LBL-14842
UC-70
Volume II c.2

Lawrence Berkeley Laboratory
UNIVERSITY OF CALIFORNIA

EARTH SCIENCES DIVISION

ANALYTICAL PERFORMANCE MODELS FOR GEOLOGIC REPOSITORIES

P.L. Chambré, T.H. Pigford, A. Fujita, T. Kanki, A. Kobayashi, H. Lung, D. Ting, Y. Sato, and S.J. Zavoshy

October 1982

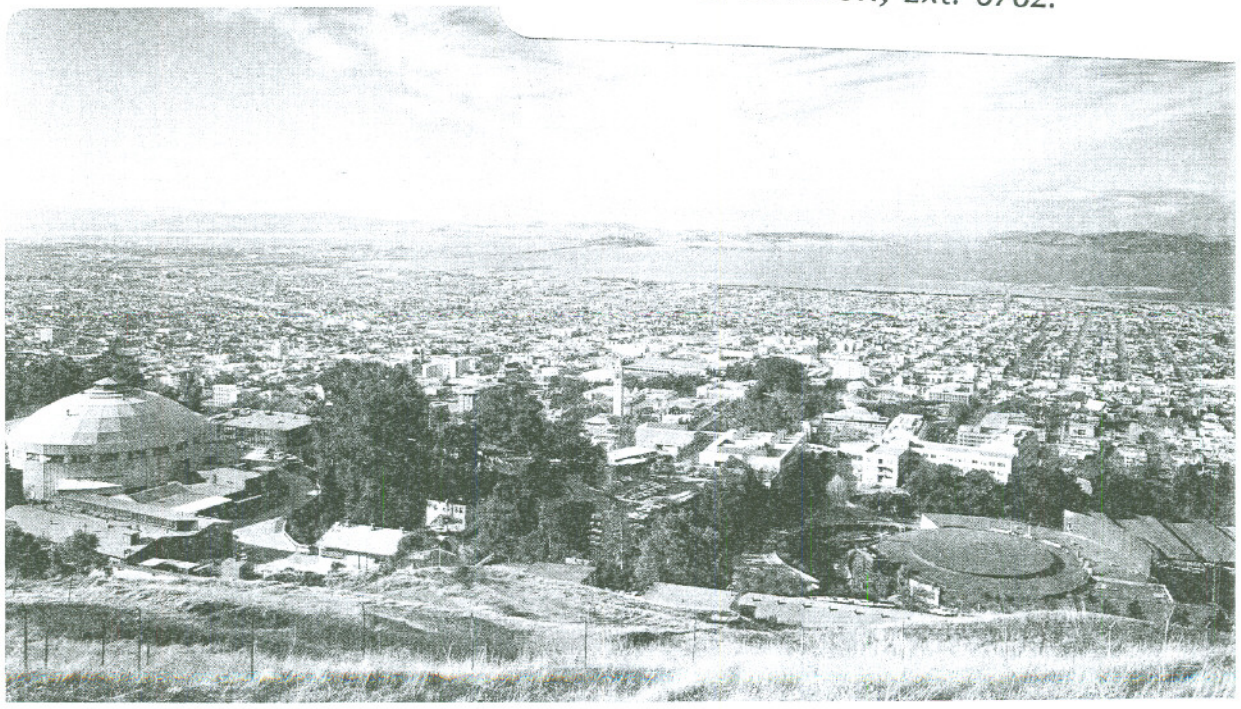

Prepared for the U.S. Department of Energy under Contract DE-AC03-76SF00098

I

LBL-14842
UCB-NE-4017
UC-70
Volume II

ANALYTICAL PERFORMANCE MODELS FOR GEOLOGIC REPOSITORIES*

P. L. Chambre', T. H. Pigford, A. Fujita, T. Kanki
A. Kobayashi, H. Lung, D. Ting, Y. Sato, S. J. Zavoshy

Earth Sciences Division, Lawrence Berkeley Laboratory

and

Department of Nuclear Engineering, University of California

Berkeley, California 94720

October 1982

---

*Prepared for the U.S. Department of Energy under contract no. DE-AC03-76SF00098 Administered by the Office of Nuclear Waste Isolation, Battelle Memorial Institute under MPO E511-05200.

The authors invite comments and would appreciate being notified of any errors in the report.

T. H. Pigford
Department of Nuclear Engineering
University of California
Berkeley, CA 94720

REPORT OUTLINE

ANALYTICAL PERFORMANCE MODELS FOR GEOLOGIC REPOSITORIES

1. Introduction and Summary

2. Three-Dimensional Transport in a One-Dimensional Flow Field, Solubility Limited Dissolution

   2.1. Introduction and Summary

   2.2. The Transport Equation and Boundary Conditions

   2.3. Solution for Point Sources

   2.4. Comparison to Concentrations From an Infinite Plane Source

   2.5. Numerical Example, Peclet No. > 4

   2.6. Numerical Example, Peclet No. < 4

   2.7. Nomenclature

   2.8. Literature References

3. Transport of a Radionuclide Chain With Nonequilibrium Chemical Reactions

   3.1. Nonequilibrium Between Two Species in a Stationary System

   3.2. Transport Without Dispersion, Local Sorption Equilibrium

      3.2.1. Transport Equations and Boundary Conditions

      3.2.2. Analytical Solutions

      3.2.3. Transport of Species of a Nuclide With No Precursor, Impulse Release

      3.2.4. Comparison With the Equilibrium Solution

      3.2.5. Duration of Nonequilibrium Characteristics

      3.2.6. Transport of Species of a Mother Nuclide, Band Release

      3.2.7. Transport of Species of a Two-Member Nuclide Chain, Band Release

Equilibrium and nonequilibrium transport of radionuclides discussed in our previous report (H1, P1) has dealt with transport in porous media, wherein radionuclides are retarded entirely by sorption. The purpose of this chapter is to develop the mathematical analysis for transport of radionuclides in fractured media, wherein radionuclides are convected by groundwater flowing through planar fissures. Here molecular diffusion into and out of micropores penetrating the rock surfaces of the fissures plays an important role in retarding the migration of radionuclides through the fissures, as has been pointed out by Neretnieks (N1).

We first formulate the equations governing fissure-flow transport of radionuclides with micropore diffusion, and we present analytical solutions to the transport of a radionuclide with no precursor, with no dispersion within the fissure, considering equilibrium sorption within the micropores. Solutions are present for an impulse release, stop release, band release, and solubility-limited dissolution.

5.1 Mathematical Modeling and Formulation

5.1.1. Transport Equations in a Finite Diffusion Field With One-Dimensional Fissure Flow

Consider a rock matrix containing planar parallel fissures extending in the direction and micropores penetrating the rock surfaces of the fissures. Within each fissure water is flowing at a constant velocity v in the z-direction, but the water in the micropores is assumed to be at rest. The spacing b between rock surfaces of each fissure and the distance d between adjacent fissures are assumed to be constants, as shown in Fig. 5.1.1. Three phases to be considered are the flowing water phase, the stationary water

phase, and the solid phase. Dispersion in the flowing water phase is neglected. Let $N_i(z,t)$, $M_i(z,y,t)$ and $S_i(z,y,t)$ be the concentrations of the nuclide i in the flowing water phase, in the stationary water phase, and in the solid phase, respectively. Since the water in the micropores is at rest, the transport of nuclides there is governed by molecular diffusion. Sorption on the planar surfaces of the fissure is assumed to be small compared to sorption on micropore surfaces and is neglected. The concentrations of the nuclide i in these three phases are then governed by the following transport equations:

$$\frac{\partial N_i}{\partial t} + v \frac{\partial N_i}{\partial z} + \lambda_i N_i = \lambda_{i-1} N_{i-1} - \frac{2}{b} J_i \qquad (5.1.1)$$

$$\varepsilon \frac{\partial M_i}{\partial t} - \varepsilon D_i \frac{\partial^2 M_i}{\partial y^2} + \varepsilon \lambda_i M_i = \varepsilon \lambda_{i-1} M_{i-1} - q_i \qquad (5.1.2)$$

$$(1-\varepsilon) \frac{\partial S_i}{\partial t} + (1-\varepsilon)\lambda_i S_i = (1-\varepsilon)\lambda_{i-1} S_{i-1} + q_i \qquad (5.1.3)$$

$$t > 0, \quad z > 0, \quad 0 < y < d/2, \quad i = 1,2,3, \ldots$$

where D_i is the diffusivity of the nuclide i in the micropore fissures which includes any goemetric factors of the micropores; ε is the volume fraction of micropores in rock, excluding the fissure; λ_i is the radioactive decay constant of the nuclide i; J_i is the diffusive rate of the nuclide i at surfaces of the fissure per unit area of fissure surface, and q_i is the rate of sorption per unit surface area within the micropores. The diffusive current and sorption rate are given by, respectively

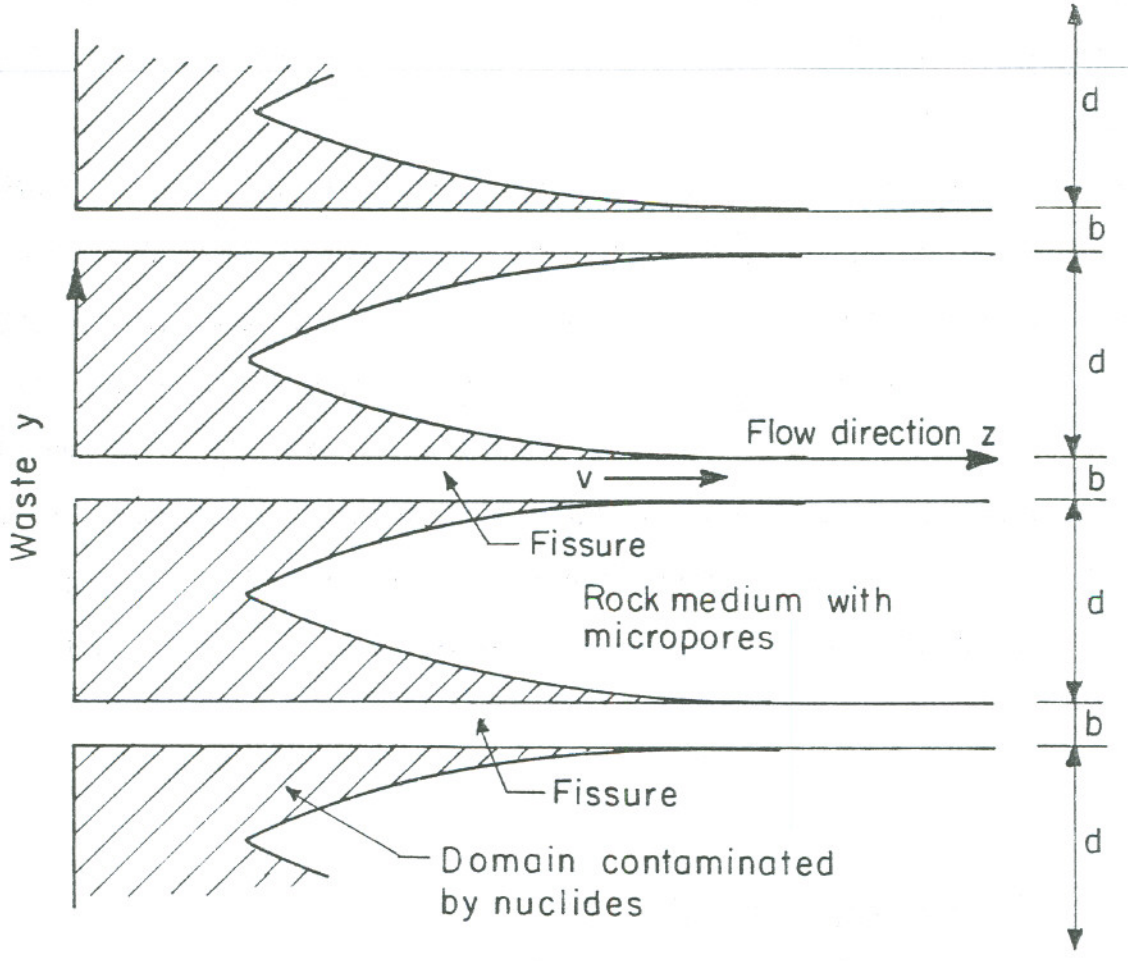

Fig. 5.1.1 Rock matrix, fissure and micropores in a fractured medium of finite spacing of fissures.

$$J_i(z,t) = -\varepsilon D_i \left.\frac{\partial M_i}{\partial y}\right|_{y=0}, \quad t > 0,\ z > 0,\ i = 1,2,.. \tag{5.1.4}$$

$$q_i(z,y,t) = k_m a \left(M_i - \frac{S_i}{K_{D,i}}\right),\ t > 0,\ z > 0,\ 0 < y < d/2,\ i = 1,2,.. \tag{5.1.5}$$

where k_m is the mass transfer coefficient, a is the interfacial area between stationary water and solid per unit volume of water, and $K_{D,i}$ is the distribution coefficient.

In this model it is noted that there are two independent transport processes which can retard the migration velocity of the nuclides. One is the removal by molecular diffusion of the nuclides into and out of micropores penetrating the surfaces of the fissures and the other is mass-transfer by sorption on the micropore surfaces. The effect of diffusion into and out of micropores will be called the "surface retardation effect" and sorption within micropores will be called "the bulk retardation effect". The surface retardation effect has not been considered in the analysis for porous-flow transport.

5.1.2 Initial and Boundary Conditions

If we assume that there are initially no nuclides in the water flow field and in the rock matrices prior to the beginning of dissolution of the nuclides, we can set the initial concentrations of nuclides in each phase as

$$N_i(z, 0) = 0, \quad z > 0 \tag{5.1.6}$$

$$M_i(z,y,0) = 0,\ z > 0, \quad d/2 > y > 0 \tag{5.1.7}$$

$$S_i(z,y,0) = 0,\ z > 0, \quad d/2 > y > 0 \tag{5.1.8}$$

The boundary condition for $N_i(z,t)$ for an infinite plane source of dissolving waste at z = 0 is:

$$N_i(0, t) = \phi_i(t), \qquad t > 0 \tag{5.1.9}$$

where the function $\phi_i(t)$ is the general time dependent concentration of the nuclide i at z = 0. We further assume that the concentration of nuclide i in the micropores should equal that of nuclide in the fissures. Then we can write the boundary condition for $M_i(z,y,t)$ at y = 0 as

$$M_i(z, 0, t) = N_i(z, t), \quad t > 0, \quad z > 0 \tag{5.1.10}$$

Another boundary condition for $M_i(z,y,t)$ to be specified at the center of spacing of the medium is, from symmetry:

$$\left.\frac{\partial M_i(z,y,t)}{\partial y}\right|_{y=d/2} = 0 \qquad z > 0, \quad t > 0 \tag{5.1.11}$$

Equations (5.1.1) through (5.1.11) give a complete set of equations for the transport problem to be solved.

i) Step release

When the radionuclides are released stepwise from the waste repository, the function $\phi_i(t)$ is given by

$$\phi_i(t) = B_i(t)\, h(t), \quad t > 0 \tag{5.1.12}$$

where the function $B_i(t)$ is the Bateman equation given by (H1):

$$B_i(t) = \sum_{j=1}^{i} b_{ij}\, e^{-\lambda_j t} \tag{5.1.13}$$

with the coefficient:

$$b_{ij} = \sum_{m=1}^{j} \frac{N_m^o \prod_{\ell=m}^{i} \lambda_\ell}{\lambda_i \prod_{\substack{\ell=m \\ (\ell \neq j)}}^{i} (\lambda_\ell - \lambda_j)} \qquad (5.1.14)$$

N_m^o is the initial concentration of the nuclide m at the waste repository.

ii) Band release

For a band release, the function $\phi_i(t)$ is given by

$$\phi_i(t) = B_i(t) \, [\, h(t) - h(t-T) \,] \qquad (5.1.15)$$

where T is the duration time of release, i.e., the leach time. If we assume that the waste and its contained radionuclides dissolve at a constant total rate over the time period T, the initial concentration of the nuclide i can be related to the initial total amount W_T^o of waste per unit cross sectional area of water flow:

$$N_i^o = \frac{n_i^o \, W_T^o}{vT} \qquad (5.1.16)$$

where n_i^o is the initial (t = 0) amount of nuclide i per unit amount of waste.

iii) impulse release

The impulse release is given by:

$$\phi_i(t) = TN_i^o \, \delta(t) \qquad (5.1.17)$$

5.1.3 Transport Equations for Shallow Penetration in Micropores

If the depth of penetration of nuclides from a fissure surface into the rock medium is much less than the fissure space d, the micropores

can be treated as being of infinite length. The transport equations presented in the foregoing section are still valid over the time and field space, so the equations to be solved are

$$\frac{\partial N_i}{\partial t} + v \frac{\partial N_i}{\partial z} + \lambda_i N_i = \lambda_{i-1} N_{i-1} - \frac{2}{b} J_i \qquad (5.1.18)$$

$$\varepsilon \frac{\partial M_i}{\partial t} - \varepsilon D_i \frac{\partial^2 M_i}{\partial y^2} + \varepsilon \lambda_i M_i = \varepsilon \lambda_{i-1} M_{i-1} - q_i \qquad (5.1.19)$$

$$(1-\varepsilon) \frac{\partial S_i}{\partial t} + (1-\varepsilon)\lambda_i S_i = (1-\varepsilon)\lambda_{i-1} S_{i-1} + q_i \qquad (5.1.20)$$

$t > 0, \quad z > 0, \quad y > 0, \quad i = 1,2,3, \ldots$

The diffusive flux J_i and the rate of sorption q_i in these equations are given by

$$J_i(z, t) = - \varepsilon D_i \left. \frac{\partial M_i}{\partial y} \right|_{y=0}, \quad t > 0, \quad z > 0 \qquad (5.1.21)$$

$$q_i(z,y,t) = k_m a(M_i - \frac{S_i}{K_{D,i}}), \quad t > 0, \quad z > 0, \quad y > 0 \qquad (5.1.22)$$

The initial and boundary conditions are

$$N_i(z, 0) = 0, \qquad z > 0 \qquad (5.1.23)$$

$$M_i(z,y,0) = 0, \qquad z > 0, \quad y > 0 \qquad (5.1.24)$$

$$S_i(z,y,0) = 0. \qquad z > 0, \quad y > 0 \qquad (5.1.25)$$

The boundary condition for $N_i(z,t)$ is

$$N_i(0,t) = \phi_i(t), \qquad t > 0 \qquad (5.1.26)$$

The surface and infinite boundary conditions for $M_i(z,y,t)$ are, respectively

$$M_i(z,0,t) = N_i(z,t), \qquad t > 0, \quad z > 0 \qquad (5.1.27)$$

$$M_i(z,\infty,t) = 0, \qquad t > 0, \quad z > 0 \qquad (5.1.28)$$

The difference of the set of governing equations in this section from that of Sect. 5.1.2 for transport in an finite diffusion field is the replacement of the symmetry boundary condition, Eq. (5.1.11) by the infinite-medium boundary condition, Eq. (5.1.28).

5.2 Diffusion Governing Transport in an Infinite Diffusion Field

In this section we present the analytical solution to fissure-flow transport in an infinite diffusion field with local sorption equilibrium and we explore the retardation due to the molecular diffusion into micropores in the rock matrix.

5.2.1 Transport Equation With Local Sorption Equilibrium

Here we consider the transport of a mother nuclide (i = 1), with no precursor. When the rate of mass transfer of nuclide between water and solid phases in micropore fissures is so rapid that the concentration of the nuclide in the solid phase is local equilibrium with that of the nuclide in the micropore water, we can write

$$S_1 = K_{D,1} M_1 \qquad (5.2.1)$$

where $K_{D,1}$ is the distribution coefficient. Adding Eq. (5.1.19) to Eq. (5.1.20) and using the above relation we obtain:

$$\frac{\partial M_1}{\partial t} - \frac{D_1}{K_1} \frac{\partial^2 M_1}{\partial y^2} + \lambda_1 M_1 = 0 \qquad t > 0, \quad y > 0 \qquad (5.2.2)$$

where K_i is the sorption coefficient defined by

$$K_i = 1 + \frac{(1-\varepsilon)\, K_{D,i}}{\varepsilon} \qquad (5.2.3)$$

In Eq. (5.2.3), ε is the porosity of rock medium excluding the fissures. Equation (5.2.2) shows that diffusion of a nuclide in micropores in the y-direction should be characterized by the ratio of diffusivity to the sorption equilibrium coefficient, rather than by the molecular diffusivity itself. This implies that a weakly sorbed species can penetrate more deep into the rock medium than a strongly sorbed species.

The transport equation for the first nuclide in the flowing water phase is

$$\frac{\partial N_1}{\partial t} + v \frac{\partial N_1}{\partial z} + \lambda_1 N_1 = - \frac{2}{b} J_1 \quad , \qquad t > 0 \quad z > 0 \qquad (5.2.4)$$

where J_1 is the diffusive flux at top surface of the fissures, given by Eq. (5.1.4)

The initial conditions are

$$N_1(z, 0) = 0 \qquad (5.2.5)$$

$$M_1(z,y,0) = 0 \qquad (5.2.6)$$

The boundary conditions are

$$N_1(0, t) = \phi_1(t) \qquad (5.2.7)$$

$$M_1(z,0,t) = N_1(z,t) \qquad (5.2.8)$$

$$M_1(z,\infty,t) = 0 \qquad (5.2.9)$$

5.2.2 Analytical Solution

The set of equations (5.2.2) through (5.2.9) can be solved by the

method of Laplace transform with the aid of initial and boundary conditions. Taking the Laplace transform of Eqs. (5.2.2) and (5.2.4), we have

$$\frac{\partial^2 \tilde{M}_1(z,y,s)}{\partial y^2} - \frac{s+\lambda_1}{D_1} K_1 \tilde{M}_1(z,y,s) = 0 \qquad (5.2.10)$$

$$\frac{\partial \tilde{N}_1(z,s)}{\partial z} + \frac{s+\lambda_1}{v} \tilde{N}_1(z,s) = - \frac{2}{bv} \tilde{J}_1(z,s) \qquad (5.2.11)$$

where s is the transformed variable with respect to time t and the functions $\tilde{M}_1(z,y,s)$ and $\tilde{N}_1(z,s)$ are the transformed subordinate functions of $M_1(z,y,t)$ and $N_1(z,t)$, respectively. $\tilde{J}_1(z,s)$ is the transformed diffusive flux at the fissure surface

$$\tilde{J}_1(z,s) = - \varepsilon D_1 \left. \frac{\partial \tilde{M}_1(z,y,s)}{\partial y} \right|_{y=0} \qquad z > 0 \qquad (5.2.12)$$

Solving Eq. (5.2.10) with the initial and boundary conditions, Eqs. (5.2.6), (5.2.8) and (5.2.9), we have the transformed solution for $\tilde{M}_1(z,y,s)$

$$\tilde{M}_1(z,y,s) = \tilde{N}_1(z,s)\, e^{-y\sqrt{\frac{K_1}{D_1}(s+\lambda_1)}} \qquad (5.2.13)$$

and the transformed diffusive flux in the form:

$$\tilde{J}_1(z,s) = \varepsilon D_1 \tilde{N}_1(z,s) \sqrt{\frac{K_1}{D_1}(s+\lambda_1)} \qquad (5.2.14)$$

Solving Eq. (5.2.10) after substitution of Eq. (5.2.14) subject to the boundary condition given by Eq. (5.2.7), we have the transformed solution

$$\tilde{N}_1(z,s) = \tilde{\phi}_1(s)\, e^{-\frac{(\lambda_1+s)}{v} - a_1 z \sqrt{s+\lambda_1}} \qquad (5.2.15)$$

where $\tilde{\phi}_1(s)$ is the transformed concentration at the repository and a_1 is the constant defined by

$$a_1 = \frac{2\varepsilon D_1}{bv}\sqrt{\frac{K_1}{D_1}} \qquad (5.2.16)$$

Also from Eq. (5.2.13),

$$\tilde{M}_1(z,y,s) = \tilde{\phi}_1(s) e^{-\frac{(s+\lambda_1)}{v} z - (a_1 z + b_1 y)\sqrt{s+\lambda_1}} \qquad (5.2.17)$$

where b_1 is the constant:

$$b_1 = \sqrt{\frac{K_1}{D_1}} \qquad (5.2.18)$$

The inverse of Eqs.(5.2.15) and (5.2.17) with respect to s can be found by using the formula:

$$L^{-1}\left\{e^{-d\sqrt{s+\lambda_1}}\right\}$$

$$= \frac{\alpha}{2\sqrt{\pi t^3}} e^{-\frac{\alpha^2}{4t} - \lambda_1 t} \equiv P_1(t;\alpha) \qquad (5.2.19)$$

The solution for aqueous concentration of the nuclide in the fissure and micropores are given by, respectively

$$N_1(z,t) = e^{-\frac{\lambda_1}{v} z} \int_0^{t-\frac{z}{v}} \phi_1(t-\tfrac{z}{v}-\tau) P_1(\tau;a_1 z)\, d\tau, \quad z<vt \qquad (5.2.20)$$

$$M_1(z,y,t) = e^{-\frac{\lambda_1}{v}z} \int_0^{t-\frac{z}{v}} \phi_1(t-\tfrac{z}{v}-\tau)P_1(\tau;a_1z+b_1y)d\tau, \quad (5.2.21)$$

$$z<vt$$

5.2.3 Transport With an Impulse Release

When the function $\phi_1(t)$ is characterized by the impulse release function given by Eq.(5.1.18), the solutions for the concentration of the nuclide in the fissure and micropores become

$$N_1(z,t)=(TN_1^o)e^{-\frac{\lambda_1}{v}z} P_1(t-\tfrac{z}{v}, a_1z) \quad , \qquad z<vt \qquad (5.2.22)$$

$$M_1(z,y,t)=(TN_1^o)e^{-\frac{\lambda_1}{v}z} P_1(t-\tfrac{z}{v}, a_1z + b_1y), \quad z<vt \qquad (5.2.23)$$

The concentration profiles of 237Np with no precursor nuclide for transport with impulse release at various migration times are shown in Fig. (5.2.1).

5.2.4 Solution For a Step Release

For a step release, the time dependent function $\phi_1(t)$ is given by Eq. (5.1.12). For the first nuclide,

$$\phi_1(t) = N_1^o\, h(t)\, e^{-\lambda_1 t} \qquad (5.2.24)$$

Substituting Eq. (5.2.24) into Eqs. (5.2.20) and (5.2.21), we have the solutions for the space-time dependent aqueous concentrations of the nuclide in the fissure and in the micropores

$$N_1(z,t) = N_1^o\, e^{-\lambda_1 t}\, \mathrm{erfc}\left(\frac{a_1 z}{2\sqrt{t-z/v}}\right), \quad z < vt \qquad (5.2.25)$$

$$M_1(z,y,t) = N_1^o\, e^{-\lambda_1 t}\, \mathrm{erfc}\left(\frac{a_1 z+b_1 y}{2\sqrt{t-z/v}}\right), \quad z < vt \qquad (5.2.26)$$

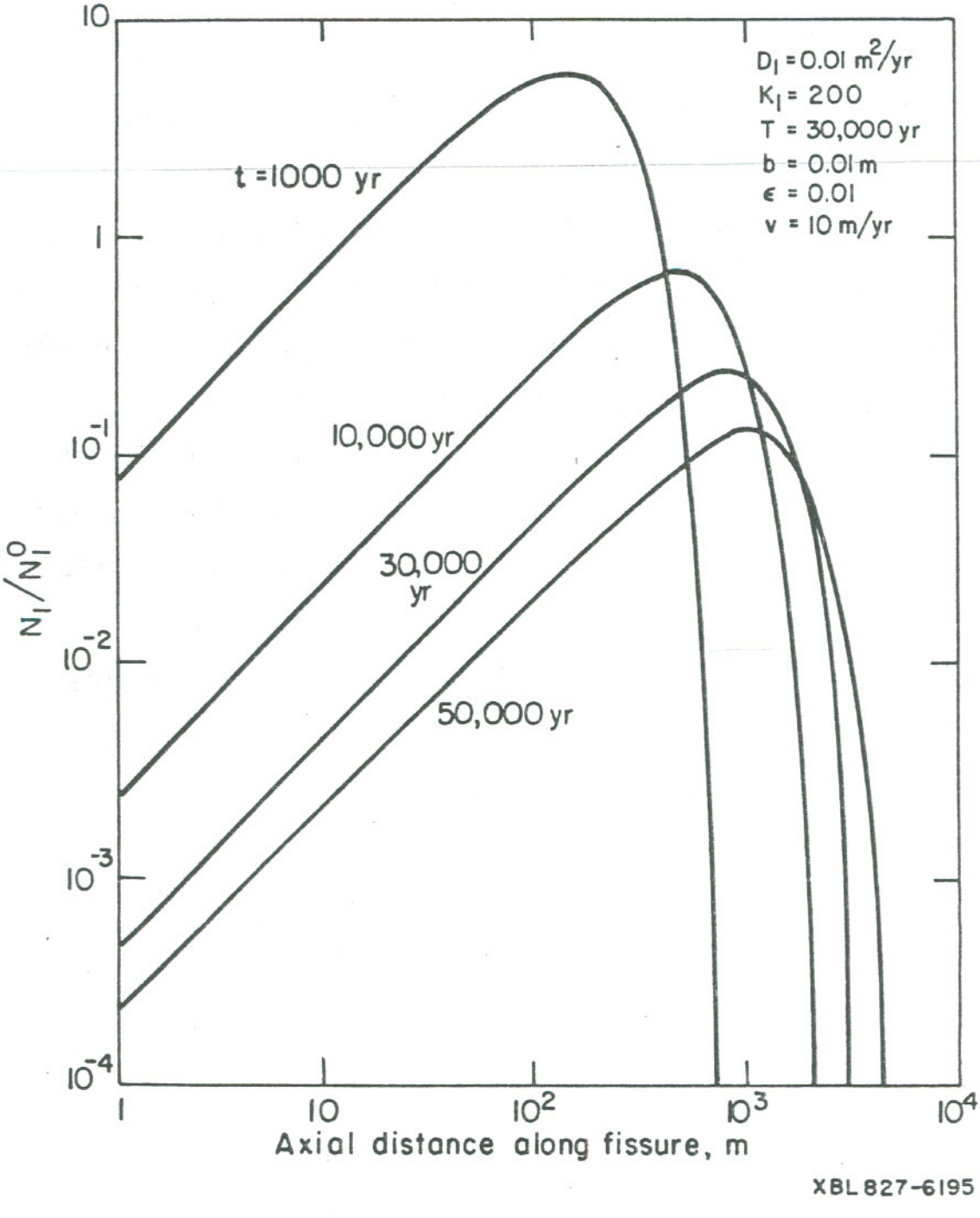

Fig. 5.2.1 Concentration profiles of ^{237}Np, fissure flow transport with impulse release.

5.2.5 Penetration Thickness of Nuclide in Fractured Medium

In Equation (5.2.2) for the diffusion of a nuclide through micropores the coefficient of the second-order space derivative of the concentration is inversely proportional to the sorption equilibrium constant K_1 of the rock medium. Hereafter this coefficient will be called an apparent diffusivity designated as D_1/K_1. In Fig. 5.2.2, the aqueous concentration profiles of ^{237}Np in the micropores at a given time t = 10,000 yr for a step release are shown for various values of the sorption retardation constant. For times of the order of one year, a weakly sorbed nuclide, with an assumed retardation constant K_1 = 1, can penetrate about 40m into the rock at a migration distance z = 100 m, whereas a strongly sorbed nuclide, with K_1 = 10,000 can penetrate only about 0.2 m. Because of long railing edge of the concentration profile, the concept of penetration depth remains ambiguous. The penetration depth or "thickness", is usually defined as a fictitious distance that corresponds to an arbitrarily specified amount of the nuclide penetrating into the medium per unit cross sectional area of the medium, normalized to the concentration at the surface of the medium. Here we define the penetration thickness $\eta(z,t)$ at a given distance z and time t as

$$\eta(z,\ t) = \frac{\int_0^\infty M_1(z,y,t)dy}{M_1(z,0,t)} \qquad (5.2.27)$$

Substituting Eq. (5.2.26) into Eq.(5.2.27), we have the local penetration thickness

$$\eta(z,t)=\frac{1}{C_2}\left\{-\frac{1}{\sqrt{\pi}\ e^{C_1^2}\ \mathrm{erfc}(C_1)} - C_1\right\} \qquad (5.2.28)$$

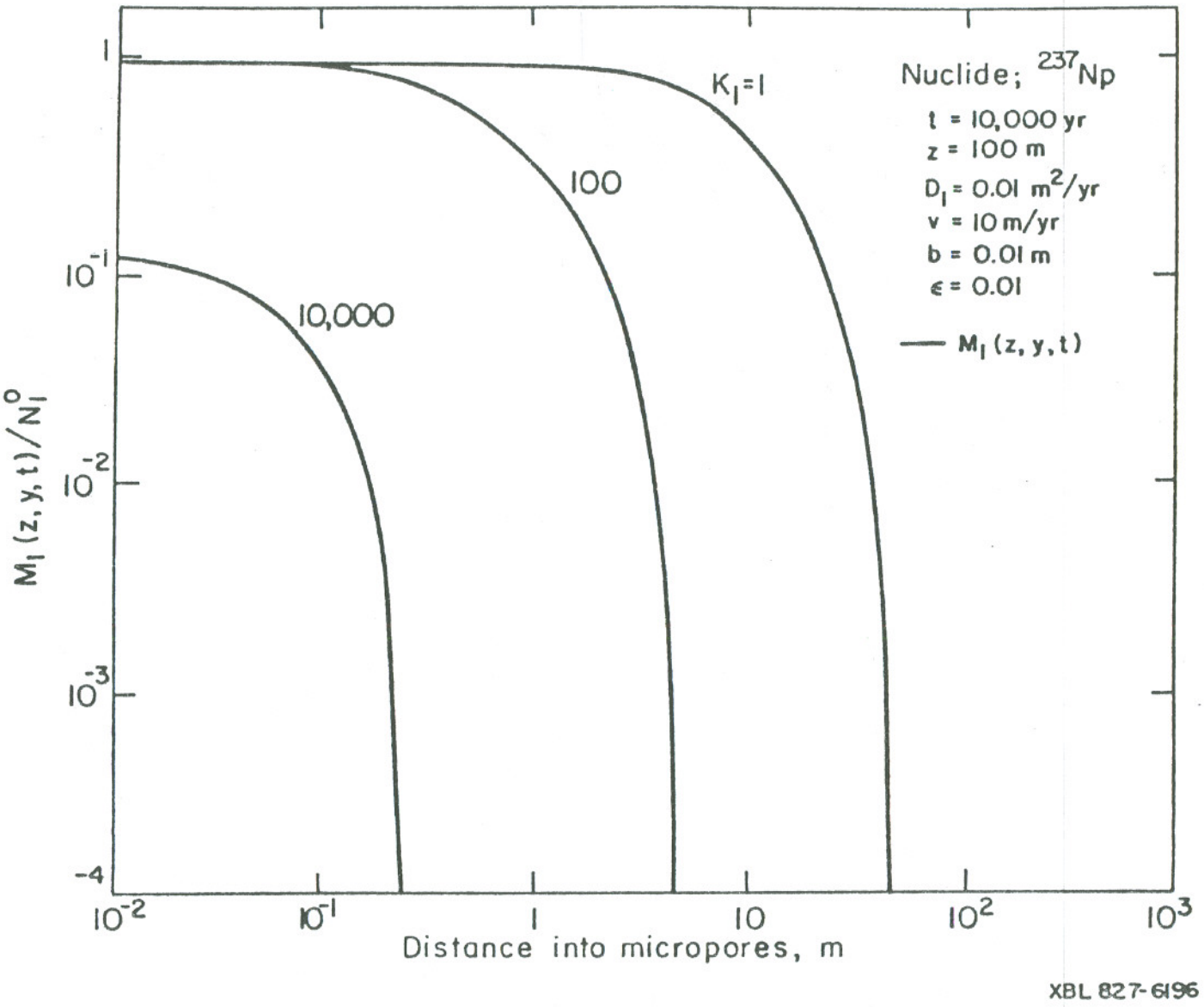

Fig. 5.2.2 Concentration profiles of ^{237}Np in micropores, step release

where

$$C_1 = \frac{\varepsilon z\sqrt{D_1 K_1}}{bv\sqrt{t-z/v}} \qquad (5.2.29)$$

$$C_2 = \frac{\sqrt{K_1 D_1}}{2\sqrt{t-z/v}} \qquad (5.2.30)$$

In Tables 5.2.1 (a) ~ 5.2.1 (c), variation of the penetration thickness with distance z at a given time which are calculated from Eq. (5.2.28) are shown for various values of the retardation constant. The assumed parameters used in calculations are listed in these tables. As seen from these tables, the penetration thickness depends strongly on the retardation constant. For t = 10,000 yr and at z = 100 m for K_1 = 1, the penetration thickness is 11 m, whereas for K_1 = 10,000 the penetration thickness is only 0.01 m. Because of the smaller penetration thickness of the strongly sorbed species, the concentration gradient of the nuclide at the fissure surface of the medium is greater, which results in a greater diffusive flux into the micropores. Also the greater diffusive flux of the nuclide into the medium results in greater retardation of the nuclide in its migration within the fissure.

5.2.6 Retardation Due to Molecular Diffusion

Profiles of the aqueous concentration of ^{237}Np in the fissure of a step release, calculated for three different values of the sorption retardation constant of the rock medium, are shown as the solid lines in Fig. 5.2.3. The diffusivity of the nuclide in micropore water, including the effect of geometric factors, is assumed to be D_1 = 0.01 m^2/yr. The

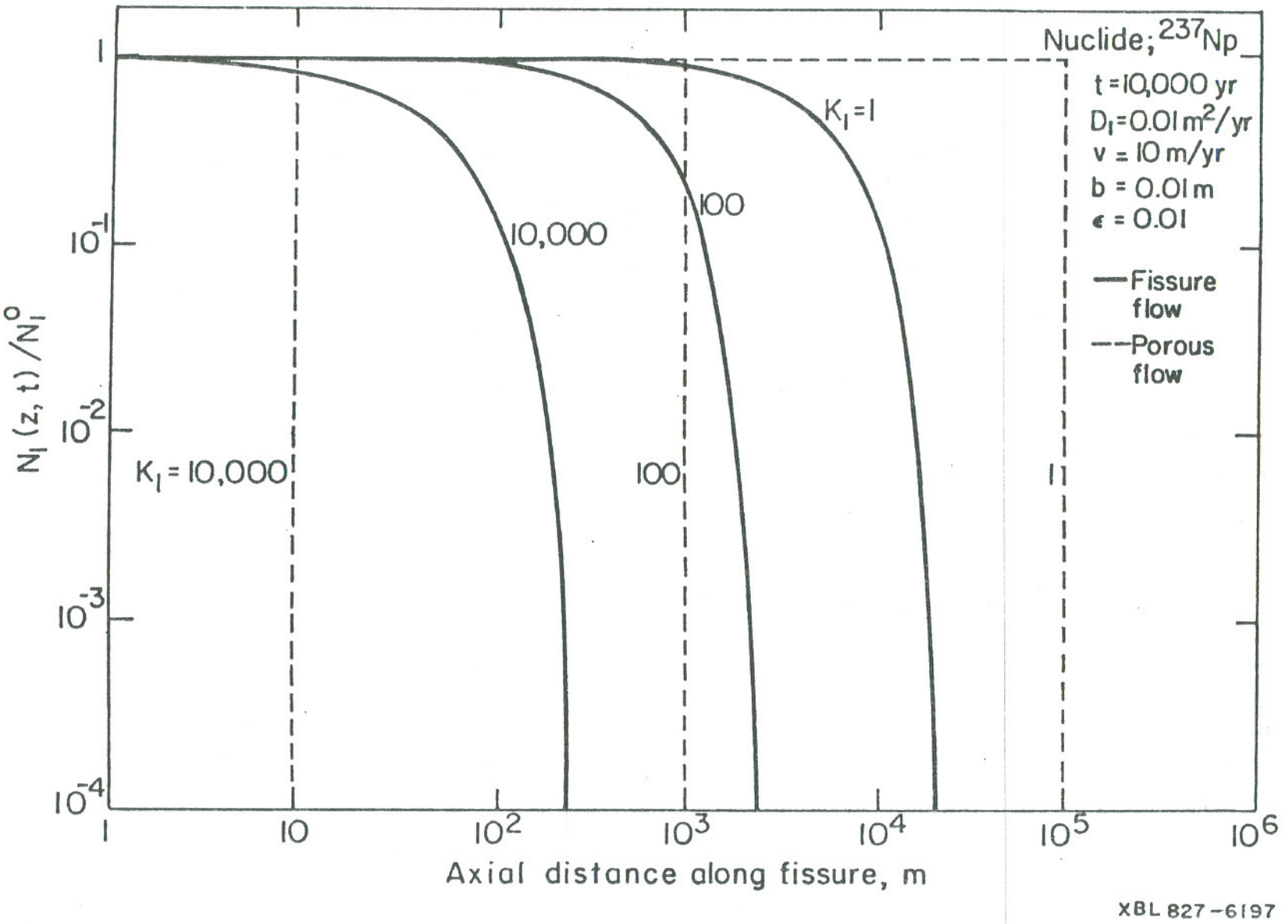

Fig. 5.2.3 Concentration profiles of ^{237}Np in fissure, step release.

Table 5.2.1 Penetration thickness for various sorption coefficients, assumed $D_1=1.0\times10^{-2}m^2/yr$, v=10 m/yr, b=$1.0\times10^{-2}$m, $\varepsilon=1.0\times10^{-2}$.

Time t (yr)	Distance z (m)	Penetration thickness, η (m) $K_1=1$	$K_1=1\times10^2$	$K_1=1\times10^4$
1×10^4	1.0×10^{-1}	1.128x10	1.128	1.128×10^{-1}
	5.0×10^{-1}	1.128x10	1.128	1.125×10^{-1}
	1.0	1.128x10	1.128	1.121×10^{-1}
	5.0	1.128x10	1.125	1.093×10^{-1}
	1.0x10	1.128x10	1.121	1.059×10^{-1}
	$5.0\times10_2$	1.124x10	1.093	8.324×10^{-2}
	1.0×10^2	1.121x10	1.058	6.388×10^{-2}
	5.0×10^2	1.090x10	8.300×10^{-1}	1.989×10^{-2}
	1.0×10^3	1.053x10	6.345×10^{-1}	9.900×10^{-3}
	5.0×10^3	8.056	1.899×10^{-1}	1.90×10^{-3}
	1.0×10^4	5.906	9.00×10^{-2}	9.00×10^{-4}
	5.0×10^4	1.00	1.00×10^{-2}	1.00×10^{-4}
	1.0×10^5	1.0×10^{-10}	1.0×10^{-12}	1.0×10^{-14}
1×10^3	1.0×10^{-1}	3.568	3.568×10^{-1}	3.561×10^{-2}
	5.0×10^{-1}	3.568	3.565×10^{-1}	3.532×10^{-2}
	1.0	3.567	3.561×10^{-1}	3.496×10^{-2}
	5.0	3.564	3.531×10^{-1}	3.227×10^{-2}
	1.0x10	3.559	3.495×10^{-1}	2.930×10^{-2}
	$5.0\times10_2$	3.523	3.219×10^{-1}	1.539×10^{-2}
	1.0×10^2	3.479	2.913×10^{-1}	6.162×10^{-3}
	5.0×10^2	3.139	1.479×10^{-1}	1.900×10^{-3}
	1.0×10^3	2.753	5.007×10^{-1}	9.00×10^{-4}
	5.0×10^3	8.110×10^{-1}	1.00×10^{-2}	1.00×10^{-4}
	1.0×10^4	1.0×10^{-10}	1.0×10^{-12}	1.0×10^{-14}
1×10^2	1.0×10^{-1}	1.128	1.128×10^{-1}	1.121×10^{-2}
	5.0×10^{-1}	1.128	1.125×10^{-1}	1.093×10^{-2}
	1.0	1.127	1.121×10^{-1}	1.058×10^{-2}
	5.0	1.122	1.090×10^{-1}	8.300×10^{-3}
	1.0x10	1.115	1.053×10^{-1}	6.345×10^{-3}
	$5.0\times10_2$	1.064	8.056×10^{-2}	1.899×10^{-3}
	1.0×10^2	1.001	5.906×10^{-3}	9.00×10^{-4}
	5.0×10^2	5.252×10^{-1}	9.999×10^{-12}	1.00×10^{-14}
	1.0×10^3	1.0×10^{-10}	1.0×10^{-12}	1.0×10^{-14}

other assumed parameters are included in the figure. For the assumed time of 10,000 yr and an assumed water velocity of 10 m/yr, the water travel distance is 10^5 m. A nuclide with K_1 = 10,000 is found to be much retarded by molecular diffusion into the micropores. Even a nonsorbed nuclide with K_1 = 1 is retarded by molecular diffusion into the micropores. The dashed lines show the concentration profiles of the same nuclide assumed to be convected by porous flow at the same water velocity with local sorption equilibrium with the porous solid. For a strongly sorbed nuclide, the migration distance of that nuclide convected by fissure flow is greater than that of the nuclide convected by porous flow, defining "migration distance" as the distance reached by the half maximum of the leading edge of the concentration profile. For a weakly sorbed nuclide, however, the migration distance in fissure flow is less than that in the porous flow. This implies that the porous flow model with local sorption equilibrium, if it is applied to the transport of nuclides in fractured media, may overestimate the retardation capacity for a strongly sorbed nuclide and may underestimate the retardation capacity for a weakly sorbed nuclide.

5.2.7 Transport With a Band Release

The solutions for space-time-dependent aqueous concentrations of the nuclide in the fissure and in the micropores for a band release can be obtained by direct application of the theorem of superposition (H1). They are given by, respectively

$$N_1(z,t) = N_1^o e^{-\lambda_1 t}\left[h(t-\frac{z}{v})\ \mathrm{erfc}\left(\frac{a_1 z}{2\sqrt{t-z/v}}\right)\right.$$

$$\left. - h(t-T-\frac{z}{v})\ \mathrm{erfc}\left(\frac{a_1 z}{2\sqrt{t-T-z/v}}\right)\right] \qquad (5.2.31)$$

$$M_1(z,y,t) = N_1^o e^{-\lambda_1 t}\left[h(t-z/v)\mathrm{erfc}\left(\frac{a_1 z+b_1 y}{2\sqrt{t-z/v}}\right)\right.$$

$$\left. - h(t-T-\frac{z}{v})\ \mathrm{erfc}\left(\frac{a_1 z + b_1 y}{2\sqrt{t-T-z/v}}\right)\right] \qquad (5.2.32)$$

where the constants a_1 and b_1 are given by Eqs. (5.2.16) and (5.2.18).

Figure 5.2.4 shows the concentration profiles of ^{237}Np in the fissures for the band release. The leach time is assumed to be T = 30,000 yr, and the other parameters used in the calculations are the same as those used for the step release. Because of the removal at the front of the band by diffusion into micropores and the release of the penetrated nuclide at the rear of the band, the concentration profiles for fissure flow, for various K_1 values, show the long smoothed curves with long trailing edges, and with highly curved leading edges. All of the fissure-flow curves converge at $N_1 = 0$ and at the water-transport distance of 5×10^5 m, because no sorption retardation occurs within the fissures. The dashed lines show the concentration bands of the nuclide calculated from the porous-flow model. The effect of diffusion into and out of the micropores is to greatly spread the concentration band, qualitatively similar to the effect of a large dispersion coefficient for dispersion in the direction of convective flow.

Because of the spreading of the concentration profile in fissure

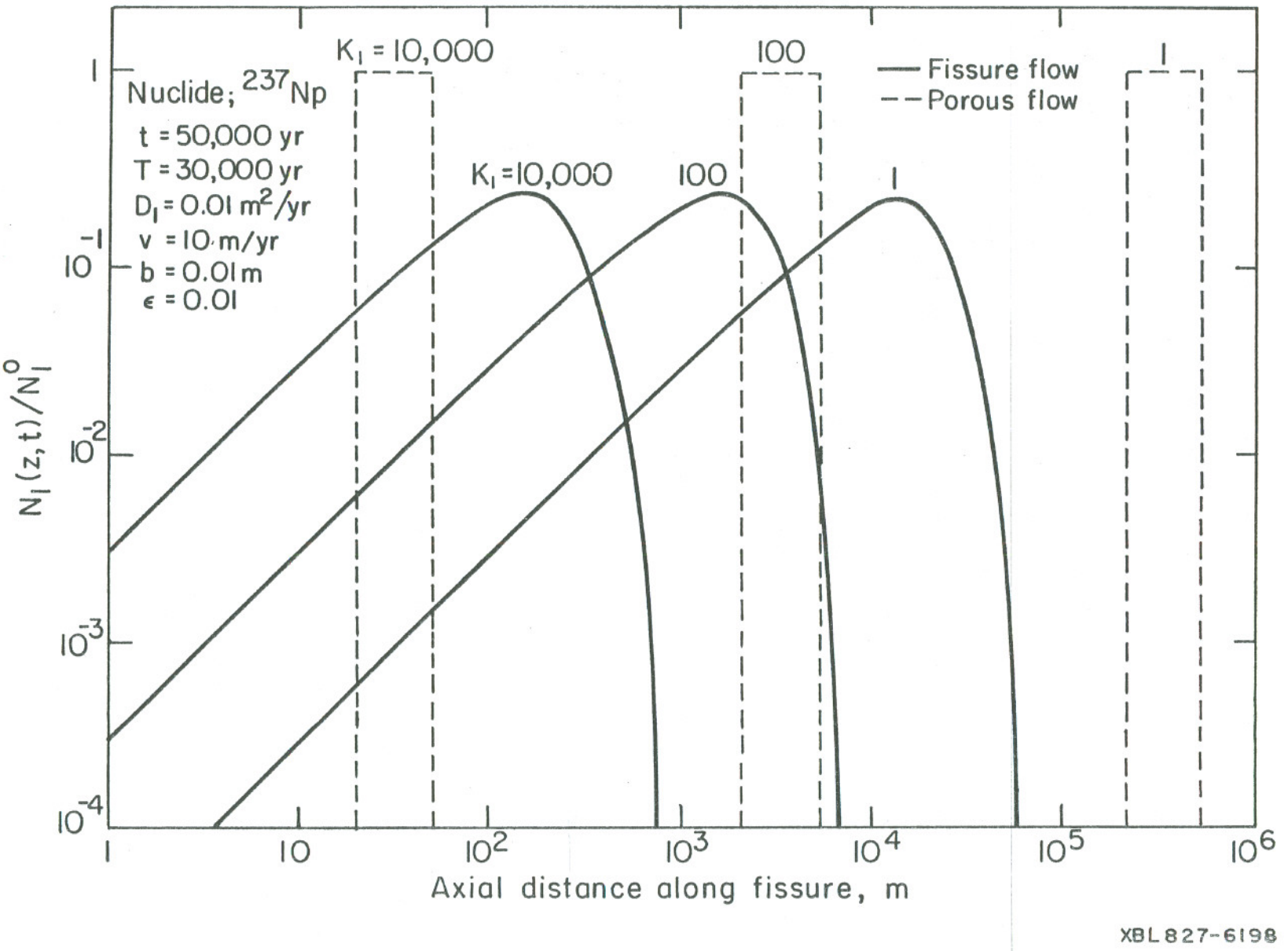

Fig. 5.2.4 Concentration profiles of ^{237}Np in the fissure, band release.

flow, the maximum concentration, even for a weakly sorbed nuclide, is much lower than that predicted from the porous-flow model. The maximum concentration is relatively unaffected by the magnitude of the sorption retardation constant.

The concentration profiles of ^{237}Np in micropores in the y-direction at a given distance z = 10 m are shown for some different migration times in Fig. 5.2.5. In this calculation, the leach time is assumed to be 10,000 yr. At t = 10,000 yr, when the band-release solution is identical to the step-release solution, the nuclide still continues to penetrate into the rock medium and the concentration gradient of the nuclide is negative throughout, i.e. the concentration decreases monotonically with distance at a time less than the leach time. At $t = 10^5$ yr, when the trailing edge of the seed concentration band has already passed the distance of z = 10 m, the concentration of the nuclide in the fissure is lower than that in the micropores, and the nuclide diffuses back out into the flowing water. Consequently, the concentration in the micropore now increases with distance at a smaller y, reaches a maximum, and decreases again with distance at a greater penetration distance. The diffusion of the nuclide at the fissure surface into the flowing water fissure causes the long trailing edges of concentration in the fissure as shown in Fig. 5.2.4. The locus of the maximum concentration of the nuclide in the micropore moves more deeply into the medium with increasing time.

In evaluating the biological hazard due to radioactive wastes, the maximum concentration of the contained nuclide is an important index. As described above the maximum concentration of the nuclide predicted for fissure flow transport shows an appreciably lower value than that

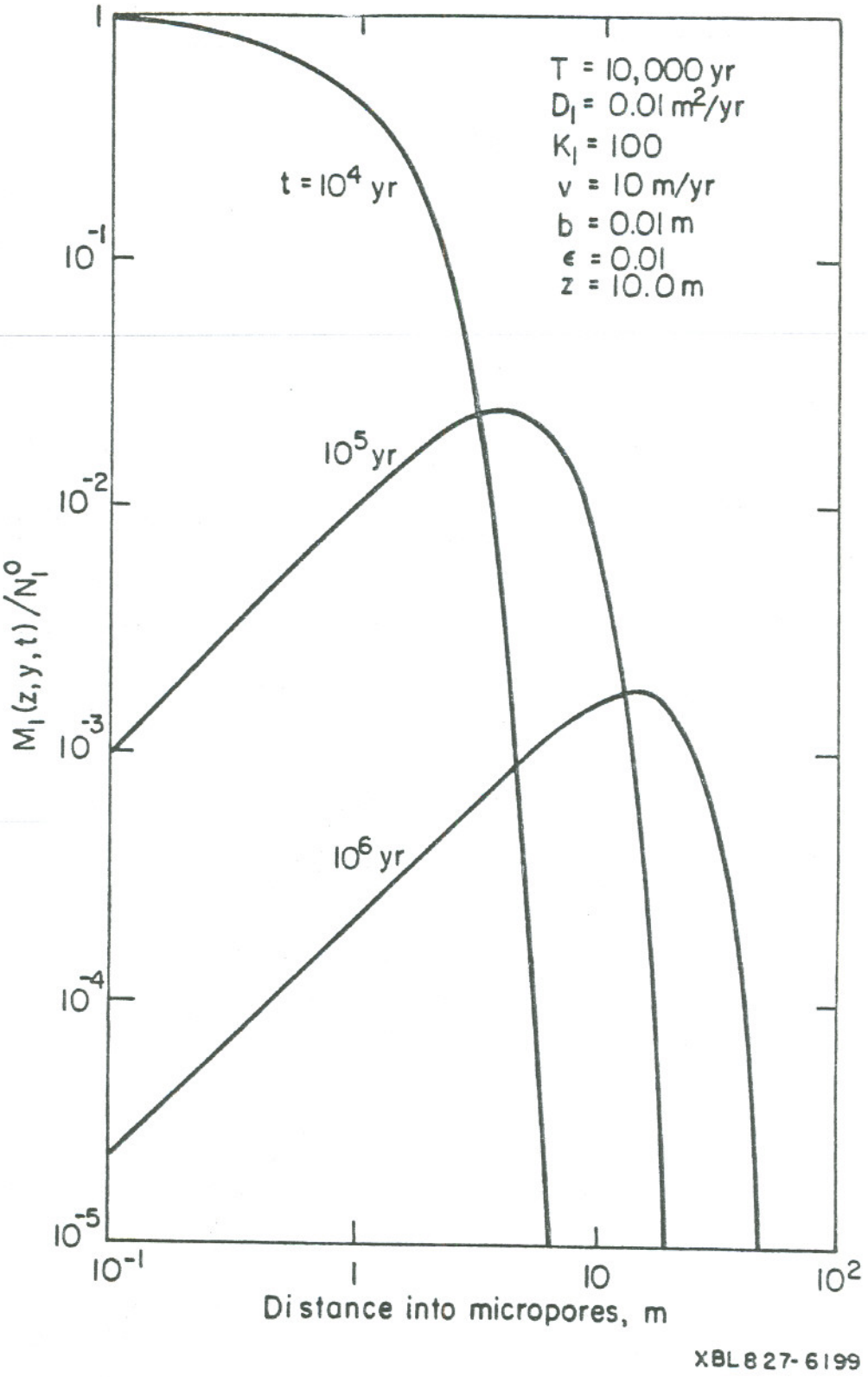

Fig. 5.2.5 Concentration profiles of ^{237}Np in micropores, band release.

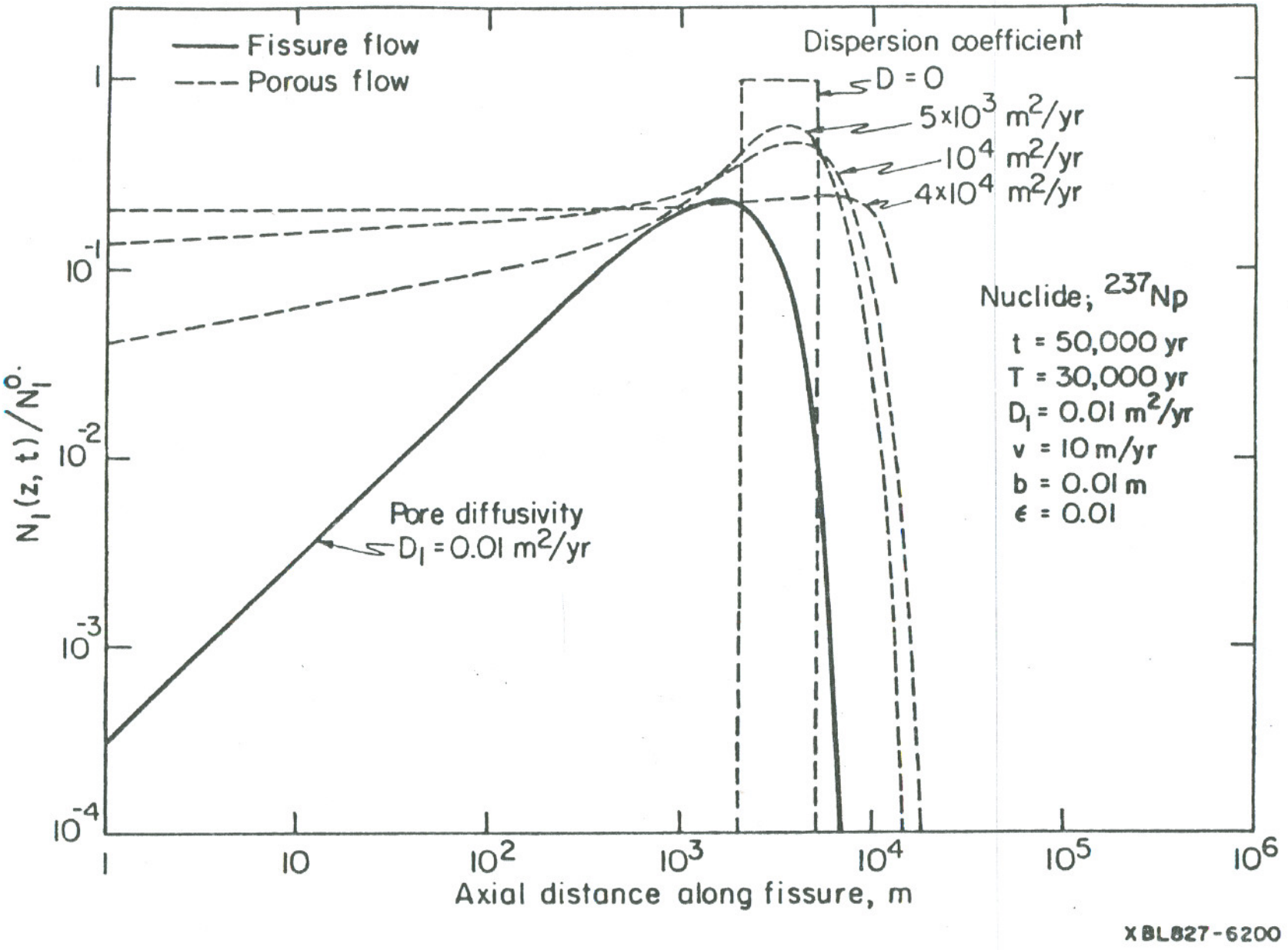

Fig. 5.2.6 Comparison of maximum concentration in fissure flow transport with that of porous flow.

predicted from the porous-flow transport model. Because the broadening of the concentration profiles in fracture flow is qualitatively like the effect of axial dispersion in porous flow, we can calculate the magnitude of an axial dispersion coefficient that would result in a porous-flow concentration maximum as low as that calculated for fissure flow. Fig. 5.2.6 shows a comparison of the maximum concentration of ^{237}Np predicted in porous-flow transport with dispersion with that predicted in fissure-flow transport without dispersion. This figure demonstrates that even with a dispersion coefficient orders of magnitude greater than commonly used, the attenuation of the concentration equivalent to that predicted in fissure flow transport cannot be expected in porous-flow transport. In this assumed case, an axial dispersion coefficient greater than about 4×10^4 m^2/yr will be needed to obtain the same attenuation as that predicted in fissure-flow transport.

5.3 Transport With a Finite Plane Source

In a real waste repository the waste sources will be arranged in a finite array. Although the analytical solutions for fissure-flow transport with an infinite plane source, which neglect transverse flow and dispersion in the fissures, give important insights into radionuclide transport in fissure flow, application of these solutions will lead to an over-estimate of the concentrations at the point of discharge to the environment. Here we consider the transport of radionuclides released from a finite plane source into infinite plane fissures surrounded by an infinite rock medium, with one-dimensional water flow in the fissures.

5.3.1 Formulation and Analysis

Consider a coordinate system with z in the flow direction, y in the direction of pore diffusion into the rock and x in the transverse direction parallel to the surface of the fissure as shown in Fig. 5.3.1. In the case of dispersion free, the convective transport of the nuclide in the z direction is usually much more effective than dispersive transport in the z direction, so the latter will be neglected. In the transverse x direction, however, because of no water flow in that direction, dispersion and even molecular diffusion play an important role in nuclide transport. Here we will solve the problem literally for infinite planar fissures, so the appropriate coefficient D_x for Fickian transport in the transverse planar direction x is the molecular diffusivity D_{ml} of the nuclide in the liquid. When sorption in the micropores is locally equilibrated, the transport equations for the aqueous concentrations of the nuclide in the fissure and in the micropores are given by

$$\frac{\partial N_1}{\partial t} + v \frac{\partial N_1}{\partial z} - D_{ml} \frac{\partial^2 N_1}{\partial x^2} + \lambda_1 N_1 = - \frac{2}{b} J_1 \qquad (5.3.1)$$

$$\frac{\partial M_1}{\partial t} - \frac{D_1}{K_1} \frac{\partial^2 M_1}{\partial y^2} + \lambda_1 M_1 = 0 \qquad (5.3.2)$$

$$t > 0, \quad z > 0, \quad -\infty < x < +\infty, \quad y > 0$$

where $N_1(z,x,t)$ and $M_1(z,y,x,t)$ are the aqueous concentrations of the mother nuclide in the fissure and micropores, respectively, v is the water

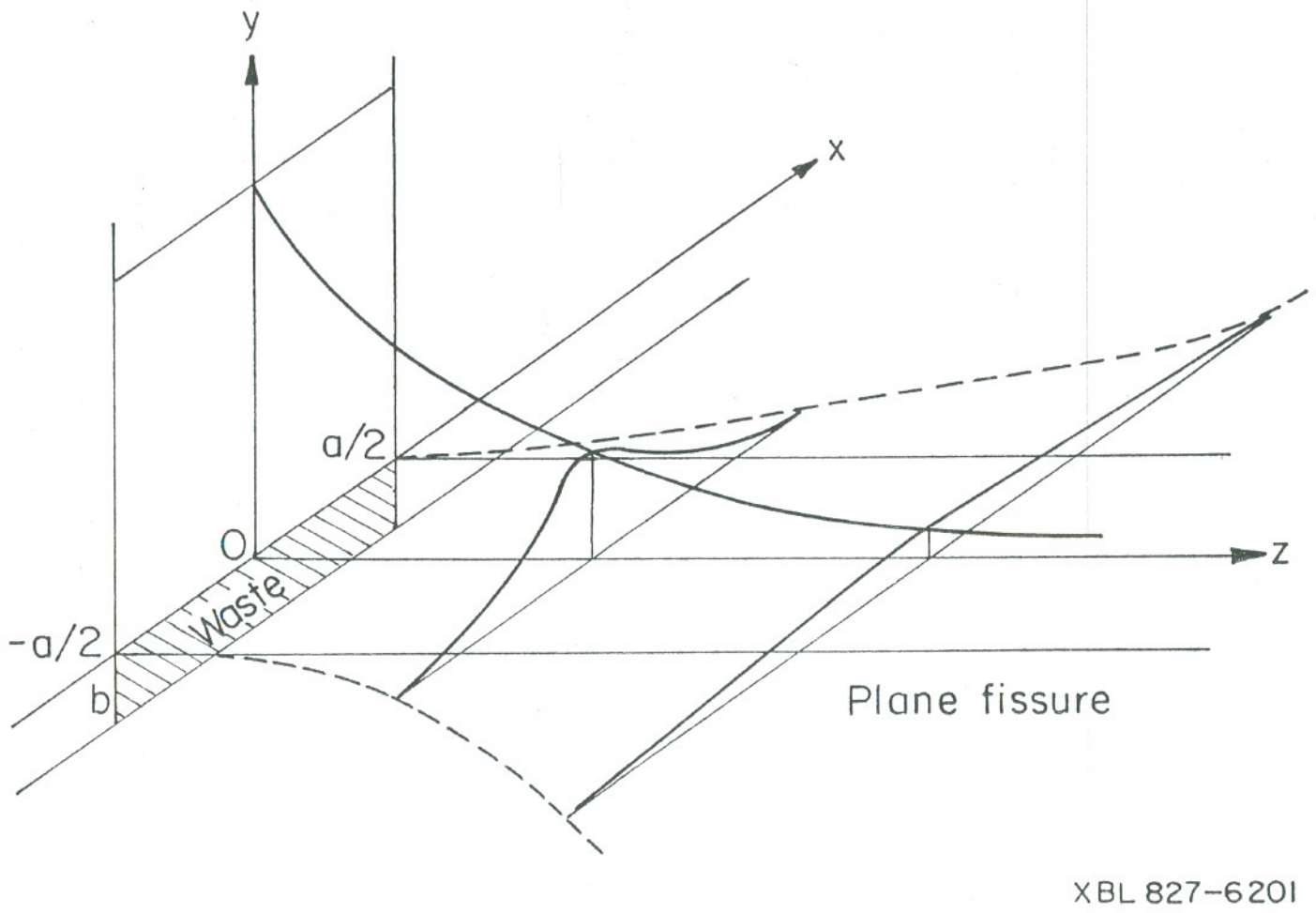

Fig. 5.3.1 Coordinate system for release from a finite source into planar fissures.

velocity, D_1 is the pore molecular diffusivity, D_{m1} is the pure molecular diffusivity, λ_1 is the radioactive decay constant, K_1 is the retardation constant, b is the spacing of the interstice fissure walls, and J_1 is the diffusive flux of the nuclide due to transport into the micropores.

$$J_1 = -\varepsilon D_1 \frac{\partial M_1}{\partial y}\bigg|_{y=0}, \quad t > 0, \; z > 0, \; -\infty < x < +\infty \tag{5.3.3}$$

where ε is the porosity of the fractured medium excluding the fissures.

The initial conditions are

$$N_1(z, x, 0) = 0, \quad z > 0, \quad -\infty < x < +\infty \tag{5.3.4}$$

$$M_1(z,y,x,0) = 0, \quad z > 0, \quad -\infty < x < +\infty, \; y > 0 \tag{5.3.5}$$

The boundary conditions are

$$N_1(0, x, t) = \begin{cases} \phi_1(t), & t > 0, \quad |x| < a/2 \\ 0, & |x| > a/2 \end{cases} \tag{5.3.6}$$

$$M_1(z,0,x,t) = N_1(z,x,t) ,$$

for

$$t > 0, \quad z > 0, \quad -\infty < x < +\infty$$

$$M_1(z,\pm\infty,x,t) = 0, \quad t > 0, \quad z > 0, \quad -\infty < x < +\infty \tag{5.3.8}$$

Taking the Laplace transform of Eq. (5.3.2) with respect to t and solving with the aid of the initial and boundary conditions, we obtain the concentration of the nuclide in the micropores and diffusive flux at the surfaces of the fissure in the transformed form:

$$\tilde{M}_1(z,y,x,s) = \tilde{N}_1(z,x,s)\, e^{-y\sqrt{\frac{K_1}{D_1}(s+\lambda_1)}} \tag{5.3.9}$$

$$\tilde{J}_1(z,x,s) = \varepsilon D_1 \tilde{N}_1(z,x,s)\sqrt{\frac{K_1}{D_1}(s+\lambda_1)} \tag{5.3.10}$$

where $\tilde{M}_1(z,y,x,s)$ is

$$\tilde{M}_1(z,y,x,s) = \int_0^\infty e^{-st} M_1(z,y,x,t)\, dt \tag{5.3.11}$$

Define

$$\hat{\tilde{N}}_1(z,\omega,s) = \int_{-\infty}^{\infty}\int_0^\infty e^{-ix\omega - st} N_1(z,x,t)\, dt\, dx \tag{5.3.12}$$

Taking Laplace and Fourier transforms of Eq.(5.3.1) with respect to t and x, and solving the resultant equation with the appropriate initial and boundary conditions, we have

$$\tilde{N}_1(z,\omega,s) = \tilde{\phi}_1(s)\, \hat{H}(\omega)\, e^{-\frac{s+\lambda_1}{v} z - a_1 z\sqrt{s+\lambda_1 + (i\omega)^2}\frac{D_{m1}}{v} z} \tag{5.3.13}$$

where a_1 is the same constant as given by Eq. (5.2.16) and the function H(w) is given by

$$H(\omega) = \frac{2 \sin(\frac{a\omega}{2})}{\omega} \tag{5.3.14}$$

Inversion of Eq. (5.3.13) can be found by using the Fourier inversion formulae:

$$F^{-1}\left\{ e^{(i\omega)^2\theta} \right\} = \frac{1}{2\sqrt{\pi}} \frac{e^{-\frac{x^2}{4\theta}}}{\sqrt{\theta}} \tag{5.3.15}$$

$$F^{-1}\left\{ H(\omega) \right\} = h(x + \tfrac{a}{2}) - h(x - \tfrac{a}{2}) \tag{5.3.16}$$

thus, from the convolution rule

$$F^{-1}\left\{H(\omega)e^{(i\omega)^2\theta}\right\} = \frac{1}{\sqrt{\pi}} \int_{-\infty}^{+\infty} \frac{e^{-\xi^2/4\theta}}{2\sqrt{\theta}} \cdot \left[h(x-\xi+\frac{a}{2}) - h(x-\xi-\frac{a}{2})\right] d\xi$$

$$= E_1\ (\frac{a}{2} \pm x, \theta) \qquad (5.3.17)$$

where ζ is a dummy integral variable and the function $E_1(a/2\pm x,\theta)$ is given by

$$E_1(\frac{a}{2} \pm x, \theta) = \frac{1}{2}\left[\text{erf}\ (\frac{\frac{a}{2} + x}{2\sqrt{\theta}}) + \text{erf}\ (\frac{\frac{a}{2} - x}{2\sqrt{\theta}})\right] \qquad (5.3.18)$$

and the Laplace inversion formula:

$$L^{-1}\left\{e^{-\alpha\sqrt{s+\lambda_1}}\right\} = \frac{\alpha}{2\sqrt{\pi t^3}}\ e^{-\frac{\alpha^2}{4t} - \lambda_1 t} \equiv P_1(t;\alpha) \qquad (5.3.19)$$

There results the solution for the concentration of the nuclide in the fissure

$$N_1(z,x,t) = E_1(\frac{a}{2} \pm x, \frac{D_{m1}}{v} z)\ e^{-\frac{\lambda_1}{v} z} \int_0^{t - \frac{z}{v}} P_1(\tau;a_1 z)\phi_1(t-\tau-\frac{z}{v})\ d\tau \qquad (5.3.20)$$

The concentration of the nuclide in the micropores is then, from Eqs. (5.3.9), (5.3.13), and (5.3.19)

$$M_1(z,y,x,t) = E_1(\frac{a}{2} \pm x, \frac{D_{m1}}{v} z)\ e^{-\frac{\lambda_1}{v} z}$$

$$\cdot \int_0^{t - \frac{z}{v}} P_1(t;a_1 z+b_1 y)\ \phi_1(t-\tau-\frac{z}{v})\ d\tau \qquad (5.3.21)$$

where the constant b_1 is given by Eq.(5.2.18).

5.3.2 Solution for an Impulse Release

When the function $\phi_1(t)$ is specified by the impulse release function:

$$\phi_1(t) = TN_1^o \delta(t) \tag{5.3.22}$$

the solutions can be written as

$$N_1(z,x,t) = T N_1^o e^{-\frac{\lambda_1}{v} z} h(t-\frac{z}{v}) E_1(\frac{a}{2} \pm x, \frac{D_{m1}}{v} z) P_1(t-\frac{z}{v}; a_1 z) \tag{5.3.23}$$

$$M_1(z,y,x,t) = T N_1^o e^{-\frac{\lambda_1}{v} z} h(t-\frac{z}{v}) E_1(\frac{a}{2} \pm x, \frac{D_{m1}}{v} z)$$

$$\cdot P_1(t-\frac{z}{v}; a_1 z + b_1 y) \tag{5.3.24}$$

where N_1^o is the initial concentration of the nuclide at the waste repository. Because of infinite characteristic of the boundary data, the concentration N_1 shows an infinite value at the leading edge at $z = vt$ when $D_1 \to 0$.

5.3.3 Solution For a Step Release

The step release function is characterized by Eq. (5.1.12), especially for the first nuclide

$$\phi_1(t) = B_1(t)\, h(t) \tag{5.3.25}$$

where the function $B_1(t)$ is given by

$$B_1(t) = b_{11} e^{-\lambda_1 t}, \quad b_{11} = N_1^o \tag{5.3.26}$$

Substitution of Eq. (5.3.25) into Eqs. (5.3.20) and (5.3.21) gives the solutions for the aqueous concentrations of the nuclide in the main and micropore fissures. They are respectively,

$$N_1(z,x,t) = N_1^o\, e^{-\lambda_1 t}\, E_1\left(\frac{a}{2} \pm x, \frac{D_{m1} z}{v}\right) \operatorname{erfc}\left(\frac{a_1 z}{2\sqrt{t-z/v}}\right) h(t-z/v) \qquad (5.3.27)$$

$$M_1(z,y,x,t) = N_1^o e^{-\lambda_1 t}\, E_1\left(\frac{a}{2} \pm x, \frac{D_{m1} z}{\quad}\right) \operatorname{erfc}\left(\frac{a_1 z + b_1 y}{2\sqrt{t-z/v}}\right) h(t-z/v) \qquad (5.3.28)$$

where a_1 and b_1 are the constants given by Eqs. (5.2.16) and (5.2.18), respectively,

5.3.4 Solution For a Band Release

For a band release, the function $\phi_1(t)$ is given by

$$\phi_1(t) = B_1(t)\left[h(t) - h(t - T)\right] \qquad (5.3.29)$$

where T is the leach time.

The solutions for a band release can be obtained directly by applying the theorem of superposition (H-1). The concentrations of the nuclide in the fissure and in the micropores are given by, respectively

$$N_1(z,y,t) = N_1(z,y,t;\, b_{11}) - N_1(z,y,x,t-T;\, b_{11}\, e^{-\lambda_1 T}) \qquad (5.3.30)$$

$$M_1(z,y,x,t) = M_1(z,y,x,t;\, b_{11}) - M_1(z,y,x,t-T;\, b_{11}\, e^{-\lambda_1 T}) \qquad (5.3.31)$$

5.3.5 Effect of Transverse Molecular Diffusion on Fissure-Flow Transport

The concentration profiles of ^{237}Np released stepwise from a finite

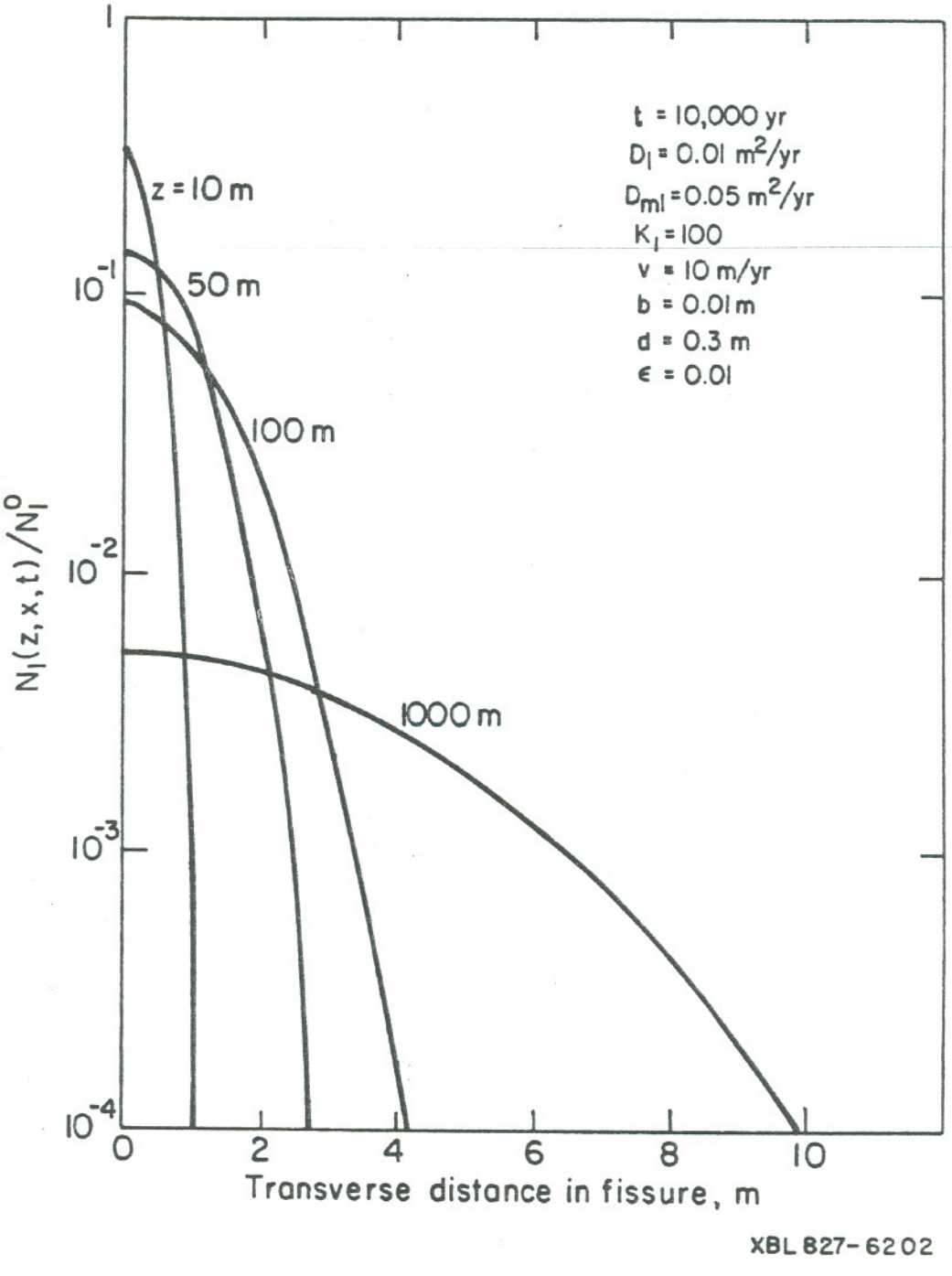

Fig. 5.3.2 Concentration profiles in transverse direction in fissure, step release (z=distance from waste source).

plane source, with the ratio of fissure width b to fissure spacing d of 30, along the transverse direction x at various values of the migration distance z are shown in Fig. 5.3.2. The molecular diffusivity in the water in the main fissure D_{mi} is assumed to be 0.05 m^2/yr, five times higher than the assumed micropore diffusivity D_l. The micropore diffusivity is usually related to the pure molecular diffusivity D_{mi} as $D_l = D_{mi}/q^2$, where q^2 is a geometric factor, the tortuosity coefficient. The assumed parameters are listed in the figure. For a relatively small axial distance z the concentration profile in the transverse direction shows a smaller diffusion path length and a greater gradient in concentration, which would cause a greater diffusive flux in that direction. The concentration gradient becomes smaller and the diffusion path length becomes greater with increasing migration distance z. This behavior is quite different from that noticed in the concentration profile in the y-direction in the rock medium. The profiles along y-direction shows a smaller diffusion path length but a greater concentration gradient at a greater distance z.

This behavior in concentration in the transverse x-direction is well understood by introducing the concept of an effective diffusion time t_e. Since the diffusion field in the transverse x-direction moves with the water at the same velocity, the effective time for the molecular diffusion in this field can be determined by $t_e = z/v$. At z = 10 m, for instance, t_e = 1 yr, whereas at a greater distance z = 1000 m, t_e = 100 yr. Therefore, at a greater distance z there is a greater effective time for diffusion in the x-direction.

The diffusion field in the y-direction in the rock medium, on the other hand, is a stationary field, since the water in the micropores is

at rest. Therefore, the effective time for diffusion in the micropores is given by $t_e = t - z/v$. At a given time, t_e at a smaller z gives a greater effective time for the diffusion in the micropore fissures. The case is just contrary to the case for the transverse diffusion in the flowing water in the main fissure. Because of the longer effective time, a nuclide at a greater z can diffuse to reach a greater distance in the transverse x direction, thereby resulting in a considerably lower concentration along z at x = 0.

The concentration gradient in micropores becomes very steep near the leading edge of the band moving through the fissures, whereas the concentration gradient in the transverse direction becomes quite low in that region far from the source but becomes infinite in the medium adjacent to the source, at the edges of the source. Therefore, attenuation of concentration at x = 0 due to transverse diffusion is very small at the leading convection edge of the band, and consequently transverse diffusion has no significant effect in retarding nuclide migration velocity, even though it does appreciably attenuate the maximum concentration of the nuclide.

In fact, taking a limit of the solution given by Eq. (5.3.27) of $D_1 \to 0$ yields

$$N_1(z,x,t) = N_1^o e^{-\lambda_1 t} h(t-\frac{z}{v}) E_1(\frac{a}{2} \pm x, \frac{D_{m1} z}{v}) \qquad (5.3.32)$$

This equation shows that the nuclide convected from the waste repository is only attenuated in concentration by a ratio of the function $E_1(a/2 \pm x, D_{m1} z/v)$. Although the E_1 function decreases with distance z at a given x, it is still finite at the water-travel edge. This means

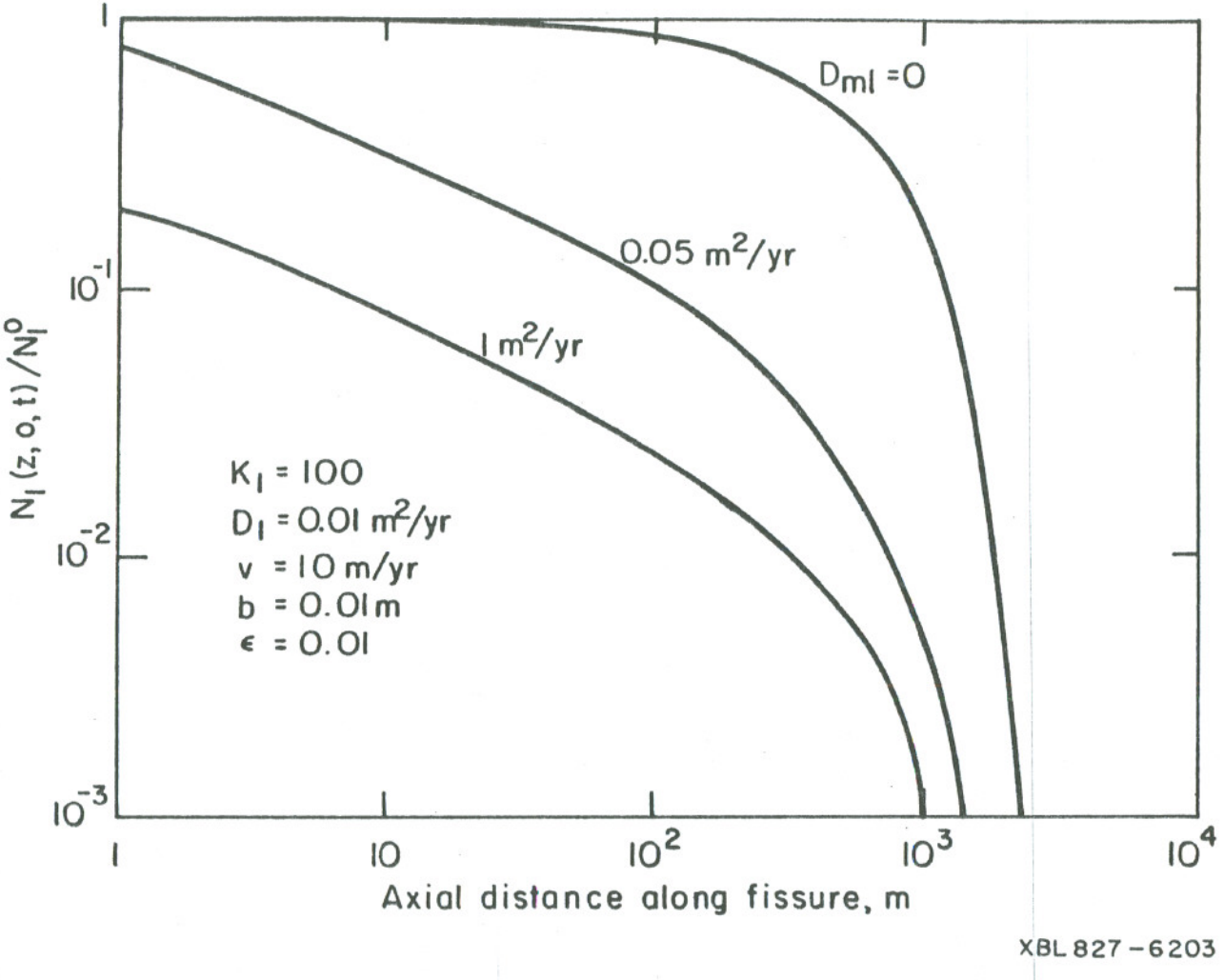

Fig. 5.3.3 Effect of transverse molecular diffusion on fissure flow transport, concentration profiles of ^{237}Np at x=0 and y=0 with different molecular diffusivities.

that E_1 function contributions has nothing characteristic of a retardation effect on the nuclide migration velocity. When the molecular diffusivity D_{mi} becomes zero, on the other hand, the solution approaches the solution for transport without transverse diffusion, namely,

$$N_1(z,x,t) = N_1(z,t) = N_1^o e^{-\lambda_1 t} h(t-\frac{z}{v}) \text{ erfc } (\frac{a_1 z}{2\sqrt{t-z/v}}) \qquad (5.3.33)$$

This equation gives zero concentration at the leading edge z = vt.

In Figure 5.3.3 the concentration profiles of ^{237}Np at the center of the repository source (x = 0) and along the z-direction, for a step release, are compared with the concentration of that nuclide in transport without transverse molecular diffusion. As seen from this figure, the concentration at a given z is reduced appreciably by transverse diffusion in the x-direction, even with a relatively smaller diffusion coefficient. Figure 5.3.4 also shows a comparison of the concentration profile along z-direction at x = 0 in transport with transverse diffusion with that in transport without transverse diffusion, but for band release. The size of the repository source is assumed to be same as that assumed in transport with step release. The figure shows that the maximum concentration is much reduced by transverse diffusion, even with a small value of the diffusivity. The maximum concentration with D_{m1} = 0.05 m^2/yr for instance, gives a value almost a hundredfold less than the maximum concentration without transverse diffusion. However, transverse diffusion has negligible effect on the locus of the maximum concentration, nor does it appreciably shift the leading edge of the concentration band.

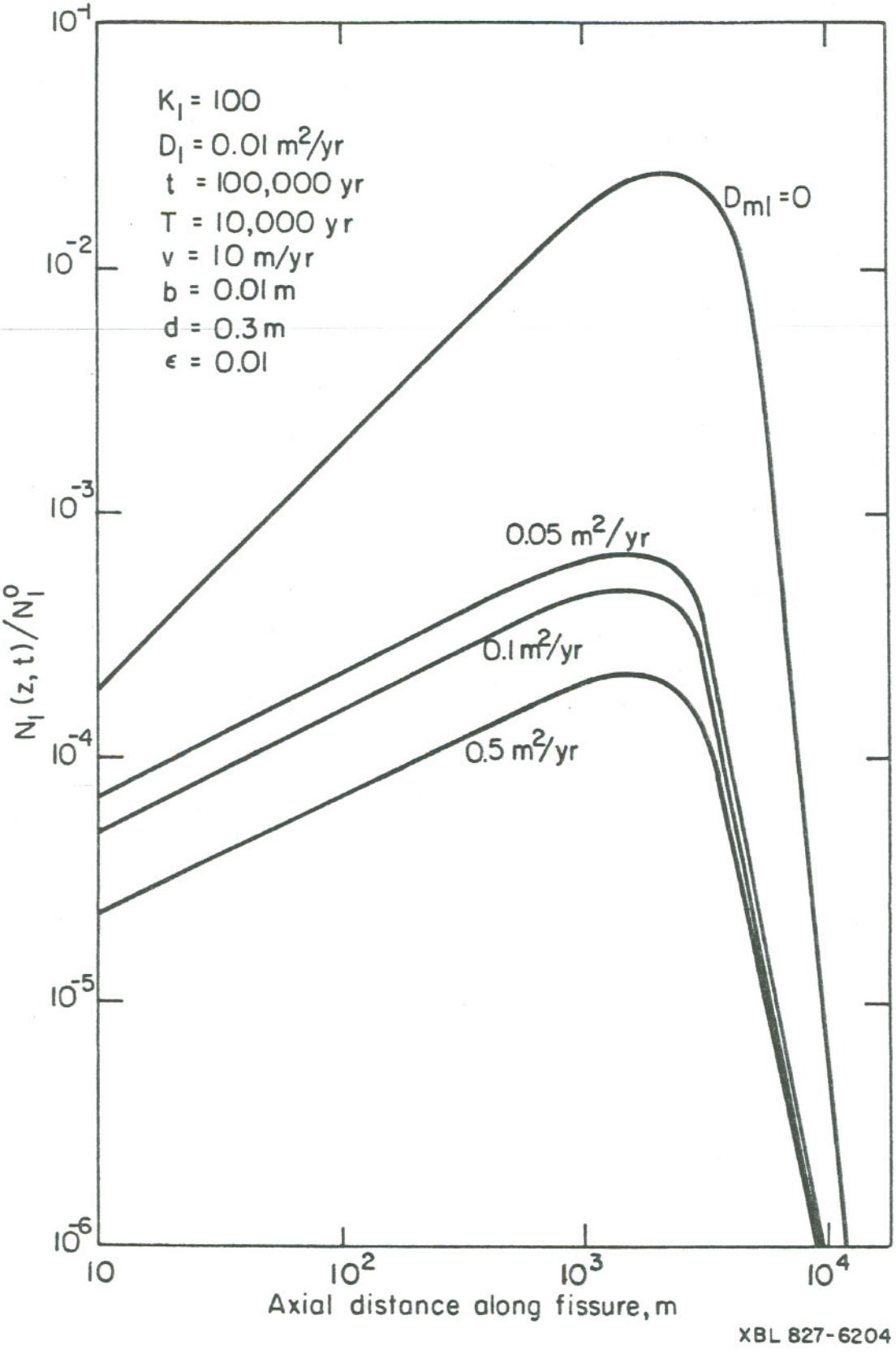

Fig. 5.3.4 Effect of transverse molecular diffusion on aqueous concentration of ^{237}Np in micropores, band release.

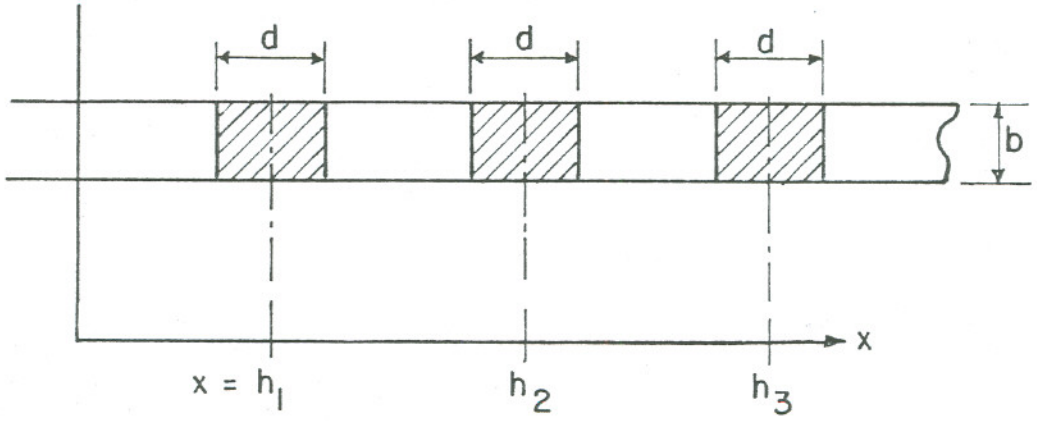

Fig. 5.3.5 Arrayed plane source in fissure flow transport.

5.3.6 Transport of a Nuclide Released From Arrayed Finite Plane Sources

When many plane sources are arrayed at a plane at z = 0 as shown in Fig. 5.3.5, nuclides released from one source will affect the concentration from another source. Let h_1, h_2, ... h_i, ... be the positions at x axis of the each plane source, then the concentrations of the nuclide in the fissure and micropores are given by the superposition of the solutions

$$N_1(z,x,t) = N_1^o e^{-\lambda_1 t} h(t-z/v) \operatorname{erfc}\left(\frac{a_1 z}{2\sqrt{t-z/v}}\right) \sum_{\ell=1}^{n} E_1\left[\frac{a}{2}+(x-h\ ), \frac{D_{m1} z}{v}\right] \quad (5.3.34)$$

$$M_1(z,y,x,t) = N_1^o e^{-\lambda_1 t} h(t-z/v) \operatorname{erfc}\left(\frac{a_1 z+b_1 y}{2\sqrt{t-z/v}}\right) \sum_{\ell=1}^{n} E_1\left[\frac{a}{2}+(x-h\ ), \frac{D_{m1} z}{v}\right] \quad (5.3.35)$$

when n is the number of finite plane sources.

The step-release concentration profiles in the transverse x-direction of ^{237}Np assumed to be released from array of finite waste sources with an assumed scale b = 0.01 m, d = 0.3 m, and Δh = 3 m, and at a given time t = 10,000 yr are shown in Fig. 5.3.6, with the migration distance z as a parameter. As seen from the figure, the distinctly separated concentration steps travel along z-direction at a smaller z, but because of the effect of transverse diffusion, the separated concentration steps superpose with each other and make a new wavelike concentration step at a greater distance z. In this assumed case, the concentration profile becomes almost flat at z = 100 m. The dashed lines show the concentration profiles resulting from transport without transverse diffusion. The figure shows that neglecting transverse diffusion can lead to significantly overestimates not only of the maximum concentration but also of the local concentration of a nuclide.

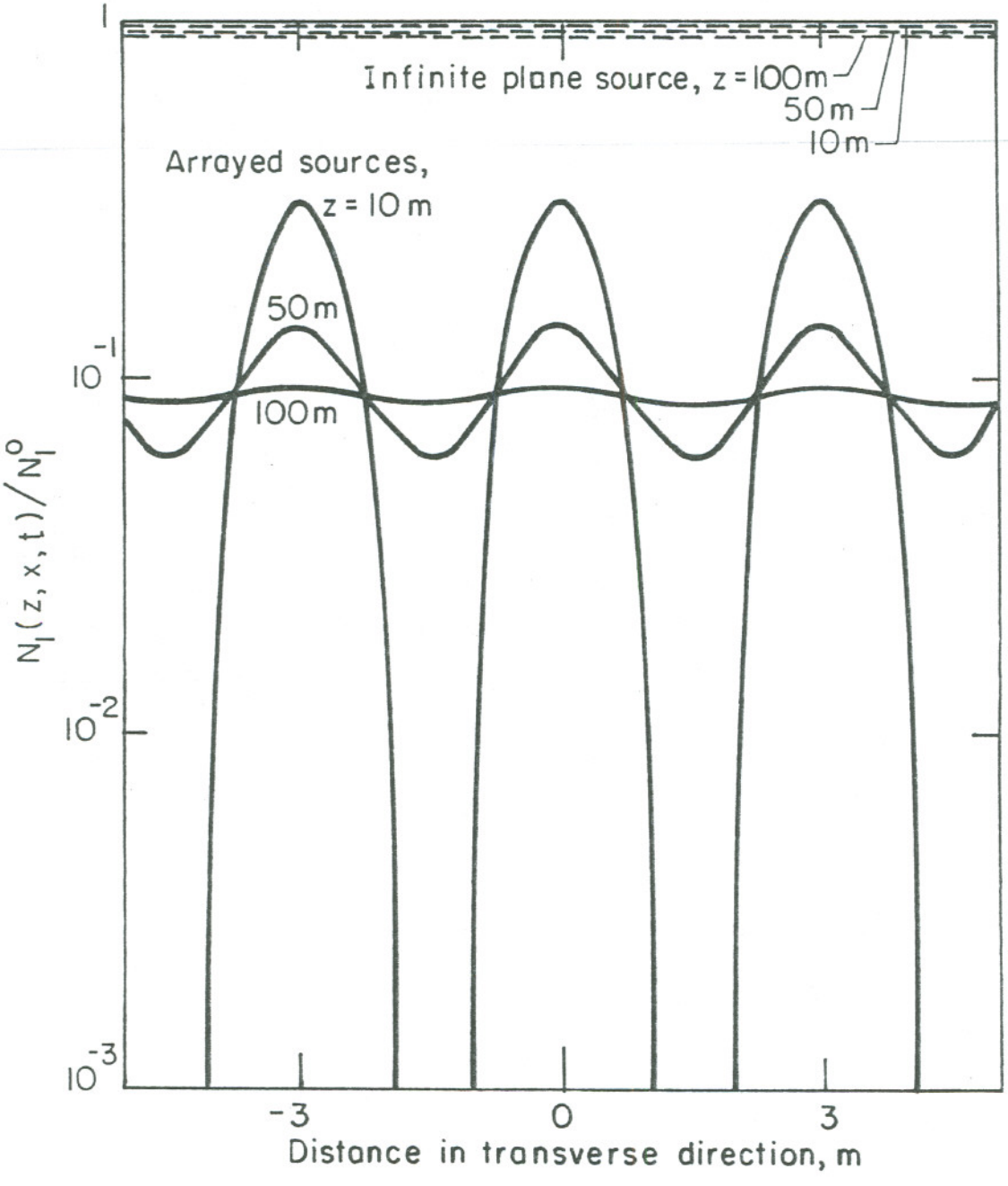

XBL 827-6206

Fig. 5.3.6 Concentration profiles of ^{237}Np released from arrayed sources in transverse direction, t=10000 yr, D_l=0.01 m^2/yr, D_{ml}=0.05 m^2/yr, v=10 m/yr, b=0.01 m, d=0.3 m, h_l=3 m.

5.4 Transport of a Nuclide in a Plane Fissure With Flow in the Surrounding Permeable Rock

In the previous analysis we have neglected water flow through micropores. However, it is possible that a transverse pressure gradient may induce very slow water flow through micropores. The purpose of this section is to derive the analytical solution to the transport of a mother nuclide through a fissure with some crossflow of water through the micropores.

5.4.1 Formulation and Analysis

Consider a single infinite-plane fissure of average interstice b, both sides of which are bounded by rock surfaces permeable to water. If there exists a pressure gradient in the direction as shown in Fig. 5.4.1, water should flow in the y+ direction in the micropores in the upper medium A, and in the negative of the y^- direction in the micropores in the lower medium B. Although water flow through micropores is usually very small, due to the considerably lower permeability of the rock, it can affect the concentration profile of the nuclide in the fissure, especially at small z distances where the concentration gradient of the nuclide in micropores near the surface of the fissure is so small that convective transport by permeating water in micropores becomes comparable to diffusive transport. Let $N_1(z,t)$ be the aqueous concentration of the nuclide in the fissure and $M_1^+(z,y+,t)$ amd $M_1^-(z,y^-,t)$ be the concentrations of the nuclide in the medium A and in the medium B, respectively. The transport equations which govern these concentrations are given by

$$\frac{\partial N_1}{\partial t} + v\frac{\partial N_1}{\partial z} + \lambda_1 N_1 = -\frac{1}{b}(J_1^+ + J_1^-) \qquad (5.4.1)$$

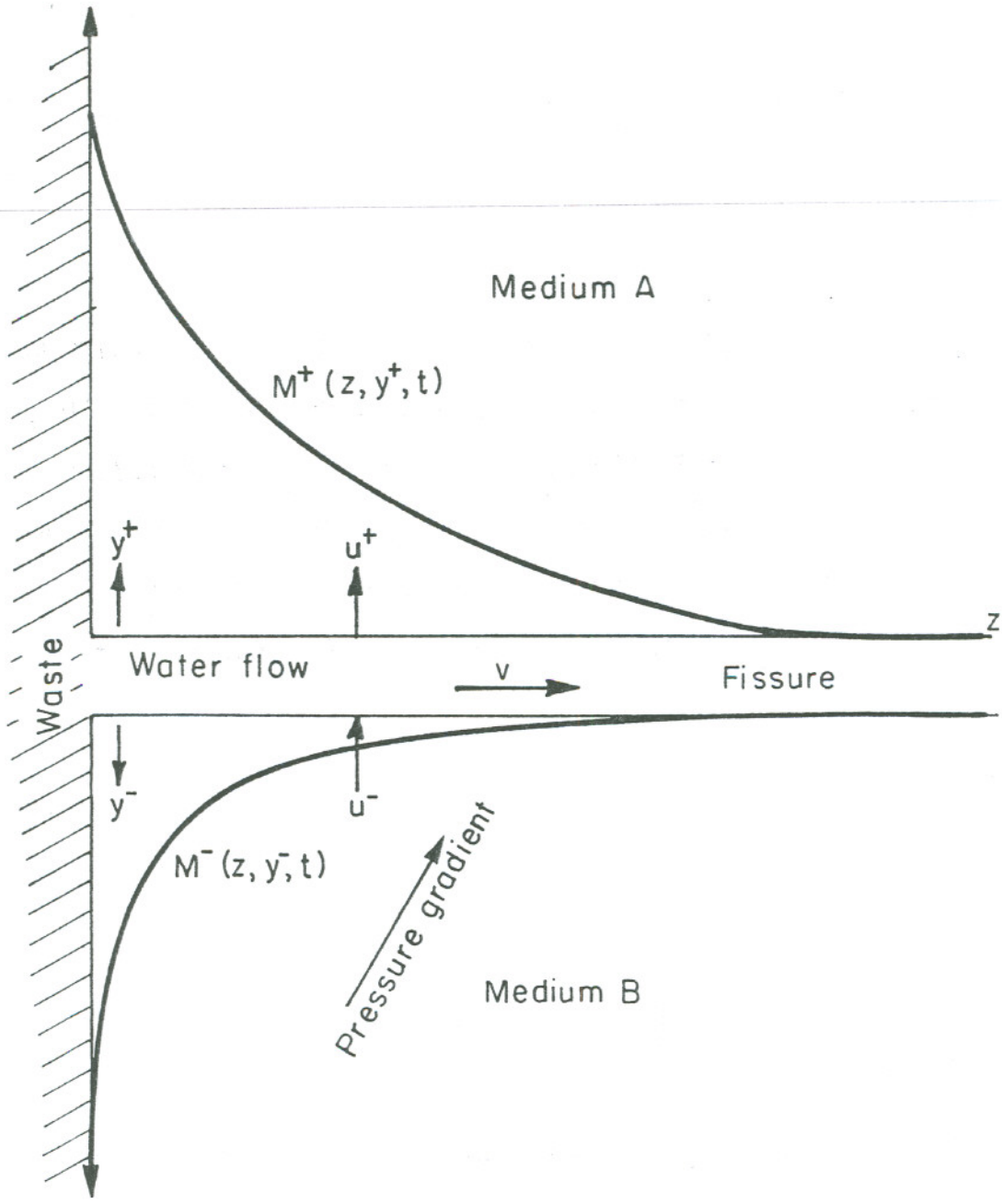

XBL 827-6207

Fig. 5.4.1 Transport of nuclides in a plane fissure surrounded by rock permeable water flow.

$$\frac{\partial M_1^+}{\partial t} + \frac{u^+}{K_1}\frac{\partial M_1^+}{\partial y^+} - \frac{D_1}{K_1}\frac{\partial^2 M_1^+}{\partial y^{+2}} + \lambda_1 M_1^+ = 0 \qquad (5.4.2)$$

$$\frac{\partial M_1^-}{\partial t} - \frac{u}{K_1}\frac{\partial M_1^-}{\partial y^-} - \frac{D_1}{K_1}\frac{\partial^2 M_1^-}{\partial y^{-2}} + \lambda_1 M_1^- = 0 \qquad (5.4.3)$$

$$t > 0, \quad z > 0, \quad y^+ > 0, \quad y^- > 0$$

where v is the water velocity in the fissure, u^+ and u^- are the velocities of the permeating water in the micropores in media A and B, respectively, D_1 is the pore molecular diffusivity of the nuclide, K_1 is the sorption retardation constant, λ_1 is the radioactive decay constant, and b is the width of the fissure. The functions J_1^+ and J_1^- are the sums of the convective and diffusive fluxes of the nuclide at the surface of the fissure given by

$$J_1^+ = -\varepsilon^+ D_1 \left.\frac{\partial M_1^+}{\partial y^+}\right|_{y^+ = 0} + \varepsilon^+ u^+ N_1 \qquad (5.4.4)$$

$$J_1^- = -\varepsilon^- D_1 \left.\frac{\partial M_1^-}{\partial y^-}\right|_{y^- = 0} - \varepsilon^- u^- N_1 \qquad (5.4.5)$$

where ε^+ and ε^- are porosities of media A and B, respectively. If we assume that the water velocity v in the fissure is independent of space and time, and there is no accumulation of the water in the fissure, we can write from the equation of continuity

$$\varepsilon^+ u^+ = \varepsilon^- u^- \qquad (5.4.6)$$

Especially, when $\varepsilon^+ = \varepsilon^-$,

$$u^+ = u^- = u \tag{5.4.7}$$

The initial conditions are

$$N_1(z, 0) = 0, \qquad z > 0 \tag{5.4.8}$$

$$M_{1-}^{+}(z,y,0) = 0, \qquad z > 0,\ y_{-}^{+} > 0 \tag{5.4.9}$$

The boundary conditions are

$$N_1(0, t) = \phi_1 (t), \qquad t > 0 \tag{5.4.10}$$

$$M_{1-}^{+}(z,y,0) = N_1(z, t), \qquad z > 0,\ t > 0 \tag{5.4.11}$$

$$M_{1-}^{+}(z,\infty,t) = 0, \qquad z > 0,\ t > 0 \tag{5.4.12}$$

Equations (5.4.1) (5.4.3) with the appropriate initial and boundary conditions of Eqs. (5.4.7) (5.4.11) can be solved by the method of Laplace transforms. Taking the Laplace transform of Eqs. (5.4.2) and (5.4.3) with respect to time t and introducing new transformed functions $\tilde{m}_{1-}^{+}(z,y_{-}^{+},s)$ defined as

$$\tilde{M}_{1-}^{+}(z,y,s) = \tilde{m}_{1-}^{+}(z,y,s)\, e^{\gamma_{-}^{+} z} \tag{5.4.13}$$

where

$$\tilde{M}_{1-}^{+}(z,y_{-}^{+},s) = \int_0^\infty e^{-st}\, M_{1-}^{+}(z,y_{-}^{+},t)dt \tag{5.4.14}$$

$$\gamma_{-}^{+} = \pm \frac{u}{2D_1} \tag{5.4.15}$$

we have the differential equations which govern the functions $\tilde{m}_{1-}^{+}(z,y,s)$

$$\frac{d^2\tilde{m}_1^+}{dy^2} - \frac{K_1}{D_1}\left(s + \lambda_1 + \frac{u^2}{4K_1D_1}\right)\tilde{m}_1^+ = 0 \qquad (5.4.16)$$

$$\tilde{m}_1^+(z,0,s) = \tilde{N}_1(z,s) \qquad (5.4.17)$$

$$\tilde{m}_1^+(z,\infty,s) = 0 \qquad (5.4.18)$$

The transformed solutions of Eq. (5.4.16) subject to the boundary conditions are

$$\tilde{m}_1^+(z,y,s) = \tilde{N}_1(z,s)\, e^{-y\sqrt{\frac{K_1}{D_1}\left(s+\lambda_1+\frac{u^2}{4D_1K_1}\right)}} \qquad (5.4.19)$$

From Eqs. (5.4.13) and (5.4.19), we can obtain the convective and diffusive transport rate of the nuclide at surface of the main fissure in the transformed form:

$$\tilde{J}_1^+(z,s) = \left[\pm\frac{\varepsilon u}{2} + \varepsilon D_1\sqrt{\frac{K_1}{D_1}\left(s+\lambda_1+\frac{u^2}{4D_1K_1}\right)}\right]\tilde{N}_1(z,s) \qquad (5.4.20)$$

Taking the Laplace transform of Eq. (5.4.1) with respect to t, and solving the resultant equation after substitution of Eq. (5.4.20) subject to the boundary condition, we have

$$\tilde{N}_1(z,s) = \tilde{B}_1(s)\, e^{-\frac{s+\lambda_1}{v}z - a_1 z\sqrt{s+\lambda_1+\frac{u^2}{4D_1K_1}}} \qquad (5.4.21)$$

where a_1 is the same constant as before, defined by

$$a_1 = \frac{2\varepsilon D_1}{bv}\sqrt{\frac{K_1}{D_1}} \qquad (5.4.22)$$

Using the Laplace inversion formula:

$$L^{-1}\left\{ e^{-a_1 z\sqrt{s+\lambda_1+u^2/4D_1K_1}} \right\}$$
$$= \frac{a_1 z}{2\sqrt{\pi t^3}}\, e^{-\frac{a_1^2 z^2}{4t} - \left(\lambda_1 + \frac{u^2}{4D_1K_1}\right)t}$$

$$\equiv \underline{P}_1\,(t;a_1 z) \tag{5.4.23}$$

we have the space-time-dependent aqueous concentration of the nuclide in the main fissure

$$N_1(z,t) = e^{-\frac{\lambda_1}{v}z} \int_0^{t-\frac{z}{v}} \phi_1\left(t-\tau-\tfrac{z}{v}\right)\underline{P}_1(\tau;a_1 z)\, d\tau \tag{5.4.24}$$

From Eq. (5.4.13) with Eqs. (5.4.19) and (5.4.21), the concentration of the nuclide in the micropores in media A and B becomes

$$M_1^{\pm}(z,y^{\pm},t) = e^{\pm\frac{u}{2D_1}y^{\pm} - \frac{\lambda_1}{v}z} \int_0^{t-\frac{z}{v}} \phi_1\left(t-\tau-\tfrac{z}{v}\right)\underline{P}_1(\tau;a_1 z+ b_1 y^{\pm})\, d\tau \tag{5.4.25}$$

where the constant b_1 is

$$b_1 = \sqrt{\frac{K_1}{D_1}} \tag{5.4.26}$$

5.4.2 Solutions For an Impulse Release

When the aqueous concentration of the nuclide at repository is given by an impulse release function,

$$\phi_1\,(t) = (T\,N_1^o)\,\delta\,(t) \tag{5.4.27}$$

the solutions become

$$N_1(z,t) = (t\ N_1^o)\ e^{-\frac{\lambda_1}{v} z}\ \underline{P}_1(t - \frac{z}{v};\ a_1 z)\ h(t - \frac{z}{v}) \qquad (5.4.28)$$

$$M_1^{\pm}(z,y^{\pm},t) = (T\ N_1^o)\ e^{\pm \frac{u}{2D_1} y^{\pm} - \frac{\lambda_1}{v} z}\ \underline{P}_1(t - \frac{z}{v};\ a_1 z + b_1 y^{\pm})\ h(t - \frac{z}{v}) \qquad (5.4.29)$$

where N_1^o is the initial concentration of the nuclide at the repository, the function $\underline{P}_1(t,\alpha)$ is given by Eq. (5.4.22), and the constants a_1 and B_1 are given by Eqs. (5.4.21) and (5.4.25).

5.4.3 Solutions for a step release

When the boundary value of the concentration of the nuclide is given by a step release, the function $\phi_1(t)$ is given by

$$\phi_1(t) = B_1(t)\ h(t) \qquad (5.4.30)$$

where the function $B_1(t)$ is given by Eq. (5.1.13)
Substituting Eq. (5.4.30) into Eqs. (5.4.23) and (5.4.24), we have the solutions for a step release,

$$N_1(z,t) = b_{11}\, e^{-\lambda_1 t} h(t-z/v)\, \frac{2}{\sqrt{\pi}} \int_{\frac{a_1 z}{2\sqrt{t-z/v}}}^{\infty} \exp\left[-\left(\eta^2 + \frac{a_1^2 u^2 z^2}{16 D_1 K_1 \eta^2}\right)\right] d\eta$$

$$= \frac{1}{2} b_{11} h(t-\tau/v)\, e^{-\lambda_1 t} \cdot \left\{ e^{\frac{a_1 u z}{2\sqrt{K_1 D_1}}} \operatorname{erfc}\left[\frac{a_1 z\sqrt{K_1 D_1} + u(t - z/v)}{2\sqrt{K_1 D_1\,(t - z/v)}}\right] \right.$$

$$\left. + e^{-\frac{a_1 u z}{2\sqrt{K_1 D_1}}} \operatorname{erfc}\left[\frac{a_1 z\sqrt{K_1 D_1} - u(t - z/v)}{2\sqrt{K_1 D_1\,(t - z/v)}}\right] \right\} \qquad (5.4.31)$$

$$M_1^{\pm}(z,y^{\pm},t) = b_{11}\, e^{-\lambda_1 t \pm \frac{u}{2D_1} y^{\pm}} h(t-z/v)\, \frac{2}{\sqrt{\pi}} \int_{\frac{a_1 z + y^{\pm}\sqrt{K_1 D_1}}{2\sqrt{t - z/v}}}^{\infty} \exp\left[-\eta^2 - \frac{(a_1 z + y^{\pm}\sqrt{K_1/D_1})^2 u^2}{16 K_1 D_1 \eta^2}\right] d\eta$$

$$= \frac{1}{2} b_{11}\, e^{-\lambda_1 t \pm \frac{u}{2D_1} y^{\pm}} h(t-z/v) \cdot \left\{ e^{\frac{(a_1 z + y^{\pm}\sqrt{K_1/D_1})u}{2\sqrt{K_1 D_1}}} \right.$$

$$\cdot \operatorname{erfc}\left[\frac{a_1 z\sqrt{K_1 D_1} + K_1 y^{\pm} + u\,(t - \frac{z}{v})}{2\sqrt{K_1 D_1\,(t - z/v)}}\right]$$

$$\left. + e^{-\frac{(a_1 z + y^{\pm}\sqrt{K_1/D_1})u}{2\sqrt{K_1 D_1}}} \operatorname{erfc}\left[\frac{a_1 z\sqrt{K_1 D_1} + K_1 y^{\pm} - u(t - z/v)}{2\sqrt{K_1 D_1 (t - z/v)}}\right] \right\} \qquad (5.4.32)$$

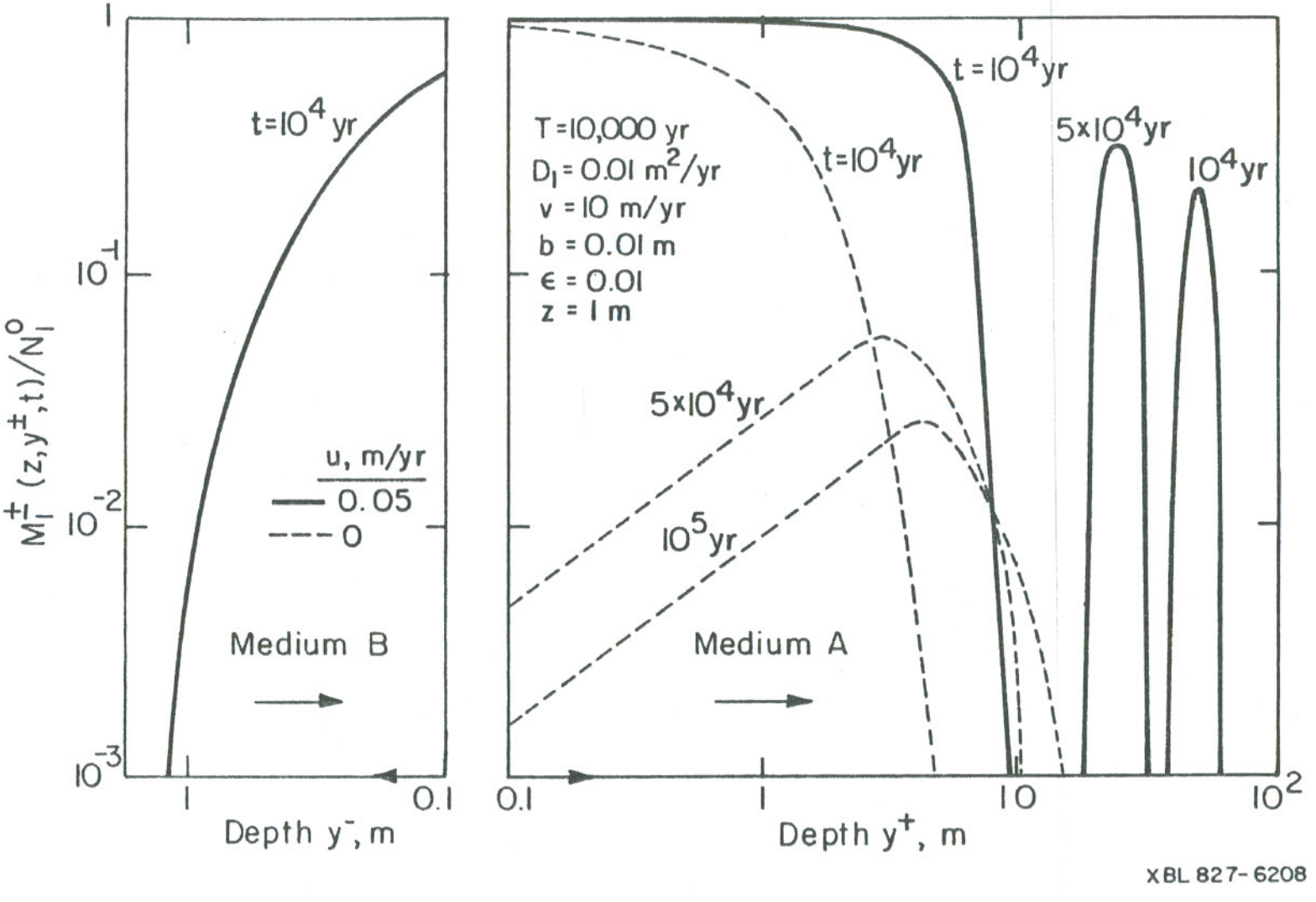

Fig. 5.4.2 Concentration profiles of ^{237}Np in micropores with permeable water.

5.4.4 Solutions for a Band Release

For a band release, the time-dependent concentration at the repository is given by

$$\phi_1 (t) = B_1 (t) \left[h(t) - h(t - T)\right] \tag{5.4.33}$$

where T is the duration time of release.

The solutions for a band release are obtained by applying the theorem of superposition (H-1). They are

$$N_1 (z,t) = N_1 (z,t; b_{11}) - N_1 (z,t-T; b_{11} e^{-\lambda_1 T}) \tag{5.4.34}$$

$$M_1^{\pm}(z,y^{\pm},t) = M_1^{\pm}(z,y^{\pm},t;b_{11}) - M_1^{\pm} (z,y^{\pm},t-T; b_{11} e^{-\lambda_1 T}) \tag{5.4.35}$$

where the functions $N_1(z,t; b_{ij})$ and $M_1^{\pm} (z,y; b_{ij})$ stand for the space and time dependent concentrations of the nuclide for the step release with Bateman coefficient b_{ij}, respectively.

5.4.5 Effect of Micropore Flow on Fissure-Flow Transport

Figure 5.4.2 shows the concentration profiles of ^{237}Np in the micropore fissures in the rock media A and B at fixed distance z = 1 m, at time = 10,000 yr and at t = 100,000 yr, with a permeating water velocity u = 0.05 m/yr in the positive y+ direction. The release mode is assumed to be a band release with a leach time T = 10,000 yr. Note that the concentrations at t = 10,000 yr are equivalent to those for the step release. The concentrations of the nuclide in transport without permeable water, i.e., with u = 0, at corresponding times are shown as

dashed lines. The concentrations with u = 0 in medium B are not given in this figure; their profiles are completely symmetrical to the profiles in medium A.

The permeating water in medium B acts on the nuclide to migrate in the negative y- direction against molecular diffusion, whereas the water in the medium A convects the nuclide in the positive y+ direction in the same direction as that of molecular diffusion. Many of the nuclides that have diffused into medium B are convected to the medium across the flowing water in the main fissure, resulting in a nonsymmetric concentration profile with a greater diffusive path length in medium A but with a smaller path length in medium B. The penetration thickness of the nuclide at t = 10,000 yr reaches almost y+ = 10 m in medium A, but the thickness in medium B is only 1 m deep.

The effect of penetrating water on the concentration along the $y^{\pm}$ direction becomes more significant as the migration time increases. At t = 100,000 yr, the concentration band of the nuclide in medium A travels a greater distance in that medium. The concentration of the nuclide in the medium B, on the other hand, is extremely small and the concentration band does not appear in this figure. Also, because of convective transport from medium A to B, nuclide transport with permeating water shows a greater maximum concentration within the micropore, and the maximum occurs at a greater distance from the fissure surface.

Fig. 5.4.3 shows the aqueous concentration profiles of ^{237}NP in the fissure with permeating water velocities of u = 0.005 and 0.01 m/yr, as well as for u = 0. This figure shows that convective transport in the medium across the flowing water decreases the concentration of the nuclide

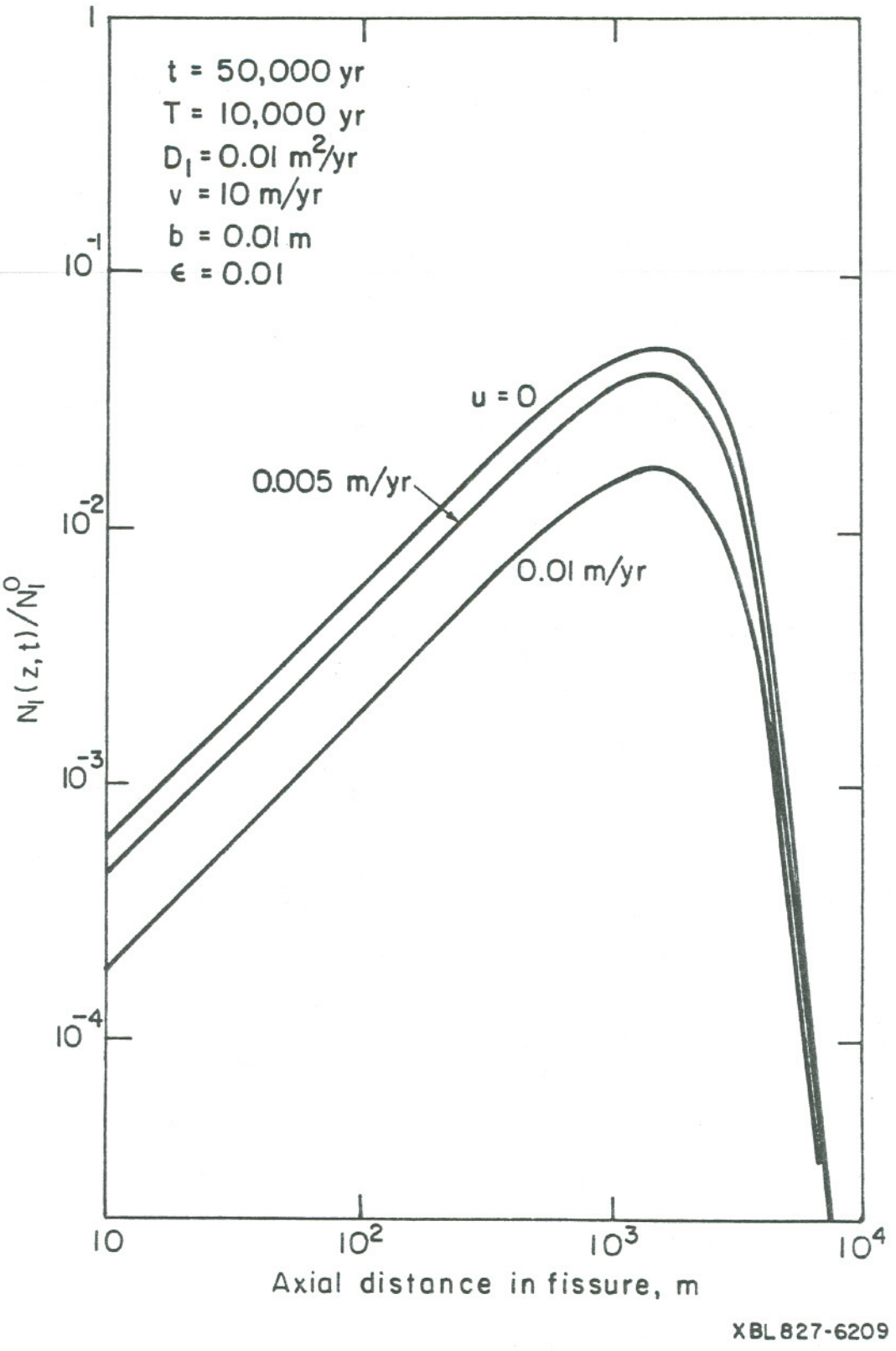

Fig. 5.4.3 Effect of permeable water on aqueous concentration profile of ^{237}Np in fissure.

over the entire migration distance. This means that the convective increase in the amount of nuclides entering the upper micropores is more important than the convective decrease in the amount of nuclides diffusing into the lower micropores. The permeating water in micropores has no effect on the retardation capacity, i.e., the maximum concentration, as well as the concentration band, occur at almost the same position, at all values of the micropore velocity shown in Figure 5.4.3.

5.5 Solubility Limited Migration of a Radionuclide in Fractured Media

In the foregoing analysis for transport of nuclides in fractured media, the effect of a solubility limit of the nuclide has not been taken into consideration. However, many of actinide elements, such as plutonium, uranium, and neptunium, may exist in chemical forms of very low solubility. Such a species of the nuclide released directly from the dissolving waste matrix can precipitate at the waste surface, and the aqueous concentration of that nuclide will remain constant at the waste location while the precipitate is present, thereby changing the boundary condition for transport of that nuclide. Neglecting the limited solubility will lead to an overestimate of the maximum concentration of the nuclide.

It is important to develop the analysis presented in this chapter to include the effect of limited solubility of the nuclide. For porous flow the solution for transport of a parent nuclide with a limited solubility has been presented in our previous report (P1). This section presents the solutions for transport of a parent nuclide in a fractured medium with a solubility-limit boundary condition. It demonstrates the

importance of limited solubility on the transport behavior. For this purpose, we first consider the material balance of the nuclide at the waste location in order to know the time-dependent aqueous concentration at the source boundary. We then derive the solutions for the concentrations of the nuclide in the fissure and in the micropores.

5.5.1 Transport Equations

The transport equations which govern the aqueous concentrations of the nuclide in the fissure and micropores are, assuming local sorption equilibrium,

$$\frac{\partial N_1}{\partial t} + v \frac{\partial N_1}{\partial z} + \lambda_1 N_1 = -\frac{2}{b} J_1 \qquad (5.5.1)$$

$$\frac{\partial M_1}{\partial t} - \frac{D_1}{K_1} \frac{\partial^2 M_1}{\partial y^2} + \lambda_1 M_1 = 0 \qquad (5.5.2)$$

$$t > 0, \quad 0 < z < \infty, \quad y > 0$$

where $N_1(z,t)$ and $M_1(z,y,t)$ are the concentrations of the nuclide in the fissure and micropores respectively, v is the water velocity, D_1 is the pore molecular diffusivity, K_1 is the sorption retardation constant, λ_1 is the decay constant of the nuclide, b is the interstice of the main fissure, and J_1 is the diffusive flux of the nuclide at surface of the main fissure

$$J_1 = - \varepsilon D_1 \left. \frac{\partial M_1}{\partial y} \right|_{y = 0} \qquad t > 0, \quad z > 0 \qquad (5.5.3)$$

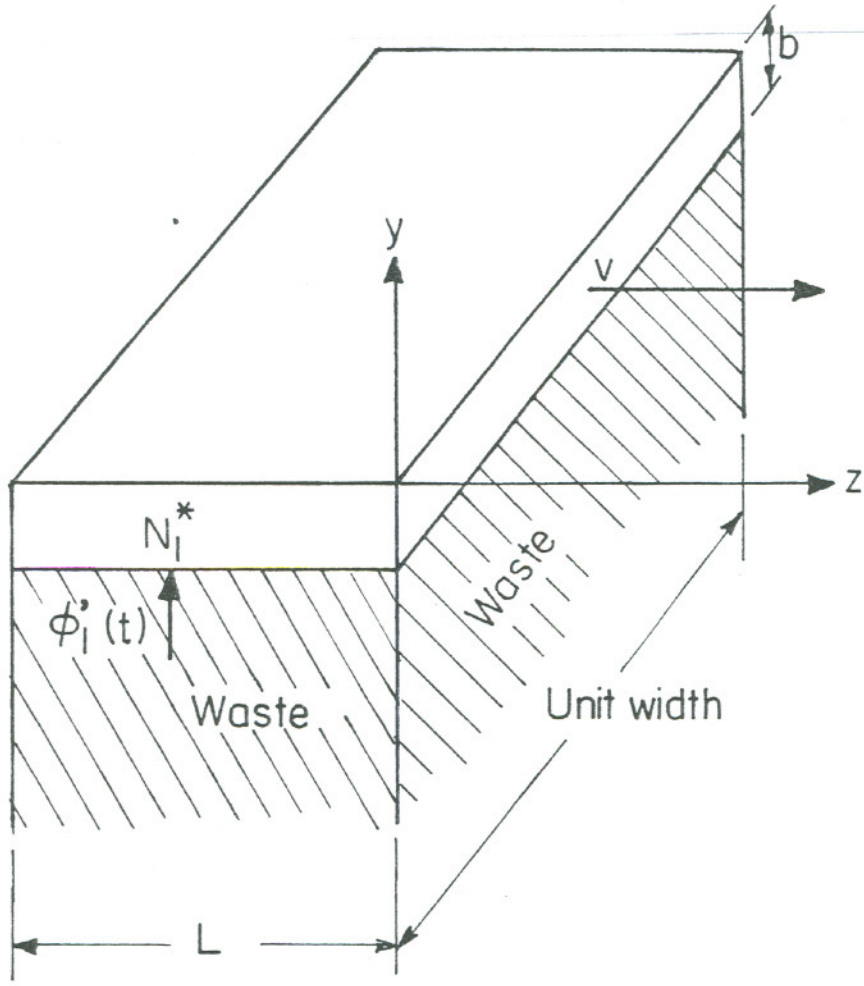

Fig. 5.5.1 Geometry of waste adjacent to a fissure.

The initial and boundary conditions are

$$N_1(z, 0) = 0, \qquad z > 0 \tag{5.5.4}$$

$$M_1(z,y,0) = 0, \qquad z > 0, \qquad y > 0 \tag{5.5.5}$$

$$N_1(0, t) = \phi_1 (t), \qquad t > 0 \tag{5.5.6}$$

$$M_1(z,0,t) = N_1(z,t), \qquad z > 0, \qquad t > 0 \tag{5.5.7}$$

$$M_1(z,\infty,t) = 0$$

The function $\phi_1 (t)$ is determined from a material balance of the nuclide at the waste surface, as shown in the next section.

5.5.2 Material Balance at the Waste Surface

Consider a waste form of length L in the axial direction z and of infinite width in the x direction of the fissure plane, as shown in Fig. 5.5.1. Suppose that the waste matrix is dissolving continuously from that surface into the water flowing in the fissure of width b. For a mother nuclide with no precursors, if its precipitate forms it will appear at the beginning of waste-form dissolution. While the precipitate is present the liquid at the waste location will be at a constant concentration N_1^* of the nuclide, where N* denotes the solubility. Assuming complete mixing of the nuclide in the water immediately above the waste surface, we can write the total material balance for the precipitate of that nuclide in the form:

$$\frac{\partial P_1}{\partial t} + \lambda_1 P_1 = \frac{1}{b\nu\tau} \phi_1' \ (t) - \frac{1}{\tau} N_1^* - \lambda_1 N_1^* \tag{5.5.8}$$

where P_1 is the amount of precipitate per unit volume of water at z = 0, $\phi_1'(t)$ is the release rate of the nuclide into the water from the waste per unit width of waste, and τ is the residence time determined by

$$\tau = \frac{L}{v} \tag{5.5.9}$$

The initial condition for P_1 is

$$P_1(0) = 0 \tag{5.5.10}$$

The solution of Eq. (5.5.8) subject to Eq. (5.5.10) is

$$P_1(t) = e^{-\lambda_1 t} \int_0^t e^{\lambda_1 \theta} \left[\frac{1}{bv\tau} \phi_1{}^1(\theta) - (\lambda_1 + \frac{1}{\tau}) N_1{}^* \right] d\theta \tag{5.5.11}$$

The release rate $\phi_1'(t)$ of the nuclide from the waste, per unit width of waste is

$$\phi_1'(t) = \frac{n_1(t) W_T^o b}{T} \tag{5.5.12}$$

where W_T^o is the total initial amount of waste per unit cross-sectional area of water flow in a fissure, b is the spacing of the fissure walls, T is the leach time, and $n_1(t)$ is the time-dependent atom fraction of the nuclide in the waste. For the mother nuclide

$$n_1(t) = n_1{}^o e^{-\lambda_1 t} \tag{5.5.13}$$

where $n_1{}^o$ is the initial atom fraction of nuclide i in the waste form by an initial total amount of nuclides in the waste form and $n_1(t)$ is the time-dependent atom fraction in the waste.

Substituting Eq. (5.5.12) into Eq. (5.5.11), we have

$$P_1(t) = \frac{N_1^o}{\tau} t\, e^{-\lambda_1 t} - N_1^*\left(1 + \frac{1}{\lambda_1 \tau}\right)\left(1 - e^{-\lambda_1 t}\right) \qquad (5.5.14)$$

where N_1^o is the initial aqueous concentration of the nuclide that would occur if there were no precipitate,

$$N_1^o = \frac{n_1^o W_T^o}{v\bar{T}} = \frac{\dot{m}_1^o}{v} \qquad (5.5.15)$$

where $\dot{m}_1^o = n_1^o M^o / bT$ is the initial release rate of nuclide i per unit cross-sectional area of water flow. We now introduce the amount $P_1^s(t)$ of precipitate per unit surface area of waste at z = 0

$$P_1^s(t) = \int_0^L P_1(t)\, dz = L\, P_1(t) \qquad (5.5.16)$$

Multiplying Eq. (5.5.14) by L and taking the limit of $L \to 0$, we have

$$P_1^s(t) = v\, N_1^o\, t\, e^{-\lambda_1 t} - N_1^* \frac{v}{\lambda_1}\left(1 - e^{-\lambda_1 t}\right) \qquad (5.5.17)$$

This is equivalent to the solution presented for porous-flow transport in our previous report (P1).

We can now evaluate the aqueous concentration of the nuclide at the waste. Since time is measured from the time at the beginning of precipitation, the aqueous concentration remains at the saturated concentration until the accumulated precipitate all dissolves. Then,

$$\phi_1(t) = N_1^*, \qquad t \leq t^* \qquad (5.5.18)$$

where t* is determined from Eq. (5.5.14) or from Eq. (5.5.17) by setting

$P_1(t)$ equal to zero. Note that Eq. (5.5.17) gives t* at the limit of $\tau \to 0$.

At $t > t^*$, the following material balance holds for the aqueous concentration of the nuclide at the waste surface

$$\frac{\partial \phi_1}{\partial t} + \lambda_1 \phi_1 + \frac{1}{\tau} \phi_1 = \frac{1}{b\nu\tau} \phi_1', \quad t > t^* \tag{5.5.19}$$

The initial condition is

$$\phi_1(t^*) = N_1^* \tag{5.5.20}$$

The solution of Eq. (5.5.19) subject to Eq. (5.5.20) gives the time-dependent aqueous concentration of the nuclide at the waste surface.

$$\phi_1(t') = N_1^o e^{-\lambda_1 t^*} \left[e^{-\lambda_1 t'} - e^{-(\lambda_1 + \frac{1}{\tau})t'} \right] + N_1^* e^{-(\lambda_1 + \frac{1}{\tau})t'},$$

$$t' > 0 \tag{5.5.21}$$

where

$$t' = t - t^* \tag{5.5.22}$$

When $\tau \to 0$, this equation reduces to

$$\phi_1(t) = N_1^o e^{-\lambda_1 t^*} e^{-\lambda_1 t'}, \quad t > t^* \tag{5.5.23}$$

This equation is equivalent to that derived in our previous report (P1) for the plane boundary condition for porous-flow transport. In this case when the residence time approaches zero, the aqueous concentration of the

nuclide at the waste surface has a discontinuous jump at $t = t^*$. The residence time usually is much smaller than the half life of the nuclide, e.g., for L = 10 m and v = 10 m/yr, $\tau = L/v = 1$ yr. This means that Eq. (5.5.23) gives a sufficiently good approximation to the time-dependent boundary concentration of a nuclide of long half life. For a nuclide of very short half life, this approximation becomes less valid. When $\tau \to \infty$, Eq. (5.5.19) reduces to a simple decay equation for the mother nuclide in a stationary system. Also, from Eq. (5.5.8) and the initial condition given by Eq. (5.5.10), we find that there no longer exists a precipitate at the repository at $t > 0$. If we consider the case wherein a finite concentration P_1^o of the precipitate designated exists initially, the solutions give a nonzero value for the concentration of the precipitate

$$P_1(t) = \begin{cases} P_1^o e^{-\lambda_1 t} - N_1^* (1 - e^{-\lambda_1 t}), & t < t^* \\ 0 & t \geq t^* \end{cases} \qquad (5.5.24)$$

The aqueous concentration of the nuclide is

$$\phi_1(t) = \begin{cases} N_1^* & t < t^* \\ N_1^* e^{-\lambda_1 (t-t^*)}, & t \geq t^* \end{cases} \qquad (5.5.25)$$

where by solving for $P_1(t') = 0$ in Eq. (5.5.24) we get:

$$t^* = \frac{1}{\lambda_1} \ln \left(1 + \frac{P_1^o}{N_1^*}\right) \tag{5.5.26}$$

The boundary condition for the transport equations is, from Eqs. (5.5.18) and (5.5.21)

$$\phi_1(t) = \begin{cases} N_1^*, & t \leq t^* \\ c_{11} e^{-\lambda_1 (t-t^*)} + c_{12} e^{-(\lambda_1 + \frac{1}{\tau})(t-t^*)}, & t > t^* \end{cases} \tag{5.5.27}$$

where

$$c_{11} = N_1^o e^{-\lambda_1 t^*}, \quad c_{12} = N_1^* - N_1^o e^{-\lambda_1 t^*} \tag{5.5.28}$$

5.5.3 Solubility-limited Transport With a Step Release

The space-time-dependent concentrations of the nuclide can be obtained by solving the basic transport equations subject to the initial conditions given by Eqs. (5.5.4) and (5.5.5) and the boundary conditions given by Eqs. (5.5.6) and (5.5.7) with the function given by Eq. (5.5.27). The solutions are

$$N_1(z,t) = N_1^* e^{\frac{-z\lambda_1}{v}} h(t-z/v)\, E_1(z,t,a_1 z) -$$

$$- N_1^* e^{\frac{-z\lambda_1}{v}} h(t-t^*-z/v)\, E_1(z,t-t^*,a_1 z) +$$

$$+ h(t-t^* - \tfrac{t}{v}) \left\{ C_{11} e^{-\lambda_1 (t-t^*)} \operatorname{erfc}\left(\frac{a_1 z}{2\sqrt{t-t^*-z/v}}\right) + \right.$$

$$\left. + C_{12} \exp\left[\frac{z}{v\tau} - (\lambda_1 + \tfrac{1}{\tau})(t-t^*)\right] \cdot E_1^+(z,t-t^*,a_1 z) \right\} \tag{5.5.29}$$

$$M_1(z,y,t) = N_1^* e^{\frac{-z\lambda_1}{v}} \left[h(t - \frac{z}{v})\, E_1\,(z,t,a_1 z + b_1 y) - \right.$$

$$\left. - h\,(t-t^* - z/v)\, E_1\,(z,t-t^*,\, a_1 z + b_1 y) \right] +$$

$$+ h\,(t-t^* - z/v) \left\{ C_{11}\, e^{-\lambda_1 (t-t^*)}\, \operatorname{erfc}\, (\frac{a_1 z + b_1 y}{2\sqrt{t-t^*-z/v}}) \right. +$$

$$\left. + C_{12} \exp\left[\frac{z}{v\tau} - (\lambda + \frac{1}{\tau})(t-t^*) \right] .\ E_1^{+}\,(z,t-t^*, a_1 z + b_1 y) \right\} \qquad (5.5.30)$$

where

$$a_1 = \frac{2\varepsilon D_1}{bv} \sqrt{\frac{K_1}{D_1}} \qquad (5.5.31)$$

$$b_1 = \sqrt{\frac{K_1}{D_1}} \qquad (5.5.32)$$

The functions $P_1(t;\alpha)$, $E_1(z,t;\alpha)$, and $E_1^{+}(z,t;\alpha)$ are given by

$$P_1(t;\alpha) = \frac{\alpha}{2\sqrt{\pi t^3}}\, e^{-\frac{\alpha^2}{4t} - \lambda_1 t} \qquad (5.5.33)$$

$$E_1(z,t;\alpha) = \frac{2}{\sqrt{\pi}} \int_{\frac{\alpha}{2\sqrt{t-z/v}}}^{\infty} e^{-\eta^2 - \frac{\lambda_1 \alpha^2}{4\eta^2}}\, d\eta \qquad (5.5.34)$$

$$E_1^{+}(z,t;\alpha) = \frac{2}{\sqrt{\pi}} \int_{\frac{\alpha}{2\sqrt{t-z/v}}}^{\infty} e^{-\eta^2 + \frac{\alpha^2}{4\eta^2}}\, d\eta \qquad (5.5.35)$$

The function $E_1(z,t;\alpha)$ can be reduced in terms of the complementary error function with the aid of the formula:

$$\int e^{-a^2x^2 - \frac{b^2}{x^2}}\, dx = \frac{\sqrt{\pi}}{4a}\left[e^{2ab}\,\mathrm{erf}(ax + \tfrac{b}{x}) + e^{-2ab}\,\mathrm{erf}\,(ax - \tfrac{b}{x})\right] \qquad (5.5.36)$$

$$E_1(z,t;\alpha) = \frac{1}{2}\left\{ e^{\alpha\sqrt{\lambda_1}}\,\mathrm{erfc}\left[\frac{\alpha + 2(t - z/v)\sqrt{\lambda_1}}{2\sqrt{t-z/v}}\right]\right.$$

$$\left. + e^{-\alpha\sqrt{\lambda_1}}\,\mathrm{erfc}\left[\frac{\alpha - 2(t - z/v)\sqrt{\lambda_1}}{2\sqrt{t-z/v}}\right]\right\} \qquad (5.5.37)$$

When $\tau \to 0$, the solutions can be simplified as

$$N_1(z,t) = N_1^*\, e^{-\frac{\lambda_1 z}{v}}\left[h(t - z/v)\, E_1\,(z,t,a_1 z) -\right.$$

$$\left. - h\,(t-t^* - z/v)\, E_1\,(z,t-t^*,a_1 z)\right] \quad +$$

$$C_{11}\, e^{-\lambda_1(t-t^*)}\, h(t-t^*-z/v)\,\mathrm{erfc}\,\left(\frac{a_1 z}{2\sqrt{(t-t^*-z/v}}\right) \qquad (5.5.38)$$

$$M_1(z,y,t) = N_1^*\, e^{-\frac{\lambda_1 z}{v}}\left[h(t-z/v)\, E_1\,(z,t,a_1 z+b_1 y) -\right.$$

$$\left. - h(t-t^* -z/v)\, E_1(z,t-t^*,a_1 z+b_1 y)\right] \quad +$$

$$+ C_{11}\, e^{-\lambda_1(t-t^*)}\, h(t-t^*-z/v)\,\mathrm{erfc}\,\left(\frac{a_1 z+b_1 y}{2\sqrt{t-t^*-z/v}}\right) \qquad (5.5.39)$$

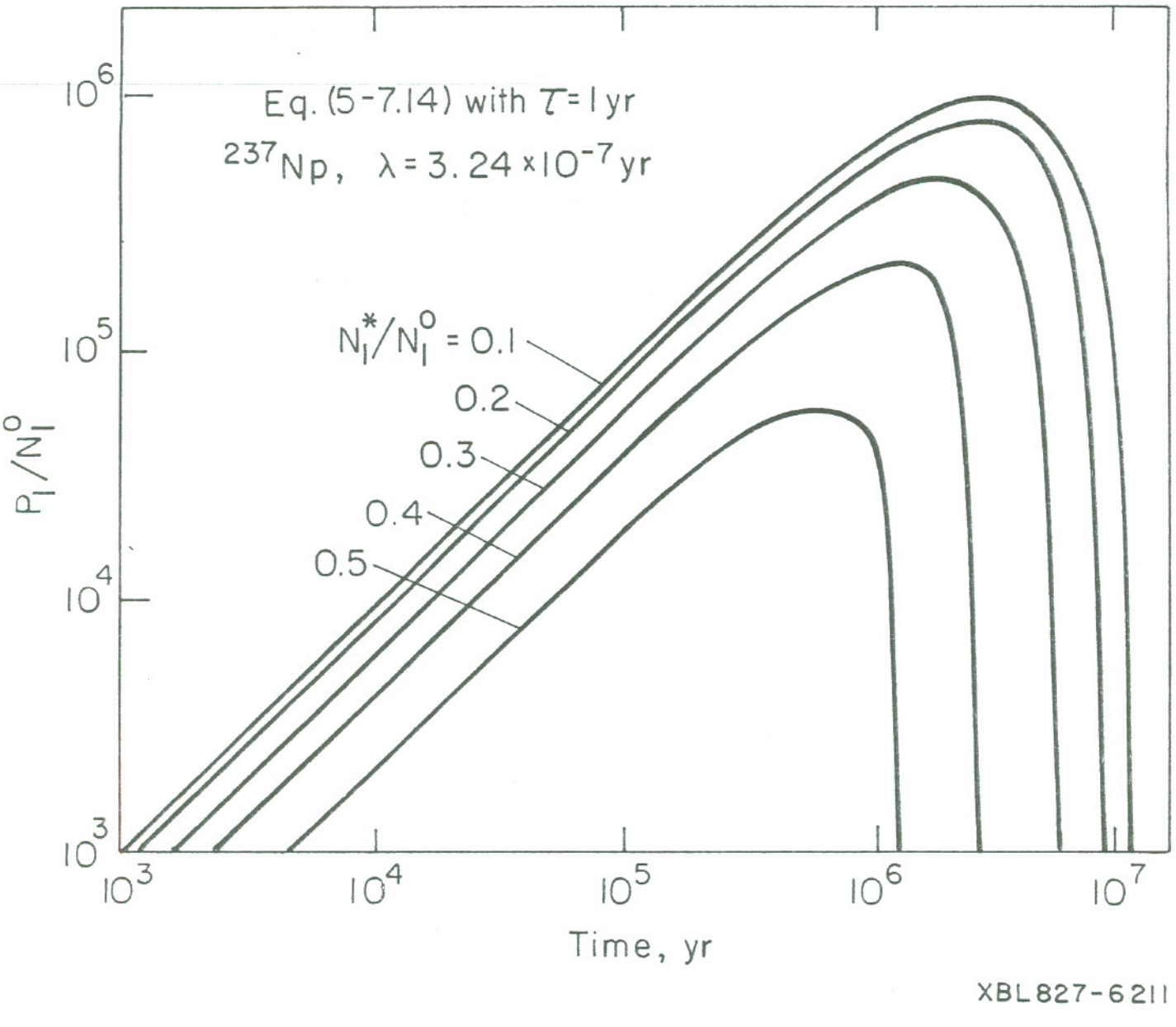

Fig. 5.5.2 Time dependent concentration of precipitate of parent nuclide.

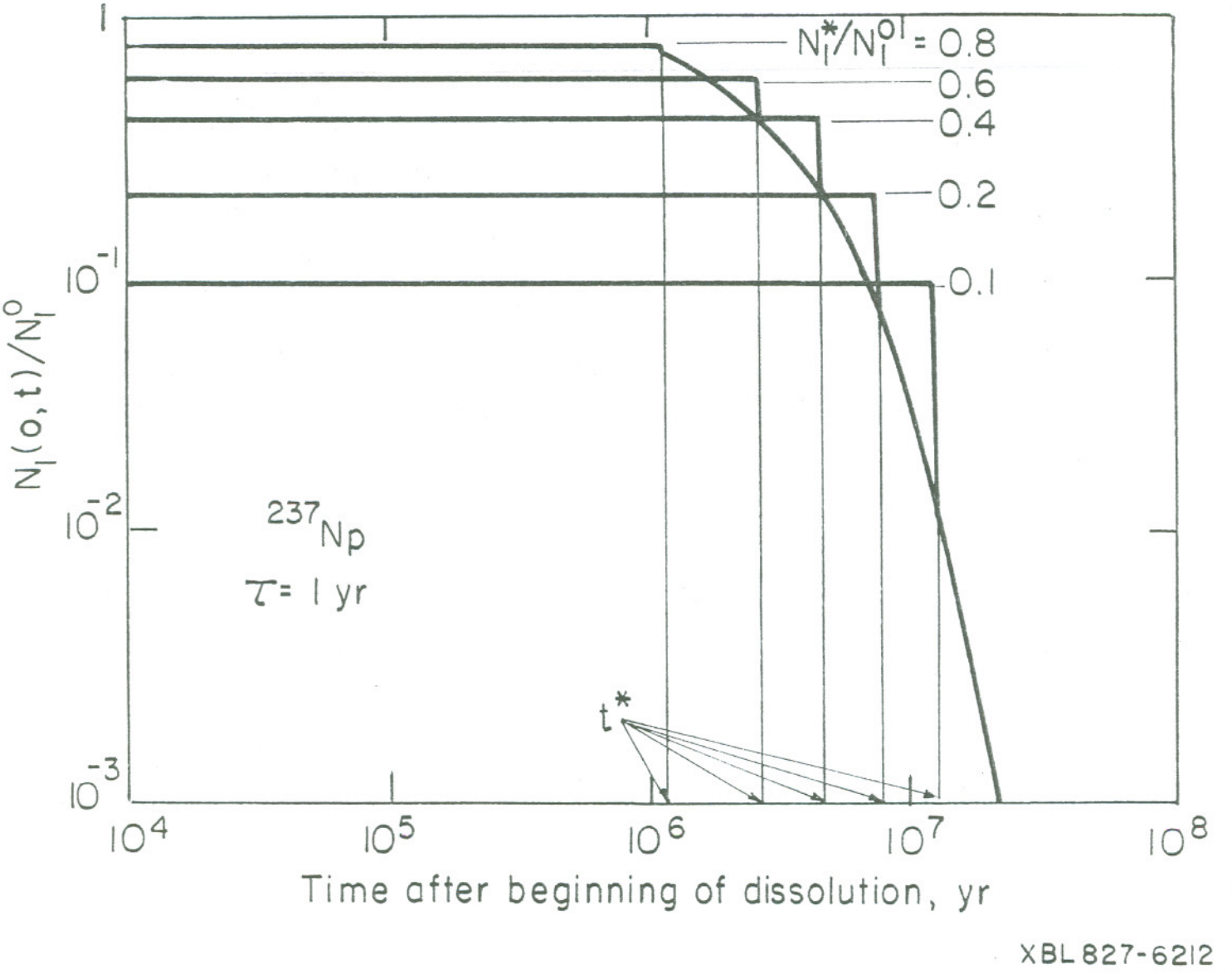

Fig. 5.5.3 Time-dependent aqueous concentration of ^{237}Np at repository with precipitate.

5.5.4 Solubility-limited Transport With a Band Release

Let T be the time of duration of the release. The function $\phi_1(t)$ for the band release can then be written as

$$\phi_1(t) = N_1^* \left[h(t) - h(t-t^*)\right] + N_1^* e^{-(\lambda_1+\frac{1}{\tau})t} h(t-t^*) +$$

$$+ N_1^{\,o} h(T-t^*) e^{-\lambda_1 t^*} (e^{-\lambda_1(t-t^*)} - e^{-(\lambda_1+\frac{1}{\tau})(t-t^*)}) .$$

$$\left[h(t-t^*) - h(t-T)\right] \qquad (5.5.40)$$

The solutions are

$$N_1(z,t) = N_1^* e^{-\frac{\lambda_1 z}{v}} \left[h(t-z/v)\ E_1(z,t,a_1 z) - h\,(t-t^*-z/v) x\ E_1(z,t-t^*,a_1 z)\right]$$

$$+ N_1^* e^{-t(\lambda_1+\frac{1}{\tau}) + \frac{z}{v\tau}} h(t-t^*-z/v) \times E_1^{+}(z,t-t^*,a_1 z)$$

$$+ N_1^{\,o} e^{-\lambda_1 t} h(T-t^*) \cdot \left[h(t-t^*-\tfrac{z}{v}) \times \operatorname{erfc}\left(\frac{a_1 z}{2\sqrt{t-t^*-z/v}}\right)\right.$$

$$\left. - h(t-T-z/v) \cdot \operatorname{erfc}\left(\frac{a_1 z}{2\sqrt{t-T-z/v}}\right)\right] +$$

$$+ N_1^{\,o} h(T-t^*) \cdot \exp\left[-\lambda_1 t - \tfrac{1}{\tau}(t-t^*-z/v)\right] \cdot \left[h(t-T-z/v) x\right.$$

$$\left. x\ E_1^{+}(z,t-T,a,z) - h(t-t^*-z/v)\ E_1^{+}(z,t-t^*,a_1 z)\right]$$

(5.5.41)

$$M_1(z,y,t) = N_1^* e^{-\frac{\lambda_1 z}{v}} \left[h(t-z/v)\ E_1(z,t,a_1 z+b_1 y) - h(t-t^*-z/v)x\right.$$

$$x\ E_1(z,t-t^*,a_1 z+b_1 y)\Big] + N_1^* e^{-\lambda_1 t-\frac{1}{\tau}(t-z/v)} h(t-t^*-z/v)\,x$$

$$x\ E_1(z,t-t^*,a_1 z+b_1 y) + N_1^o e^{-\lambda_1 t} h(T-t^*)\Big[h(t-t^*-z/v)\,x$$

$$x\ \grave{e}rfc\left(\frac{a_1 z+b_1 y}{2\sqrt{t-t^*-z/v}}\right) - h(t-T-z/v).\ erfc\left(\frac{a_1 z+b_1 y}{2\sqrt{t-T-z/v}}\right)\Big] +$$

$$+ N_1^o h(T-t^*)\ exp\left[-\lambda_1 - \frac{1}{\tau}(t-t^*-z/v)\right].\left[h(t-T-z/v)x\right.$$

$$x\ E_1^+(z,t-T,a_1 z+b_1 y) - h(t-t^*-z/v).\ E_1^+(z,t-t^*,a_1 z+b_1 y)\Big] \qquad (5.5.42)$$

when $\tau \to 0$ the solutions become

$$N_1(z,t) = N_1^* e^{-\frac{\lambda_1 z}{v}}\left[h(t-z/v)\ E_1(z,t,a,z) - h(t-t^*-z/v)x\right.$$

$$x\ E_1(z,t-t^*,a_1 z)\Big] + N_1^o e^{-\lambda_1 t} h(T-t^*)\Big[h(t-t^*-z/v)\,x$$

$$x\ erfc\left(\frac{a_1 z}{2\sqrt{t-t^*-z/v}}\right) - h(t-T-z/v).\ erfc\left(\frac{a_1 z}{2\sqrt{t-T-z/v}}\right)\Big] \qquad (5.5.43)$$

$$M_1(z,y,t) = N_1^* e^{-\frac{\lambda_1 z}{v}}\left[h(t-z/v)\quad E_1(z,t,a,z+b,y) - h(t-t^*-z/v)x\right.$$

$$x\ E_1(z,t-t^*,a_1 z+b_1 y)\Big] + N_1^o e^{-\lambda_1 t} h(T-t^*)\Big[h(t-t^*-z/v)x$$

$$x\ erfc\left(\frac{a_1 z+b_1 y}{2\sqrt{t-t^*-z/v}}\right) - h(t-T-z/v).erfc\left(\frac{a_1 z+b_1 y}{2\sqrt{t-T-z/v}}\right)\Big] \qquad (5.5.44)$$

where t* is the solution to the following equation

$$\frac{N_1^o}{\tau} e^{-\lambda_1 t^*} \left[t^* - (t^*-T)h(t^*-T) \right] = N_1^* (1+\frac{1}{\lambda_1 \tau}) (1-e^{-\lambda_1 t^*}) \qquad (5.5.45)$$

5.5.5 Aqueous and Precipitate Concentrations of a Nuclide at Repository

Figure 5.5.2 shows a variation of relative concentration of precipitate at repository with the time measured from the beginning of precipitating. These curves show the concentrations of ^{237}Np which are calculated for various assumed values of saturated concentration from Eq. (5.5.14) with a parameter assumed to be unity. As is expected, the precipitate first increases from zero with the time, reaches a maximum, and then decreases to redissolve into the water with increase of the time. All of these curves intercept zero concentration, the time axis. Each of these interceptions is corresponding to the time t* defined in Eq. (5.5.18). After that the precipitate no longer exists. The figure shows that a lower saturated concentration causes a higher concentration of the precipitate and a greater time of t*.

The variation of aqueous concentration of ^{237}Np with the time for various assumed normalized values of saturated concentration are given in Fig. 5.5.3. The time t* when the precipitate has all dissolved is determined from Eq. (5.5.14) by setting the precipitate $P_1(t)$ equal to zero. The concentration of the nuclide at the waste surface remains constant at N_1^* until the time t* decreases almost discontinuously at t = t*, and then decreases smoothly subject to the exponential function as given by Eq. (5.5.23). The concentration jump at t = t* is attributed to the resident time, τ assumed here to be extremely small compared with

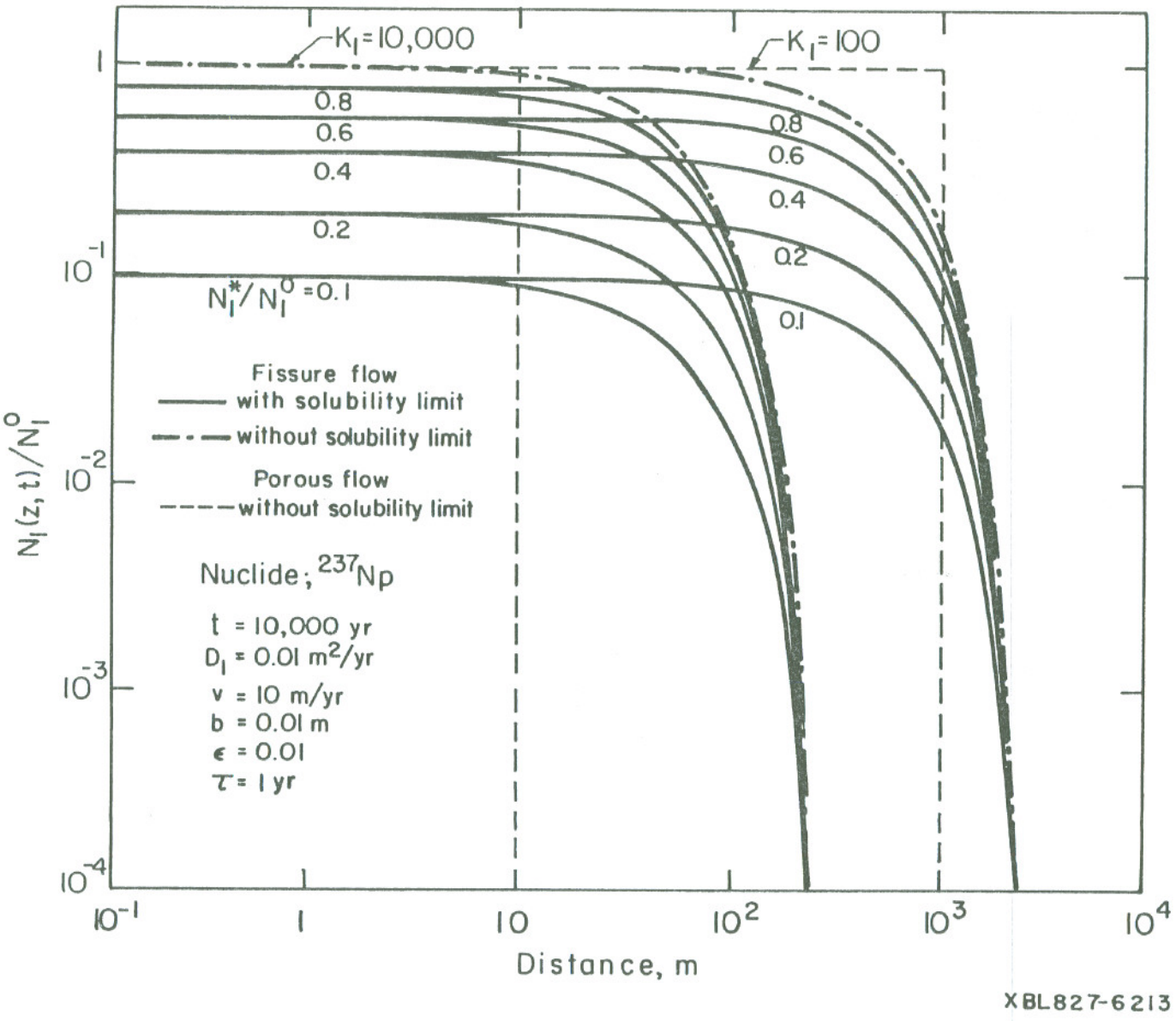

Fig. 5.5.4 Concentration profiles of ^{237}Np in fissure flow transport with limited solubility, step release.

the inverse of the radioactive decay constant of the nuclide. For $\tau << 1/\lambda_1$, Eq. (5.5.23) is a good approximation for the time-dependent concentration of the nuclide with precipitation. For a short-lived nuclide, Eq. (5.5.23) becomes less exact, and the exact solution Eq. (5.5.27), which gives a continuous concentration profile at $t = t^*$, should be used.

5.5.6 Effect of Limited Solubility on Fissure-flow Transport

Relative concentrations of ^{237}NP for step release calculated from Eq. (5.5.29), with different normalized values of the solubility concentration, are shown in Fig. (5.5.4). The solid lines show the concentration profiles for transport with solubility limit and broken lines show those without solubility limit. Two typical cases, with the retardation constant assumed to be $K_1 = 10000$ and with $K_1 = 100$, are considered. The pore diffusivity and the other relevant parameters are listed in the figure. For this case with no precursor, precipitation occurs only at the waste surface, causing a decrease in the aqueous concentration of the nuclide over the whole range of migration space. The concentrations shown by the broken lines for $K_1 = 10000$ and for $K_1 = 100$ are reduced to a lower concentration by a factor almost equal to the ratio N_1^o/N_1^* of the maximum possible initial concentration to the solubility concentration. However, because of the accumulated precipitate, the aqueous concentration at the saturated level can persist at a greater time than expected when neglecting the limited solubility. The space-time concentration surface is shown in Fig. 5.5.5.

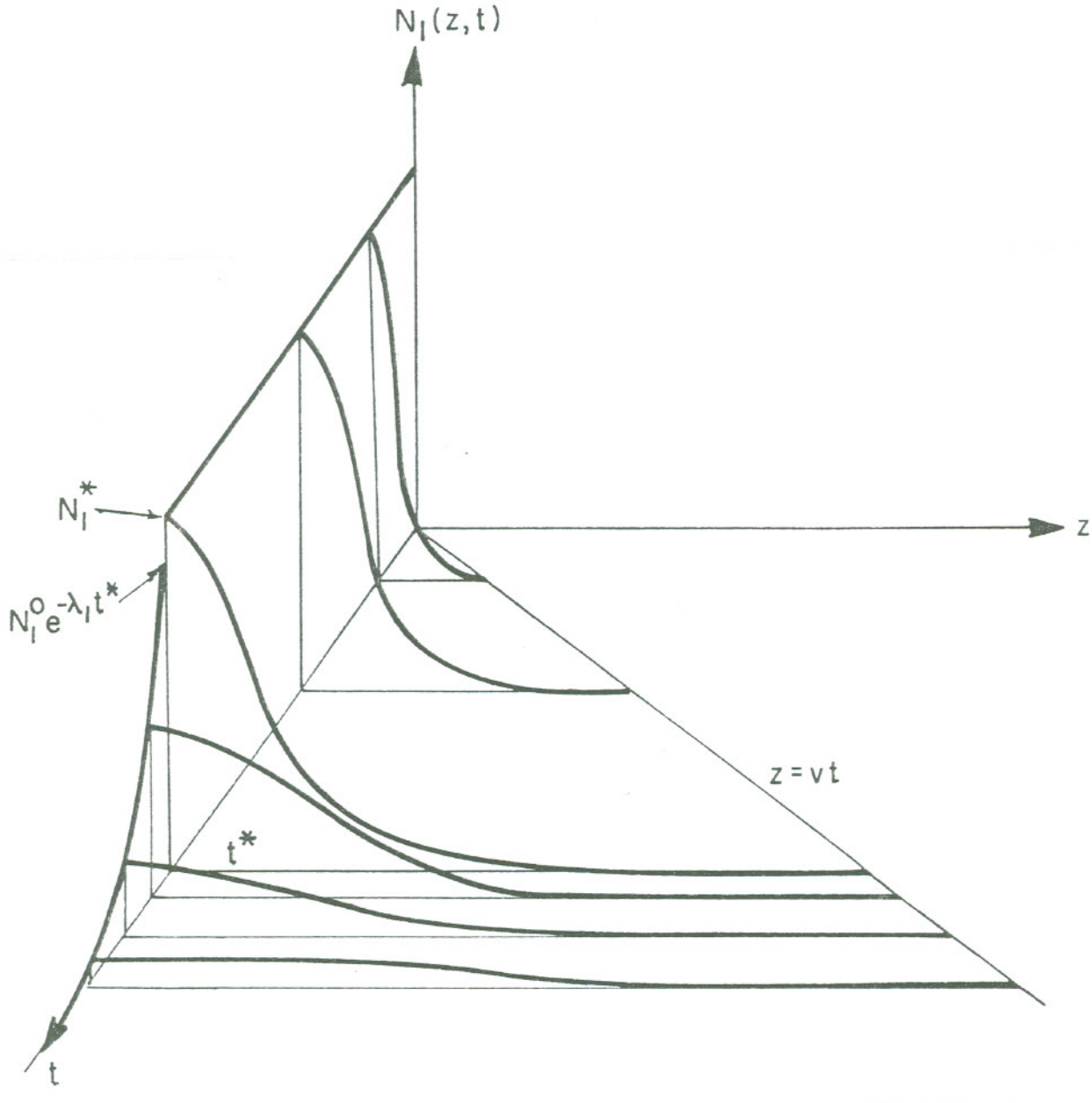

Fig. 5.5.5 Space-time-dependent aqueous concentration in fissure-flow transport with step release and solubility limit.

transport by porous flow, assuming the same porosity as the fractured medium excluding the main fissure. As is already discussed in section 5.2 for transport without solubility limit, the porous-flow model gives an overestimate of the retardation capacity for transport with a larger retardation coefficient and an underestimate of the retardation capacity for transport with a smaller retardation coefficient. In concluding, precipitation of the nuclide at the repository has two important effects, one is to reduce the maximum concentration as well as the local concentration of the nuclide and the other is to shift the concentration band at a given distance to a greater time.

5.6 Transport of a Radionuclide in Multi-Layered Fractured Media

Fissures and micropores in fractured media usually form a geometrically complicated matrix with layered solid phases of different geophysical properties, and it is important to analyze radionuclide transport in layered fractured media. We here consider the transport of a mother nuclide through a series of many planar fissures, each bounded by surfaces of rock of different physiochemical properties.

5.6.1 Formulation and Analysis

Consider the transport of a mother nuclide through series of fissures

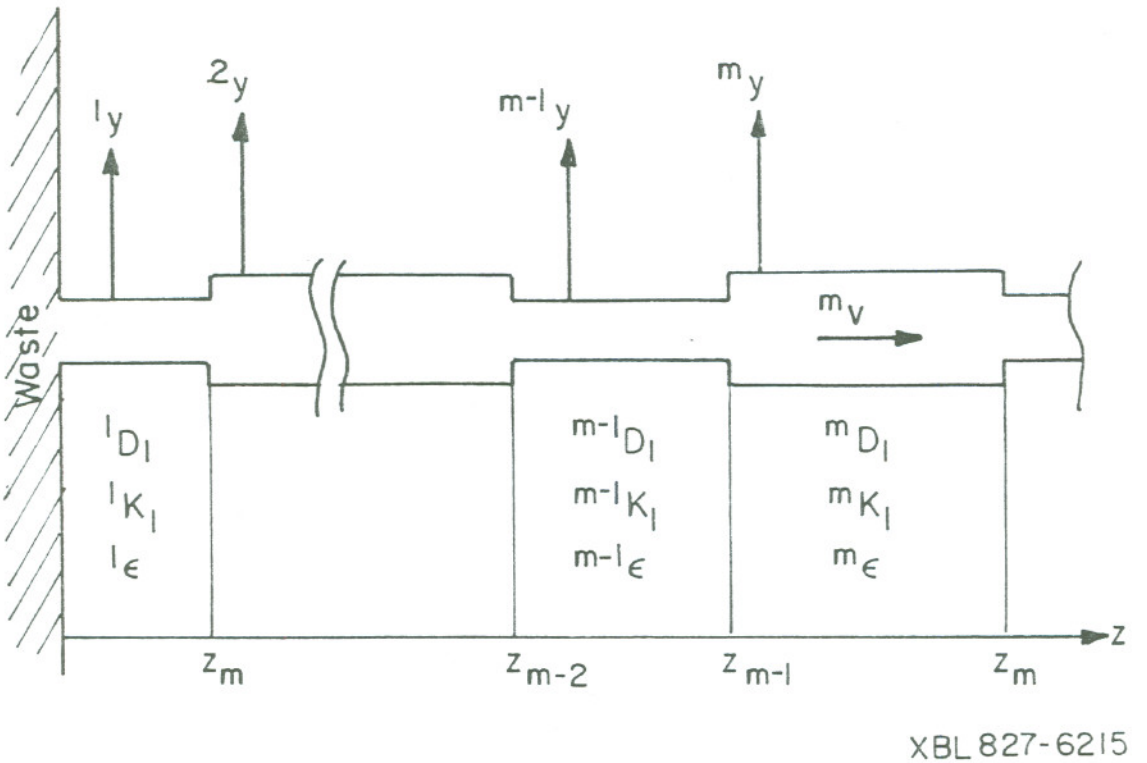

Fig. 5.6.1 Physical scheme of fissure-flow transport in a series of fissures.

of different interstices, as shown in Fig. 5.6.1. Let us designate the fissure of interstice ${}^{m}b$ and the surrounding rock medium, located between distances $z=z_{m-1}$ and $z=z_m$ as, the mth fissure and mth medium, respectively. We take a distance z from the waste in the flow direction and the distance ${}^{m}y$ from surface of the mth fissure in the mth rock medium. If we assume that the concentration of the nuclide in the solid phase is equilibrated locally with that in the water phase in the micropores, the transport equations which govern the concentrations of the nuclide in the mth fissure and micropores are given by, respectively

$$\frac{\partial {}^{m}N_1}{\partial t} + {}^{m}v \frac{\partial {}^{m}N_1}{\partial z} + \lambda_1 {}^{m}N_1 = - \frac{2}{{}^{m}b} {}^{m}J_1 \qquad (5.6.1)$$

$$\frac{\partial {}^{m}M_1}{\partial t} + \frac{{}^{m}D_1}{{}^{m}K_1} \frac{\partial^2 {}^{m}M_1}{\partial ({}^{m}y)^2} + \lambda_1 {}^{m}M_1 = 0 \qquad (5.6.2)$$

$$t > 0, \quad z > 0, \quad y > 0, \quad m = 1,2,3, \ldots$$

where ${}^{m}N_1(z,t)$ and ${}^{m}M_1(z,y,t)$ are aqueous concentrations of the nuclide in the mth fissure and micropores, respectively, ${}^{m}D_1$, is the pore molecular diffusivity, ${}^{m}K_1$ is the sorption retardation constant, ${}^{m}v$ is the water velocity, and ${}^{m}J_1$ is the diffusive flux of the nuclide at surface of the mth fissure.

$${}^{m}J_1 = - {}^{m}\varepsilon \, {}^{m}D_1 \left. \frac{\partial {}^{m}M_1}{\partial {}^{m}y} \right|_{{}^{m}y = 0} \qquad (5.6.3)$$

$$m = 1,2,3 \ldots$$

Initial conditions are

$$ {}^{m}N_{1}(z, 0) = 0, \qquad z > 0, \qquad m = 1,2, \ldots \tag{5.6.4} $$

$$ {}^{m}M_{1}(z, y, 0) = 0, \quad z > 0, \qquad my > 0 \quad m = 1,2, \ldots \tag{5.6.5} $$

From the equation of continuity, assuming a constant density of water,

$$ {}^{m-1}v \; {}^{m-1}b = {}^{m}v \; {}^{m}b \;, \qquad m = 2,3, \ldots \tag{5.6.6} $$

Also from the mass conservation of the nuclide, assuming transport without longitudinal diffusion

$$ {}^{m-1}N_{1} \; {}^{m-1}v \; {}^{m-1}b = {}^{m}N \; {}^{m}v \; {}^{m}b \;, \qquad m = 2,3, \ldots \tag{5.6.7} $$

The boundary condition for ${}^{m}N_{1}(z,t)$ at $z = z_{m-1}$ is given by

$$ {}^{m}N_{1}(z_{m-1},t) = {}^{m-1}N\,(z_{m-1}, t) \;, \qquad m = 2,3, \ldots \tag{5.6.8} $$

The boundary conditions for ${}^{m}M_{1}(z,y,t)$ are

$$ {}^{m}M_{1}(z,0,t) = {}^{m}N_{1}(z,t) \;, \qquad m = 1,2, \ldots \tag{5.6.9} $$

$$ {}^{m}M_{1}(z,\infty,t) = 0 \;, \qquad m = 1,2, \ldots \tag{5.6.10} $$

Let us introduce a new variable:

$$ {}^{m}z = z - z_{m-1} \;, \qquad z_{m} - z_{m-1} > {}^{m}z > 0 \tag{5.6.11} $$

Then the transport equations can be rewritten as

$$\frac{\partial {}^{m}N_1}{\partial t} + {}^{m}v \frac{\partial {}^{m}N_1}{\partial {}^{m}z} + \lambda_1 {}^{m}N_1 = - \frac{2}{{}^{m}b} {}^{m}J_1 \tag{5.6.12}$$

$$\frac{\partial {}^{m}M_1}{\partial t} + \frac{{}^{m}D_1}{{}^{m}K_1} \frac{\partial^2 {}^{m}M_1}{\partial ({}^{m}y)^2} + \lambda_1 {}^{m}M_1 = 0 \tag{5.6.13}$$

$$t > 0, \quad {}^{m}y > 0, \quad z_m - z_{m-1} > {}^{m}z > 0 , \quad m = 1,2, \ldots$$

The initial and boundary conditions become

$${}^{m}N_1 ({}^{m}z,0) = 0, \quad z_m - z_{m-1} > {}^{m}z > 0 \tag{5.6.14}$$

$${}^{m}M_1 ({}^{m}z, {}^{m}y,0) = 0, \quad z_m - z_{m-1} > z > 0, \quad {}^{m}y > 0 \tag{5.6.15}$$

$${}^{m}N_1 (0,t) = {}^{m-1}\chi_1(t), \quad t > 0 \tag{5.6.16}$$

$${}^{m}M_1 ({}^{m}z,0,t) = {}^{m}N_1 ({}^{m}z,t), \quad t > 0, \quad z_m - z_{m-1} > {}^{m}z > 0 \tag{5.6.17}$$

$${}^{m}M_1 ({}^{m}z,\infty,t) = 0, \quad z_m - z_{m-1} > {}^{m}z > 0, \quad t > 0 \tag{5.6.18}$$

where the function ${}^{m-1}\chi(t)$ is defined as

$${}^{m-1}\chi(t) = \begin{cases} \phi_1(t), & t \geq 0, \quad m = 1 \\ {}^{m-1}N_1(z_{m-1},t), & t > 0, \quad m = 2,3, \ldots \end{cases} \tag{5.6.19}$$

The system of Eqs. (5.6.12) (5.6.19) is the same as the equations for the transport of a nuclide in a single fissure as presented in section 5.2. Therefore the solutions in that section can be directly applied to this problem. The solutions are given in the recursive form by

$$m_{N_1}(m_z,t) = e^{-\frac{\lambda_1}{m_v} m_z} \cdot \int_0^{t-\frac{m_z}{m_v}} {}_{m-1}\chi_1(t-\tau-\frac{m_z}{m_v}) P_1(\tau;{}^{m}a_1 {}^{m}z)\,d\tau \qquad (5.6.20)$$

$$m_{M_1}(m_z,m_y,t) = e^{-\frac{\lambda_1}{m_v} m_z} \cdot \int_0^{t-\frac{m_z}{m_v}} {}_{m-1}\chi_1(t-\tau-\frac{m_z}{m_v}) P_1(\tau;{}^{m}a_1 {}^{m}z+{}^{m}b_1 {}^{m}y)\,d\tau \qquad (5.6.21)$$

where

$$m_{a_1} = \frac{2\, m_\varepsilon\, m_{D_1}}{m_b m_v} \frac{m_{K_1}}{m_{D_1}} \qquad (5.6.22)$$

$$m_{b_1} = \sqrt{\frac{m_{K_1}}{m_{D_1}}} \qquad (5.6.23)$$

The function $P_1(t;\alpha)$ is given by Eq. (5.2.19), i.e.,

$$P_1(t;\alpha) = \frac{\alpha}{2\sqrt{\pi t^3}} e^{-\frac{\alpha^2}{4t} - \lambda_1 t} \qquad (5.6.24)$$

5.6.2 Transport in a Two-layered Fractured Medium

Equations (5.6.20) and (5.6.21) are still in recursive form. We now

apply these solutions to the transport of a nuclide in a two-layered fractured medium for three different release modes

i) Impulse release

When the function $\phi_1(t)$ in Eq. (5.6.19) is given by the impulse release function, the solutions become

$$ {}^1N_1(z,t) = (TN_1{}^o)\, e^{-\frac{\lambda_1}{{}^1v} z}\, P_1(t - \frac{z}{{}^1v}; {}^1a_1 z)\, h(t - \frac{z}{{}^1v}) \quad z_1 > z > 0 \qquad (5.6.25) $$

$$ {}^2N_1(z,t) = (TN_1{}^o)\, e^{-\lambda_1(\frac{z-z_1}{{}^2v} + \frac{z_1}{{}^1v})}\, P_1(t - \frac{z-z_1}{{}^2v} - \frac{z_1}{{}^1v}; {}^2a_1(z-z_1) + {}^1a_1 z)\, h(t - \frac{z-z_1}{{}^2v} - \frac{z_1}{{}^1v}), \quad z_2 > z > z_1 \qquad (5.6.26) $$

$$ {}^1M_1(z,t) = (TN_1{}^o)\, e^{-\frac{\lambda_1}{{}^1v} z}\, P_1(t - \frac{z}{{}^1v}; {}^1a_1 z + {}^1b_1\, {}^1y)\, h(t - \frac{z}{{}^1v}) $$

$$ {}^1y > 0, \quad z_1 > z > 0 \qquad (5.6.27) $$

$$ {}^2M_1(z,t) = (TN_1{}^o)\, e^{-\lambda_1(\frac{z-z_1}{{}^2v} + \frac{z_1}{{}^1v})}\, P_1(t - \frac{z-z_1}{{}^2v} - \frac{z_1}{{}^1v}; {}^2a_1(z-z_1) + {}^1a_1 z + {}^2b_1\, {}^2y)\, h(t - \frac{z-z_1}{{}^2v} - \frac{z_1}{{}^1v}), \quad {}^2y > 0, z_2 > z > z_1 \qquad (5.6.28) $$

ii) Step release

For a step release, the solution for the concentration of the nuclide in the fissure is given by

$$ {}^{1}N_1(z,t) = N_1{}^{o}\, e^{-\lambda_1 t}\,(t - \tfrac{z}{{}^{1}v})\ \mathrm{erfc}\left(\frac{{}^{1}a_1 z}{2\sqrt{t-\frac{z}{v}}}\right),\quad z_1>z>0 \qquad (5.6.29) $$

$$ {}^{2}N_1(z,t) = N_1{}^{o}\, e^{-\lambda_1 t}\, h(t - \tfrac{z-z_1}{{}^{2}v} - \tfrac{z_1}{{}^{1}v})\ \mathrm{erfc}\left(\frac{{}^{2}a_1(z-z_1)+{}^{1}a_1 z_1}{2\sqrt{t-\frac{z-z_1}{{}^{2}v}-\frac{z_1}{{}^{1}v}}}\right), $$

$$ z_2>z>z_1 \qquad (5.6.30) $$

The concentration of the nuclide in the micropores is given by

$$ {}^{1}M_1(z,t) = N_1{}^{o}\, e^{-\lambda_1 t}\, h(t - \tfrac{z}{{}^{1}v})\ \mathrm{erfc}\left(\frac{{}^{1}a_1 z+{}^{1}b_1{}^{1}y}{2\sqrt{t-z/v}}\right) .\ {}^{1}y>0, z_1>z>0 $$

(5.6.31)

$$ {}^{2}M_1(z,t) = N_1{}^{o}\, e^{-\lambda_1 t}\, h(t - \tfrac{z-z_1}{{}^{2}v} - \tfrac{z_1}{{}^{1}v})\ \mathrm{erfc}\left(\frac{{}^{2}a_1(z-z_1)+{}^{1}a_1 z_1+{}^{2}b_1{}^{2}y}{2\sqrt{t-\frac{z-z_1}{{}^{2}v}-\frac{z_1}{{}^{1}v}}}\right), $$

$$ {}^{2}y>0,\ z_2>z>z_1 \qquad (5.6.32) $$

iii) Band release

The band-release solutions can be obtained by employing the superposition theorem (H-1).

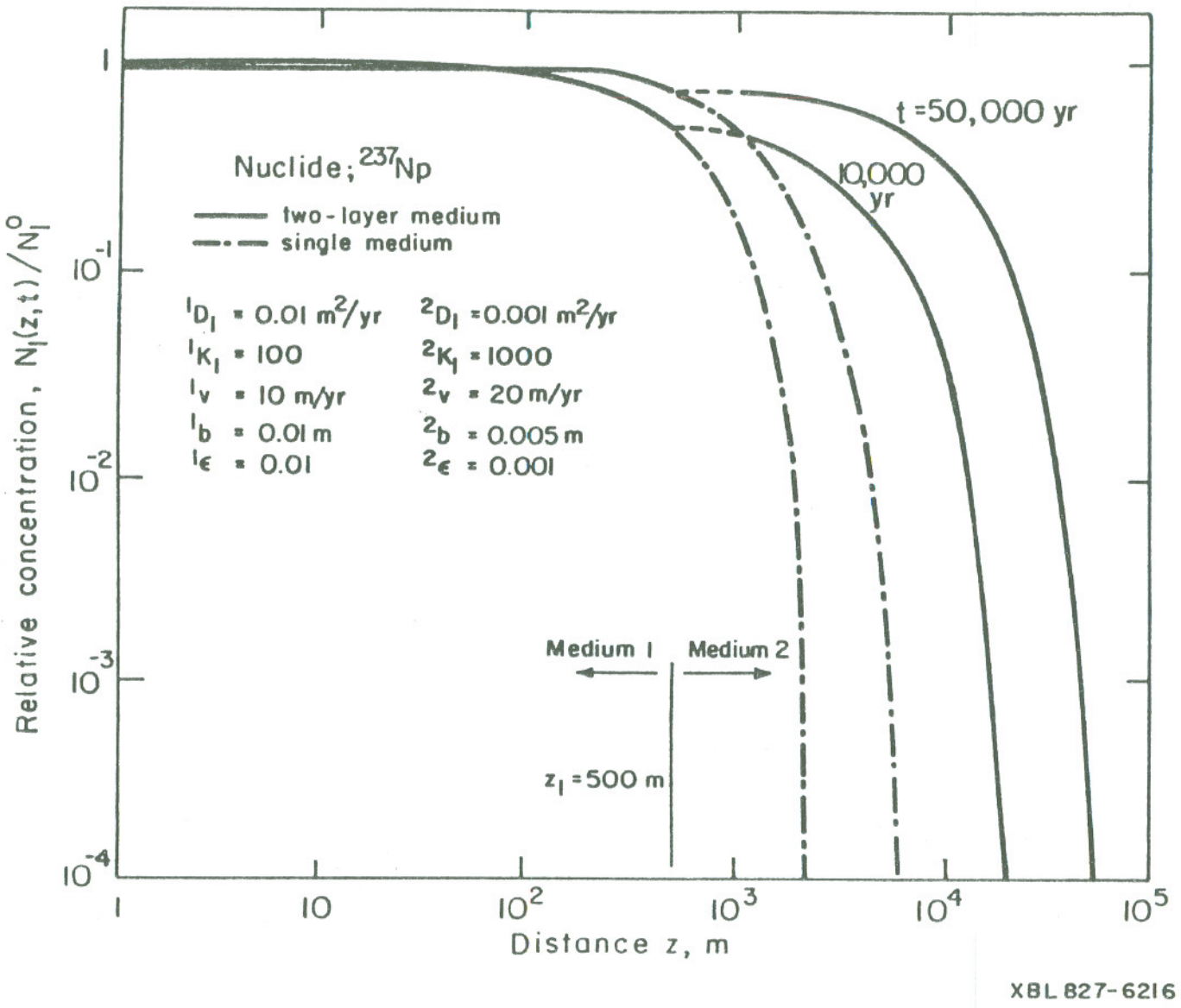

Fig. 5.6.2 Concentration profiles of ^{237}Np in a two-layered fractured medium.

5.6.3 Migration Behavior in a Two-Layered Fractured Medium

The aqueous concentration profiles of ^{237}Np in a two-layered fractured medium with a contact surface at $z = z_1$ (= 500 m) for a step release are compared in Fig. 5.6.2 with the concentration profiles of the nuclide in transport in a single layered fractured medium. The solid lines show the concentrations of the nuclide in the two-layer medium and the broken lines show the concentrations in the single-layer medium. (The dashed line which connects the solid line in each phase shows an expected asymptote. Numerical integration of Eq. (5.6.30) gives a less exact value for a smaller value of $z - z_1$.) The assumed parameters are included in the figure. Because of the assumption of transport without dispersion in the fissure, the nuclide at a distance less than $z = z_1$ is not affected by the existence of the second layer. Here we assume a greater water velocity and a smaller pore diffusivity in the second layer, so the nuclide can migrate a greater distance than would be predicted for in a single layered medium, even though there is a greater assumed value of the sorption retardation constant for the second layer.

5.7 Transport in an Infinite Diffusion Field With Nonequilibrium Sorption

Analytical solutions for transport in a porous medium without local chemical equilibrium of radionuclides in the liquid and solid have been presented in our previous report. In fissure-flow transport, as described in section 5.2, the retardation effect originates not only from the sorption process but also from the molecular diffusion into and out of micropores within the rock medium. Here the effect of nonequilibrium sorption becomes more important than expected in porous flow transport, even for the transport of long-lived radionuclides. In this section, we consider

the more general case of fissure-flow transport with nonequilibrium sorption in micropores.

5.7.1 Analysis

The governing transport equations to be solved are from Eqs. (5.1.18) through (5.1.20)

$$\frac{\partial N_1}{\partial t} + v \frac{\partial N_1}{\partial z} + \lambda_1 N_1 = -\frac{2}{b} J_1 \tag{5.7.1}$$

$$\frac{\partial M_1}{\partial t} - D_1 \frac{\partial^2 M_1}{\partial y^2} + \Lambda_1^m M_1 - K_1^m S_1 = 0 \tag{5.7.2}$$

$$\frac{\partial S_1}{\partial t} + \Lambda_1^s S_1 - K_1^s M_1 = 0 \tag{5.7.3}$$

$$t > 0, \quad z > 0, \quad y > 0$$

where

$$\Lambda_1^m = \lambda_1 + \frac{k_m a}{\varepsilon} \tag{5.7.5}$$

$$\Lambda_1^s = \lambda_1 + \frac{k_m a}{(1-\varepsilon) K_{D\,1}} \tag{5.7.5}$$

$$K_1^m = \frac{k_m a}{\varepsilon K_{D1}} \tag{5.7.6}$$

$$K_1^s = \frac{k_m a}{1-\varepsilon} \tag{5.7.7}$$

and J_1 is given by

$$J_1(z,t) = - \varepsilon D_1 \left. \frac{\partial M_1}{\partial y} \right|_{y=0} , \qquad t > 0, \quad z > 0 \tag{5.7.8}$$

The initial and boundary conditions are, from Eqs. (5.1.23) through (5.1.28)

$$N_1 (z,0) = 0, \qquad z > 0, \tag{5.7.9}$$

$$M_1(z,y,0) = 0, \qquad z > 0, \qquad y > 0 \tag{5.7.10}$$

$$S_1(z,y,0) = 0, \qquad z > 0, \qquad y > 0 \tag{5.7.11}$$

$$N_1(0,t) = \phi_1(t), \qquad t > 0 \tag{5.7.12}$$

$$M_1(z,0,t) = N_1(z,t), \quad t > 0, \qquad z > 0 \tag{5.7.13}$$

$$M_1(z,\infty,t) = 0, \qquad t > 0, \qquad z > 0 \tag{5.7.14}$$

The solutions of these equations can be obtained by the method of Laplace transform. Taking the Laplace transform of Eqs. (5.7.1), (5.7.2), and (5.7.3), we have

$$\frac{d\tilde{N}_1}{dz} + \frac{s+\lambda_1}{v} \tilde{N}_1 + \frac{2}{bv} \tilde{J}_1 = 0 \tag{5.7.15}$$

$$s\,\tilde{M}_1 - D_1 \frac{d^2\tilde{M}_1}{dy^2} + \Lambda_1^{\,m}\,\tilde{M}_1 - K_1^{\,m}\,\tilde{S}_1 = 0 \qquad (5.7.16)$$

$$s\,\tilde{S}_1 + \Lambda_1^{\,s}\,\tilde{S}_1 - K_1^{\,s}\,\tilde{M}_1 = 0 \qquad (5.7.17)$$

Eliminating the transformed concentration of the nuclide in the solid phase from Eqs. (5.7.16) and (5.7.17) and solving the diffusion equation subject to the boundary conditions given by Eqs. (5.7.13) and (5.7.14), we can find the transformed solution for the concentration of the nuclide in the micropores

$$\tilde{M}_1(z,y,s) = \tilde{N}_1(z,s)\, e^{-\frac{y}{\sqrt{D_1}}\sqrt{s+\Lambda_1^{\,m} - \frac{K_1^{\,m}K_1^{\,s}}{(s+\Lambda_1^{\,s})}}} \qquad (5.7.18)$$

and the transformed diffusive flux:

$$\tilde{J}_1(z,s) = \varepsilon\sqrt{D_1}\,\tilde{N}_1(z,s)\sqrt{s+\Lambda_1^{\,m} - \frac{K_1^{\,m}K_1^{\,s}}{(s+\Lambda_1^{\,s})}} \qquad (5.7.19)$$

Also from Eq. (5.7.17)

$$\tilde{S}_1(z,y,s) = K_1^{\,s}\,\tilde{N}_1(z,s)\,\frac{e^{-\frac{y}{\sqrt{D_1}}\sqrt{s+\Lambda_1^{\,m} - \frac{K_1^{\,m}K_1^{\,s}}{D_1(s+\Lambda_1^{\,s})}}}}{s+\Lambda_1^{\,s}} \qquad (5.7.20)$$

Substituting Eq. (5.7.19) into Eq. (5.7.15) and solving the resultant equation with the boundary condition given by Eq. (5.7.12), we have

$$\tilde{N}_1(z,s) = \tilde{\phi}_1(s)\exp\left(-\frac{\lambda_1+s}{\underline{v}}z - d_1 z\sqrt{s+\Lambda_1^{\,m} - \frac{K_1^{\,m}K_1^{\,s}}{s+\Lambda_1^{\,s}}}\right) \qquad (5.7.21)$$

where d_1 is the constant defined by

$$d_1 = \frac{2\varepsilon\sqrt{D_1}}{bv} \tag{5.7.22}$$

The transformed function of the form similar to Eq. (5.7.21) has been studied by Lapidus and Amundson in their analysis in adsorption of species in bed (L-1). In order to find the inverse of Eq. (5.7.21), we use the following general formula for the Laplace transform:

$$L\left\{\int_o^t \left(\frac{t-u}{au}\right)^{\nu} J_{2\nu}\left[2\sqrt{aut-au^2}\right] f(u)du\right\} = \frac{1}{s^{2s+1}}\, g(s+\frac{a}{s}) \tag{5.7.23}$$

where g(s) is the transformed function of f(t) with respect to t,

$$L\left[f(t)\right] = g(s) \tag{5.7.24}$$

Especially, when $\nu = 0$, we can write

$$L\left\{\int_o^t J_o\left[2\sqrt{aut-au^2}\right] f(u)du\right\} = \frac{1}{s}\, g(s+\frac{a}{s}) \tag{5.7.25}$$

From the displacement rule,

$$L\left\{e^{-\Lambda_1 s t} \int_o^t J_o\left[2\sqrt{au(t-u)}\right] f(u)\, du\right\}$$

$$= \frac{1}{s+\Lambda_1 s}\, g(s+\Lambda_1 s + \frac{a}{s+\Lambda_1 s}) \tag{5.7.26}$$

Let

$$H(s) = e^{- d_1 z \sqrt{s+\Lambda_1{}^m - \frac{K_1{}^m K_1{}^s}{s+\Lambda_1{}^s}}} \tag{5.7.27}$$

For a direct application of Eq. (5.7.26), we split the function g(s) into two parts, thus

$$H(s) = \Lambda_1{}^s h(s) + s\, h(s) \tag{5.7.28}$$

where the function h(s) is defined by

$$h(s) = \frac{e^{- d_1 z \sqrt{\frac{s^2+(\Lambda_1{}^m+\Lambda_1{}^s)s+\Lambda_1{}^m\Lambda_1{}^s-K_1{}^m K_1{}^s}{s+\Lambda_1{}^s}}}}{s+\Lambda_1{}^s} \tag{5.7.29}$$

Now consider the function g(s) which takes the form:

$$g(s) = e^{- d_1 z \sqrt{s+c}} \tag{5.7.30}$$

of which the inversion is

$$f(t;d_1 z) = \frac{d_1 z}{2\sqrt{\pi t^3}}\; e^{- \frac{d_1{}^2 z^2}{4t} - ct} \tag{5.7.31}$$

Then

$$\frac{g(s+\Lambda_1{}^s + \frac{a}{s+\Lambda_1{}^s})}{s+\Lambda_1{}^s} = \frac{e^{- d_1 z \sqrt{\frac{s^2+(2\Lambda_1{}^s+c)s+(\Lambda_1{}^s)^2+c\Lambda_1{}^s+a}{s+\Lambda_1{}^s}}}}{s+\Lambda_1{}^s} \tag{5.7.32}$$

Equating Eq. (5.7.32) with Eq. (5.7.29), we find

$$\left.\begin{aligned} c &= \Lambda_1^{\,m} - \Lambda_1^{\,s} \\ a &= -K_1^{\,m} K_1^{\,s} \end{aligned}\right\} \tag{5.7.33}$$

Noting that the relation among Eqs. (5.7.30)∿(5.7.32), we can write the inverse of function h(s) directly from Eq. (5.7.26)

$$\begin{aligned} & L^{-1}\left\{h(s)\right\} \\ &= e^{-\Lambda_1^{\,s} t} \int_0^t \frac{d_1 z}{2\sqrt{\pi u^3}}\, e^{-\frac{d_1^{\,2} z^2}{4u} - (\Lambda_1^{\,m} - \Lambda_1^{\,s})u} \cdot I_o\left[2\sqrt{K_1^{\,m} K_1^{\,m} u(t-u)}\right] du \\ &= F(t;d_1 z) \end{aligned} \tag{5.7.34}$$

where $I_o(x)$ is the modified Bessel function of zero order. Also since $F(0;d_1 z) = 0$,

$$\begin{aligned} L^{-1}\left\{s\, h(s)\right\} &= \frac{\partial F(t;d_1 z)}{\partial t} \\ &= e^{-\Lambda_1^{\,s} t} f(t;d_1 z) - \Lambda_1^{\,s} F(t;d_1 z) + G(t;d_1 z) \end{aligned} \tag{5.7.35}$$

where the function $f(t;d_1 z)$ is given by Eq. (5.7.31) and the function $G(t;d_1 z)$ is given by

$$G(t;d_1z) = e^{-\Lambda_1^s t}\int_0^t \frac{\sqrt{K_1^m K_1^s u}}{\sqrt{t-u}}\frac{d_1 z}{2\sqrt{\pi u^3}} e^{-\frac{d_1^2 z^2}{4u} - (\Lambda_1^m - \Lambda_1^s)u} I_1\left[2\sqrt{K_1^m K_1^s u(t-u)}\right] du \tag{5.7.36}$$

where $I_1(x)$ is the modified Bessel function of first order. From Eqs. (5.7.34) and (5.7.35), we have the inversion of the function H(s),

$$L\left\{H(s)\right\} = e^{-\Lambda_1^s t} f(t;d_1z) + G(t;d_1z) \tag{5.7.37}$$

Applying the equation directly to Eq. (5.7.21) and using the shift rule, we can finally obtain the solution for the aqueous concentration of the nuclide in the fissure

$$N_1(z,t) = e^{-\frac{\lambda_1}{v}z}\int_0^{t-\frac{z}{v}} \phi_1(t-\tau-\tfrac{z}{v})\left[e^{-\Lambda_1^s \tau} f(\tau;d_1z) + G(\tau;d_1z)\right] d\tau \tag{5.7.38}$$

The concentration of the nuclide in the micropores is, from Eq. (5.7.18)

$$M_1(z,y,t) = \int_0^t N_1(z,t-\tau)\left[e^{-\Lambda_1^s \tau} f(\tau;e_1y) + G(\tau;e_1y)\right] d\tau \tag{5.7.39}$$

where

$$e_1 = \frac{1}{\sqrt{D_1}} \tag{5.7.40}$$

Also, the concentration of the nuclide in the solid phase is given by

$$S_1(z,y,t) = K_1^s \int_0^t e^{-\Lambda_1^s \tau} M_1(z,y,t-\tau)d\tau \tag{5.7.41}$$

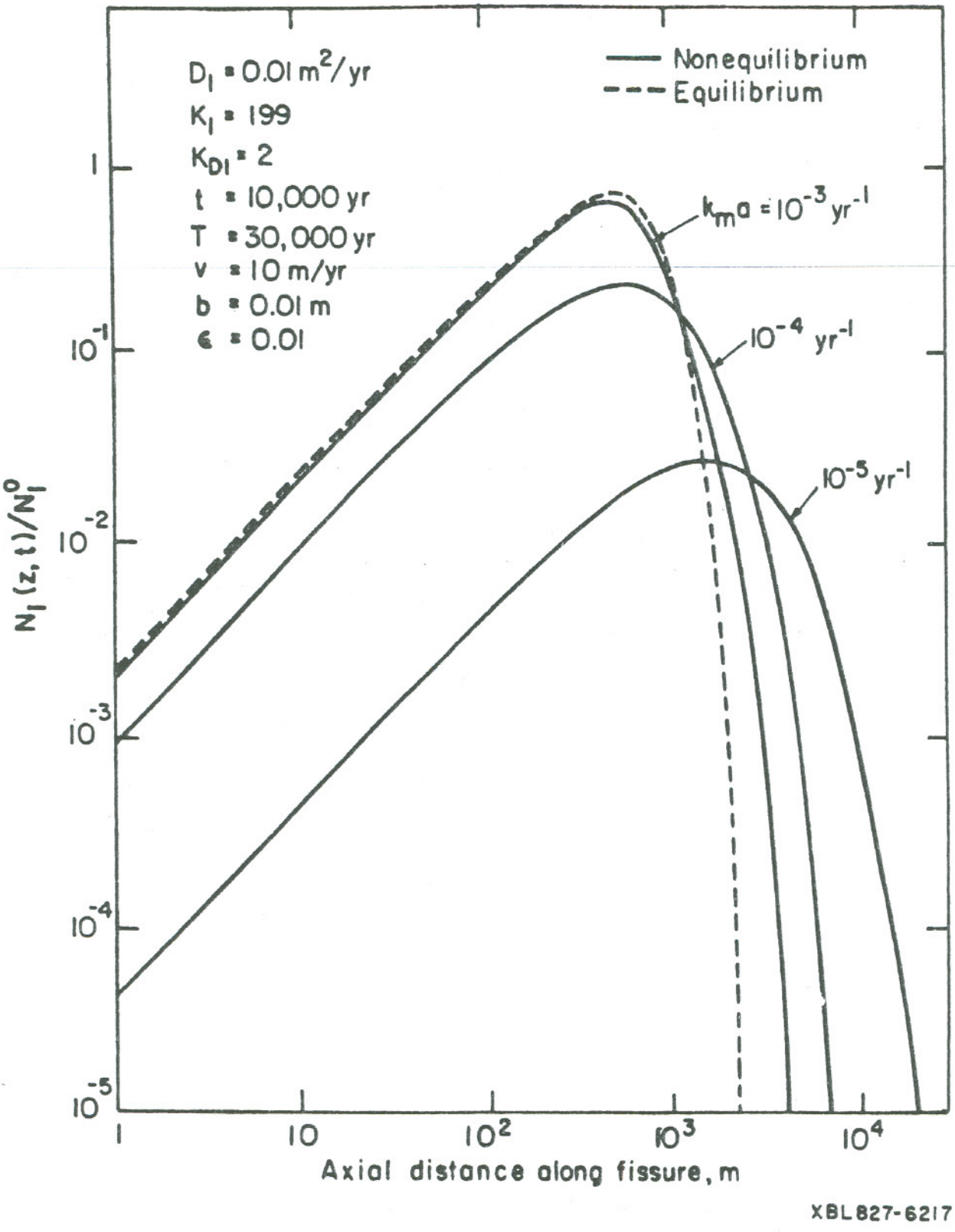

Fig. 5.7.1 Effect of nonequilibrium sorption on fissure-flow transport, concentration profiles of ^{237}Np in the fissure, impulse release.

5.7.2 Transport With an Impulse Release

The solution for the concentration of the nuclide in the fissure, Eq. (5.7.38), involves a double integral term and is not suitable for direct numerical calculations. However, if the boundary value of the concentration at the repository is given by the impulse function given by Eq. (5.1.18), the solution can be simplified, and is given by

$$N_1(z,t) = (TN_1{}^o)\, h(t - \tfrac{z}{v}) \left[e^{-\Lambda_1{}^s (t - \frac{z}{v})} f(t - \tfrac{z}{v}; d_1 z) + G(t - \tfrac{z}{v}; d_1 z) \right] \quad (5.7.42)$$

where the functions $f(t;d_1z)$ and $G(t;d_1z)$ are given by Eqs. (5.7.31) and (5.7.42). The solutions for the concentrations of the nuclide in the micropores and in the solid phase are given by Eqs. (5.7.39) and (5.7.41), with substitution of Eq. (5.7.42).

The concentration profiles of ^{237}Np at t = 10,000 yr for transport with nonequilibrium sorption, which are calculated from Eq. (5.7.42) are shown as the solid lines in Fig. 5.7.1 for different assumed values of the mass-transfer coefficient k_m and the interfacial area $\underline{a}$ per unit volume. Each nonequilibrium curve shows a higher concentration at greater distances than the concentration given by the equilibrium curve, whereas the nonequilibrium concentration is lower at the smaller distances. For the migration times considered here, the "seed pulse" has moved with the water velocity to a distance of 10^5m. Therefore the long concentration tail results from nuclides emerging from the micropores by molecular diffusion. The penetration thickness within the micropores is greater for nonequilibrium sorption, resulting in a smaller concentration gradient and a smaller diffusive flux of nuclides returning to the fissure in the

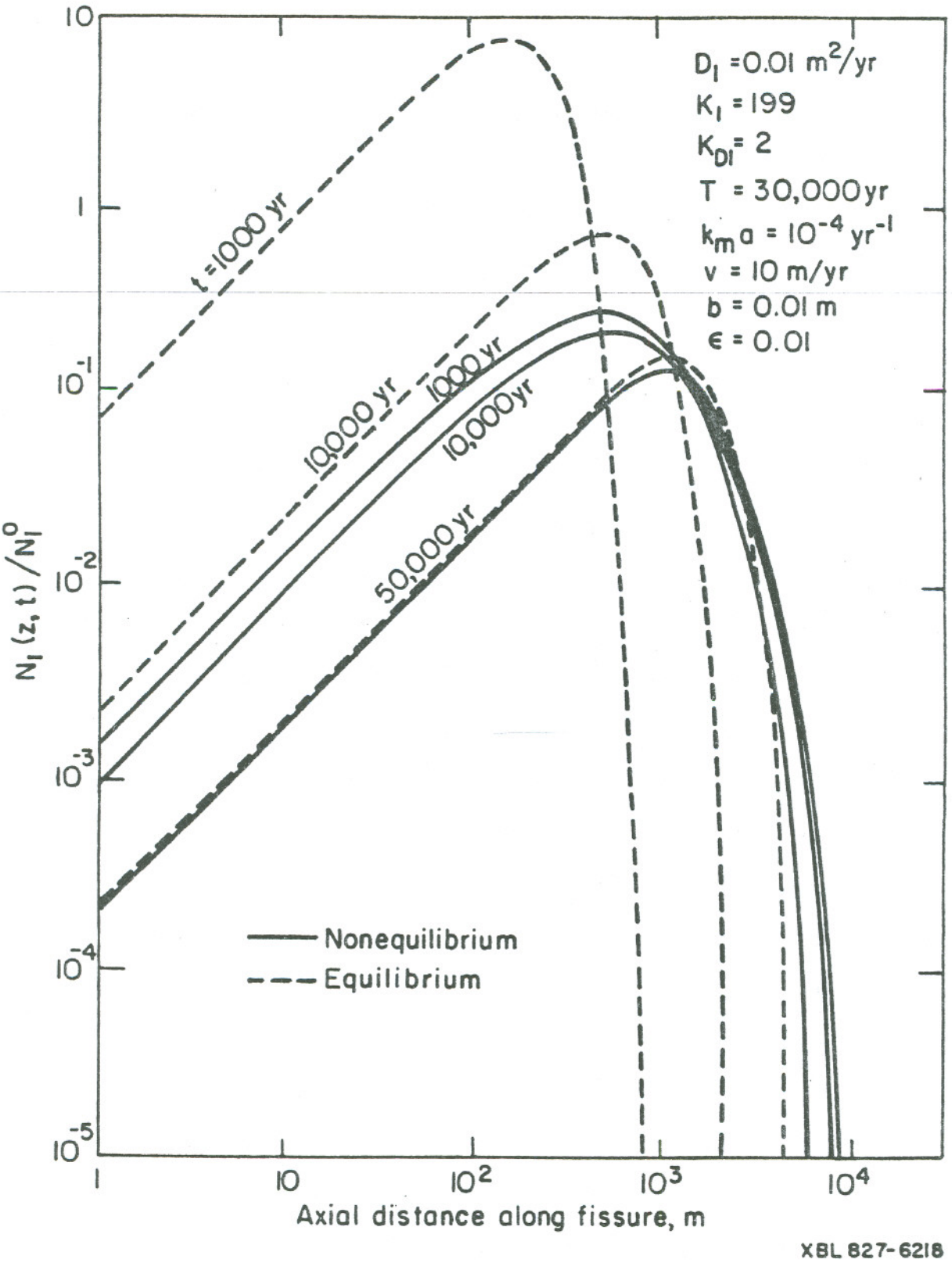

Fig. 5.7.2 Concentration profiles of ^{237}Np for transport with non-equilibrium sorption.

region of the concentration tail. The effect at the greater distances in the region of the leading edge of the concentration band, non-equilibrium sorption promotes faster penetration into the micropores, thereby lowering the concentration in that region. As seen from the figure, nonequilibrium sorption spreads the concentration profile over a greater distance than for equilibrium sorption, resulting in a lower maximum concentration. As the mass-transfer coefficient increases, the nonequilibrium concentration curve approaches the equilibrium curve.

Shown in Fig. 5.7.2 is the variation of the concentration profile of ^{237}Np with migration time. The pore diffusivity and the mass-transfer coefficient are assumed to be $D_l = 0.01\ m^2/yr$ and $k_m a = 10^{-4}\ 1/yr$. The time required to reach equilibrium depends mainly on these two parameters. For a greater diffusivity, the nonequilibrium characteristic is governed predominantly by sorption, whereas for a smaller diffusivity, the transport is governed by diffusion process. In this assumed case, the nonequilibrium effect persists until a time of almost 50,000 yr.

5.8 Transport of a Multi-Member Nuclide Chain, Convective Transport in Micropores

In the foregoing sections the fissure-flow transport of a single mother nuclide has been discussed. In evaluating the biological hazard due to long-lived actinide elements which are possibly released into a migration field from high-level waste repositories, it is desired to provide the analytical solutions for the transport of a multi-member nuclide chain, in order to estimate the chromatographic behavior of daughter nuclides. Among the nuclide chains contained in radioactive wastes, the following

nuclide chains are considered to be important, because of the relatively high biological hazard of the radium daughters.

$$^{246}Cm \rightarrow {}^{242}Pu \rightarrow {}^{238}U \rightarrow {}^{234}U \rightarrow {}^{230}Th \rightarrow {}^{226}Ra$$
$$^{242m}Am \rightarrow {}^{242}Cm \nearrow$$
$$^{237}Np \rightarrow {}^{233}Pa \rightarrow {}^{233}U \rightarrow {}^{227}Th \rightarrow {}^{225}Ra$$

In succeeding sections the transport of a multi-member nuclide chain in fractured media is considered. Numerical demonstration of the solutions applied to three-member nuclide chains are also given.

As one of the simplest cases, we first consider the fissure flow transport of a nuclide chain with convective transport of the nuclides in the micropores.

5.8.1 Formulation and Transport Equations

Consider water flow in the z-direction in an infinite plane fissure of interstice b. The fissure is bounded by surfaces of rock of porosity ε, through which the water can penetrate outwards in the transverse y-direction at a constant velocity w, as shown in Fig. 5.8.1. Because of the water flow through the medium, the water velocity v in the fissure is space-dependent and is specified by the conservation equation:

$$\frac{\partial v}{\partial z} = -\frac{2\varepsilon w}{b} \tag{5.8.1}$$

Thus the water velocity is given by

$$v(z) = v_o - \frac{2\varepsilon w z}{b} \tag{5.8.2}$$

where v_o is the water velocity in the z-direction at the repository site.

The transport equations which govern the concentrations of the nuclide i in the main and micropore fissures are given by, with assuming local sorption equilibrium in the micropore fissures

$$\frac{\partial N_i}{\partial t} + v \frac{\partial N_i}{\partial z} + \lambda_i N_i = - \varepsilon \frac{2}{b} w N_i + \lambda_{i-1} N_{i-1} \qquad (5.8.3)$$

$$\frac{\partial M_i}{\partial t} + \frac{w}{K_i} \frac{\partial M_i}{\partial y} + \lambda_i M_i = \frac{\lambda_{i-1} K_{i-1}}{K_i} M_{i-1} \qquad (5.8.4)$$

$t > 0, \quad z > 0, \quad y > 0, \quad i = 1,2,3, \ldots$

where $N_i(z,t)$ is the concentration of the nuclide i in the main fissure, $M_i(z,y,t)$ is the concentration of the nuclide i in the micropore fissures, λ_i is the radioactive decay constant, and K_i is the sorption equilibrium coefficient.

The initial conditions are given by

$$N_i(z,0) = 0, \quad z > 0 \qquad (5.8.5)$$

$$M_i(z,y,0) = 0, \quad z > 0, \quad y > 0 \qquad (5.8.6)$$

The boundary conditions are

$$N_i(0,t) = \phi_i(t), \quad t > 0, \qquad (5.8.7)$$

$$M_i(z,0,t) = N_i(z,t), \quad t > 0, \quad z > 0 \qquad (5.8.8)$$

where the function $\phi_i(t)$ is the time-dependent concentration of the nuclide i

at the repository, given in section 5.1.2. The $M_i(z,y,t)$ tends to zero as $y \to \infty$.

5.8.2 Solutions to Pore Convection Transport

Since Eqs. (5.8.3) and (5.8.4) are related to each other only by the boundary condition given by Eq. (5.8.8) and are not coupled; they can be solved independently.

Now we introduce a new variable z' defined as

$$z' = \int_0^z \frac{1}{v(z)}\, dz, \qquad z' > 0, \qquad z > 0 \tag{5.8.9}$$

then Eq. (5.8.3) becomes

$$\frac{\partial N_i}{\partial t} + \frac{\partial N_i}{\partial z'} + \lambda_i N_i = - \varepsilon \frac{2}{b} w N_i + \lambda_{i-1} N_{i-1} \quad , t > 0, z' > 0 \tag{5.8.10}$$

The initial and boundary conditions for $N_i(z',t)$ are, from Eqs. (5.8.5) and (5.8.7)

$$N_i(z',0) = 0, \qquad z' > 0 \tag{5.8.11}$$

$$N_i(0,t) = \phi_i(t), \qquad t > 0 \tag{5.8.12}$$

The solution for the space-time-dependent concentration of nuclide i in the fissure can be obtained by Laplace transform, and is given in the general form:

$$N_i(z',t) = e^{-(\lambda_i+\frac{2\varepsilon w}{b})z'} h(t-z')\ \phi_i(t-z')$$

$$+\sum_{j=1}^{i-1} \prod_{q=j}^{i-1} (\lambda_q) \sum_{\ell=j}^{i} \frac{e^{-(\lambda_\ell+\frac{2\varepsilon}{b}w)z'}}{\prod_{\substack{r=j \\ r\neq\ell}}^{i} (\lambda_r-\lambda_\ell)}\ \phi_j(t-z')h(t-z') \qquad (5.8.13)$$

In the original coordinate system, the solution becomes

$$N_i(z,t) = e^{-(\lambda_i+\frac{2\varepsilon w}{b})q(z)} h(t-q(z))\ \phi_i(t-q(z))$$

$$+\sum_{j=1}^{i-1} \prod_{q=j}^{i-1} (\lambda_q) \sum_{\ell=j}^{i} \frac{e^{-(\lambda_\ell+\frac{2\varepsilon w}{b})\,q(z)}}{\prod_{\substack{r=j \\ r\neq\ell}}^{i} (\lambda_r-\lambda_\ell)}\ h(t-q(z))\ \phi_j(t-q(z)) \qquad (5.8.14)$$

where

$$q(z) = -\frac{b}{2\varepsilon w} \ln\left(1-\frac{2\varepsilon w z}{b v_o}\right) \qquad (5.8.15)$$

The system of Eqs. (5.8.4), (5.8.6), and (5.8.8) is just the same form as that employed in analysis for the porous flow transport, with the exception of a slight difference in the expression of the boundary condition. Therefore, we can directly apply our previous solution for porous flow transport (H-1) to this problem. The solution for the concentration of the nuclide i in the micropores is then given by

$$M_i(z',y,t) = e^{-(\lambda_i/w_i)y} N_i(z',t-\frac{y}{w_i})$$

$$+ \sum_{j=1}^{i-1} \underline{A}_i^{(j)} \sum_{m=j}^{i} \frac{e^{-(\lambda_m/w_m)y}}{\underline{B}_m^{(j)}} \sum_{\substack{r=j \\ r\neq m}}^{i} \underline{D}_{rm}^{(j)} \int_0^t \underline{g}_{rm}(t-\tau) N_j(z',\tau)\, d\tau \qquad (5.8.16)$$

where

$$w_i = w/K_i \qquad (5.8.17)$$

$$\underline{A}_{\ell}^{(j)} = \prod_{r=j}^{i-1} \left(\frac{\lambda_r K_r}{w_{r+1} K_{r+1}}\right) \qquad (5.8.18)$$

$$\underline{B}_m^{(j)} = \prod_{\substack{r=j \\ r\neq m}}^{i} \left(\frac{1}{w_r} - \frac{1}{w_m}\right) \qquad (5.8.19)$$

$$\underline{D}_{rm}^{(j)} = \frac{1}{\prod_{\substack{q=j \\ q\neq m\neq r}}^{i} (\underline{\Delta}_{qr} - \underline{\Delta}_{rm})} \qquad (5.8.20)$$

with

$$\underline{\Delta}_{rm} = \frac{\lambda_r w_r - \lambda_m w_r}{w_m - w_r} \qquad (5.8.21)$$

The function $\underline{g}_{rm}(t)$ is given by

$$\underline{g}_{rm}(t) = h(t-\frac{y}{w_m})\, e^{-\underline{\Delta}_{rm}(t-\frac{y}{w_m})} \qquad (5.8.22)$$

5.8.3 Transport With an Impulse Release

When the function $\phi_i(t)$ is given by an impulse release function given by Eq. (5.1.17), Eq. (5.8.14) becomes

$$N_i(z,t) = T\, N_i^o\, e^{-(\lambda_i + \frac{2\varepsilon w}{b})\, q(z)}\, \delta(t - q(z))$$

$$+ T \sum_{j=1}^{i-1} \prod_{q=j}^{i-1} (\lambda_q) \sum_{\ell=j}^{i} \frac{e^{-(\lambda_\ell + \frac{2\varepsilon w}{b})\, q(z)}}{\prod_{\substack{r=j \\ r\neq\ell}}^{i} (\lambda_r - \lambda_\ell)}\, N_j^o\, \delta(t - q(z)) \quad (5.8.23)$$

This equation shows that every concentration pulse travels along the z-t line given by $t = q(z)$. Thus, if the removal mechanism of the nuclide in the fissure is only from convective transport, every nuclide can migrate at the same velocity with no retardation. The only effect to be expected is attenuation in concentration of the nuclide.

The concentration of the nuclide i in the micropores can be obtained by substitution of Eq. (5.8.23) into Eq. (5.8.16), and is given by

$$M_i(z,y,t) = e^{-(\lambda_i/w_i)y} \left[T\, N_i^o\, e^{-(\lambda_i + \frac{2\varepsilon w}{b})q(z)}\, \delta(t - \frac{y}{w_i} - q(z)) \right]$$

$$+ T \sum_{j=1}^{i-1} \prod_{q=j}^{i-1} (\lambda_q) \sum_{\ell=j}^{i} \frac{e^{-(\lambda_\ell + \frac{2\varepsilon w}{b})q(z)}}{\prod_{\substack{r=j \\ r\neq\ell}}^{i} (\lambda_r - \lambda_\ell)}\, N_j^o\, \delta(t - \frac{y}{w_i} - q(z))$$

$$+ T \sum_{j=1}^{i-1} \frac{A_i(j)}{B_m(j)} \sum_{m=j}^{i} e^{-(\lambda_m/w_m)y} \sum_{r=j}^{i} D_{rm}(j) \left[N_j^o\, e^{-(\lambda_i + \frac{2\varepsilon w}{b})q(z)}\, g_{rm}(t - q(z)) \right.$$

$$\left. + T \sum_{k=1}^{j-1} \prod_{q=k}^{j-1} (\lambda_q) \sum_{\ell=k}^{j} N_k^o \frac{e^{-(\lambda_k + \frac{2\varepsilon w}{b})q(z)}}{\prod_{\substack{r=k \\ r\neq\ell}}^{i} (\lambda_r - \lambda_\ell)}\, g_{rm}(t - q(z)) \right] \quad (5.8.24)$$

The characteristics of the solution given by Eq. (5.8.24) have already been discussed in our previous reports (H-1, P-1).

5.9 Transport of a Multi-Member Radionuclide Chain, Diffusive Transport in Micropores

In sections 5.2∿5.7, analytical solutions to the transport of a single mother nuclide in a planar fissure, with diffusive transport in micropores, are presented. In this section we develop the analysis for the equilibrium transport of a multi-member nuclide chain in a fractured media, with diffusive transport in micropores. Here we present the exact solutions to the problem in recursive form. Because of mathematical difficulty in reduction of the recursive solutions, the nonrecursive solutions in general form are not given here. Mathematical approximations yield nonrecursive formulae which describe the space-time-dependent concentrations of the nuclide in the fissure and micropores, as given in the following section.

5.9.1 Recursive Exact Solutions

The transport equations of an arbitrary radionuclide chain with one-dimensional fissure flow are, assuming local sorption equilibrium

$$\frac{\partial N_i}{\partial t} + v \frac{\partial N_i}{\partial z} + \lambda_i N_i = - \frac{2}{b} J_i + \lambda_{i-1} N_{i-1} \qquad (5.9.1)$$

$$\frac{\partial M_i}{\partial t} - \frac{D_i}{K_i} \frac{\partial^2 M_i}{\partial y^2} + \lambda_i M_i = \frac{\lambda_{i-1} K_{i-1}}{K_i} M_{i-1} \qquad (5.9.2)$$

$$t > 0, \quad \infty > z > 0, \quad y > 0, \quad i = 1,2,3 \ldots$$

where $N_i(z,t)$ is the aqueous concentration of the nuclide i in the main fissure, $M_i(z,y,t)$ is the aqueous concentration of the nuclide i in the micropore fissures, v is the water velocity, D_i is the pore molecular diffusivity, K_i is the sorption equilibrium coefficient, λ_i is the radioactive decay constant, and b is the interstice of the main fissure. The function $J_i(z,t)$ is the diffusive flux at the fissure surface, given by

$$J_i(z,t) = - \varepsilon D_i \frac{\partial M_i}{\partial y}\bigg|_{y=0}, \qquad z > 0, \qquad t > 0, \quad i = 1,2,3, .. \tag{5.9.3}$$

The initial and boundary conditions are

$$N_i(z,0) = 0 \qquad z > 0 \tag{5.9.4}$$

$$M_i(z,y,0) = 0, \quad z > 0, \quad y > 0 \tag{5.9.5}$$

$$N_i(0,t) = \phi_i(t), \qquad t > 0 \tag{5.9.6}$$

$$M_i(z,0,t) = N_i(z,t), \qquad z > 0, \quad t > 0 \tag{5.9.7}$$

where the function $\phi_i(t)$ is the general time-dependent concentration of the nuclide i at the waste repository. The function $\phi_i(t)$ is given by Eq. (5.1.12) for a step release, by Eq. (5.1.15) for a band release, and by Eq. (5.1.17) by an impulse release. The pore concentration $M_i(z,y,t)$ approaches zero as y approaches infinity.

Equations (5.9.1) and (5.9.2) are connected by Eq. (5.9.3), subject to the appropriate initial and boundary conditions given by Eqs. (5.9.4) - (5.9.7), and can be solved by Laplace and Fourier sine

transforms. The transformed solutions for $\tilde{N}_i(z,s)$ and $\hat{\tilde{M}}_i(z,\omega,s)$ are given in recursive form:

$$\tilde{N}_i(z,s) = \tilde{\phi}_i(s)\, e^{-\frac{s+\lambda_i}{v} z - \frac{2\varepsilon D_i z}{bv}\sqrt{\frac{K_i}{D_i}(s+\lambda_i)}}$$

$$+ \frac{\lambda_{i-1}}{v} \int_0^z N_{i-1}(z-\zeta,s)\, e^{-\frac{s+\lambda_i}{v}\zeta - \frac{2\varepsilon D_i \zeta}{bv}\sqrt{\frac{K_i}{D_i}(s+\lambda_i)}}\, d\zeta$$

$$+ \frac{2\varepsilon D_i}{bv} \sum_{j=1}^{i-1} \frac{D_j}{\lambda_i K_i} \prod_{\ell=j}^{i} \left(\frac{\lambda_\ell K_\ell}{D_\ell}\right)$$

$$\cdot \sum_{r=j}^{i} \sum_{\substack{q=j \\ q\neq r}}^{i} B_q^{ji} \sqrt{\frac{\frac{K_r}{D_r}(s+\lambda_r)}{s+D^*_{qr}}} \int_0^z \tilde{N}_j(z-\zeta,s) e^{-\frac{s+\lambda_i}{v}\zeta - \frac{2\varepsilon D_i \zeta}{bv}\sqrt{\frac{K_i}{D_i}(s+\lambda_i)}}\, d\zeta \qquad (5.9.8)$$

$$\hat{\tilde{M}}_i(z,\omega,s) = \sum_{j=1}^{i} \frac{D_j}{\lambda_i K_i} \prod_{\ell=j}^{i} \left(\frac{\lambda_\ell K_\ell}{D_\ell}\right) \prod_{r=j}^{i} \left(\frac{1}{\omega^2 + \frac{K_r}{D_r}(s+\lambda_r)}\right) \omega \tilde{N}_j(z,s) \qquad (5.9.9)$$

where s and ω are the transformed variables with respect to t and y, respectively.

Inversion of these equations gives the aqueous concentrations of the nuclide i in the fissure and micropores in recursive form:

$$N_i(z,t) = e^{-\frac{\lambda_i}{v} z} \int_0^t \phi_i(\tau - \frac{z}{v})\, P_i(t-\tau; a_i z)\, d\tau$$

$$+ \frac{\lambda_{i-1}}{v} \int_0^z \int_0^t e^{-\frac{\lambda_i}{v}\zeta}\, N_{i-1}(z-\zeta, t-\frac{\zeta}{v})\, P_i(t-\tau; a_i z)\, d\tau\, d\zeta$$

$$- \frac{2\varepsilon D_i}{bv} \sum_{j=1}^{i-1} \frac{D_j}{\lambda_i K_i} \prod_{\ell=j}^{i} \left(\frac{\lambda_\ell K_\ell}{D_\ell}\right) \sum_{r=j}^{i} \sum_{\substack{q=j \\ q\neq r}}^{i} B_q^{ji}$$

$$\cdot \int_0^z \int_0^t \int_0^{t-\tau_1} e^{-\frac{\lambda_i}{v}\zeta}\, N_j\,(z-\zeta, \tau_2 - \frac{\zeta}{v})\, P_i(t-\tau, -\tau_2; a_i\zeta)$$

$$\cdot Q_r^{\,q}(\tau_1)\, d\tau_2\, d\tau_1\, d\zeta \qquad (5.9.10)$$

$$M_i(z,y,t) = \int_0^t N_i(z,t-\tau)\, P_i(\tau; b_i y)\, d\tau$$

$$+ \sum_{j=1}^{i-1} \frac{D_j}{\lambda_i K_i} \prod_{\ell=j}^{i} \left(\frac{\lambda_\ell K_\ell}{D_\ell}\right) \sum_{r=j}^{i} \sum_{\substack{q=j \\ q\neq r}}^{i} B_q^{ji} \int_0^t N_j(z,t-\tau) R_r^{\bar{q}}(y,\tau)\, d\tau \qquad (5.9.11)$$

where

$$a_i = \frac{2\varepsilon\sqrt{D_i K_i}}{bv}, \quad i = 1,2,3 \ldots. \qquad (5.9.12)$$

$$b_i = \sqrt{\frac{K_i}{D_i}}, \quad i = 1,2,3, \ldots \qquad (5.9.13)$$

and the function $P_i(t;\alpha)$, $Q_r^q(t)$, and $R_r^q(y,t)$ are given by

$$P_i(t;\alpha) = \frac{\alpha}{2\sqrt{\pi}} \frac{e^{-\frac{\alpha^2}{4t} - \lambda_i t}}{t^{3/2}} \tag{5.9.14}$$

$$Q_r^q(t) = \begin{cases} -\sqrt{\frac{K_r}{D_r}} \cdot \sqrt{D^*_{qr} - \lambda_r} \cdot \frac{1}{\sqrt{\pi}} \int_{1/\sqrt{(D^*_{qr} - \lambda_r)t}}^{\infty} e^{\frac{1}{\xi^2}} d\xi, \lambda_r < D^*_{qr} \\ \sqrt{\frac{K_r}{D_r}} \left\{ \frac{e^{-\lambda_r t}}{\sqrt{\pi t}} + \sqrt{\lambda_r - D^*_{qr}}\ e^{-D^*_{qr} t} . \operatorname{erf}\left[\sqrt{(\lambda_r - D^*_{qr})t}\right] \right\} \\ \qquad \lambda_r > D^*_{qr} \end{cases} \tag{5.9.15}$$

$$R_r^q(y,t) = e^{-D^*_{qr} t} \frac{2}{\sqrt{\pi}} \int_{\frac{y}{\sqrt{4D_r t/K_r}}}^{\infty} \exp\left(- \xi^2 - (\lambda_r - D^*_{qr}) \frac{y^2 K_r}{4 D_r \xi^2} \right) d\xi, \lambda_r < D^*_{qr}$$

$$\frac{1}{2} e^{-D^*_{qr} t} \left[e^{y\sqrt{(\lambda_r - D^*_{qr})\frac{K_r}{D_r}}} \operatorname{erfc}\left(\frac{y + 2t\sqrt{(\lambda_r - D^*_{qr})D_r/K_r}}{\sqrt{4D_r t/K_r}} \right) \right.$$

$$\left. + e^{-y\sqrt{(\lambda_r - D^*_{qr})\frac{K_r}{D_r}}} \operatorname{erfc}\left(\frac{y - 2t\sqrt{(\lambda_r - D^*_{qr})D_r/K_r}}{\sqrt{4D_r t/K_r}} \right) \right]$$

$$\lambda_r > D^*_{qr} \tag{5.9.16}$$

with the constants:

$$B_q^{ji} = \frac{1}{d_{qr}} \prod_{\substack{\ell=j \\ \ell\neq q \\ \ell\neq r}}^{i} \left[d_{\ell r} \left(D^*_{\ell r} - D^*_{qr} \right) \right]^{-1}$$

$$D^*_{qr} = e_{qr} / d_{qr}$$

$$e_{qr} = \lambda_q K_q / D_q - \lambda_r K_r / D_r$$

$$d_{qr} = K_q / D_q - K_r / D_r \qquad (5.9.17)$$

For the mother nuclide, Eqs. (5.9.10) and (5.9.11) give, for a step release

$$N_1(z,t) = N_1^o e^{-\lambda_1 t} \operatorname{erfc}\left(\frac{a_1 z}{2\sqrt{t - z/v}}\right) h(t - \tfrac{z}{v}) \qquad (5.9.18)$$

$$M_1(z,y,t) = N_1^o e^{-\lambda_1 t} \operatorname{erfc}\left(\frac{a_1 z + b_1 y}{2\sqrt{t - z/v}}\right) h(t - \tfrac{z}{v}) \qquad (5.9.19)$$

The equations are just the same as those given by Eqs. (5.2.25) and (5.2.26). Equations (5.9.10) and (5.9.11) give the recursive expressions for the space-time-dependent aqueous concentrations of nuclide i in the fissure and micropores. Our remaining problem is to reduce the solutions into nonrecursive expressions. However, because of the rather complicated mathematical forms, it is difficult to derive nonrecursive solutions directly from these recursive solutions. In the following section, the approximations that allow us to derive nonrecursive solutions will be presented.

5.10 Approximate Solutions in Fissure-Flow Transport of a Multi-Member Nuclide Chain, With Diffusion in Micropores

In the foregoing section, the exact solutions to the transport of radionuclide chain of arbitrary length, in fractured media with one-dimensional fissure flow, is given in recursive form. We here present approximate solutions in which the radioactive decay of an individual daughter nuclide in the micropore liquid and in the solid phase are neglected. For a chain of long lived radionuclides, the resulting solutions can give a good approximation to the exact recursive solutions described in the foregoing section.

5.10.1 Formulation

Consider an infinite plane fissure of interstice b in which water is flowing in the z-direction at a constant velocity v. The nuclides released from the waste repository located at z = 0 migrate in this fissure and can diffuse into the stationary water in the micropores. The transport equation that describes the aqueous concentration of the nuclide i in the fissure is

$$\frac{\partial N_i}{\partial t} + v \frac{\partial N_i}{\partial z} + \lambda_i N_i = - \frac{2}{b} J_i + \lambda_{i-1} N_{i-1} \qquad (5.10.1)$$

$$t > 0, \qquad 0 < z < \infty, \qquad y > 0, \qquad i = 1,2,3, \ldots$$

where $N_i(z,t)$ is the concentration of the nuclide i in the fissure, $J_i(z,t)$ is the removal rate of the nuclide i at surfaces of the fissure, and λ_i is the radioactive decay constant of the nuclide i.

For diffusive transport in the micropores, and neglecting the radioactive decay of the nuclides in the micropores, the transport equation is

$$\frac{\partial M_i}{\partial t} - \frac{D_i}{K_i} \frac{\partial^2 M_i}{\partial y^2} = 0 \qquad t > 0, \quad y > 0, \quad i = 1,2,3, \ldots \qquad (5.10.2)$$

where $M_i(z,y,t)$ is the concentration of the nuclide i in the stationary water in the micropores, D_i is the pore molecular diffusivity, and K_i is the sorption retardation constant of nuclide i in the rock medium.

The diffusive flux $J_i(z,t)$ which relates Eq. (5.10.1) to Eq. (5.10.2) is given by

$$J_i(z,t) = - \varepsilon D_i \left. \frac{\partial M_i}{\partial y} \right|_{y=0}, \qquad z > 0, \quad t > 0, \quad i = 1,2, \ldots \qquad (5.10.3)$$

The initial conditions are

$$N_i(z,0) = 0, \qquad z > 0, \quad i = 1,2,3 \ldots \qquad (5.10.4)$$

$$M_i(z,y,0) = 0, \quad z > 0, \quad y > 0, \quad i = 1,2,3 \ldots \qquad (5.10.5)$$

The boundary conditions are

$$N_i(0,t) = \phi_i(t), \qquad t > 0, \quad i = 1,2,3, \ldots \qquad (5.10.6)$$

$$M_i(z,0,t) = N_i(z,t), \quad t > 0, \quad y > 0, \quad i = 1,2,3, \ldots \qquad (5.10.7)$$

where the function $\phi_i(t)$ is the general time-dependent concentration of the nuclide i at the waste location. The $M_i(z,y,t)$ approaches zero as y approaches infinity.

5.10.2 Nonrecursive Solution

Let s be the Laplace transformed variable with respect to time t, the transformed solution of Eq. (5.10.2) subject to the initial and boundary conditions given by Eqs. (5.10.5) and (5.10.7) is

$$\tilde{M}_i(z,y,s) = \tilde{N}_i(z,s)\, e^{-y\sqrt{\frac{K_i}{D_i}}\sqrt{s}} \tag{5.10.8}$$

The diffusive flux in the transformed form is then given by

$$\tilde{J}_i(z,s) = \varepsilon D_i \sqrt{\frac{K_i}{D_i}}\sqrt{s}\ \tilde{N}_i(z,s) \tag{5.10.9}$$

Taking the Laplace transform of Eq. (5.10.1) with respect to t and with respect to z with the aid of the initial and boundary conditions, and solving the resultant equation with substitution of Eq. (5.10.9), we have

$$\hat{\tilde{N}}_i(p,s) = \frac{\tilde{\phi}_i(s) + \frac{\lambda_{i-1}}{v}\hat{\tilde{N}}_{i-1}(p,s)}{p + \frac{s+\lambda_i}{v} + a_i\sqrt{s}} \tag{5.10.10}$$

where p is the transformed variable with respect to z.

Let the solution take the form:

$$N_i(z,t) = \sum_{j=1}^{i} N_{ij}(z,t) \tag{5.10.11}$$

the general form of $N_{ij}(p,s)$ is then

$$N_{ij}(p,s) = \begin{cases} \dfrac{\tilde{\phi}_i(s)}{p + \dfrac{s+\lambda_i}{v} + a_i\sqrt{s}} , & i=j \\ \dfrac{\prod_{\ell=j}^{i-1}(\lambda_\ell)}{v^{i-j}} \sum_{\ell=j}^{i-1} C_\ell^{ij} \dfrac{\tilde{\phi}_j(s)}{p + \dfrac{s+\lambda_\ell}{v} + a_\ell\sqrt{s}} , & i\neq j \end{cases} \tag{5.10.12}$$

with constants:

$$C_\ell^{ij} = \prod_{\substack{r=j \\ r\neq\ell}}^{i} \left(\frac{1}{\Lambda_{r\ell} + \mu_{r\ell}\sqrt{s}}\right) \tag{5.10.13}$$

$$\mu_{r\ell} = a_r - a_\ell , \quad r \neq \ell \tag{5.10.14}$$

$$\Lambda_{r\ell} = \frac{\lambda_r}{v} - \frac{\lambda_\ell}{v} \tag{5.10.15}$$

$$a_r = \frac{2\varepsilon D_r}{bv}\sqrt{\frac{K_r}{D_r}} \tag{5.10.16}$$

Inversion of Eq. (5.10.10) gives

$$N_{ij}(z,t) = \begin{cases} e^{-\frac{\lambda_i}{v}z}\, \phi_i(t-\frac{z}{v}) \,.\, P_i(t;a_i z) , & i=j \\ \dfrac{\prod_{\ell=j}^{i-1}(\lambda_\ell)}{v^{i-j}} \sum_{\ell=j}^{i} \sum_{\substack{r=j \\ r\neq\ell}}^{i} \dfrac{A_\ell^{ij}}{\prod_{\substack{r=j \\ r\neq\ell}}^{i}(\mu_{r\ell})} e^{-\frac{\lambda_\ell}{v}z} .\phi_i(t-\tfrac{z}{v}).G_{r\ell}(z,t) , & i\neq j \end{cases} \tag{5.10.17}$$

with the functions $P_i(t;\alpha)$ and $G_{r\ell}(z,t)$:

$$P_i(t;\alpha) = \frac{\alpha}{2\sqrt{\pi}} \frac{e^{-\frac{\alpha^2}{4t}}}{\sqrt{t^3}} \tag{5.10.18}$$

$$G_{r\ell}(z,t) = \frac{e^{-a_\ell^2 z^2/4t}}{\sqrt{\pi t}} - \delta_{r\ell}\, e^{a_\ell \delta_{r\ell} z + \delta_{r\ell}^2 t} \operatorname{erfc}\left(\frac{a_\ell z}{2\sqrt{t}} + \delta_{r\ell}\sqrt{t}\right) \tag{5.10.19}$$

and the constants:

$$A_\ell^{ij} = \prod_{\substack{q=j \\ r\neq\ell \\ q\neq r}}^{i} \left(\frac{1}{\delta_{q\ell} - \delta_{r\ell}}\right) \tag{5.10.20}$$

$$\delta_{r\ell} = \frac{\Lambda_{r\ell}}{\mu_{r\ell}} = \frac{\lambda_r - \lambda_\ell}{v(a_v - a_\ell)} \tag{5.10.21}$$

Substituting Eq. (5.10.17) into Eq. (5.10.11), we have the space and time dependent concentration of the nuclide i in the fissure in the nonrecursive form:

$$N_i(z,t) = e^{-\frac{\lambda_i}{v} z} \int_0^t \phi_i\left(t-\tau-\frac{z}{v}\right) P_i(\tau;a_i z)\, d\tau$$

$$+ \sum_{j=1}^{i-1} \frac{\prod_{\ell=j}^{i-1} (\lambda_\ell)}{v^{i-j}} \sum_{\ell=j}^{i} \sum_{\substack{r=j \\ r\neq\ell}}^{i} \frac{A_\ell^{ij}}{\prod_{\substack{r=j \\ r\neq\ell}}^{i} (\mu_r)} e^{-\frac{\lambda_\ell}{v} z} \int_0^{t-\frac{z}{v}} \phi_j\left(t-\tau-\frac{z}{v}\right) G_{r\ell}(z,\tau)\, d\tau \tag{5.10.22}$$

The concentration of the nuclide i in the micropores is given by, from Eq. (5.10.8)

$$M_i(z,y,t) = \int_0^t N_i(z,t-\tau)\, P_i(\tau, b_i y)\, d\tau \qquad (5.10.23)$$

where

$$b_i = \sqrt{\frac{K_i}{D_i}} \qquad (5.10.24)$$

i) Solution for a step release

When the function $\phi_i(t)$ is given by the step release concentration given by Eq. (5.1.12), the solution becomes

$$N_i(z,t) = \sum_{n=1}^{i} b_{ni}\, e^{-\lambda_n\left(t-\frac{z}{v}\right)}\, f_2^{in}(z,t)\, e^{-\frac{\lambda_i z}{v}}$$

$$+\sum_{j=1}^{i-1}\sum_{\ell=j}^{i}\sum_{\substack{r=j\\ r\neq\ell}}^{i}\frac{\prod_{q=j}^{i-1}(\lambda_q)}{\prod_{\substack{q=j\\ q\neq\ell\\ r\neq\ell}}^{i}(\mu_{q\ell})}\,\frac{A_\ell^{ij}}{v^{i-j}}\sum_{n=1}^{j}\left\{\frac{b_{nj}}{\sqrt{\lambda_n}}\, e^{-\lambda_n t-\frac{\lambda_\ell-\lambda_n}{v}z}.f_1^{\ell n}(z,t)\right.$$

$$-\frac{b_{nj}\,\delta_{r\ell}}{\lambda_n+\delta_{r\ell}^2}\, e^{\left(a_\ell\delta_{r\ell}z+\delta_{r\ell}^2\left(t-\frac{z}{v}\right)-\frac{\lambda_\ell}{v}z\right)}.\operatorname{erfc}\left(\frac{a_\ell z}{2\sqrt{t-z/v}}+\delta_{r\ell}\sqrt{t-z/v}\right.$$

$$\left.\left.-\frac{b_{nj}\,\delta_{r\ell}}{\lambda_n+\delta_{r\ell}^2}\, e^{-\lambda_n t-\frac{\lambda_\ell-\lambda_n}{v}z}\left[\frac{\delta_{r\ell}}{\sqrt{\lambda_n}}\, f_1^{\ell n}(z,t)-f_2^{\ell n}(z,t)\right]\right\} \qquad (5.10.25)$$

where the function $f_1^{\ell n}(z,t)$ and $f_2^{\ell n}(z,t)$ are given by

$$f_1^{\ell n}(z,t) = \frac{2}{\sqrt{\pi}} \int_0^{\sqrt{\lambda_n/t-z/v)}} e^{\eta^2 - \frac{\lambda_n a_\ell^2 z^2}{4\eta^2}} d\eta \; h(t-z/v) \qquad (5.10.26)$$

$$f_2^{\ell n}(z,t) = \frac{2}{\sqrt{\pi}} \int_{\frac{a_\ell z}{2\sqrt{t-z/v}}}^{\infty} e^{-\eta^2 + \lambda_n \frac{a_\ell^2 z^2}{4\eta^2}} d\eta \; h(t-z/v) \qquad (5.10.27)$$

ii) Solution for a band release

The solution for a band release is given by, from the superposition theorem (H-1)

$$N_i(z,t) = N_i(z,t;b_{ij})h(t) - N_i(z,t,b_{ij}\, e^{-\lambda_j T})h(t-T) \qquad (5.10.28)$$

$$M_i(z,y,t) = M_i(z,t;b_{ij})h(t) - M_i(z,t,b_{ij}\, e^{-\lambda_j T})h(t-T) \qquad (5.10.29)$$

where the functions $N_i(z,t;\, b_{ij})$ and $M_i(z,y,t;\, b_{ij})$ mean the solutions for the aqueous concentrations of the nuclide i for step release with the Bateman coefficient b_{ij}.

5.10.3 Accuracy of Approximate Model

In Table 5.10.1, the time-dependent concentration profiles of the mother nuclide 2.14×10^6-yr ^{237}Np, calculated from Eq. (5.10.25), are compared with the exact profiles given by Eq. (5.9.18). The approximate solution gives a fairly good approximation to the exact solution over the

Table 5.10.1 Comparison of approximate solution, neglecting radioactive decay in the micropores, with the exact solution for a first-member nuclide ^{237}Np, step release, K_1=100, D_1=0.01 m^2/hr, v=10 m/yr, b=0.01 m, ε=0.01.

Distance	$N_1(z,t)/N_1^0 \times 10$					
m	$t=1.0\times10^4$ yr		$t=1.0\times10^5$ yr		$t=1.0\times10^6$ yr	
	approx.	exact	approx.	exact	approx.	exact.
0.1	9.967	9.967	9.681	9.681	7.233	7.233
0.2	9.965	9.965	9.681	9.681	7.233	7.233
0.4	9.963	9.963	9.680	9.680	7.233	7.233
0.6	9.961	9.961	9.679	9.679	7.233	7.233
0.8	9.959	9.959	9.679	9.679	7.233	7.233
1.0	9.956	9.956	9.678	9.678	7.232	7.232
2.0	9.945	9.945	9.674	9.674	7.232	7.232
4.0	9.923	9.923	9.668	9.667	7.230	7.230
6.0	9.900	9.900	9.661	9.661	7.228	7.228
8.0	9.878	9.878	9.654	9.654	7.227	7.227
10.	9.855	9.855	9.647	9.647	7.225	7.225
20.	9.743	9.743	9.614	9.612	7.218	7.217
40.	9.519	9.518	9.547	9.543	7.206	7.201
60.	9.295	9.293	9.480	9.474	7.194	7.184
80.	9.072	9.069	9.413	9.405	7.183	7.168
100	8.849	8.846	9.346	9.336	7.172	7.152
200	7.751	7.746	9.011	8.991	7.119	7.070
400	5.696	5.690	8.342	8.307	7.009	6.907
600	3.941	3.934	7.680	7.633	6.895	6.744
800	2.556	2.552	7.030	6.974	6.776	6.582
1000	1.550	1.547	6.398	6.337	6.655	6.420
2000	0.04273	0.04261	3.646	3.588	6.013	5.622
4000	0.00000	0.00000	0.7239	0.7073	4.650	4.134
6000	0.00000	0.00000	0.07076	0.06889	3.349	2.864
8000	0.00000	0.00000	0.003268	0.003176	2.246	1.864
10000	0.00000	0.00000	0.000070	0.000067	1.401	1.136
20000	0.00000	0.00000	0.000000	0.000000	0.04401	0.03354

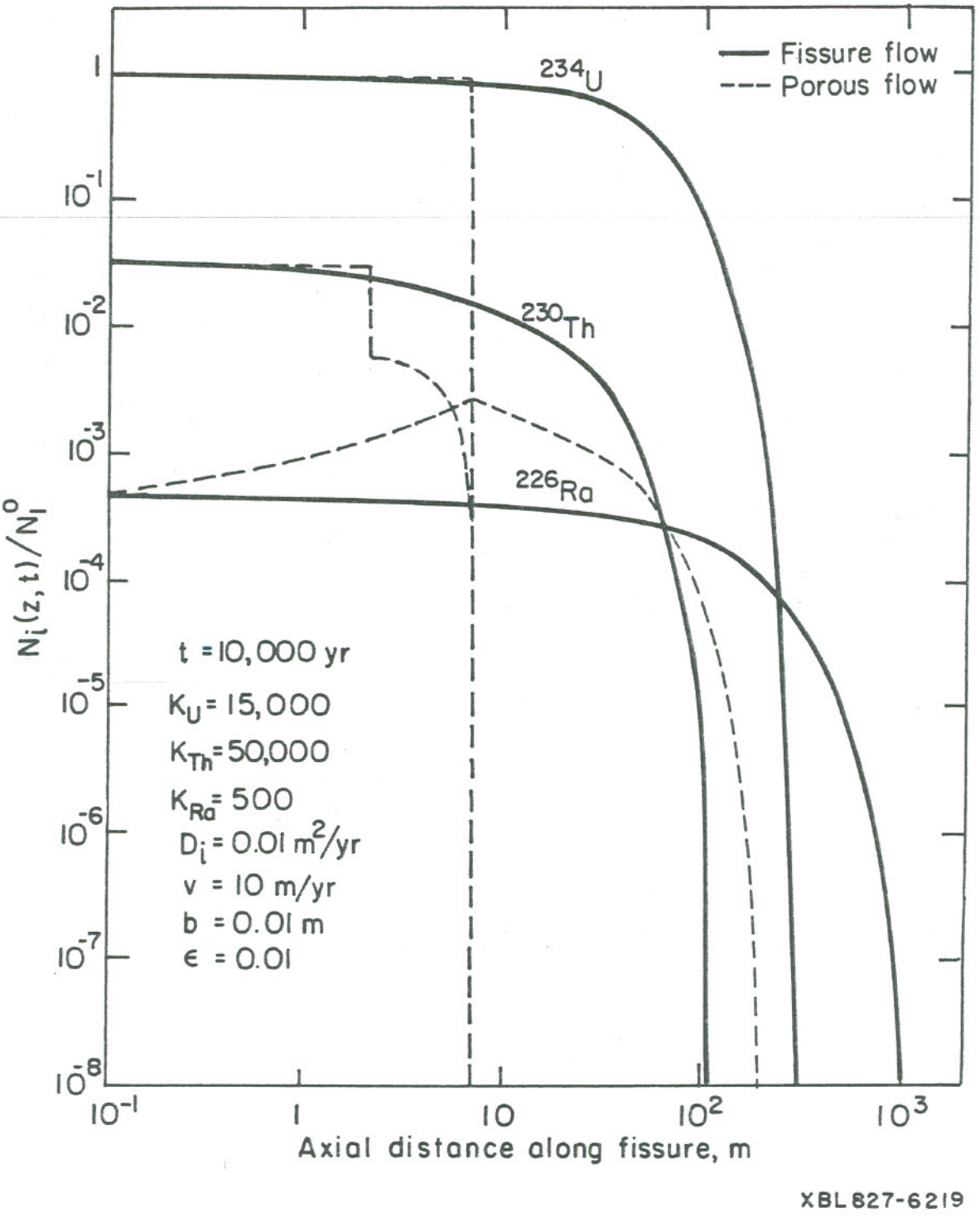

Fig. 5.10.1 Concentration profiles of the decay chain, $^{234}U \rightarrow {}^{230}Th \rightarrow {}^{226}Ra$, for a step release.

entire range of migration distance, for times smaller than and comparable to the half life.

5.10.4 Transport of Three-Member Nuclide Chain

The relative concentrations of a three member-nuclide chain $^{234}U \rightarrow {}^{230}Th \rightarrow {}^{226}Ra$ at t = 10,000 yr, with no daughter initially present, calculated from Eq. (5.10.25) for a step release, are shown as the solid lines in Fig. 5.10.1. The pore diffusivity of each nuclide is assumed to be a constant value, $D_1 = 0.01\ m^2/yr$. The other parameters used in this calculation are listed in the figure. At this assumed migration time of 10,000 yr, the water can travel in the fissure to a distance of 100,000 meters from the waste. Because of the surface retardation effect due to the molecular diffusion into the micropores, however, all of these nuclides cannot arrive at such a great distance during this time. At 200 m from the concentration of ^{234}U, waste is attenuated a thousand-fold below the concentration at the waste. Because of its relatively low assumed retardation constant, ^{226}Ra can migrate farther than its precursor nuclides ^{234}U and ^{230}Th. The dashed lines show the concentration profiles of the nuclide chain calculated from the porous-flow transport model. The migration path length for each nuclide in porous-flow transport is less than for fissure-flow transport. In fissure flow transport, the maximum concentration for both parent and daughter nuclides occurs always at the waste location.

In Fig. 5.10.2, the concentration profiles of $^{237}Np \rightarrow {}^{233}U \rightarrow {}^{229}Th$ in fissure-flow transport with step release and those in porous flow transport with step release are compared.

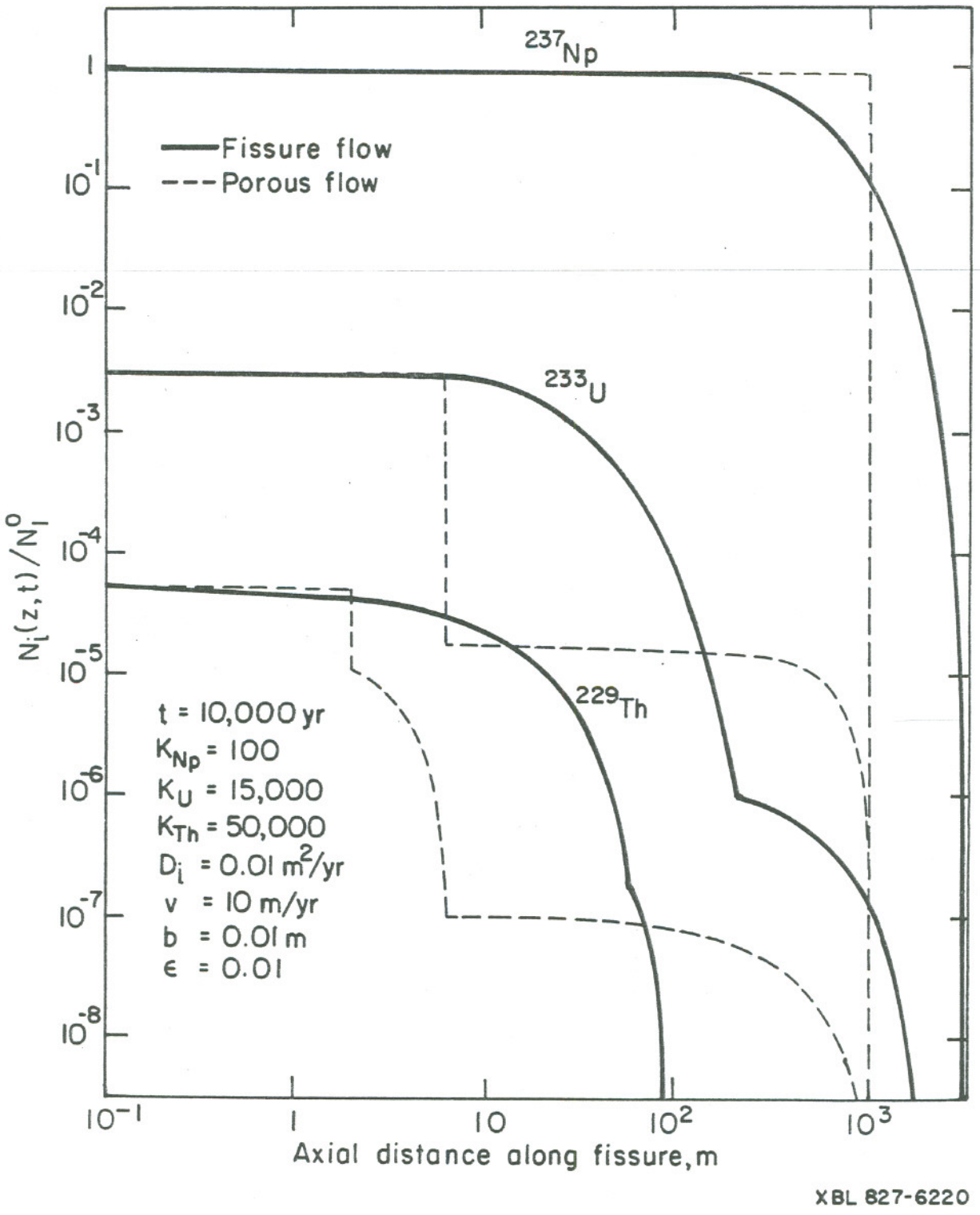

Fig. 5.10.2 Concentration profiles of the decay chain, $^{237}Np \rightarrow {}^{233}U \rightarrow {}^{229}Th$, for a step release.

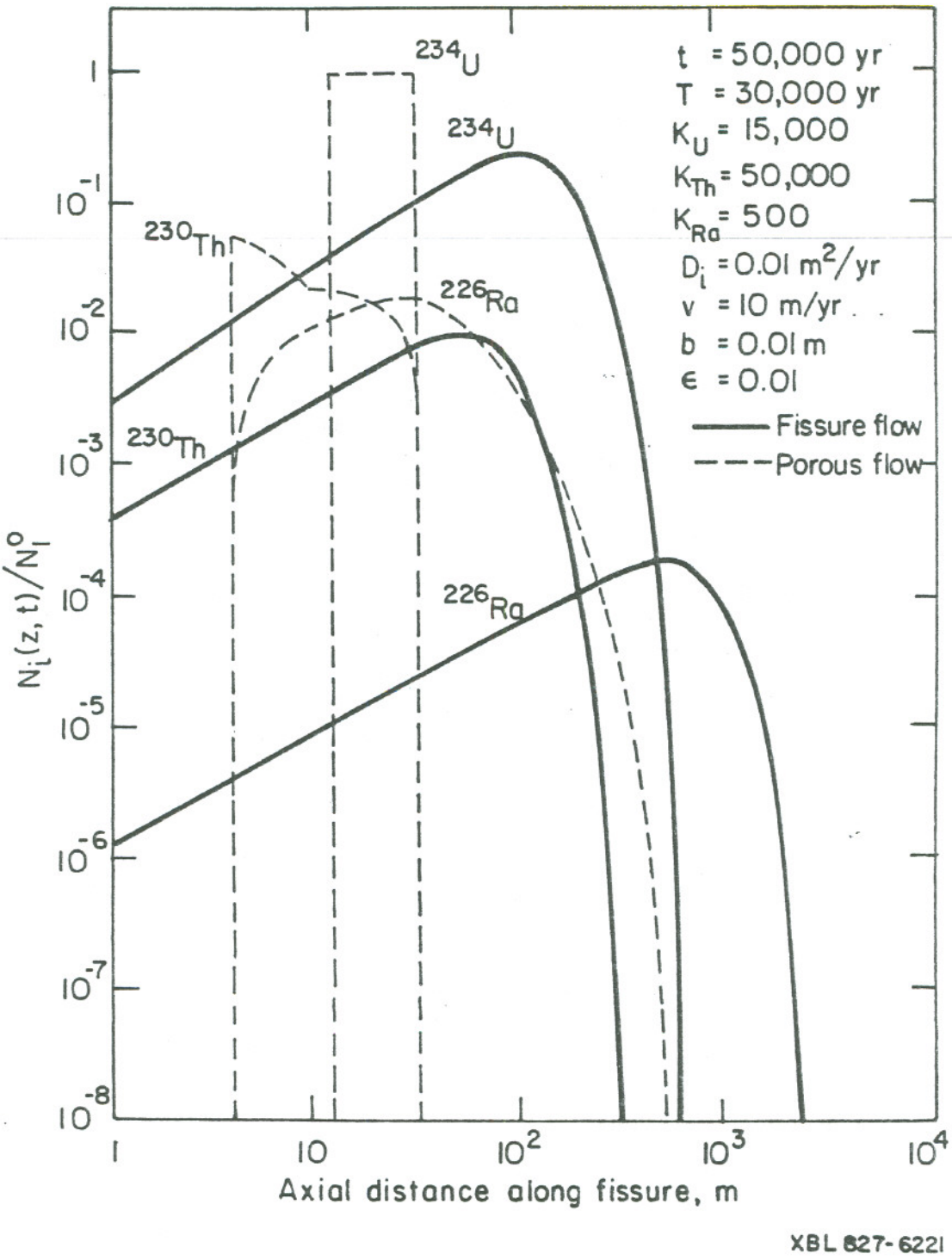

Fig. 5.10.3 Concentration profiles of the decay chain, $^{234}U \rightarrow {}^{230}Th \rightarrow {}^{226}Ra$, for a band release.

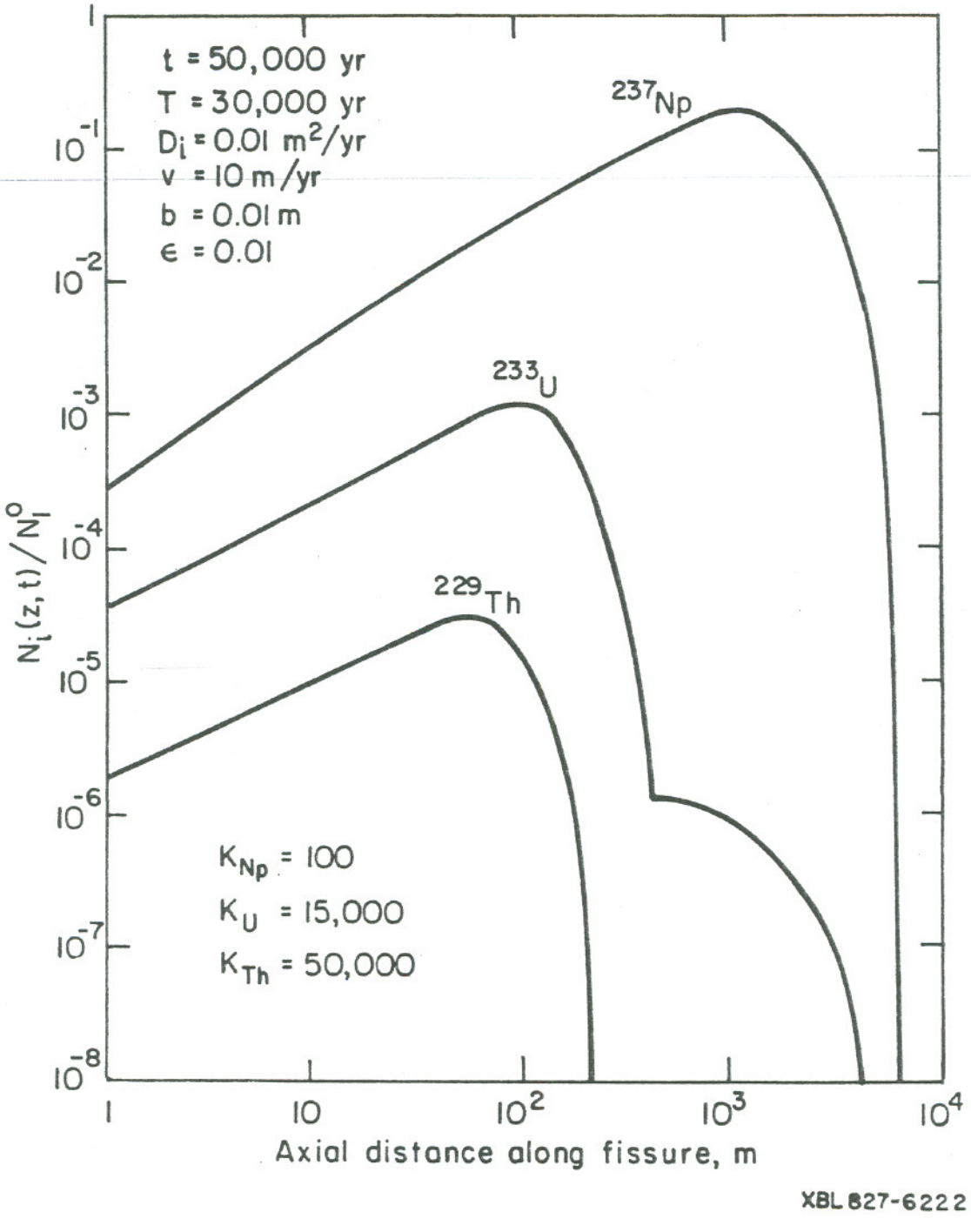

Fig. 5.10.4 Concentration profiles of the decay chain, $^{237}Np \rightarrow {}^{233}U \rightarrow {}^{229}Th$, for a band release.

The concentration profiles of $^{234}U \rightarrow {}^{230}Th \rightarrow {}^{226}Ra$ at t = 50000 yr, with no daughter nuclide initially present, calculated for a band release from Eq. (5.10.28), are shown as the solid lines in Fig. (5.10.3). The dashed curves show the concentration profiles calculated for the porous-flow transport. Assumed values used in these calculations are included in the figure. The relatively sharp concentration band of the nuclides in porous flow transport is smoothed in fissure-flow transport by pore diffusion, with a lower maximum concentration than in porous-flow transport. Even at a time exceeding the leach time, a nuclide can still remain at the waste location, because of re-release of the nuclide from the rock medium by molecular diffusion.

Concentration profiles of $^{237}Np \rightarrow {}^{233}U \rightarrow {}^{229}Th$ for a band release are shown in Fig. 5.10.4. For the nuclide ^{237}Np, with a lower retardation constant, the maximum concentration occurs at a smaller distance than expected in porous-flow transport, whereas for the daughter nuclides, ^{233}U and ^{229}Th, with higher retardation constants, the maximum concentrations are found at greater distances than in porous-flow transport. The maximum concentration of each nuclide is an order of magnitude less than in porous flow transport.

5.11 Nomenclature

a : interfacial area between stationary water and solid phases

width of waste repository/ constant defined by Eq. (5.7.33)

a_i : constant defined by Eq. (5.2.16) or by Eq. (5.9.12)

$^{m}a_i$: constant defined by Eq. (5.6.22)

$\underline{A}_i^{(j)}$: constant defined by Eq. (5.8.18)

A_ℓ^{ij} : constant defined by Eq. (5.10.20)

b : interstice of main fissure (distance between planer walls)

b_i : constant defined by Eq. (5.2.18) or by Eq. (5.9.13)

$^{m}b_i$: constant defined by Eq. (5.6.23)

b_{ji} : Bateman coefficient, Eq. (5.1.14)

$B_m^{(j)}$: constant defined by Eq. (5.8.19)

$\underline{B}_m^{(j)}$: constant defined by Eq. (5.8.19)

B_q^{ji} : constant defined by Eq. (5.9.17)

$B_i(t)$: Bateman function, Eq. (5.1.13)

c : constant defined by Eq. (5.7.32)/ integration constant in Eq. (5.5.36)

c_1 : constant defined by Eq. (5.2.29)

c_2 : constant defined by Eq. (5.2.30)

$C_i(t)$: relative concentration of nuclide i normalized by total concentration at repository

C_i^o : initial concentration of nuclide i at repository, Eq. (5.5.13)

C_{ij} : constant defined by Eq. (5.5.28)

C_ℓ^{ij} : constant defined by Eq. (5.10.13)

d : width of repository/ spacing of fissures

d_1 : constant defined by Eq. (5.7.22)

d_{qr} : constant defined by Eq. (5.9.17)

D : dispersion coefficient

D_i : molecular diffusivity of nuclide i in micropores

$^{m}D_i$: molecular diffusivity of nuclide i in micropores in the mth medium

D_{mi} : molecular diffisivity of nuclide i in water

$\underline{D}_{rm}^{(j)}$: constant defined by Eq. (5.8.20)

D_{qr} : constant defined by Eq. (5.9.17)

e_1 : constant defined by Eq. (5.7.40)

e_{qr} : constant defined by Eq. (5.9.17)

$E_1(x,\theta)$: function defined by Eq. (5.3.18)

$E_1(z,t;\alpha)$: function defined by Eq. (5.5.4)

$E(z,t;\alpha)$: function defined by Eq. (5.5.5)

$f(t;\alpha)$: function defined by Eq. (5.7.31)

$f_1^{\ell n}(z,t)$: function defined by Eq. (5.10.26)

$f_2^{\ell n}(z,t)$: function defined by Eq. (5.10.27)

$F(t;\alpha)$: function defined by Eq. (5.7.34)

$g(s)$: function defined by Eq. (5.7.30)

$\underline{g}_{rm}(t)$: function defined by Eq. (5.8.22)

$G(t;\alpha)$: function defined by Eq. (5.7.36)

$G_{r\ell}(z,t)$: function defined by Eq. (5.10.19)

h_ℓ : spacing of repositories

$h(s)$: function defined by Eq. (5.7.29)

$h(t)$: Heaviside unit step function

$H(s)$: function defined by Eq. (5.7.27)

$J_i(z,t)$: diffusive flux of nuclide i at surface of fissure

$^{m}J_i(z,t)$: diffusive flux of nuclide i at surface of fissure in mth medium

k_m : mass transfer coefficient

$K_{D,i}$: distribution coefficient

K^i : sorption equilibrium coefficient defined by Eq.(5.2.3)

L : length of waste repository in direction at water flow

$m_i(z,y,t)$: function defined in Eq. (5.4.12)

$\dot{m}_i$: release rate of nuclide i per unit time and unit cross-sectional area of water flow

$M_i(z,y,t)$: concentration of nuclide i in stationary water in micropores

$M_i^+(z,y,t)$: concentration of nuclide i in water in micropores with permeating water

$^{m}M_i(z,y,t)$: concentration of nuclide i in stationary water in micropores in mth medium

n_i : amount of nuclide i in waste per unit amount of total waste, Eq. (5.1.16)

$N_i(z,t)$: aqueous concentration of nuclide i in fissure

$^{m}N_i(z,t)$: aqueous concentration of nuclide i in fissure in mth medium

N_i : initial concentration of nuclide i at waste location

N_i^* : saturated concentration of nuclide i in water

P_i : concentration of precipitate of nuclide i

P_i^s : concentration of precipitate defined by Eq. (5.5.16)

P_i^o : initial concentration of precipitate of nuclide i

$p_i(t;\alpha)$: function defined by Eq. (5.10.18)

$P_i(t;\alpha)$: function defined by Eq. (5.2.19) or by Eq. (5.9.14)

$\underline{P}_i(t;\alpha)$: function defined by Eq. (5.4.23)

q : geometric factor, tortuosity coefficient

q_i : rate of mass transfer of nuclide i at interface between water and solid phases

$q(z)$: function defined by Eq. (5.8.15)

s : Laplace transform variable

$S_i(z,y,t)$: concentration of nuclide i in solid phase

t : migration time

t^* : duration of a finite amount of precipitate

t' : relative time defined by Eq. (5.5.22)

T : duration of release, leach time

T' : time defined by Eq. (5.5.45)

u : dummy integration variable

u, u^+, u^- : velocity of permeating water

v : velocity of water in fissure

v : water velocity main fissure at waste location

w : velocity of water in micropores

w_i : migration velocity of nuclide i defined by Eq. (5.8.17)

W_T^o : dissolution rate of total waste per unit width of fissure

x : distance in transverse direction parallel to the fissure surface

$y, y^{\pm}$: depth of rock medium, distance in rock medium measured from surface of main fissure

m_y : depth of mth rock medium

z : distance from waste in direction of water flow

z' : time variable defined by Eq. (5.8.9)

z_m : distance of interface surface of (m-1)th and mth media from waste

m_z : distance defined by Eq. (5.6.11)

α : arbitrary parameter

γ^{+}_{-} : constant defined by Eq. (5.4.14)

$\delta_{r\ell}$: constant defined by Eq. (5.10.21)

$\delta(t)$: delta function

$\underline{\Delta}_{rm}$: constant defined by Eq. (5.8.21)

ε : porosity of fractured medium excluding main fissure

$^{m}\varepsilon$: porosity of mth rock medium

ζ : dummy integration variable

η : dummy integration variable

$\eta(z,t)$: penetration thickness defined by Eq. (5.2.30)

θ : parameter in Eq. (5.3.15)/ dummy integration variable

λ_i : radioactive decay constant of nuclide i

Λ_l^m : constant defined by Eq. (5.7.4)

$\Lambda_{r\ell}$: constant defined by Eq. (5.10.15)

$\mu_{r\ell}$: constant defined by Eq. (5.10.14)

ξ : dummy integral variable

τ : resident time defined by Eq. (5.5.9)/ dummy integral variable

$\phi_i(t)$: time-dependent aqueous concentration of nuclide i at waste location

$\phi_i(t)$: time-dependent source of nuclide i

$^{m}x(t)$: function defined by Eq. (5.6.19)

ω : Fourier transform variable

5.12 Literature references

B-1 H. Bateman, "Tables of Integral Transforms", Vol. 1, McGraw-Hill Book Co., Inc. (1954).

H-1 M. Harada, P. L. Chambre', M. Foglia, K. Higashi, F. Iwamoto, D. Leung, T. H. Pigford, and D. Ting, "Migration of Radionuclides Through Sorbing Media, Analytical Solutions I", LBL-10500 (1980).

L-1 L. Lapidus and N. Amundson, "Mathematics of Adsorption in Bed VI, The Effect of Longitudinal Diffusion in Ion Exchange and Chromatographic Column", J. Phys. Chem., 56, 984 (1952).

N-1 I. Neretnieks, "Diffusion in the Rock Matrix, An Important Factor in Radionuclide Retardation", J. Geophys. Res., 85, 4379 (1980).

P-1 T. H. Pigford, P. L. Chambre', M. Albert, M. Foglia, M. Harada, F. Iwamoto, T. Kanki, D. Leung, S. Masuda, S. Muraoka, and D. Ting, "Migration of Radionuclides Through Sorbing Media, Analytical Solutions II", LBL-11616 (1980).

6. Radionuclide Transport Based on EPA Assumptions for Generic Repositories

6.1. Introduction

As technical support for its draft proposed standard for a geologic repository, EPA has applied a one-dimensional calculation to estimate the long-term release of radionuclides from conceptual repositories and to estimate the health effects therefrom (S1). EPA has included in its model the effects of solubility limit of radionuclides and the time-dependent thermally driven buoyant flow of groundwater within the host rock due to decay heat. These effects have not been included in analyses by DOE contractors (C1) of the long-term radionuclide release from conceptual repositories in salt, granite, and basalt. The EPA approach also differs in that it provides for element-specific release rates of radionuclides from the dissolving waste form, due to solubility effects, whereas the DOE contractors have assumed congruent dissolution.

However, the EPA analysis is limited to the transport of a single radionuclide, with no decay precursor, so EPA's consideration has been limited to the fission products and the first member of actinide decay chains. EPA has neglected the important daughter nuclides, such as radium-226, that contribute significantly to the total release and health effects. As an aid to understanding the EPA analysis and conclusions of the performance of conceptual repositories and the implications therefrom, we present here our derivation of the analytical solutions of radionuclide transport consistent with the assumptions stated by EPA. We have extended the EPA-type analysis to deal with the transport of radionuclide decay chains. The results are illustrated for the radionuclides considered in the EPA calculations and for the decay chains leading to radium-226.

6.2 EPA's assumptions

In reviewing EPA's calculations of the transport of radionuclides to the accessible environment, it was concluded that EPA made the following assumptions:

1. The repository is a porous medium containing a finite volume of water, in which the dissolved radionuclides are well-mixed.
2. The repository lies between an underlying lower aquifer and an overlying upper aquifer, with a natural flow of groundwater from a lower aquifer to an upper one.
3. Time-dependent thermally driven buoyant flow, due to decay heat, is superimposed on the natural flow which was described in 2.
4. Contaminated water from the repository is injected as an equivalent plane source into the upper aquifer.
5. There is one-dimensional advective transport of a radionuclide in a one-dimensional flow field in the upper aquifer.
6. The effect of dispersion is neglected.

6.3 Time-Dependent Concentrations Within The Repository

6.3.1 General Concentration Equation

Although EPA's assumption of complete mixing of water within the repository is of questionable validity, we will adopt this assumption for the purpose of developing a general analytical solution to compare with EPA's calculated results. For complete mixing within the repository, the time-dependent concentration $C_i(t)$ of radionuclide i within the repository is given by:

$$\frac{dC_i(t)}{dt} + \frac{Q_r(t)C_i(t)}{V} + \lambda_i C_i(t) = \frac{B_i(t)}{V} + \lambda_{i-1}\, C_{i-1}(t)$$

$$t > 0, \quad \lambda_0 = 0, \quad i = 1,2,3... \qquad (6.1)$$

where $Q_r(t)$ is the time-dependent volumetric flow rate of water through the repository, V is the volume of water within the repository, λ_i is the decay constant of the ith member and $B_i(t)$ is the time-dependent rate of dissolution of nuclide i within the repository. EPA's analysis does not include the terms relating to the precursor radionuclide i-1.

Assuming that at time t = 0 the dissolution begins, the initial condition is:

$$C_i(0) = 0 \quad i = 1,2,3... \tag{6.2}$$

According to our previous studies (H1,P1), the dissolution rate $B_i(t)$ can be expressed by any one of four different release modes, or by combinations thereof:

(1) band release, wherein the waste dissolution rate is constant during the leaching process, i.e., congruent release.

(2) exponential release, wherein all radionuclides in the undissolved waste undergo dissolution at the same constant fractional amount per unit time,

(3) preferential release, wherein the fractional dissolution rate constant of (2) can differ for different radionuclides,

(4) solubility-limited release, wherein the dissolution rate of each element is controlled by its solubility limit in groundwater.

Applying the technique of our earlier study (H1), the solution for Eq. (6.1) with Eq. (6.2) can be obtained recursively:

$$C_i(t) = \exp\left[-\lambda_i t - R(t)\right] \int_0^t \exp\left[\lambda_1 \tau + R(\tau)\right] x$$

$$x \left[\lambda_{i-1} C_{i-1}(\tau) + B_i(\tau)/v\right] d\tau \tag{6.3}$$

or generally

$$C_i(t) = \frac{1}{V} \exp\,[-\lambda_i t - R(t)]\ x$$

$$x \sum_{j=1}^{i} \prod_{l=j}^{i-1} \lambda_l \int_0^t \exp[(\lambda_i-\lambda_{i-1})\tau_i] \int_0^{\tau_i} \exp[(\lambda_{i-1}-\lambda_{i-2})\tau_{i-1}]x \int_0^{\tau_{i-1}} \cdots$$

$$\cdots \int_0^{\tau_{j+1}} \exp\,[\lambda_j\tau_j+R(\tau_j)]\ B_j(\tau_j)d\tau_j \cdots\cdots d\tau_{i-1}d\tau_i \qquad (6.4)$$

where

$$R(t) = \int_0^t \frac{Q_r(t)}{V}\,dt \qquad (6.5)$$

R(t) is the number of repository water volumes that have flowed through the repository during a time period t.

For a radionuclide with no precursors, i = 1, and Eq. (6.4) becomes:

$$C_1(t) = \frac{1}{V} \exp\,[-\lambda_1 t - R(t)\,] \int_0^t \exp[\,\lambda_1\tau+R(\tau)\,]\,B_1(\tau)d\tau$$

$$t > 0 \qquad (6.6)$$

For a nuclide whose concentration reaches a solubility limit C_1^*, the time-dependent concentration is studied in greater detail in Section 6.3.3.

6.3.2 Time-Dependent Flow Through The Repository

The time-dependent volumetric flow rate of water through the repository is given by:

$$Q_r(t) = k_r A_r G_r(t) \qquad (6.7)$$

where k_r (m/yr) is the time independent hydraulic conductivity (m/yr) of the repository, A_r (m^2) is the cross-sectional area of the repository, and $G_r(t)$ is the time-dependent potential gradient for flow through the repository. EPA approximates the latter by:

$$G_r(t) = a_1 e^{-\alpha_1 t} + a_2 e^{-\alpha_2 t} + G_0(1 + a_3 e^{-\alpha_3 t}) \qquad (6.8)$$

where G_0 is the constant gradient between the lower and upper aquifer, and a_i and α_i (i = 1,2,3) are constants determined empirically from separate calculations of the time-dependent thermally induced flow through the repository.

Substituting Eqs.(6.7) and (6.8) into (6.5) yields:

$$R(t) = \frac{k_r A_r}{V}\left[-\frac{a_1}{\alpha_1} e^{-\alpha_1 t} - \frac{a_2}{\alpha_2} e^{-\alpha_2 t} + G_0\left(t - \frac{a_3}{\alpha_3} e^{-\alpha_3 t}\right)\right] \qquad (6.9)$$

where R(0) = 0.

6.3.3 Concentration of a Single Radionuclide With a Solubility Limit

Here we consider the time-dependent concentration of the first member of a radionuclide chain in the repository. In EPA's model of rapid mixing of liquid and dissolved radionuclides in the repository, the concentration $C_1(t)$ of a radionuclide is initially zero at the beginning of dissolution (t = 0). It increases with time, and if it reaches a solubility limit C_1^*, it does so at a time t_1^*. From Eq. (6.9), C_1^* and t_1^* are related by:

$$C_1^* = \frac{1}{V} \exp\left[-\lambda_1 t_1^* - R(t_1^*)\right] \int_0^{t_1^*} \exp\left[\lambda_1 \tau + R(\tau)\right] R_1(\tau) d\tau \qquad (6.10)$$

The radionuclide will begin precipitating at time t_1^*. To determine the length of time that the precipitate will exist within the repository, we write a material balance on the amount $P_1(t)$ of precipitate of species 1 per unit volume of water in the repository:

$$\frac{dP_1(t)}{dt} + \frac{Q_r(t) C_1^*}{V} + \lambda_1 P_1 = \frac{B_1(t)}{V} - \lambda_1 C_1^*$$

$$t > t_1^* , \qquad (6.11)$$

The initial condition is

$$P_1(t_1^*) = 0 \tag{6.12}$$

Equation (6.11) can be solved with Eq. (6.12) to yield

$$P_1(t) = \frac{1}{V} \exp(-\lambda_1 t) \int_{t_1^*}^{t} \exp(\lambda_1 \tau) [\, B_1(\tau) - C_1^* (\lambda_1 V + Q_r(\tau)) \,] \, d\tau$$

$$t_1^* < t \,, \tag{6.13}$$

As a result of radioactive decay, convective transport from the repository, and complete dissolution of the solid waste, the precipitate will eventually dissolve at a time t_2^*, which satisfies the equation:

$$P_1(t_2^*) = 0 \quad , \; t_1^* < t_2^* \tag{6.14}$$

After the precipitate disappears, the concentration of the nuclide again becomes time-dependent, as given by Eq.(6.1) for $t > t_2^*$ and with the initial condition:

$$C_1(t_2^*) = C_1^* \tag{6.15}$$

Equation (6.1) for i = 1 is solved with the side condition Eq.(6.15) to yield:

$$C_1(t) = \frac{1}{V} \exp[-\lambda_1 t - R(t)] \left\{ \int_{t_2^*}^{t} \exp[\lambda_1 \tau + R(\tau)] \; B_1(\tau) \, d\tau + \right.$$

$$\left. + V C_1^* \exp[\lambda_1 t_2^* + R(t_2^*)] \right\}, \; t_2^* < t \tag{6.16}$$

In summary, the concentration $C_1(t)$ for a mother nuclide with a solubility limit C_1^* is given by:

$$C_1(t) = \begin{cases} \text{Eq.(6.6)} \,, & t_1^* > t > 0 \\ C_1^* \,, & t_1^* \leq t \leq t_2^* \\ \text{Eq.(6.16)} \,, & t_2^* < t \end{cases} \tag{6.17}$$

6.3.4 Approximate Solution For Concentration in the Repository

The time-dependent concentrations given in Section 6.3 and 6.5 are complicated because of the time-dependent integral R(t) of repository flow. To simplify, and to obtain a nonrecursive solution for the nuclide chain, we approximate the time-dependent normalized water flow rate $Q_r(t)/V$ by a constant value λ_r averaged over a time period from t = 0 to $t = t_f$, so that

$$\lambda_r = \frac{1}{Vt_f} \int_0^{t_f} Q_r(t')dt' \tag{6.18}$$

Substitution of (6.18) in (6.1) yields:

$$\frac{dC_i(t)}{dt} + (\lambda_r + \lambda_i)\, C_i(t) = \frac{B_i(t)}{V} + \lambda_{i-1}\, C_{i-1}\,(t)$$

$$t > 0, \quad \lambda_0 = 0\ , \quad i = 1,2,3, \ldots \tag{6.19}$$

The initial condition is the same as Eq.(6.2). Taking the Laplace transform of Eq.(6.18) with respect to time:

$$s\bar{C}_i + (\lambda_r + \lambda_1)\, \bar{C}_i = \frac{\bar{B}_i}{V} + \lambda_{i-1}\, \bar{C}_{i-1} \tag{6.20}$$

where $\bar{C}_i$ is the transformed concentration:

$$\bar{C}_i = \bar{C}_i(s) = \int_0^{\infty} \exp\,(-st)\, C_i(t)\, dt \tag{6.21}$$

From Eq.(6.20), $\bar{C}_i$ is

$$\bar{C}_i = \frac{\bar{B}_i}{V(s+k_i)} + \frac{\lambda_{i-1}\, \bar{C}_{i-1}}{s+k_i} \tag{6.22}$$

where

$$k_i = \lambda_r + \lambda_i \tag{6.23}$$

For i = 1 through n:

$$C_1 = \frac{\overline{B}_1}{V(s+k_1)}$$

$$C_2 = \frac{1}{V}\left[\frac{\overline{B}_2}{s+k_2} + \frac{\lambda_1 \overline{B}_1}{(s+k_1)(s+k_2)}\right]$$

$$C_n = \frac{1}{V}\left[\frac{\overline{B}_n}{s+k_n} + \frac{\lambda_{n-1}\,\overline{B}_{n-1}}{(s+k_{n-1})(s+k_n)} + \cdots\right.$$

$$\left. \cdots + \frac{\lambda_1 \cdots \lambda_{n-1}\,\overline{B}_1}{(s+k_1)(s+k_2)\cdots(s+k_n)}\right] \qquad (6.24)$$

The general form for C_i is:

$$\overline{C}_i = \frac{1}{V\lambda_i} \sum_{j=1}^{i} \frac{\left(\prod_{k=j}^{i} \lambda_k\right) \overline{B}_j}{\prod_{1=j}^{i} (s+k_1)} \qquad (6.25)$$

By using the same technique as in our previous report (H1, p4-40), Eq.(6.25) can be rewritten as

$$\overline{C}_i = \frac{1}{V\lambda_i} \sum_{j=1}^{i} E_j{}^i \sum_{1=j}^{i} F_{j1}{}^i \frac{\overline{B}_j}{s+k_1} \qquad (6.26)$$

where:

$$E_j{}^i = \prod_{q=j}^{i} \lambda_q \qquad (6.27)$$

$$F_{j1}{}^i = \left[\prod_{\substack{q=j \\ q\neq 1}}^{i} (k_q - k_1)\right]^{-1} \qquad (6.28)$$

The inverse of Eq.(6.26) is

$$C_i(t) = \frac{1}{V\lambda_i} \sum_{j=1}^{i} E_j{}^i \sum_{1=j}^{i} F_{j1}{}^i \exp(-k_1 t) \circledast B_j(t) \qquad (6.29)$$

where

$$\exp(-k_1 t) \circledast B_j(t) \equiv \int_0^t \exp(-k_1 t) B_j(t-\tau) d\tau \qquad (6.30)$$

Equation (6.29) is the general expression of the approximate solution for the radionuclide concentration in the repository, under the constant-flow approximation. As mentioned in Section 6.3 we have four different dissolution modes for $B_i(t)$. The constant-flow solution for the three different release modes which does not include the solubility limits of individual radionuclides is derived below.

(a) Band release mode: Here $B_i(t)$ is given by

$$B_i(t) = \frac{n_i(t) M^0}{T} [h(t)-h(t-T)] \qquad (6.31)$$

and

$$n_i(t) = \sum_{j=1}^{i} b_{ij} \exp(-\lambda_j t) \qquad (6.32)$$

where $n_i(t)$ is the concentration of nuclide i in the solid waste, M^0 is the initial amount of waste, h(t) is the Heaviside step function, T is the leach time, i.e., the time for total dissolution, and b_{ij} is the Bateman coefficient

$$b_{ij} = \sum_{m=1}^{j} n_m^0 \frac{1}{\lambda_i} \left[\prod_{q=m}^{i} \lambda_q \Big/ \prod_{\substack{l=m \\ l \neq j}}^{i} (\lambda_l - \lambda_j) \right] \qquad (6.33)$$

By substituting (6.31) in (6.29) one obtains the concentration of nuclide i in the repository as

$$C_i(t) = \frac{M^0}{VT\lambda_i} \sum_{j=1}^{i} E_j^i \sum_{l=j}^{i} F_{jl}^i \sum_{m=1}^{j} \left(\frac{b_{jm}}{\lambda_m - k_l} \right) W_{lm}(t) \qquad (6.34)$$

where $W_{lm}(t)$ is:

$$W_{lm}(t) = [\exp(-k_l t) - \exp(-\lambda_m t)]\, h(t) -$$

$$- \exp(-k_l T)\, [\exp(-k_l (t-T)) - \exp(-\lambda_m (t-T))]\, h(t-T) \qquad (6.35)$$

(b) Exponential release mode: In this case the $B_i(t)$ is defined as

$$B_i(t) = f n_i(t) M^0 h(t) \tag{6.36}$$

and

$$n_i(t) = \sum_{j=1}^{i} b_{ij} \exp(-\Omega_j t) \tag{6.37}$$

where f is the fractional release rate for all nuclides, and Ω_j is

$$\Omega_j \equiv \lambda_1 + f \tag{6.38}$$

The Bateman coefficient b_{ij} is given by Eq.(6.33).

The concentration of nuclide i in the repository is then

$$C_i(t) = \frac{fM^0}{V\lambda_i} \sum_{j=1}^{i} E_j^i \sum_{l=j}^{i} F_{jl}^i \sum_{m=1}^{j} \frac{b_{jm}}{\Omega_m - k_l} X_{lm}(t) \tag{6.39}$$

where $X_{lm}(t)$ is

$$X_{lm}(t) = \left[\exp(-k_l t) - \exp(-\Omega_m t)\right] h(t) \tag{6.40}$$

(c) Preferential release mode: For this release mode the $B_i(t)$ is given by

$$B_i(t) = f_i n_i(t) M^0 h(t) \tag{6.41}$$

and

$$n_i(t) = \sum_{j=1}^{i} b_{ij} \exp(-\Omega_j t) \tag{6.42}$$

where

$$\Omega_j \equiv \lambda_j + f_j \tag{6.43}$$

The Bateman coefficient b_{ij} now becomes:

$$b_{ij} = \sum_{m=1}^{j} \left\{ N_m^0 \left[\prod_{q=m}^{i} \lambda_q \Big/ \prod_{\substack{l=m \\ l \neq j}}^{i} (\Omega_l - \Omega_j) \right] \left(\frac{f_i}{f_m} \right) \right\} \tag{6.44}$$

The concentration of nuclide i in the repository is then

$$C_i(t) = \frac{f_i M^o}{V\lambda_i} \sum_{j=1}^{i} E_j^i \sum_{l=j}^{i} F_{jl}^i \sum_{m=1}^{j} \left(\frac{b_{jm}}{\Omega_m - k_l}\right) Y_{lm}(t) \qquad (6.45)$$

where $Y_{lm}(t)$ is

$$Y_{lm}(t) = \left[\exp(-k_l t) - \exp(-\Omega_m t)\right] h(t) \qquad (6.46)$$

6.4 Far-Field Concentration of Radionuclides

6.4.1 Exact Solution for a Single Nuclide

The contaminated water from the repository is assumed to mix uniformly with the upper aquifer which it crosses. The mixing point is designated by z = 0. Assuming that the flow rate Q_a of the upper aquifer is constant and is much greater than the repository flow rate $Q_r(t)$, the concentration boundary condition $N_i(0,t)$ in the upper aquifer at z = 0 is:

$$N_i(0,t) = \frac{C_i(t)Q_r(t)}{Q_a}, \quad t > 0 \qquad (6.47a)$$

The governing equation in the one-dimensional flow field without dispersion given by:

$$\frac{\partial N_i}{\partial t} + v_i \frac{\partial N_i}{\partial z} + \lambda_i N_i = \frac{K_{i-1}}{K_i} \lambda_{i-1} N_{i-1}, \text{ with } \lambda_o = 0 \quad i=1,2,3... \qquad (6.47b)$$

By substituting the $C_1(t)$ given by Eq.(6.6), and the general solution to the above transport problem (H1, Eq.(6.11)) one obtains

$$N_1(z,t) = \frac{1}{VQ_a} \exp\left[-\lambda_1 t - R(t-z/v_1)\right] Q_r(t-z/v_1) \; x$$

$$x \int^{t-z/v_1} \exp\left[\lambda_1 \tau + R(\tau)\right] B_1(\tau) d\tau, \quad t > z/v_1 \qquad (6.48)$$

where z is the distance from the discharge point in the upper aquifer, and v_1 is the migration velocity of nuclide 1:

$$v_1 = v/K_1 \tag{6.49}$$

where v is the pore velocity in the upper aquifer and K_1 is the sorption retardation constant for nuclide 1. In general, for local sorption equilibrium

$$v_i = v/K_i \tag{6.50}$$

The far-field concentration $N_1(z,t)$ of the mother nuclide with a solubility limit is obtained by substituting the $C_1(t)$ from Eq.(6.17) into (6.47a);

$$N_1(z,t) = \text{Eq.(6.48)} \quad , \; 0 < t-z/v_1 < t_1^* \tag{6.51a}$$

$$= \frac{C_1^* \, Q_r(t-z/v_1)}{Q_a} \exp\,(-\lambda_1 \, z/v_1) \quad ,$$

$$t_1^* \leq t-z/v_1 \leq t_2^* \tag{6.51b}$$

$$= \frac{Q_r(t-z/v_1}{} \exp\left[-\lambda_1 t - R(t-z/v_1)\right] \quad x$$

$$x\left\{\int_{t_2^*}^{t-z/v_1} \exp\left[\lambda_1\tau + R(\;\;)\right] B_1(\tau)d\tau + VC_1^* \exp\left[\lambda_1 t_2^* + R(t_2^*)\right]\right\}$$

$$, \; t_2^* < t-z/v_1 \tag{6.51c}$$

Equations (6.48) and (6.51b,c) have been numerically integrated to obtain the results shown later in Section 6.5.

6.4.2 Approximate Solution for Daughter Nuclides

For the daughter radionuclides we adopt the approximation in Section 6.3.4 that the repository flow rate Q_r is constant. Substituting

into Eq.(6.47) the equations (6.34), (6.39), and (6.45) derived for band exponential, and preferential release modes, respectively, one obtains the general expression for the concentration of the above release modes as:

$$N_i(z,t) = \frac{\lambda_w M^o}{VQ_a} \exp(-\lambda_i z/v_i) \sum_{j=1}^{i} E_j^i \sum_{l=j}^{i} F_{jl}^i \times$$

$$\times \sum_{m=1}^{j} \frac{b_{jm}}{\lambda_m - k_l} \chi_{lm}(t-z/v_i) h(t-z/v_i) +$$

$$+ \frac{\lambda_w M^o}{VQ_a} \sum_{j=1}^{i} A_i^j \sum_{m=j}^{i} (\exp(-\lambda_m z/v_m)/B_m^j) \sum_{\substack{l=j \\ l\neq m}}^{i} D_{lm}^j \times$$

$$\times \sum_{p=1}^{j} E_p^i \sum_{q=p}^{j} F_{qp}^j \sum_{s=1}^{p} \frac{b_{ps}}{\Omega_s - k_q} \times$$

$$\times \int_0^t g_{lm}(\tau) \chi_{qs}(t-\tau) Q_r(t-\tau) d\tau \qquad (6.52)$$

where $N_i(z,t)$ is the concentration of nuclide i at distance z and time t, and

$$\lambda_w = \begin{cases} 1/T \text{ ; band release} \\ f \text{ ; exponential release} \\ f_i \text{ ; preferential release} \end{cases} \qquad (6.53)$$

$$A_j^i = \prod_{q=j}^{i-1} (\lambda_q / v_q) \qquad (6.54)$$

$$B_m^j = \prod_{\substack{q=j \\ q\neq m}}^{i} (1/v_q - 1/v_m) \qquad (6.55)$$

$$D_{lm}^j = \left[\prod_{\substack{q=j \\ q\neq m, l\neq m}}^{i} (\Delta_{qm} - \Delta_{lm}) \right]^{-1} \qquad (6.56)$$

$$g_{lm}(t) = \exp\left[-\Delta_{lm} (t-z/v_m)\right] h(t-z/v_m) \qquad (6.57)$$

$$\Delta_{lm} = \frac{(\lambda_l/v_l - \lambda_m/v_m)}{(1/v_l - 1/v_m)} \tag{6.58}$$

$$\chi_{qs} = \begin{cases} W_{qs}; \text{ band release} \\ \chi_{qs}; \text{ exponential release} \\ Y_{qs}; \text{ preferential release} \end{cases} \tag{6.59}$$

The convolution integral in Eq.(6.52) has been performed analytically, and $N_i(z,t)$ can be easily calculated from Eq.(6.52).

6.5 Numerical Demonstration Using EPA Parameters

Here we demonstrate the application of the foregoing analytical equations to calculate the time-dependent concentrations and cumulative releases of radionuclides from the generic repositories considered by EPA. The same parameters adopted by EPA (S1) were used in numerical evaluations. Principal assumptions and parameters are:

1. The repository contains unreprocessed spent fuel initially containing 100,000 Mg of uranium.
2. Dissolution begins 500 years after emplacement.
3. Dissolution follows the exponential release mode, with a rate constant $f = 10^{-4}$/yr.
4. The effective transport distance in upper aquifer from the mixing point z=0 to the biosphere is 1600 m.
5. The average groundwater velocity in the upper aquifer is 2.1 m/yr, resulting in a water transport time to the biosphere of 760 years.

Table 6.1 shows the radionuclide inventories (S1), sorption retardation constants (S1), solubilities (S1), and health effects per curie released to the environment (S2) used by EPA.

Table 6.1 EPA's Properties of Radionuclides [a/]

Nuclide	Half Life	Inventory	Retardation Coefficient	Solubility Limit	Health Effect Factor
	Yr	Ci		ppm	
C-14	5730	2.8×10^{4}	1	-	4.58×10^{-2}
Sr-90	28	6.0×10^{9}	1	-	1.21×10^{-1}
Zr-93	1.5×10^{6}	1.9×10^{5}	100	0.001	-
Tc-99	2.12×10^{5}	1.4×10^{6}	1	0.001	2.86×10^{-4}
Sn-126	1.0×10^{5}	5.6×10^{4}	10	1.0	1.20×10^{-1}
I-129	1.7×10^{7}	3.8×10^{3}	1	-	1.09×10^{-2}
Cs-135	2.0×10^{6}	2.3×10^{5}	1	-	3.83×10^{-3}
Cs-137	30.2	8.6×10^{9}	1	-	1.98×10^{-2}
U-234	2.5×10^{5}	1.5×10^{5}	100	-	-
Np-237	2.1×10^{6}	3.3×10^{4}	100	0.001	5.98×10^{-1}
Pu-238	86.4	2.2×10^{8}	100	0.001	2.29×10^{-2}
Pu-239	2.44×10^{4}	3.3×10^{7}	100	0.001	6.93×10^{-2}
Pu-240	6600	4.9×10^{7}	100	0.001	6.54×10^{-2}
Pu-242	3.87×10^{5}	1.7×10^{5}	100	0.001	6.77×10^{-2}
Am-241	458	1.7×10^{8}	100	50	7.31×10^{-1}
Am-243	7370	1.7×10^{6}	100	50	2.77
Ra-226	1620	-	1	-	3.11

a/ All values, except for radium-226, were taken from (S1). For radium the retardation coefficient is set to be equal to that of strontium, and the health effects factor is derived from data in (S2).

6.5.1 Repository Characteristics and Groundwater Flow Specifications

Two different conceptual repository sites were considered by EPA which are discussed here. The first site considered is basalt which is characterized as a host rock of high permeability (conductivity) and with an underlying aquifer. The second site is granite which has a low permeability and no underlying aquifer. EPA assumes that those of a geological characteristic are identical to basalt site. For the same retardation constants and solubilities calculated results for EPA's basalt repository will be identical to EPA's tuff repository. EPA also considers a salt repository, but the emphasis is on the unexpected failure mechanisms so the salt repository is not considered here.

Eqs.(6.7) and (6.8) are the governing equations for the thermally driven buoyant flow in basalt and granite repositories respectively. Fig. 6.1 shows the buoyant flow as a function of time given by Eqs.(6.7) and (6.8) and are shown for these sites. Empirical constants of Eq.(6.8), dimensions of the repositories, and the conductivities of host rocks are listed in Table 6.2. EPA has adopted for granite a hydraulic conductivity and hydraulic gradient which is tenfold smaller than that of a basalt site. Water flowrate in the basalt repository decreases by about tenfold during the thermal period. After 20,000 years of implacement a constant flowrate of 2,400 m^3/yr is obtained. In the first two hundred years after waste implacement the water flow rate in the granite repository is 1/100 that of the basalt site. The water flow rate in granite decreases rapidly thereafter and eventually reaches zero. This is caused by lack of lower aquifer to supply water.

Dissolution of the radioactive waste is assumed to begin 500 years after waste implacement. The flowrates through the repositories are

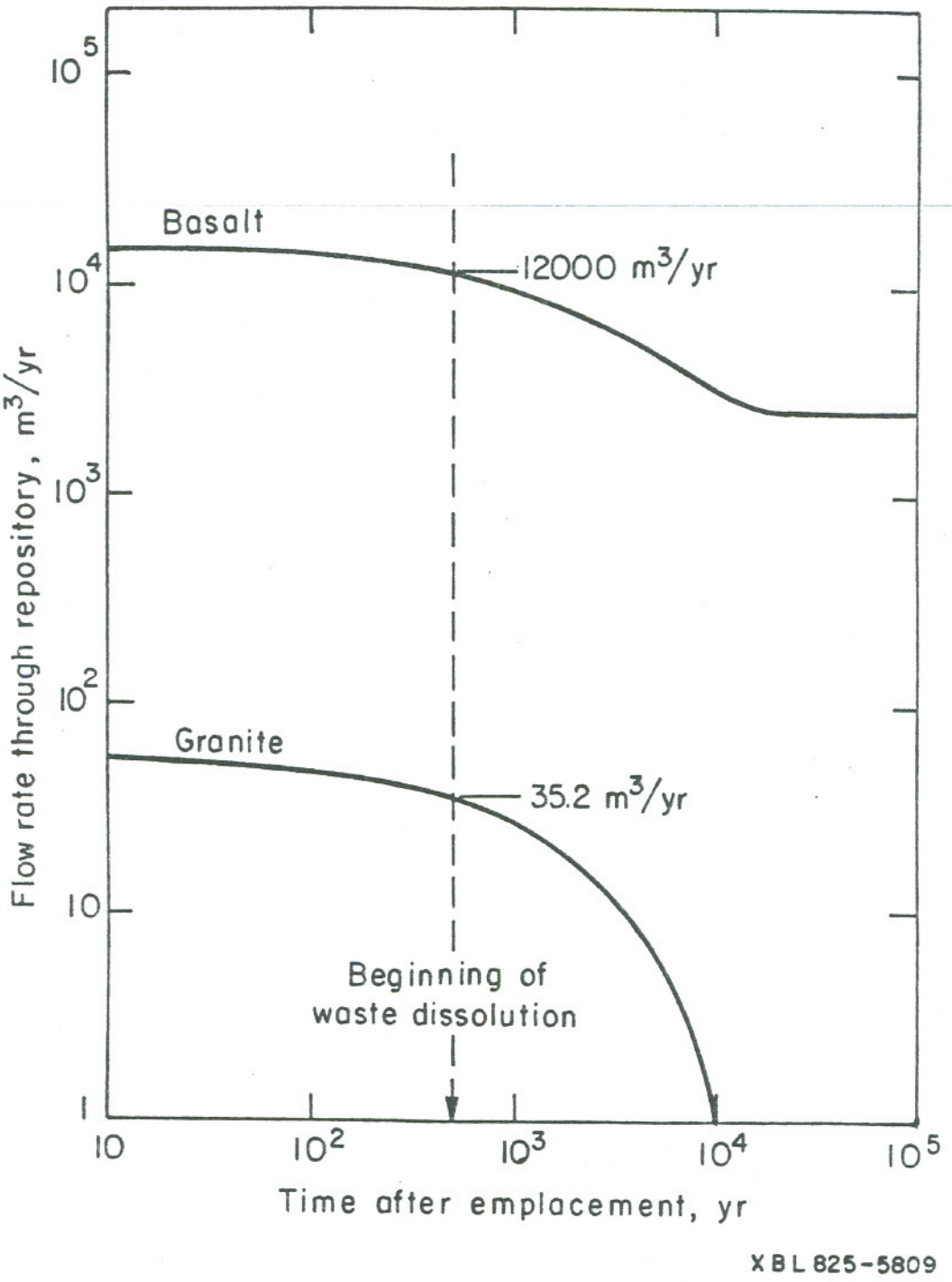

Fig. 6.1 Time-dependent flow through repository (EPA calculation(S1))

Table 6.2 Parameters used by EPA in calculating thermally driven buoyant flow (S1)

		basalt	granite
Empirical constants for thermally driven buoyant gradient	a_1	1.32×10^{-1}	1.32×10^{-2}
	a_2	1.02×10^{-1}	1.02×10^{-2}
	a_3	2.88	-
	α_1, yr^{-1}	1.6×10^{-3}	
	α_2, yr^{-1}	3.1×10^{-4}	
	α_3, yr^{-1}	2.6×10^{-4}	
Constant gradient from lower aquifer	G_0	1.0×10^{-1}	-
Conductivity of host rock	k_r, m/yr	3.0×10^{-3}	3.0×10^{-4}
Cross-sectional area of repository	A_r, m^2	8.0×10^{6}	
Volume of water in the repository	V, m^3	2.0×10^{6}	
Holdup time of repository water, yr, at 500 yr		1.67×10^{2}	5.7×10^{4}

12,000 m^3/yr for basalt and 35.2 m^3/yr for granite.

6.5.2 Radionuclide Concentrations

Fig. 6.2 shows the variation of the concentration of plutonium-239 in the repositories with time, in absence of solubility limit. The higher concentration of Pu^{239} in the granite repository is due to lower groundwater flow in the site. Figure 6.3 shows the calculated time-dependent rate of discharge of plutonium-239 from the dissolving waste and from the repository, neglecting the plutonium solubility limit. The discharge rate of plutonium-239 from the dissolving waste to the repository water is almost the same as the discharge rate from the repository to the upper aquifer, because of the relatively small assumed holdup time of the groundwater in the basalt repository. From EPA's data we estimate a holdup time of groundwater in the basalt repository of 170 yr at the beginning of dissolution, increasing to 830 yr at 20,000 yr after emplacement. The discharge rate in the basalt repository will decrease eventually because of the exponentially decreasing dissolution rate of the undissolved waste.

From the EPA data we estimate the holdup time of groundwater in the granite repository to be about 6×10^4 yr when dissolution begins, increasing to 2×10^6 yr at 10,000 yr after emplacement. Because of this relatively long holdup time, the increase in the concentration and discharge rate in granite is slower than that of a basalt repository. During the period of concentration increase, the groundwater flowrate is continuously decreasing, and the product of the concentration (Fig.6.2) and flowrate in (Fig.6.1) yields a maximum at about 2,500 yr. As the flowrate tends to zero so does the product of concentration and flowrate. After 10^4 yrs radioactive decay of plutonium-239 further decreases this product.

EPA assumes a plutonium solubility of 1 part per billion (ppb) in

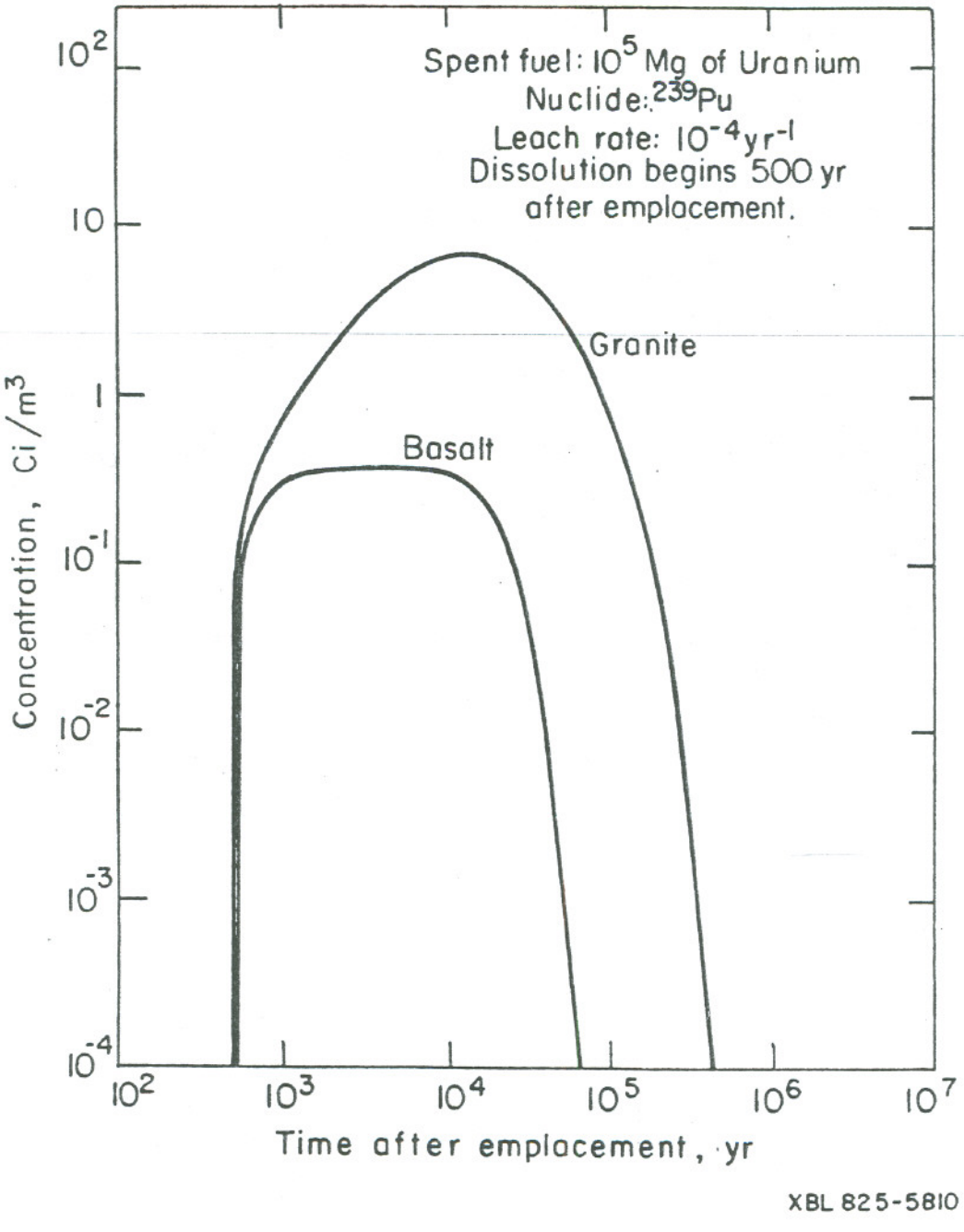

Fig. 6.2 Time-dependent concentration of ^{239}Pu in repository

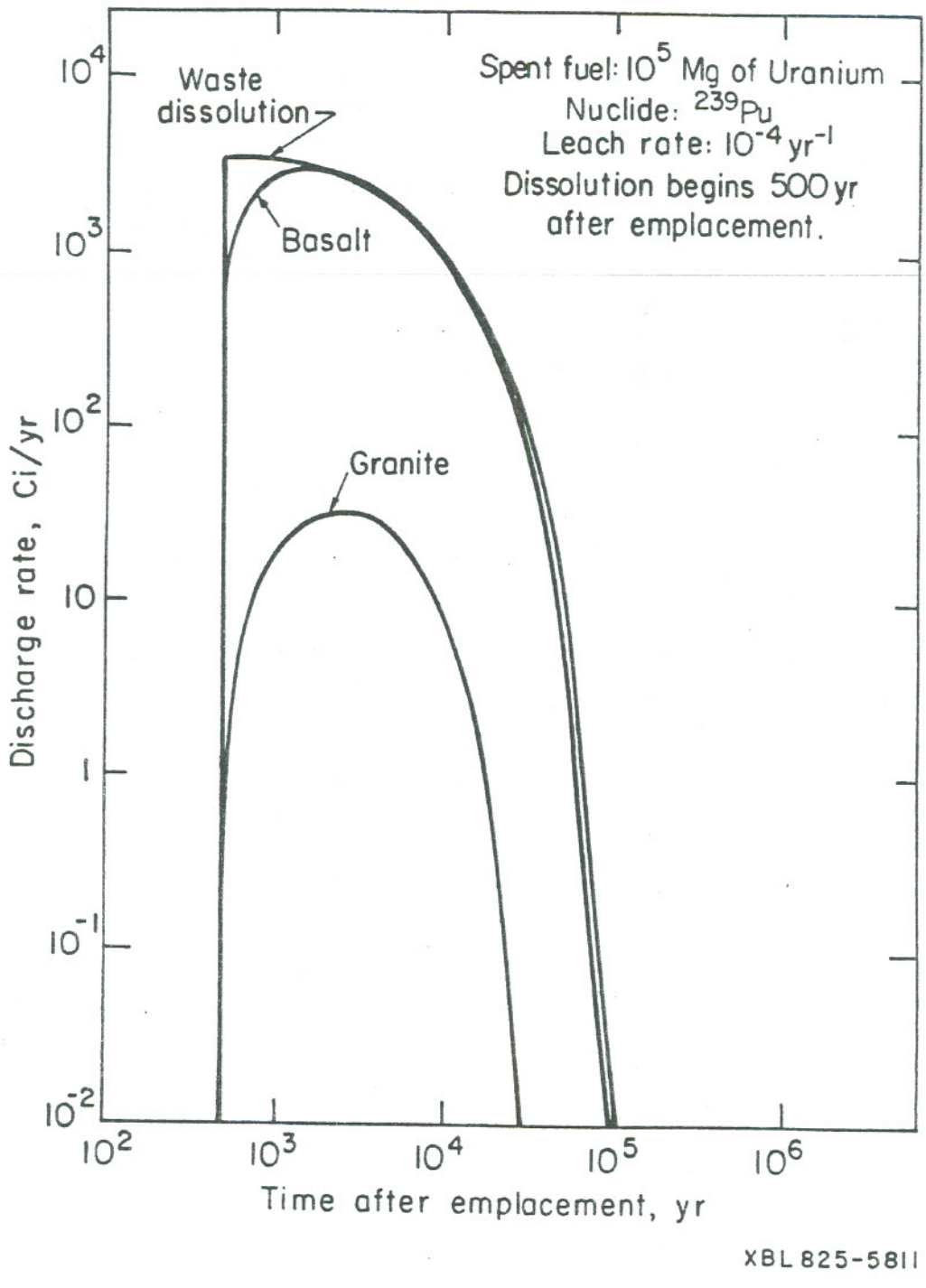

Fig. 6.3 Discharge rate of ^{239}Pu from repository

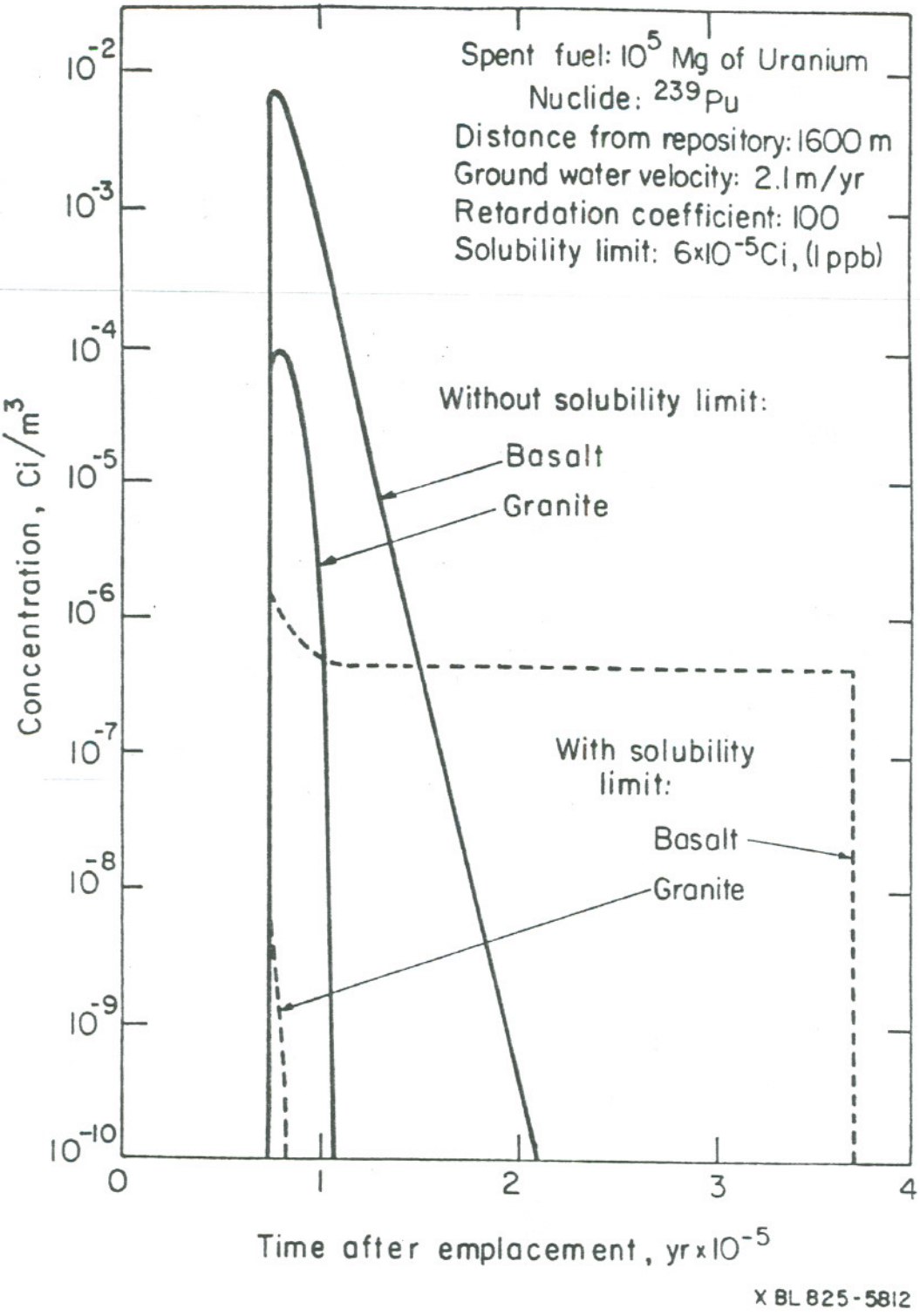

Fig. 6.4 Concentrations of 239-Pu reaching the biosphere, with and without solubility limit

groundwater, which corresponds to 6×10^{-5} Ci/m^3 for plutonium-239. Solubility interference from other plutonium isotopes is neglected. The calculated concentrations shown in Fig. 6.2 for basalt and granite repositories exceed the solubility, so the results shown in Figs. 6.2 and 6.3 are unrealistically high. The calculated concentrations of plutonium-239 at EPA's assumed distance of 1600 m to the biosphere are shown in Fig. 6.4. The concentrations are calculated with and without the solubility limit. There is a thousand fold reduction in maximum concentration due to solubility limit. For basalt, the solubility limit causes an increase in discharge of Pu^{239} to the biosphere. This is due to formation of precipitate in the repository. This broadening of the release band is not seen for granite within the concentration range of Fig. 6.4. The solubility limit greatly decreases the maximum concentration of plutonium discharged to the environment from EPA's granite repository, because the lower water flow rate through granite reduces the rate of dissolution of plutonium and the rate of discharge of plutonium to the upper aquifer.

6.5.3 Cumulative Releases

In EPA's analysis, the cumulative amount of radionuclides released during 10,000 years is used to evaluate the total health effects from the geologic repository. Here we will calculate the cumulative release as a function of time, but the time period of this release will not be arbitrarily terminated at 10,000 years.

The cumulative release $U_i(z,t)$ of radionuclide i at position z and up to time t is obtained by:

$$U_i(z,t) = Q_a \int_0^t N_i(z,\tau)d\tau \qquad (6.60)$$

Fig. 6.5 shows the increase of the cumulative release with time at z = 1600 m for basalt; similar results for granite are shown in Fig. 6.6. Parameters

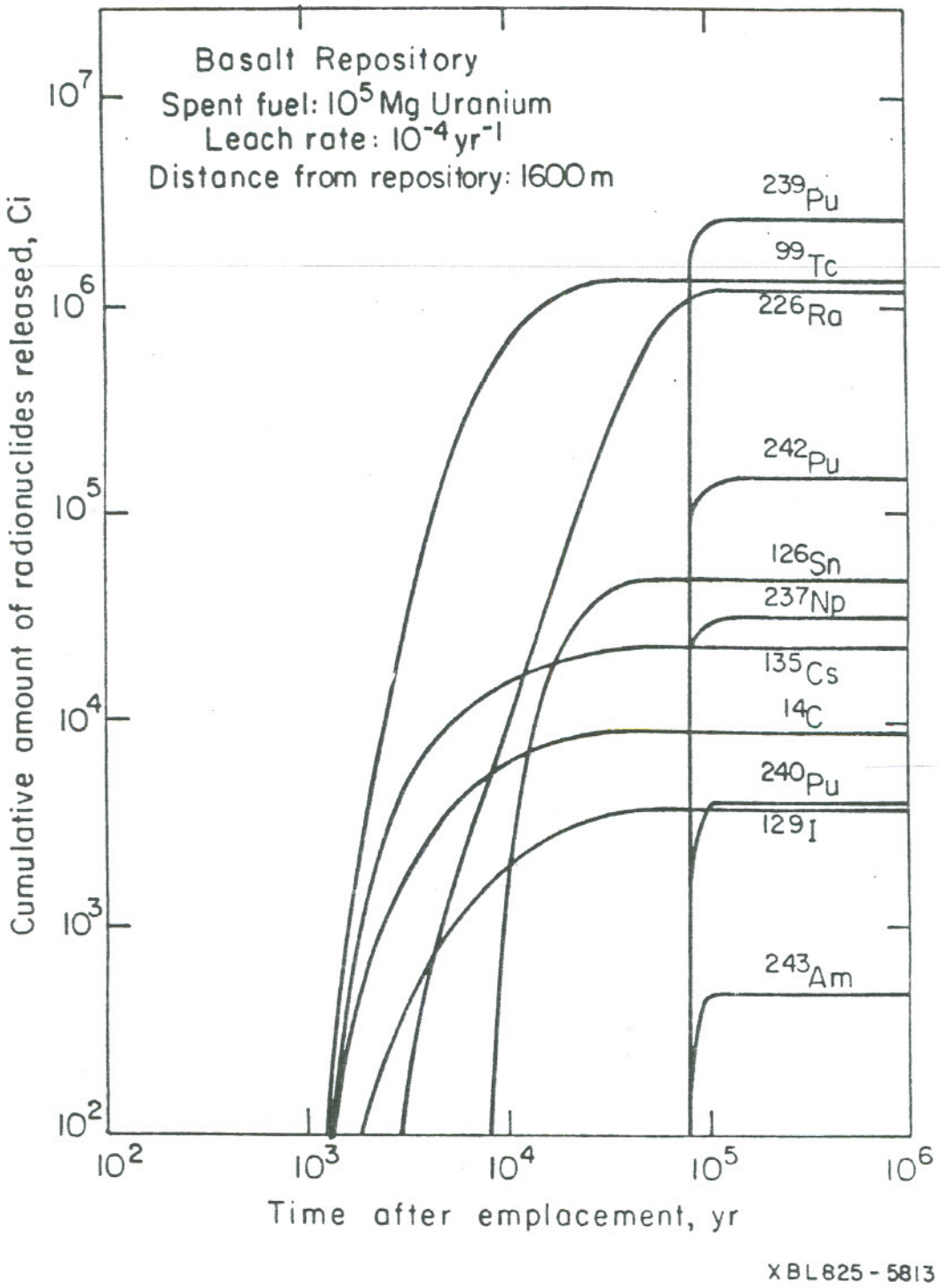

Fig. 6.5 Cumulative amount of radionuclides released from EPA's basalt repository, without solubility limit.

used by EPA (S1) in calculating these releases are listed in Table 6.2. As shown in Figs. 6.6 and 6.7, carbon-14, technetium-99, iodine-129, and cesium-135, which are the radionuclides with no sorption retardation, appear in the environment after a time delay of 1262 yrs, which is the sum of two delay times, a 500-year delay in the onset of dissolution plus EPA's assumed water transport time of 762 years. The Tin-126 with assumed retardation constant of 10 is released to the biosphere after 8100 years. EPA assumes retardation constants of 100 for the actinides, so actinides are released to the biosphere after 76,700 years. Consequently, health effects from released actinides do not enter into EPA's analysis of the potential health effects of its conceptual repositories, because EPA does not consider radionuclides released after 10,000 years.

EPA's analysis (S1) does not include radium-226, possibly because this radionuclide is not the first member of a decay chain. Radium-226 is not initially present in the radioactive waste, but is a decay product of plutonium-238, americium-242m, and curium-242, which are present in the waste. Although the precursors of radium-226 are all actinides and, according to EPA's assumptions, until well after EPA's cut-off time of 10,000 years, the daughter radium-226 is more mobile and must be considered. In our analysis we include the effect of Ra^{226}. We assume that the radium sorption constant is the same as that of the other alkaline earth, e.g., strontium, for which EPA assumes no retardation, i.e., $K = 1$. On this basis some amount of radium will appear in the environment, along with the other non-sorbing radionuclides, after 1,260 years.

The curves for radium-226 in Figs. 6.5 and 6.6 are examples of the application of the equations developed in this chapter for the transport of radionuclides in a decay chain of arbitrary length. In the first 1000 years

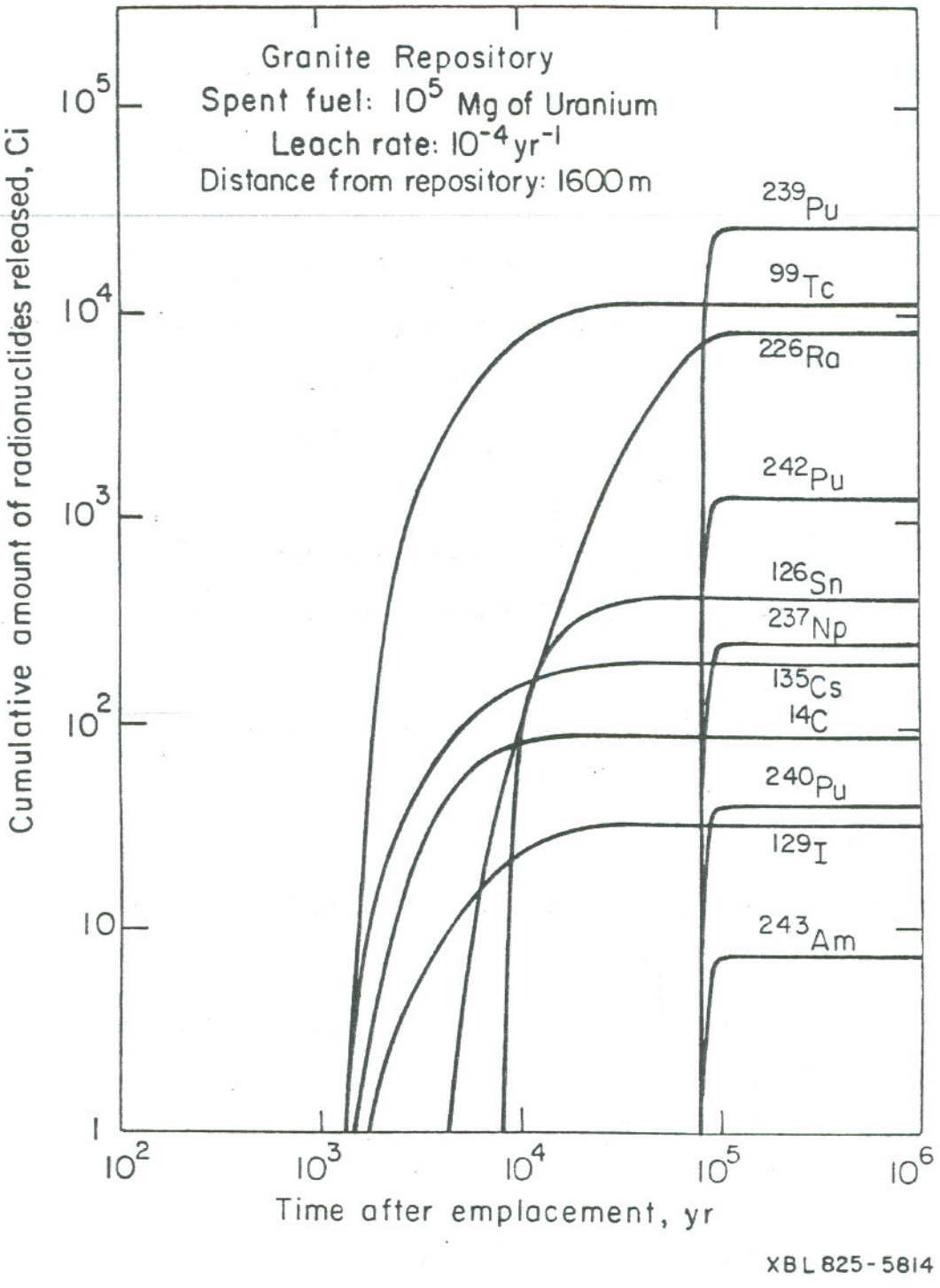

Fig. 6.6 Cumulative amount of radionuclides released from EPA's granite repository, without solubility limit.

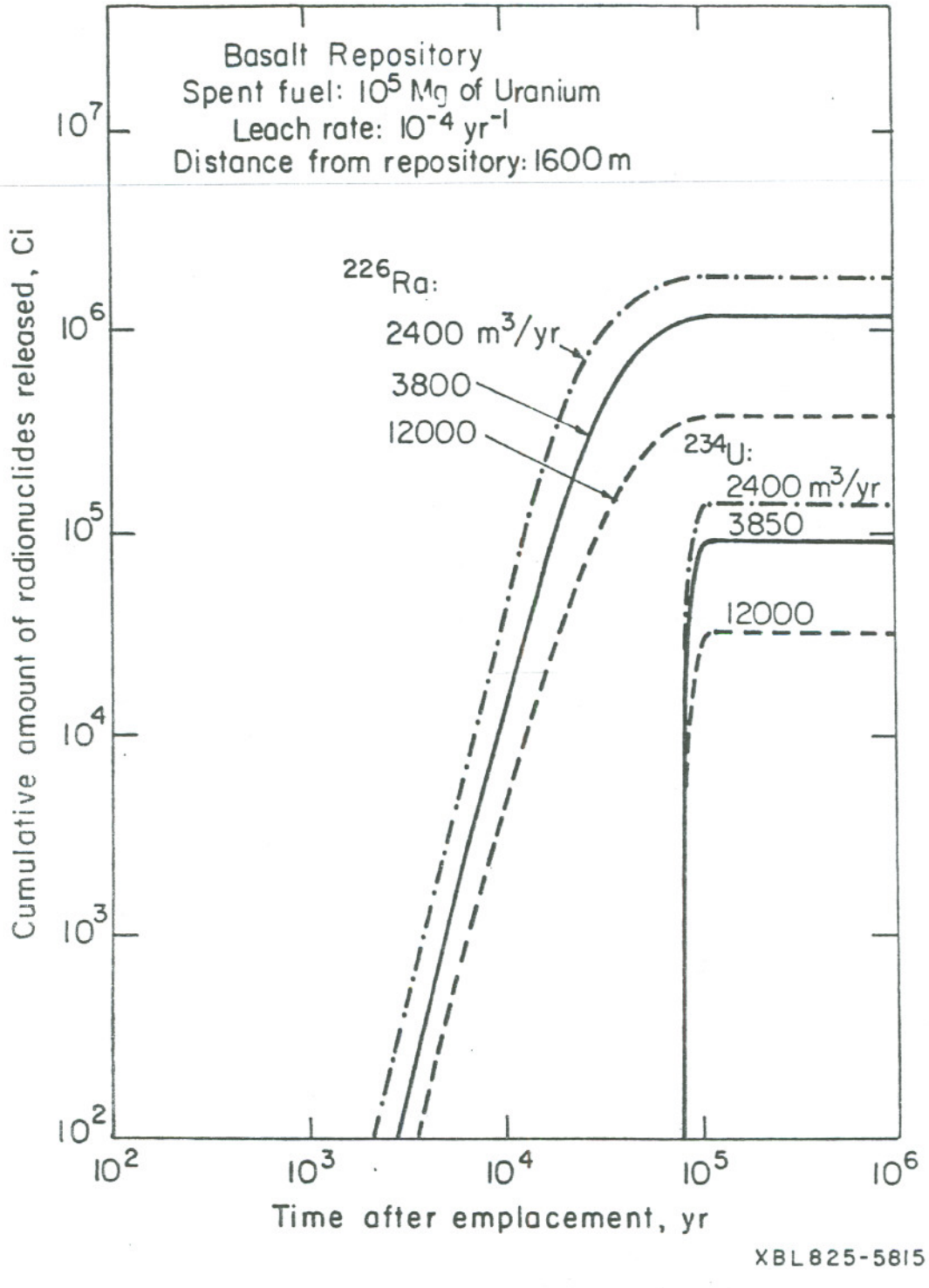

Fig. 6.7 Cumulative amount of ^{234}U and ^{226}Ra released, effect of repository flow rate (EPA's basalt repository).

after emplacement for the basalt and granite repositories, neglecting solubility limit, only technetium-99 and cesium-135 are predicted to have curie releases exceeding that of radium-226. As we shall see later, the calculated health effects from released radium-226 far outweigh those from the other radionuclides released during this time period. It is apparent that the release of radium-226 must be considered in a realistic analysis of the potential hazards from a geologic repository, even during the relatively short time period of 10,000 years assumed by EPA. The equations for the transport of radionuclide decay chains are vital for this analysis.

The equations used to predict the transport and release of radium-226 are the approximate exponential-release solutions of Section 6.4.2, where it is assumed that the flowrate of groundwater through the repository is constant. To estimate the value of the flowrate to use in these calculations, the cumulative release of uranium-234 predicted for time-dependent flow is compared in Fig. 6.7 with that predicted for constant flow. The calculated curve for uranium-234 for an assumed constant repository flowrate of 3,850 m^3/yr is identical with the exact curve for uranium-234, calculated by applying Eq.(6.6) and using the time-dependent repository flowrate deduced by EPA. A constant flowrate of 3,850 m^3/yr through the basalt repository is used to estimate the cumulative release of radium, in the absence of solubility limits. It is this average flowrate that has been used in the calculations for Figs. 6.5 and 6.6.

6.5.4 Cumulative Health Effects From Released Radionuclides

A stated objective of EPA's draft proposed standard is that there shall be no more than 1,000 calculated health effects over 10,000 yr from the environmental releases of radionuclides from a repository containing waste from 10^5 Mg of uranium fuel. EPA has provided data (S2), shown in Table 6.1,

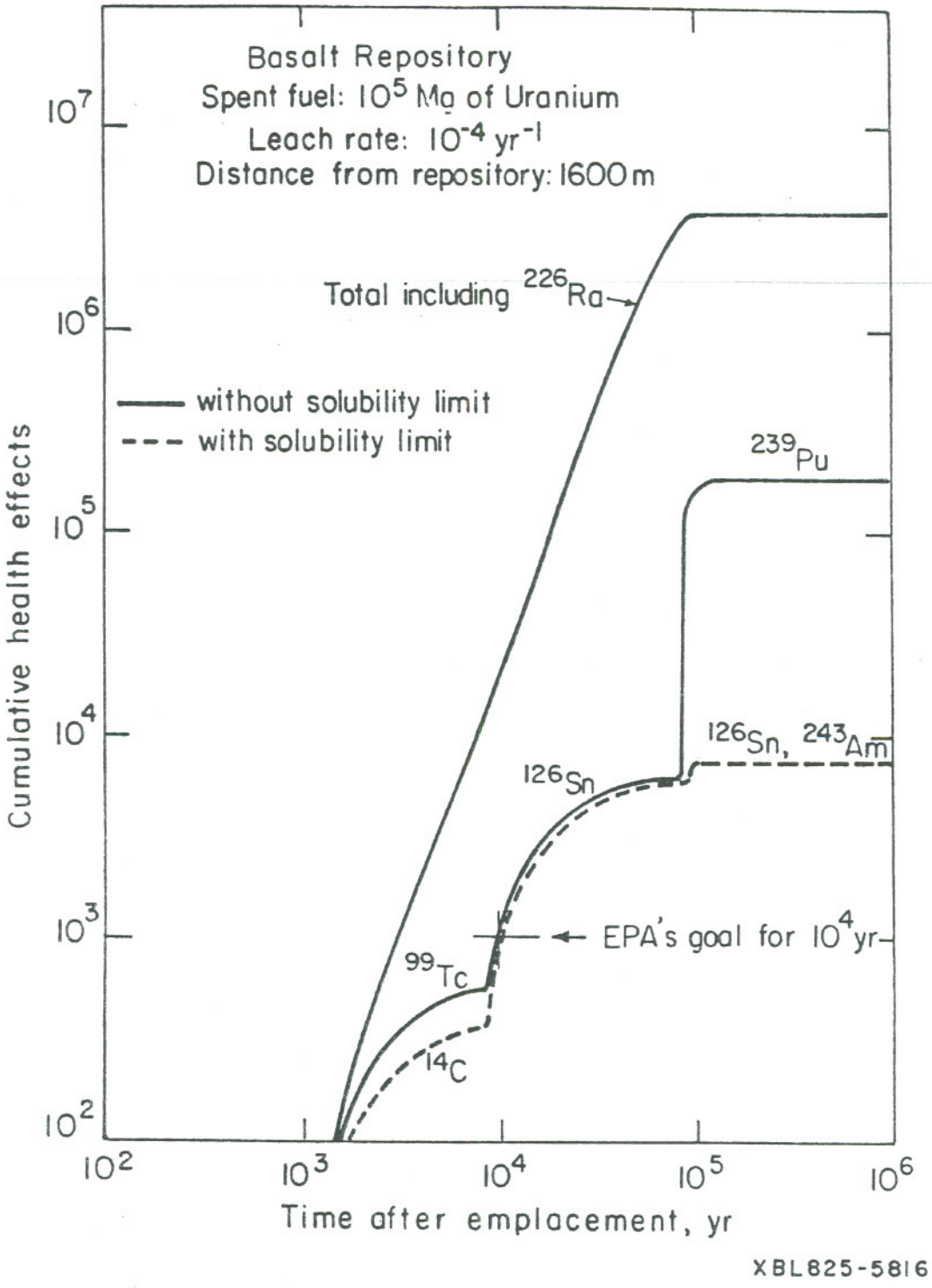

Fig. 6.8 Cumulative health effects from radionuclides released from EPA's basalt repository.

to be used in calculating the number of health effects per curies of activity released to the biosphere, based upon its estimates of world population and worldwide averages for the consumption of surface water for drinking and for the consumption of food grown in or irrigated by water. Our resulting calculations of the cumulative health effects as a function of time for EPA's basalt and granite repositories are shown in Fig. 6.8, and 6.9. The labels on the curves for the total health effects of all radionuclides other than radium-226 indicate the radionuclides that are the main contributors to the cumulative health effects during the period indicated. Within this mixed group, technetium-99 is the main contributor during the period up to 10,000 yr, except when the solubility limit of technetium is considered. In the latter case carbon-14 becomes the main contributor. Tin-126 is the main contributor from 10^4 to 10^5 yr. From 10^5 to 10^6 yr plutonium-239 is the main contributor if solubility limits are not considered, and tin-126 and americium-243 are the main contributors when solubility limits are considered.

EPA's draft proposed standard lists curie releases of individual radionuclides that are upper-limit releases for 10,000 yr. The upper-limit release for technetium-99 is 2×10^3 Ci per 1000 Mg of U, which corresponds to 2×10^5 Ci for a 10^5 Mg repository. This compares to our calculated cumulative release of 6.4×10^5 Ci of technetium-99 in 10^4 yr, as shown in Fig. 6.5, ignoring solubility limit. There is an apparent inconsistency, in that the calculated curie releases of technetium-99 for basalt are tenfold greater than allowed in EPA's draft standard, yet the calculated health effects from technetium-99 just meet EPA's goal of 1,000 health effects in 10,000 yr. The discrepancy occurs because EPA has decreased the allowable curie release of technetium-99 tenfold below that which is calculated by EPA data to result in 1,000 health effects (P1). This results

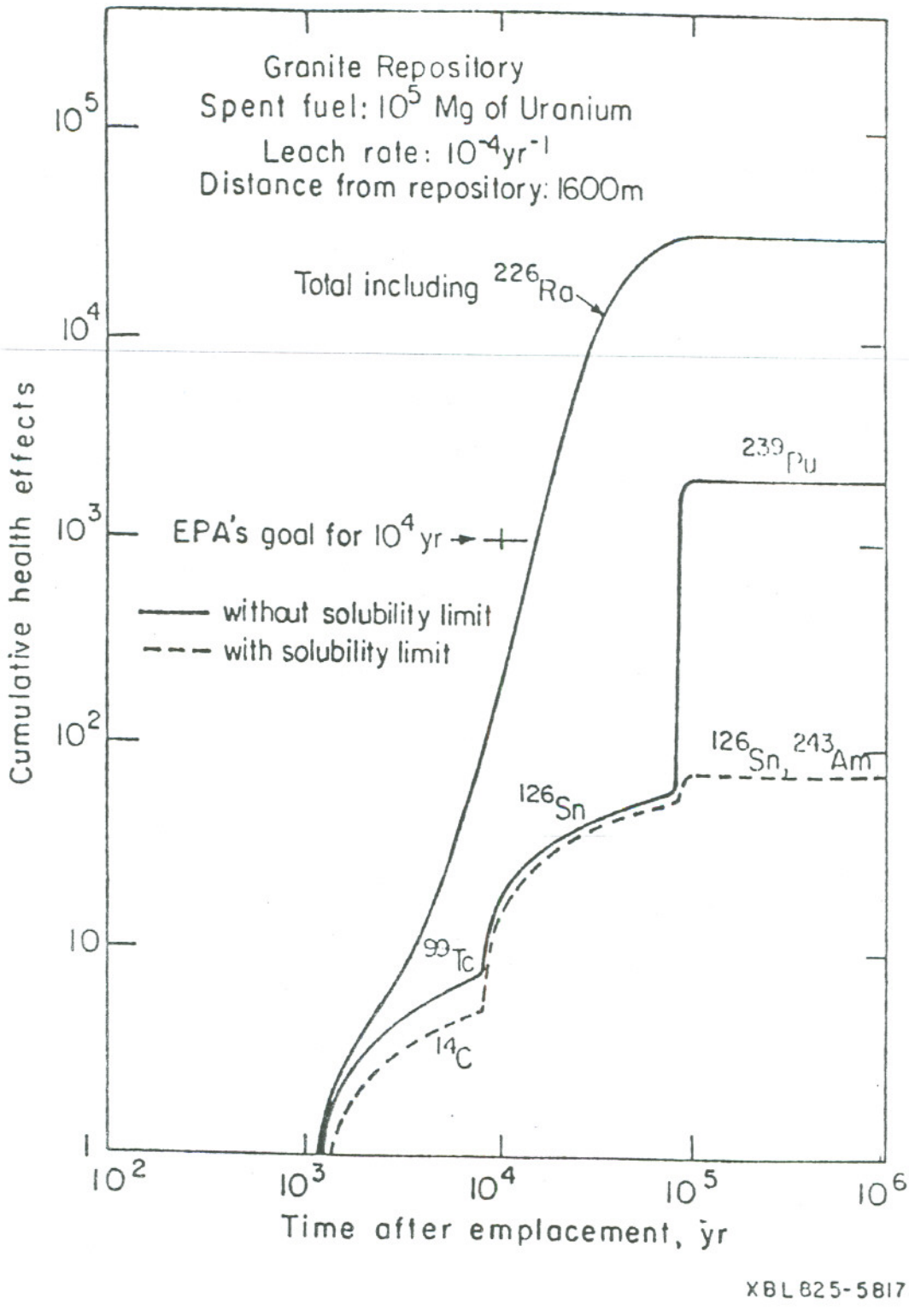

Figure 6.9 Cumulative health effects from radionuclides released from EPA's granite repository.

from EPA's view that uncertainties in the data on uptake of technetium-99 by plants justify this reduction in the allowable curie release limit for technetium-99.

The curves for the health effects from radium-226 are calculated on the basis of no solubility limit of the uranium precursors of radium-226. It is apparent that even during the 10,000 yr period adopted by EPA radium-226 contributes over an order of magnitude more health effects than the sum of all the other radionuclides released during this period. The cumulative health effects increase rapidly and level off only after about 10^5 yr, based upon the use of EPA's assumptions and parameters. Separate calculations, to be reported later, show a decrease in the cumulative health effects from radium-226 when the solubility of uranium is taken into account, but the conclusions concerning the importance of radium-226 remain valid.

It is apparent from Fig. 6.8 that when radium-226 is considered EPA's goal of no more than 1,000 health effects in 10,000 yr is not met by EPA's basalt repository. This is a consequence of the large flowrate of groundwater within the basalt repository, as estimated by EPA.

6.6 Nomenclature

a_i, (i=1,2..)	Emperically fitted constant for buoyancy
A_i^j	Defined by Eq.(6.54)
A_r	Cross-sectional area of repository, (m^2)
B_{ij}	Bateman coefficient, Eqs.(6.33) and (6.44)
$B_i(t)$	Release rate of nuclide i from waste, (atoms/yr)
B_{jl}^i	Defined by Eq.(6.55)
$C_i(t)$	Concentration of nuclide i at repository, (atoms/m^3)
$C_i(s)$	Defined by Eq.(6.21)
C_i^*	Solubility limit of nuclide i, (atoms/m_3)
D_{lm}^j	Defined by Eq.(6.56)
E_j^i	Defined by Eq.(6.27)
f	Fractional release rates of all nuclides, (1/yr)
f_i	Fractional release rate for nuclide i, (1/yr)
F_{jl}^i	Defined by Eq.(6.28)
$g_{lm}(t)$	Defined by Eq.(6.57)
G_0	Constant hydraulic gradient from lower aquifer
$G_r(t)$	Hydraulic gradient from repository
k_r	Permeability of host rock, (m/yr)
K_i	Retardation coefficient of nuclide i

M^0	Initial amount of nuclide i, (atoms)
n_i^0	Initial concentration of nuclide i in the solid waste
$n_i(t)$	Concentration of nuclide i in the solid waste
$N_i(zt)$	Concentration of nuclide i in groundwater, (atoms/m^3)
$P_i(t)$	Amount of precipitate at repository, (atoms/m^3)
Q_a	Volumetric water flow rate in upper aquifer, (m^3/yr)
$Q_r(t)$	Time dependent water flow rate from repository, (m^3/yr)
$R(t)$	Defined by Eq.(6.5)
t	Time after beginning of leach, (yr)
t_1^*	Beginning time for precipitation, (yr)
t_2^*	Time at precipitate disappears, (yr)
T	Leach time for band release, (yr)
$U_i(z,t)$	Cumulative amount of nuclide i at distance z and up to time t, (atoms)
v	Groundwater velocity in upper aquifer, (m/yr)
v_i	Migration velocity of nuclide i, (m/yr)
V	Volume of water within the repository, (m^3)
$W_{1m}(t)$	Defined by Eq.(6.35)
$X_{1m}(t)$	Defined by Eq.(6.40)
$Y_{1m}(t)$	Defined by Eq.(6.46)

z	Distance from repository, (m)
$\alpha_T (i=1,2,3)$	Emperically fitted constant for buoyancy flow, (1/yr)
Δ_{1m}	Constant defined by Eq.(6.58)
K_i	Constant defined by Eq.(6.23)
λ_i	Decay constant of nuclide i, (1/yr)
λ_r	Constant defined by Eq.(6.18)
Ω_i	Constant defined by Eqs.(6.38) or (6.43)

6.7 References

C1 M. O. Cloninger and C. R. Cole, "A Reference Analysis on the Use of Engineered Barriers for Isolation of Spent Fuel in Granite and Basalt", PNL-3530, August, 1981.

H1 M. Harada, P. L. Chambre', M. Foglia, K. Higashi, F. Iwamoto, D. Leung, T. H. Pigford, D. Ting, "Migration of Radionuclides Through Sorbing Media, Analytical Solutions -- I", LBL-10500, 1980.

P1 T. H. Pigford, P. L. Chambre', M. Albert, M. Foglia, M. Harada, F. Iwamoto, T. Kanki, D. Leung, S. Masuda, and D. Ting, "Migration of Radionuclides Through Sorbing Media: Analytical Solutions -- II", LBL-11616, October, 1980.

P2 T. H. Pigford, "EPA Proposed Standard for Geologic Isolation of High-Level Waste", UCB-NE-4006, March, 1981.

P3 T. H. Pigford, "Derivation of EPA Proposed Standard for Geologic Isolation of High-Level Waste", UCB-NE-4006 (Addendum 1), August, 1981.

S1 G. Bruce Smith, Daniel J. Egan, Jr., W. A. Williams, James M. Gruhlke, Cheng-Yeng Hung, Barry L. Serini, "Population Risks from Disposal of High-Level Radioactive Waste in Geologic Repositories", EPA 520/3-80-006 (Draft), July, 1981.

S2 J. Michael Smith, Ted W. Fowler, Abraham S. Goldin, "Environmental Pathway Models for Estimating Population Health Effects from Disposal of High-level Radioactive Waste in Geologic Repositories", EPA 520/5-80-002 (Draft), July, 1981.

7.1 Mass Transfer From a Fuel Canister by Diffusion

Paul L. Chambré

Consider a cylinder of finite length imbedded in a porous medium. The cylinder matrix contains a diffusing specie such as $Si(OH)_x$ or UO_2 which is set free at the surface of the cylinder at the solubility limit $\hat{c}_s$ of this specie in water and then diffuses into the exterior unbounded space. The diffusion coefficient is assumed constant. The governing equation for the conservation of mass of the diffusing species outside the cylinder in absence of any losses is

$$K \frac{\partial \hat{c}}{\partial t} = D_f \nabla^2 \hat{c} \tag{7.1.1a}$$

Here D_f is the diffusion coefficient of the species in water and K its retardation coefficient.

The boundary conditions are respectively

$$\hat{c} = \hat{c}_s \tag{7.1.1b}$$

on the surface of the cylinder and

$$\hat{c} = 0 \tag{7.1.1c}$$

on an infinite spherical surface enclosing the cylinder. If the concentration at infinity is non-zero, a change in the reference datum of $\hat{c}$ reduces that problem to the above formulation. Prior to the time t = 0 the diffusing nuclide has zero concentration in the exterior (porous) medium.

For a cylinder of finite length, the Laplace operator in eq. (7.1.1a) has the form

$$\nabla^2(\ ) = \frac{\partial^2(\ )}{\partial r^2} + \frac{1}{r}\frac{\partial(\ )}{\partial r} + \frac{1}{r^2}\frac{\partial(\ )}{\partial \theta^2} + \frac{\partial^2(\ )}{\partial z^2} \tag{7.1.2}$$

where r, θ, z are cylindrical coordinates. For the exterior diffusion problem which we wish to solve, compact analytical solutions of eqs. (7.1.1) and (7.1.2) are not possible because the interior bounding surface is a cylinder and the exterior surface is a sphere. This of course does not mean that the posed problem does not possess a solution. Indeed one can obtain it in numerical form or by analytical approximations. Since we wish to retain a compact analytical solution to this problem, a suitable approximation is made for the shape of the cylinder. The finite cylinder shape is approximated by a slender prolate spheriod which is generated by rotating a family of confocal ellipses about their major axis. This family generates not only the replacement for the finite cylinder, but produces also the outer spherical boundary which is a member of this family.

One might consider also other forms for the approximation. Suppose the inner surface of the domain is maintained in the exact form of a finite cylinder and the outer boundary is now a cylinder, but of infinite extent. For simplicity, consider furthermore that a steady state prevails so that one deals with the solution of Laplaces equation in the exterior field. Subject to the boundary condition (7.1.1b) the solution sought is mathematically equivalent to the problem of determining the capicitance of a cylinder in an infinite cylindrical box. It is well known that this problem does not possess an exact closed form solution although it can be readily shown that such a solution exists and is unique and can be approximated by various means. With these comments in mind, we reiterate that the interior cylinder surface will be approximated by a slender prolate spheroid which is described by the prolate spheroidal coordinates (α,β,ψ). Since the reader may not be familiar with this coordinate system,

we review and summarize in the following its main characteristics.

The relationship between prolate spheroidal coordinates (α,β,ψ) and the common rectangular coordinates (x,y,z) are given by

$$\begin{aligned} x &= f \sinh\alpha \sin\beta \cos\psi \\ y &= f \sinh\alpha \sin\beta \sin\psi \\ z &= f \cosh\alpha \cos\beta \end{aligned} \tag{7.1.3}$$

where f is the focal distance of the prolate spheroid measured from the coordinate origin, see Fig. 7.1.1. To exhibit the geometric significance of α, take α to be constant and let

$$a = f \cosh\alpha, \quad b = f \sinh\alpha \tag{7.1.4}$$

in eq. (7.1.3). If these three equations are squared and added, there results

$$\left(\frac{x}{b}\right)^2 + \left(\frac{y}{b}\right)^2 + \left(\frac{z}{a}\right)^2 = 1 \tag{7.1.5}$$

Since α and hence a and b are constants, this represents a prolate spheroid in the x,y,z coordinate system (see Fig. (7.1.1)). One observes from (7.1.4) that as α becomes small, the prolate spheroid tends to a small diameter "cylinder". This "cylinder" has a radius b and a length given by (7.1.5) as 2a. In the following, we shall approximate the cylinder by small positive values of α. On the other hand, as α becomes very large, so do both a and b and (7.1.5) tends to the description of a sphere of large radius. The entire α range generates a family of prolate ellipsoids.

In order to exhibit the geometric significance of β, take β to be a constant and let

$$\bar{a} = f \cos\beta, \quad \bar{b} = f \sin\beta \tag{7.1.6}$$

Again square the equations in (7.1.3) and add so that

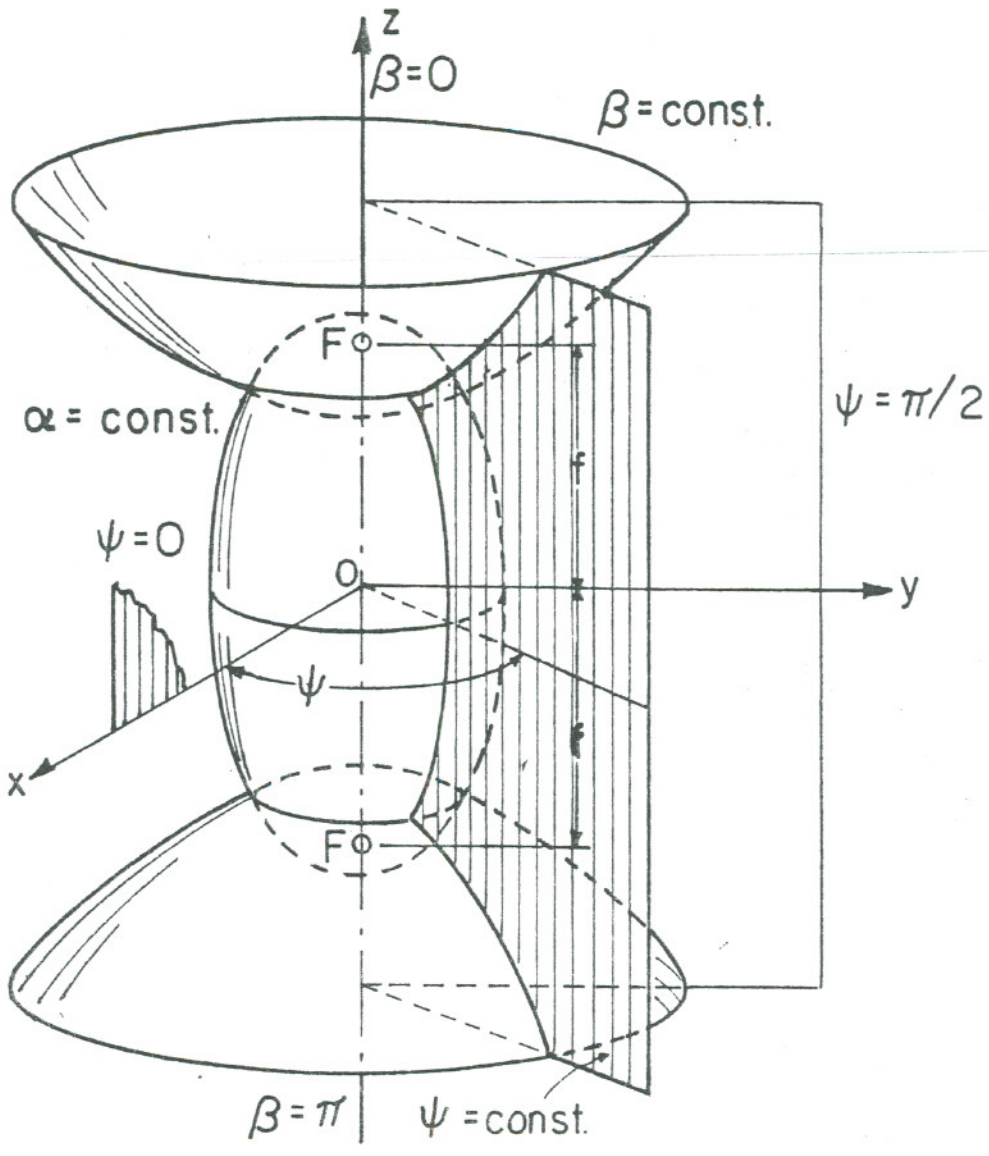

Fig. 7.1.1. Prolate spheroidal coordinates (α,β,ψ). Coordinate surfaces are prolate spheroids (α = const), hyperboloids of revolution (β = const), and half-planes (ψ = const).

$$-\left(\frac{x^2+y^2}{\bar{b}^2}\right)+\left(\frac{z}{\bar{a}}\right)^2=1 \qquad (7.1.7)$$

Hence for β constant and thus $\bar{a}$ and $\bar{b}$ constant, this equation represents a family of hyperboloids of two sheets with foci at $\pm$ f as shown in Fig. (7.1.1). When $\beta = 0$, $\bar{a} = f$ and $\bar{b} = 0$, while when $\beta = \pi$, $\bar{a} = -f$ and $\bar{b} = 0$. For either of these cases (7.1.7) reduces in the limit to the collapsed hyperboloid, i.e., the positive and negative z axis from f to ∞ and -f to $-\infty$ respectively. When $\beta = \frac{\pi}{2}$, $\bar{a} = 0$, $\bar{b} = f$ for which (7.1.7) reduces in the limit to $z = 0$, i.e., the x-y plane. Finally, as can be seen from Fig. (7.1.1), the family of half planes ψ = constant with $0 \leq \psi \leq 2\pi$ forms the third member of orthogonal coordinate system α, β, ψ which has the range

$$0 \leq \alpha \leq \infty \; ; \; 0 \leq \beta \leq \pi \; ; \; 0 \leq \psi \leq 2\pi \qquad (7.1.8)$$

In this coordinate system the square of the element of arc length is given with help of (7.1.3) by

$$(ds)^2 = f^2 \; (\sinh^2\alpha + \sin^2\beta) \left[(d\alpha)^2 + (d\beta)^2\right] + \\ + f^2 \sinh^2\alpha \, \sin^2\beta (d\psi)^2 \qquad (7.1.9)$$

From this one obtains the metric coefficients of this coordinate system as

$$h_\alpha = h_\beta = f\,(\sinh^2\alpha + \sin^2\beta)^{1/2}; \; h_\psi = f \sinh\alpha \sin\beta \qquad (7.1.10)$$

Now the form of the governing eq. (7.1.1a) in this curvilinear orthogonal coordinate system is

$$K\frac{\partial \hat{c}}{\partial t} = D_f \left[\frac{1}{h_\alpha h_\beta h_\psi}\left\{\frac{\partial}{\partial\alpha}\left(\frac{h_\beta h_\psi}{h_\alpha}\frac{\partial \hat{c}}{\partial\alpha}\right) + \frac{\partial}{\partial\beta}\left(\frac{h_\alpha h_\psi}{h_\beta}\frac{\partial \hat{c}}{\partial\beta}\right) + \right.\right. \\ \left.\left. \frac{\partial}{\partial\psi}\left(\frac{h_\alpha h_\beta}{h_\psi}\frac{\partial \hat{c}}{\partial\psi}\right)\right\}\right] \qquad (7.1.11)$$

which reduces with help of (7.1.10) to

$$K\frac{\partial\hat{c}}{\partial t} = D_f\left[\frac{1}{f^2(\sinh^2\alpha+\sin^2\beta)}\left\{\frac{1}{\sinh\alpha}\frac{\partial}{\partial\alpha}\left(\sinh\alpha\frac{\partial\hat{c}}{\partial\alpha}\right)+\right.\right.$$

$$\left.\left.+\frac{1}{\sin\beta}\frac{\partial}{\partial\beta}\left(\sin\beta\frac{\partial\hat{c}}{\partial\beta}\right)+\left(\frac{1}{\sinh^2\alpha}+\frac{1}{\sin^2\beta}\right)\frac{\partial^2\hat{c}}{\partial\psi^2}\right\}\right] \qquad (7.1.12)$$

$$\alpha_s < \alpha < \infty,\ 0 < \beta \leqslant \pi,\ 0 < \psi \leqslant 2\pi$$

An alternate form of this equation is useful. Let

$$\zeta = \cosh\alpha,\ \mu = \cos\beta,\ \psi = \psi \qquad (7.1.13)$$

then (7.1.11) transforms into

$$K\frac{\partial\hat{c}}{\partial t} = \frac{D_f}{f^2\left(\zeta^2-\mu^2\right)}\left\{\frac{\partial}{\partial\zeta}\left[(\zeta^2-1)\frac{\partial\hat{c}}{\partial\zeta}\right]+\frac{\partial}{\partial\mu}\left[(1-\mu^2)\frac{\partial\hat{c}}{\partial\mu}\right]+\right.$$

$$\left.+\frac{\zeta^2-\mu^2}{(\zeta^2-1)(1-\mu^2)}\frac{\partial^2\hat{c}}{\partial\psi^2}\right\} \qquad (7.1.14)$$

$$\zeta_s < \zeta < \infty,\ -1 \leqslant \mu \leqslant 1,\ 0 < \psi \leqslant 2\pi$$

as one can readily show. In (7.1.12) and (7.1.14) α_s and ζ_s describe the cylinder (prolate spheroid) surface. Particular solutions to this equation can be constructed by separation of variables. With

$$\hat{c}(\zeta,\mu,\psi,t) = e^{-s^2t}\ \phi\ (\zeta,\mu,\psi) \qquad (7.1.15)$$

ϕ satisfies the Helmholtz equation in prolate spheroidal coordinates

$$\frac{\partial}{\partial\zeta}\left[(\zeta^2-1)\,\frac{\partial\phi}{\partial\zeta}\right] + \frac{\partial}{\partial\mu}\left[(1-\mu^2)\,\frac{\partial\phi}{\partial\mu}\right] + \frac{\zeta^2-\mu^2}{\left(\zeta^2-1\right)\left(1-\mu^2\right)}\,\frac{\partial^2\phi}{\partial\psi^2} +$$

$$+ k^2\left(\zeta^2-\mu^2\right)\,\phi = 0, \quad \text{where } k^2 = \frac{(sf)^2K}{D_f} \tag{7.1.16}$$

This equation can be separated again with

$$\phi\,(\zeta,\mu,\psi) = R_{mn}\,(k,\zeta)\,S_{mn}\,(k,\mu)\,\begin{matrix}\cos\\ \sin\end{matrix}\,(m\psi) \tag{7.1.17}$$

Here the radial function $R_{mn}\,(k,\zeta)$ and the angular function $S_{mn}\,(k,\mu)$ satisfy the differential equations

$$\frac{d}{d\zeta}\left[(\zeta^2-1)\,\frac{d}{d\zeta}\,R_{mn}\,(k,\zeta)\right] - \left(\kappa_{mn} - k^2\zeta^2 + \frac{m^2}{\zeta^2-1}\right)R_{mn}(k,\zeta) = 0$$

$$\frac{d}{d\mu}\left[\left(1-\mu^2\right)\,\frac{d}{d\mu}\,S_{mn}\,(k,\mu)\right] + \left(\kappa_{mn}-k^2\mu^2 - \frac{m^2}{1-\mu^2}\right)S_{mn}\,(k,\mu) = 0 \tag{7.1.18}$$

The separation constants k^2 and κ_{mn}, which are eigenvalues in our problem, would be determined by boundary conditions imposed on R_{mn} and S_{mn}. This method of solution is not pursued in the following since the determination of the spheriodal eigenfunctions and eigenvalues for the exterior problem are mathematically quite involved. We will instead obtain the necessary information about the solution by application of Laplace transform techniques.

Before proceeding with this, we make the simplication that the concentration of the diffusing element on the cylinder surface is independent of

the angle ψ and constant over the entire surface so that $c(\zeta,\mu,\tau)$ obeys, see eq. (7.1.14).

$$\frac{\partial c}{\partial \tau} = \frac{1}{\left(\zeta^2 - \mu^2\right)} \left\{ \frac{\partial}{\partial \zeta} \left[(\zeta^2 - 1) \frac{\partial c}{\partial \zeta} \right] + \frac{\partial}{\partial \mu} \left[(1-\mu^2) \frac{\partial c}{\partial \mu} \right] \right\} ,$$

$$\zeta_s < \zeta < \infty, \; -1 \leqslant \mu \leqslant 1 \tag{7.1.19}$$

$$c(\zeta,\mu,o) = 0, \; \zeta_s \leqslant \zeta < \infty , \; -1 \leqslant \mu \leqslant 1 \tag{7.1.20}$$

$$c(\zeta_s,\mu,\tau) = 1, \; -1 \leqslant \mu \leqslant 1, \; \tau > 0 \tag{7.1.21}$$

$$c(\infty,\mu,\tau) = 0 \quad -1 \leqslant \mu \leqslant 1, \; \tau \geqslant 0 \tag{7.1.22}$$

$$\frac{\partial c(\zeta,o,\tau)}{\partial \mu} = 0 \quad \zeta_s \leqslant \zeta < \infty , \; \tau \geqslant 0 \tag{7.1.23}$$

where

$$c(\zeta,\mu,\tau) = \frac{\hat{c}(\zeta,\mu,\tau)}{\hat{c}_s} \; ; \; \tau = \frac{D_f t}{K f^2} \tag{7.1.24}$$

The initial condition is given by (7.1.20). The boundary conditions on the surface of the cylinder and on the spherical surface at the point at infinity are given by (7.1.21) and (7.1.22) respectively. Eq. (7.1.23) describes the symmetry of c about the midplane $\mu = 0$ of the cylinder. We now develop the steady solution as well as the early time and large time (approach to the equilibrium) behavior of this solution.

The Steady State Solution

For this case the governing equation for $c(\zeta)$ and its side conditions reduce to

$$\frac{d}{d\zeta} \left[(\zeta^2 - 1) \frac{dc}{d\zeta} \right] = 0 , \quad \zeta_s \leqslant \zeta < \infty \tag{7.1.25}$$

$$c(\zeta_s) = 1 \tag{7.1.26}$$

$$c(\infty) = 0 \tag{7.1.27}$$

If the concentration at infinity is non-zero, a change in the reference datum ($\hat{c}$) reduces that problem to the above formulation. Here c has no μ dependence because the boundary conditions (7.1.21) to (7.1.23) can be met in the indicated way. The solution to this problem is elementary and is given by

$$c(\zeta) = \frac{Q_o(\zeta)}{Q_o(\zeta_s)} \qquad \zeta_s \leq \zeta < \infty \tag{7.1.28}$$

where

$$Q_o(\zeta) = \frac{1}{2} \log \frac{\zeta+1}{\zeta-1} \tag{7.1.29}$$

is the Legendre function of the second kind and zero order. In view of

$$\frac{\zeta+1}{\zeta-1} = \frac{\cosh\alpha + 1}{\cosh\alpha - 1} = \coth^2 \frac{\alpha}{2} \tag{7.1.30}$$

Eq. (7.1.28) yields

$$c(\alpha) = \frac{\log \coth \frac{\alpha}{2}}{\log \coth \frac{\alpha_s}{2}}, \quad \alpha_s \leq \alpha < \infty \tag{7.1.31}$$

The diffusion flux is then given by

$$\vec{j} = -D_e \hat{c}_s \text{ grad } c$$

$$= \frac{-D_e \hat{c}_s}{h_\alpha} \frac{dc}{d\alpha} \tag{7.1.32}$$

Here $D_e = \varepsilon D_f$ is the effective diffusion coefficient of the species in the water saturated porous medium, and ε is the porosity of the medium. Eq.(7.1.32) with the help of (7.1.10), yields the diffusion flux from the surface of the prolate spheroid

$$\vec{j}_s = \left(\frac{D_e \hat{c}_s}{f}\right) \frac{1}{(\sinh^2\alpha_s + \sin^2\beta)^{1/2} \log(\coth \frac{\alpha_s}{2}) \sinh \alpha_s} \tag{7.1.33}$$

One observes that although the concentration is uniformly distributed over the surface $\alpha = \alpha_s$, the surface flux is a function of position β. The flux is largest over the top and bottom caps of the cylinder where β is close to o and π as shown in Fig. (7.1.1). The expression (7.1.33) is typical of the surface flux from an arbitrarily shaped body, in a diffusion field governed by Laplace's equation, subject to boundary conditions of type (7.1.26), (7.1.27). Dimensional analysis shows that

$$\vec{j}_s = \left(\frac{D_e \hat{c}_s}{\ell}\right) \text{function of body geometry}$$

where ℓ is some characteristic body dimension, which in the present case can be readily identified from (7.1.33). In order to obtain the total rate of mass transport from the cylinder, one must integrate $\vec{j}_s$ over the surface S of the prolate spheroid

$$\dot{m} = \int_S |\vec{j}_s| \, dS \tag{7.1.34}$$

Since $dS = h_\beta h_\psi \, d\beta d\psi$ one obtains with (7.1.10) and (7.1.33) the formula for the total rate of mass transport from a prolate spheroid

$$\dot{m} = \frac{4\pi D_e \hat{c}_s f}{\log(\coth \frac{\alpha_s}{2})} \quad . \tag{7.1.35}$$

For a slender prolate spheroid which is to approximate a cylinder of length to radius ratio $\frac{L}{b} \geq 10$, $\alpha_s << 1$. Hence one can approximate

$$\coth\left(\frac{\alpha_s}{2}\right) \simeq \frac{2}{\alpha_s} \quad , \quad b \simeq f \alpha_s \text{ by using (7.1.4) and } f \simeq \frac{L}{2}$$

thus,

$$b = \frac{L}{2} \alpha_s \text{ or } \frac{2}{\alpha_s} = \frac{L}{b} \quad .$$

With this (7.1.35) yields

$$\dot{m} = \frac{2\pi D_e \hat{c}_s L}{\log\left(\frac{L}{b}\right)} \tag{7.1.36}$$

an approximation for the total rate of mass transport from a slender cylinder of length L and radius b.

The principal physical feature of this formula is that $\dot{m}$ diminishes with decreasing radius b (L being held constant) but for a fixed radius $\dot{m}$ increases with L. These formulas and the equation for the fractional dissolution rate will be illustrated in section 7.5.

We consider next the question of the length of time required to establish the steady state solution.

The Transient Solution

The analysis is conducted in two parts, the early time behavior and the large time behavior of the solution to equations (7.1.19-23), since the complete solution to these equations is difficult to obtain. The large time behavior is of greatest interest since it gives an indication of the time span necessary to establish the steady state. We will compute only the dominant leading term of the solutions since it will furnish the desired information.

The Large Time Behavior

The governing equation (7.1.19) and its side conditions are subjected to a Laplace transform with respect to the variable τ and a Legendre transform with respect to the variable μ. $c(\zeta,\mu,\tau)$ thereby changes in succession into

$$c(\zeta,\mu,p) = \int_0^\infty e^{-p\tau}\, c(\zeta,\mu,\tau)\, d\tau \tag{7.1.37}$$

$$c(\zeta,2n,p) = \int_0^1 c(\zeta,\mu,p)\, P_{2n}(\mu)\, d\mu \qquad (7.1.38)$$

where the $P_{2n}(\mu)$ are the Legendre polynomials of even order. Only even members of the set are required on account of the symmetry condition (7.1.23). We have shown that for the leading term of the solution, only $P_0(\mu) = 1$ and thus $c(\zeta,o,p)$ are required. The details are omitted.

Applying (7.1.37) to (7.1.19) yields with help of (7.1.20).

$$\frac{\partial}{\partial\zeta}\left[(\zeta^2-1)\,\frac{\partial c(\zeta,\mu,p)}{\partial\zeta}\right] + \frac{\partial}{\partial\mu}\left[(1-\mu^2)\,\frac{\partial c(\zeta,\mu,p)}{\partial\mu}\right] = p(\zeta^2-\mu^2)c(\zeta,\mu,p) \qquad (7.1.39)$$

Then applying (7.1.38) gives with n = o,

$$\frac{d}{d\zeta}\left[(\zeta^2-1)\,\frac{dc(\zeta,o,p)}{d\zeta}\right] + (1-\mu^2)\,\frac{\partial c(\zeta,\mu,p)}{\partial\mu}\Bigg|_0^1 = p\int_0^1 (\zeta^2-\mu^2).$$

$$.\,c(\zeta,\mu,p)\, d\mu \qquad (7.1.40)$$

One observes, having first Laplace transformed equations (7.1.19) - (7.1.23), that the second (integrated) term in (7.1.40) vanishes by (7.1.23). The integral on the right hand side of (7.1.40) has the form

$$\int_0^1 (\zeta^2-\mu^2)\, c(\zeta,\mu,p)d\mu = \left(\zeta^2 - \frac{1}{3}\right)c(\zeta,o,p) - \frac{2}{3}\int_0^1 c(\zeta,\mu,p)P_2(\mu)d\mu \qquad (7.1.41)$$

The last integral can be shown to have no contribution to the leading term, so there results for $c(\zeta,o,p) \equiv c(\zeta,p)$

$$\frac{d}{d\zeta}\left[(\zeta^2-1)\,\frac{dc}{d\zeta}\right] = p\left(\zeta^2 - \frac{1}{3}\right)c,\ \zeta_s < \zeta < \infty \qquad (7.1.42)$$

with the boundary conditions

$$c(\zeta_s,p) = \frac{1}{p}\ ;\ c(\infty,p) = 0 \qquad (7.1.43)$$

We propose a solution to (7.1.42) of the form

$$c(\zeta,q) = \phi(\zeta,q)e^{-q(\zeta-\zeta_s)} \quad , \quad q = \sqrt{p} \tag{7.1.44}$$

where $\phi(\zeta,q)$ is to be determined by substitution into (7.1.42). There results

$$\frac{d}{d\zeta}\left[(\zeta^2-1)\frac{d\phi}{d\zeta}\right] = R(\phi,q) \tag{7.1.44a}$$

where

$$R(\phi,q) \equiv 2q\left[(\zeta^2-1)\frac{d\phi}{d\zeta} + \zeta\phi\right] + \frac{2}{3}q^2\phi \tag{7.1.44b}$$

In view of eq. (7.1.43) we take the boundary conditions on $\phi(\zeta,q)$ to be

$$\phi(\zeta_s,q) = \frac{1}{q^2}$$
$$\phi(\infty,q) = 0 \tag{7.1.45}$$

We now define the Green's function $G(\zeta,\xi)$ for the differential operator in (7.1.44a) in order to solve that equation. Let

$$\frac{d}{d\zeta}\left[(\zeta^2-1)\frac{dG(\zeta,\xi)}{d\zeta}\right] = -\delta(\zeta-\xi) \tag{7.1.46}$$

$$G(\zeta_s,\xi) = G(\infty,\xi) = 0$$

Then with $F(a,b) = \int_a^b \frac{d\zeta}{(\zeta^2-1)}$ (7.1.47)

we have

$$(\zeta^2-1)\frac{dG}{d\zeta} = A \text{ or } G(\zeta,\xi) = AF(\zeta_s,\xi) \ , \ \zeta_s < \zeta < \xi \tag{7.1.48}$$

$$(\zeta^2-1)\frac{dG}{d\zeta} = -B \text{ or } G(\zeta,\xi) = -BF(\xi,\infty) \ , \ \xi < \zeta < \infty$$

The continuity of $G(\zeta,\xi)$ and the unit jump discontinuity of $(\zeta^2-1)\frac{dG}{d\zeta}$ at $\zeta = \xi$.

determines

$$A = D^{-1}F(\xi,\infty) \ , \ B = D^{-1}F(\zeta_s,\xi) \ ; \ D = F(\zeta_s,\infty) \tag{7.1.49}$$

so that

$$G(\zeta,\xi) = \begin{cases} \left[D^{-1}F(\xi,\infty)\right] \ F(\zeta_s,\zeta) \ , \ \zeta_s \leqslant \zeta \leqslant \xi \\ \\ \left[D^{-1}F(\zeta_s,\xi)\right] \ F(\zeta,\infty) \quad \xi \leqslant \zeta < \infty \end{cases} \tag{7.1.50}$$

On evaluating D and F there results

$$G(\zeta,\xi) = \begin{cases} \dfrac{Q_o(\xi)}{Q_o(\zeta_s)} \quad \left[Q_o(\zeta) - Q_o(\zeta_s)\right] \ , \ \zeta_s \leqslant \zeta < \xi \\ \\ \dfrac{Q_o(\zeta)}{Q_o(\zeta_s)} \quad \left[Q_o(\xi) - Q_o(\zeta_s)\right] \ , \ \xi \leqslant \zeta < \infty \end{cases} \tag{7.1.51}$$

Returning now to the solution of eq. (7.1.44) we consider as our starting point Green's theorem

$$\int_{\zeta_s}^{\infty} \left\{ G \frac{d}{d\zeta} \left[(\zeta^2-1) \frac{d\phi}{d\zeta}\right] - \phi \frac{d}{d\zeta} \left[(\zeta^2-1) \frac{dG}{d\zeta}\right] \right\} d\zeta =$$

$$= \left\{ (\zeta^2-1) \left[G \frac{d\phi}{d\zeta} - \phi \frac{dG}{d\zeta} \right] \right\} \Bigg|_{\zeta_s}^{\infty} \tag{7.1.52}$$

One substitutes for the differential operators under the integral sign the equations (7.1.44a) and (7.1.46), then one makes use of the integral property of the delta function and applies the boundary conditions (re-stated)

$$G(\infty,\xi) = \phi(\infty,\xi) = 0; \ G(\zeta_s,\xi) = 0, \ \phi(\zeta_s,q) = \frac{1}{q^2} \tag{7.1.53}$$

There results

$$\phi(\xi,q) = (\zeta_s^2-1)\,\frac{dG(\zeta_s,\xi)}{d\zeta}\,\frac{1}{p} - \int_{\zeta_s}^{\infty} G(\zeta,\xi)\,R\,(\phi(\zeta),q)\,d\zeta \qquad (7.1.54)$$

But by (7.1.48)

$$(\zeta_s^2-1)\,\frac{dG(\zeta_s,\xi)}{d\zeta} = A \qquad (7.1.55)$$

where A is given by (7.1.49). If one evaluates the integrals, substitutes the result into (7.1.54) and interchanges the labels ξ and ζ, there results the Fredholm integral equation

$$\phi(\zeta,q) = \frac{Q_o(\zeta)}{Q_o(\zeta_s)}\,\frac{1}{q^2} - \int_{\zeta_s}^{\infty} G(\xi,\zeta)\,R\,(\phi(\xi),q)\,d\xi \qquad (7.1.56)$$

The large time behavior of the solution is determined by the "small p" behavior of its transform. For this reason, one usually expands the transform of the solution ϕ in powers of p or q. This amounts to the iterative solution of the integral equation in form of a Neuman series. For our purpose (7.1.56) shows that the leading term in such a series is the first (integrated) term on the right hand side, i.e.,

$$\phi^o(\zeta,q) = \frac{Q_o(\zeta)}{Q_o(\zeta_s)}\,\frac{1}{q^2} \qquad (7.1.57)$$

Higher approximations can be computed by substituting this into (7.1.44b) and then evaluating the integral (7.1.56) provided that this is done to the correct order of the dismissed μ terms. In the present, we restrict ourselves to the zeroth, i.e., the leading approximation to $c(\zeta,q)$ which is a combination of eqs. (7.1.44) and (7.1.57)

$$c(\zeta,q) = \frac{Q_o(\zeta)}{Q_o(\zeta_s)}\,\frac{e^{-q(\zeta-\zeta_s)}}{q^2} \qquad (7.1.58)$$

The Laplace and Legendre inversions produce then the desired approximation for the large time solution

$$c(\zeta,\mu,\tau) = \frac{Q_o(\zeta)}{Q_o(\zeta_s)} \operatorname{erfc}\left(\frac{\zeta-\zeta_s}{2\tau^{1/2}}\right) \tag{7.1.59}$$

As $\tau \to \infty$, the complementary error function tends towards unity so that this expression agrees with the steady solution given by Eq.(7.1.28).

The diffusion flux from the surface of the prolate spheroid is given in the ζ coordinate system by

$$\vec{j} = -\frac{D_e \hat{c}_s}{h_\zeta} \left.\frac{\partial c}{\partial \zeta}\right|_{\zeta=\zeta_s} \quad \text{where } h_\zeta = f\sqrt{\frac{\zeta^2-\mu^2}{\zeta^2-1}}$$

$$\vec{j} = -\frac{D_e \hat{c}_s}{h_{\zeta_s}} \left\{\frac{Q_o'(\zeta_s)}{Q_o(\zeta_s)} - \frac{1}{\sqrt{\pi\tau}}\right\} \tag{7.1.60}$$

The time span necessary to establish the steady state to 1% requires that

$$\frac{1}{\sqrt{\pi\tau}} = 10^{-2} \left|\frac{Q_o'(\zeta_s)}{Q_o(\zeta_s)}\right| \tag{7.1.61}$$

With $(L/_b) = 20$, $\left|\frac{Q_o'(\zeta_s)}{Q_o(\zeta_s)}\right| \simeq \frac{1}{4}\frac{(20)^2}{\log(20)} = 33.5$ $D_f = 5\times10^{-5}\ \frac{cm^2}{sec}$, K=100

and f = 150 cm, eq (7.1.24) yields

$$t_{\text{steady state}} = \frac{10^4 \times 2.25 \times 10^4 \times 10^2}{3.14 \times 5 \times 10^{-5} \times (33.5)^2} = 1.28 \times 10^{11} \text{ sec}$$

$$= 4000 \text{ yrs} \tag{7.1.62}$$

This is an appreciably long time period and its consequence in establishing the steady state in laboratory experiments must be appreciated. For increased retardation this time span increases.

It is within the context of such experiments that the early time behavior of the solution is of interest. We turn next to the analysis of

The Early Time Behavior

In contrast to the large time behavior which is characterized by small values of the Laplace transform parameter p, we are now interested in the large valued parameter case as $p \to \infty$.

The starting point of the analysis is eq. (7.1.42) for $c(\zeta,p)$

$$\frac{d}{d\zeta}\left[(\zeta^2-1)\ \frac{dc}{d\zeta}\right] = p\ (\zeta^2 - \tfrac{1}{3})\ c\ ,\ \zeta_s < \zeta < \infty \qquad (7.1.63)$$

with the boundary conditions (7.1.43)

$$c(\zeta_s,p) = \frac{1}{p}\ ;\quad c(\infty,p) = 0 \qquad (7.1.64)$$

One of the most useful techniques for obtaining the asymptotic solution of (7.1.63) for $p \to \infty$ is with help of the Liouville approximation. For this introduce the new independent variable

$$\eta = \int_{\zeta_s}^{\zeta} \left(\frac{(\zeta')^2 - \frac{1}{3}}{(\zeta')^2 - 1}\right)^{1/2} d\zeta' \qquad (7.1.65)$$

and the new dependent variable

$$N = \left(\left[\zeta^2-1\right]\left[\zeta^2 - \tfrac{1}{3}\right]\right)^{1/4} c \qquad (7.1.66)$$

There results the greatly simplified equation

$$\frac{d^2N}{d\eta^2} = \left[p + g(\eta)\right]\ N \qquad (7.1.67)$$

for which

$$N(\infty,p) = 0 \tag{7.1.68}$$

Since one treats $p \to \infty$, the function $g(\eta)$ is as usual treated as a negligible contribution and its specific form is of no further interest in the following except for the fact that it is a continuous and bounded function.

The dominant solution of (7.1.67) which satisfies (7.1.68) is

$$N(\eta,p) = Ae^{-p^{1/2}\eta} \tag{7.1.69}$$

If this is substituted into (7.1.66) and the boundary condition (7.1.64) is applied there results

$$c(\zeta,p) = \left(\frac{\left[\zeta_s^2-1\right]\left[\zeta_s^2-\frac{1}{3}\right]}{\left[\zeta^2-1\right]\left[\zeta^2-\frac{1}{3}\right]} \right)^{1/4} \frac{e}{p}^{-p^{1/2}\eta} \tag{7.1.70}$$

On inversion there results

$$c(\zeta,\mu,\tau) = \left(\frac{\left[\zeta_s^2-1\right]\left[\zeta_s^2-\frac{1}{3}\right]}{\left[\zeta^2-1\right]\left[\zeta^2-\frac{1}{3}\right]} \right)^{1/4} \operatorname{erfc}\left(\frac{\eta}{2\tau^{1/2}}\right) \tag{7.1.71}$$

where $\eta(\zeta)$ is given by (7.1.65). The early time surface diffusion flux can be determined from this equation and it exhibits, analogous to the second term in eq. (7.1.60), a $\tau^{-1/2}$ behavior, but with a different numerical coefficient.

7.2 Mass Transfer From a Fuel Canister by Diffusion and Forced Convection

Paul L. Chambré

Consider a cylinder of infinite length imbedded in a porous medium through which water is flowing steadily in accordance with Darcy's law. The cylinder matrix contains a diffusing nuclide which is set free at the surface of the cylinder at the solubility limit of the species in water and then diffuses into the exterior unbounded space. All material properties are assumed constant. The flow is taken normal to the axis of the cylinder, but inclined flows can also be treated by the analysis given below. The governing equation for the conservation of mass of the diffusing species from a cylinder of radius r_o in the presence of radioactive decay is

$$K\frac{\partial \hat{c}}{\partial t} + u(\hat{r},\theta)\frac{\partial \hat{c}}{\partial \hat{r}} + \frac{v(\hat{r},\theta)}{\hat{r}}\frac{\partial \hat{c}}{\partial \theta} = D_f\left(\frac{\partial^2 \hat{c}}{\partial \hat{r}^2} + \frac{1}{\hat{r}}\frac{\partial \hat{c}}{\partial \hat{r}} + \frac{1}{\hat{r}^2}\frac{\partial^2 \hat{c}}{\partial \theta^2}\right) - \lambda K\hat{c}\ ,$$

$$r_o < \hat{r} < \infty\ ,\ 0 \leq \theta \leq 2\pi,\ t > 0 \qquad (7.2.1)$$

Here

$$u(r,\theta) = -U\left(1 - \frac{r_o^2}{\hat{r}^2}\right)\cos\theta;\ v(\hat{r},\theta) = U\left(1 + \frac{r_o^2}{\hat{r}^2}\right)\sin\theta \qquad (7.2.2)$$

are the radial and tangential pore velocity components derived from D'Arcy's potential flow in the porous medium with U the free stream pore velocity far away from the cylinder. $\hat{r}$ is the radial distance from the center of the cylinder and θ the angle measured in the tangential flow direction from the frontal stagnation point at the cylinder surface. K is the retardation coefficient and D_f is the diffusion coefficient of the species in the liquid.

Prior to the time t = 0, the diffusing nuclide has zero concentration

in the porous medium. At time t = 0 the concentration at the surface of the cylinder is changed to a constant value c_s

$$\hat{c}(r_o,\theta,t) = c_s,\ 0 \leqslant \theta \leqslant 2\pi,\ t \geqslant 0 \tag{7.2.3}$$

and maintained at this surface concentration c_s subsequently. The boundary condition far from the cylinder is held at zero concentration

$$\hat{c}(\infty,\theta,t) = 0\ ,\ 0 \leqslant \theta \leqslant 2\pi,\ t \geqslant 0 \tag{7.2.4}$$

It is convenient to introduce non-dimensional variables with

$$\tau = \frac{Ut}{Kr_o}\ ,\ r = \frac{\hat{r}}{r_o}\ ,\ c(r,\theta,\tau) = \frac{\hat{c}(\hat{r},\theta,t)}{c_s}\ e^{\lambda t}$$

$$Pe = \frac{Ur_o}{D_f}\ ,\ \text{the Peclet number} \tag{7.2.5}$$

$$Da = \frac{K\lambda r_o}{U},\ \text{the Damkohler number for convective mass transport.}$$

Then the governing equations for $c(r,\theta,\tau)$ transform to

$$\frac{\partial c}{\partial \tau} - \left(1 - \frac{1}{r^2}\right)\cos\theta\ \frac{\partial c}{\partial r} + \left(1 + \frac{1}{r^2}\right)\frac{\sin\theta}{r}\ \frac{\partial c}{\partial \theta} = \frac{1}{Pe}\left(\frac{\partial^2 c}{\partial r^2} + \frac{1}{r}\frac{\partial c}{\partial r} + \frac{1}{r^2}\frac{\partial^2 c}{\partial \theta^2}\right)$$

$$1 < r < \infty,\ 0 \leqslant \theta \leqslant 2\pi\ \tau > 0 \tag{7.2.6}$$

$$c(1,\theta,\tau) = e^{Da\tau}\ ,\ 0 \leqslant \theta \leqslant 2\pi,\ \tau \geqslant 0 \tag{7.2.7}$$

$$c(\infty,\theta,\tau) = 0,\ 0 \leqslant \theta \leqslant 2\pi,\ \tau \geqslant 0 \tag{7.2.8}$$

with the initial condition that $c(r,\theta,0) = 0$.

For typical porous media flows the Peclet number Pe may be large. Typically, with U=2 m/yr, r_o = 0.15 m, and $D_f = 1x10^{-5}$ cm^2/sec will yield a Peclet number of 10.

This suggests an asymptotic solution of the equation system for large Peclet numbers. In this case the principal resistance to mass transfer from the cylinder surface is in a direction normal to the fluid layer surrounding the cylinder, i.e., in the r direction. The diffusion transport tangential to the surface, i.e., the term $\frac{1}{r^2}\frac{\partial^2 c}{\partial \theta^2}$, can then be neglected as will be shown below. To obtain the asymptotic form of the equations, introduce the new independent variable R in place of r

$$r = 1 + \frac{R}{\sqrt{Pe}} \quad , \tag{7.2.9}$$

then eq. (7.2.6) takes on the form

$$\frac{\partial c}{\partial \tau} - 2R\cos\theta\,\frac{\partial c}{\partial R} + 2\sin\theta\,\frac{\partial c}{\partial \theta} = \frac{\partial^2 c}{\partial R^2} + O\left(Pe^{-1/2}\right) \tag{7.2.10}$$

This is to be solved for $c(R,\theta,\tau)$ subject to, see (7.2.7), (7.2.8)

$$c(o,\theta,\tau) = e^{Da\tau} \quad , \; o \leqslant \theta \leqslant 2\pi, \; \tau \geqslant o \tag{7.2.11}$$

$$c(\infty,\theta,\tau) = 0, \; o \leqslant \theta \leqslant 2\pi, \; \tau \geqslant o \tag{7.2.12}$$

with zero initial condition.

For large Pe numbers the last term in eq. (7.2.10) is neglected. By an additional change of the independent variables, one can reduce the time dependent diffusion and convection equation (7.2.10) to a simpler time dependent diffusion problem without convection. New independent variables $\eta(R,\theta)$, $\zeta(\tau,\theta)$ are introduced which transform $c(R,\theta,\tau)$ into $\bar{c}(\eta,\zeta)$

$$\text{i.e.,}\quad \bar{c}(\eta,\zeta) = c(R,\theta,\tau) \tag{7.2.13}$$

These variables are given by

$$\zeta(\tau,\theta) = -\frac{1}{2}\cos\theta + \frac{1}{2}\left\{\frac{1-f(\tau,\theta)}{1+f(\tau,\theta)}\right\} \tag{7.2.14a}$$

where $f(\tau,\theta) = e^{-4\tau}\,\frac{a(\theta)}{b(\theta)}$ with $a(\theta) = \left(\frac{2}{1+\cos\theta}\right)$, $b(\theta) = \left(\frac{2}{1-\cos\theta}\right)$

and

$$\eta(R,\theta) = R\sin\theta\ . \tag{7.2.14b}$$

As the reader can readily verify, these transformations, which are deduced by group-theoretical considerations, change eq. (7.2.10) to a very simple equation for $\bar{c}(\eta,\zeta)$, i.e.,

$$\frac{\partial\bar{c}}{\partial\zeta} = \frac{\partial^2\bar{c}}{\partial\eta^2}\ ,\ \eta > 0,\ \zeta > 0 \tag{7.2.15}$$

subject to the side conditions

$$\bar{c}(0,\zeta) = 1\ ,\ \zeta \geq 0 \tag{7.2.16}$$

$$\bar{c}(\infty,\zeta) = 0,\ \zeta \geq 0 \tag{7.2.17}$$

with the condition that $\bar{c}(\eta,0) = 0$.

The solution to this problem is

$$\bar{c}(\eta,\zeta) = \operatorname{erfc}\left(\frac{\eta}{2\sqrt{\zeta}}\right) \tag{7.2.18}$$

The solution in R,θ,τ variables is obtained by substituting $\eta(R,\theta)$, and $\zeta(\theta,\tau)$ in (7.2.18). One obtains after some simplifications that:

$$c(R,\theta,\tau) = \operatorname{erfc}\left(R\sqrt{\frac{\coth 2\tau + \cos\theta}{2}}\right) \tag{7.2.19}$$

This solution satisfies (7.2.10) with side condition (7.2.11) replaced by unity. To obtain the τ dependent boundary condition given

by (7.2.11) we use Duhamel's integral, i.e.,

$$c(R,\theta,\tau) = \int_0^\tau c(o,\theta,\tau') \frac{\partial}{\partial\tau} \left[\operatorname{erfc}\left(R\sqrt{\frac{\coth 2(\tau-\tau') + \cos\theta}{2}} \right) \right] d\tau' \qquad (7.2.20)$$

Integrating by parts and transforming back to the original variable $\hat{c}$ one obtains

$$\hat{c}(\hat{r},Pe,Da,t,\theta) = c_s \exp\left(-\frac{Da\ Ut}{Kr_o}\right) \operatorname{erfc}\left[\left(\frac{\hat{r}}{r_o} - 1\right) \sqrt{\frac{Pe}{2}\left(\coth\frac{2Ut}{Kr_o} + \cos\theta\right)} \right] +$$

$$+ c_s\ Da \int_0^{\frac{Ut}{Kr_o}} e^{-Da\tau} \operatorname{erfc}\left[\left(\frac{\hat{r}}{r_o} - 1\right) \sqrt{\frac{Pe}{2}\left(\coth 2\tau + \cos\theta\right)} \right] d\tau \qquad (7.2.21)$$

This solution (7.2.21) describes the time dependent concentration field in the presence of radioactive decay in a Darcy flow about a cylinder.

The surface mass flux for a diffusing nuclide is

$$\vec{j}(Pe,Da,t,\theta) = - D_e \left.\frac{\partial\hat{c}}{\partial\hat{r}}\right|_{\hat{r}=r_o}$$

$$= \frac{D_e c_s}{r_o} \sqrt{\frac{2Pe}{\pi}} \left[\exp\left(-\frac{Da\ Ut}{Kr_o}\right) \sqrt{\coth\frac{2Ut}{Kr_o} + \cos\theta} + \right.$$

$$\left. + Da \int_0^{\frac{Ut}{Kr_o}} e^{-Da\tau} \sqrt{\coth 2\tau + \cos\theta}\ d\tau \right] \qquad (7.2.22)$$

where $D_e = \varepsilon D_f$ in the effective diffusion coefficient of the diffusing nuclide and ε the porosity of the medium.

The surface mass flux, according to (7.2.22) depends on time and the angular position. The angular dependence is removed by averaging the surface mass flux over the cylinder perimeter. On the account of symmetry we have

$$\vec{J}_{av}\,(Pe,Da,t) = \frac{1}{\pi}\int_0^{\pi} \vec{j}\,(Pe,Da,t,\theta)\,d\theta$$

$$= \frac{D_e c_s}{\pi r_o}\sqrt{\frac{2Pe}{\pi}}\left[\exp\left(-\frac{Da\ Ut}{Kr_o}\right)\ I\left(\frac{Ut}{Kr_o}\right) + Da\int_0^{\frac{Ut}{Kr_o}} e^{-Da\tau}\ I(\tau)\,d\tau\right] \qquad (7.2.23)$$

where

$$I(\tau) \equiv \int_0^{\pi} (\coth 2\tau + \cos\theta)^{1/2}\,d\theta$$

To evaluate $I(\tau)$ we proceed as follows

$$I(\tau) = \int_0^{\pi}\left(-1 + \frac{2e^{2\tau}}{e^{2\tau}-e^{-2\tau}} + \cos\theta\right)^{1/2} d\theta$$

$$= 2\int_0^{\pi/2}\left(\frac{2}{1-e^{-4\tau}} - 2\sin^2\phi\right)^{1/2} d\phi$$

$$= \frac{2\sqrt{2}}{m(\tau)}\ E\,[m^2(\tau)] \qquad (7.2.24)$$

where $m(\tau) \equiv (1-e^{-4\tau})^{1/2}$ and $E[x]$ is the complete elliptic integral of the second kind. Substituting for $I(\tau)$ in (7.2.23) one obtains

$$\vec{J}_{av}(Pe,Da,t) = \frac{4D_e c_s}{\pi r_o}\sqrt{\frac{Pe}{\pi}}\left\{\frac{\exp\left(-\frac{Da\ Ut}{Kr_o}\right)E\left[m^2\left(\frac{Ut}{Kr_o}\right)\right]}{m\left(\frac{Ut}{Kr_o}\right)} + Da\int_0^{\frac{Ut}{Kr_o}} e^{-Da\tau}\,\frac{E[m^2(\tau)]}{m(\tau)}\,d\tau\right\}$$

(7.2.25)

In absence of radioactive decay (λ=Da=0) there results

$$\vec{j}_{av}(Pe,o,t) = \frac{4D_e c_s}{\pi r_o}\sqrt{\frac{Pe}{\pi}}\ \frac{E[m^2(\frac{Ut}{Kr_o})]}{m(\frac{Ut}{Kr_o})} \qquad (7.2.26)$$

For application in section (7.5), we require the steady state, average surface mass flux in absence of radioactive decay. Hence, (7.2.26) yields as $t\to\infty$, with $m(\infty) = 1$ and $E[1] = 1$, that

$$\vec{J}_{av} = \frac{4D_e c_s}{\pi r_o}\sqrt{\frac{Pe}{\pi}} \qquad (7.2.27)$$

The mass transfer per unit length of cylinder under steady state condition is then given by

$$\dot{m} = \vec{J}_{av} \times 2\pi r_o = 4.5135\ D_e c_s\ \sqrt{Pe} \qquad (7.2.28)$$

a result well known in heat and mass transfer studies where it is shown to be valid for a range of Pe>4 (K2),(L1).

From (7.2.26) one can estimate the time necessary to establish the surface mass flux to 99% of the steady state mass flux. From table of complete elliptic integral of the second kind one obtains that the criteria is given by

$$\frac{Ut}{Kr_o} = 1.2 \qquad (7.2.29)$$

For a flow of U = 1 m/yr, r_o = 0.15 m, and K = 100, t = 18 years, a relatively short time for the establishment of a steady state when compared with the case of pure diffusion. There t = 4000 years was obtained (see 7.1.62).

The analysis leading to the solution (7.2.21) for the time independent boundary condition is readily generalized to a time dependent boundary condition. The starting point for this analysis is Eq.(7.2.20). If in (7.2.3), c_s is replaced by $c_s\,\phi(t)$, one must change $c(o,\theta,\tau')$ in (7.2.20) to $e^{Da\tau'}\,\phi\left(\frac{\tau' Kr_o}{U}\right)$

As an illustration consider the radioactive decay of the surface concentration according to

$$\hat{c}(r_o,\theta,t) = c_s\, e^{-\lambda t} \qquad o<\theta \leq 2\pi, \quad t\geq o \tag{7.2.30}$$

in place of Eq.(7.2.3). Here $\phi(t) \equiv e^{-\lambda t}$. Hence, we have

$$c(o,\theta,\tau') = e^{Da\tau'}\, e^{\frac{-\lambda\tau' Kr_o}{U}} = 1 \tag{7.2.31}$$

After substitution of $c(o,\theta,\tau')$ into (7.2.20) one can perform the integration analytically. Transforming back to the $\hat{c}$ and evaluating surface mass flux one obtains

$$\vec{j}\,(Pe,Da,\theta,t) = \frac{D_e c_s}{r_o} \exp\left(-\frac{Da\ Ut}{Kr_o}\right) \sqrt{\frac{2P_e}{\pi}\left[\coth\left(\frac{2Ut}{Kr_o}\right) + \cos\theta\right]}\ . \tag{7.2.32}$$

This shows that the surface mass flux no longer reaches a steady state but tends toward zero as $t \to \infty$.

For a flow parallel to the cylinder axis the mass transfer can be approximated as follows. The lateral cylinder surface is unwrapped into a flat plate of length L and width $2\pi r_o$, and subjected to a flow in the direction of the plate length. The steady mass transfer from a flat plate of width $2\pi r_o$ and length L under longitudinal flow is given by

$$\dot{M}_{long} = 2.257\ D_e c_s \left(\frac{UL}{D_f}\right)^{1/2} 2\pi r_o\ , \tag{7.2.33}$$

while the mass transfer from a cylinder of length L with the flow normal to the cylinder axis is in view of (7.2.25)

$$\dot{M}_{norm} = 4.513\ D_e c_s \left(\frac{Ur_o}{D_f}\right)^{1/2} L \tag{7.2.34}$$

Hence

$$\frac{\dot{M}_{norm}}{\dot{M}_{long}} = \frac{4.513}{(2.257)\sqrt{2\,\pi}} \left(\frac{L}{2r_o}\right)^{1/2}$$

For a canister, with an aspect ratio $\frac{L}{2r_o} = 13.2$

$$\frac{\dot{M}_{norm}}{\dot{M}_{long}} \simeq 1.63$$

This indicates that for flow parallel to the cylinder axis, the mass transfer is decreased by about 63% compared to that due to the flow normal to the cylinder axis because the thickness of the diffusion boundary layer is greater for $\dot{M}_{long}$ than for $\dot{M}_{norm}$.

Finally we note that the large Peclet number approximation made in the analysis prevents one from letting the free stream Darcy velocity U become small. If $U \to o$, in eq. (7.2.1), the convection terms drop out and the equation describes then a temporal balance between the effects of diffusion and radioactive decay. For a constant surface concentration, given by eq. (7.2.3), the modified eq. (7.2.1) generates then a steady state solution as $t \to \infty$. Since the θ dependence is no longer needed, the governing equation is

$$\frac{\partial^2 \hat{c}}{\partial r^2} + \frac{1}{r}\,\frac{\partial \hat{c}}{\partial r} - \beta^2 \hat{c} = 0, \quad r > 1$$

where

$$\beta^2 = \frac{r_o^{\,2}\lambda K}{D_f}\,, \quad r = \frac{\hat{r}}{r_o}\,, \tag{7.2.35}$$

with the boundary conditions

$$\hat{c}(1) = c_s\,, \quad \hat{c}(\infty) = 0. \tag{7.2.36}$$

The solution is given by

$$\hat{c}(r) = c_s \frac{K_o(\beta r)}{K_o(\beta)} , \quad r > 1 \tag{7.2.37}$$

so that the surface mass flux is

$$\vec{J}(r_o) = \frac{D_e c_s}{r_o} \left\{ \beta \frac{K_1(\beta)}{K_o(\beta)} \right\} \tag{7.2.38}$$

Here $K_o(\eta)$, $K_1(\eta)$ are the modified Bessel functions of zero and first order respectively.

A detailed numerical evaluation of the mass transfer without radioactive decay, i.e., eq. (7.2.28), as well as the fractional dissolution rate are given in section 7.5. The other formulae derived above including their dependence on radioactive decay will be investigated in the future.

7.3 Mass Transfer From a Fuel Canister by Diffusion and Free Convection

Paul L. Chambré

The problem concerns the mass transfer from a heated vertical cylinder which is imbedded in a water saturated porous medium. The temperature of the cylinder exceeds that of the surrounding with the result that a free convection pattern develops which drives the fluid along the cylinder surface. This induced velocity affects the mass transport of a diffusing species from the cylinder surface into the surrounding medium. It is thought that the effects of free convection might be important during that time when the fuel canister generates a sufficiently large amount of decay heat to maintain a temperature difference of about 50°C (or more) between the canister surface and the surrounding medium. The aim of the analysis is to determine the velocity, temperature and concentration fields and to develop a formula for the surface mass flux.

The following assumptions are made:

a) A steady state description is adopted.

b) The vertical cylinder surface is replaced by a flat plate surface having the same length as the cylinder and a width equal to the cylinder circumference.

c) The pore water is assumed to have temperature independent properties except for its density. The water flow obeys Darcy's law. The fluid filling the porous medium is assumed to be a single phase.

d) Boundary layer theory simplifications are assumed valid, see eq. (7.3.14) below.

The governing equations are:

Conservation of Mass

$$\frac{\partial u}{\partial x} + \frac{\partial v}{\partial y} = 0 \qquad (7.3.1)$$

Conservation of Momentum (Darcy's Law)

$$u = -\frac{k}{\mu}\left(\frac{\partial p}{\partial x} + \rho g\right) \tag{7.3.2}$$

$$v = -\frac{k}{\mu}\frac{\partial p}{\partial y} \tag{7.3.3}$$

Conservation of Energy

$$u\frac{\partial T}{\partial x} + v\frac{\partial T}{\partial y} = \alpha_e \nabla^2 T \quad , \alpha_e \equiv \frac{\lambda_e}{\rho c_p} \tag{7.3.4}$$

Conservation of Species

$$u\frac{\partial \hat{c}}{\partial x} + v\frac{\partial \hat{c}}{\partial y} = \varepsilon D_f \nabla^2 \hat{c} \tag{7.3.5}$$

Equation of State of Liquid

$$\rho = \rho_\infty \left\{1 - \beta\,(T - T_\infty)\right\} \tag{7.3.6}$$

where

$$\nabla^2 \equiv \frac{\partial^2}{\partial x^2} + \frac{\partial^2}{\partial y^2} \tag{7.3.7}$$

The coordinate system is shown in Fig. (7.3.1). The velocity components u,v point respectively into the x and y direction. In the above equations p, T, ρ, c_p are the pressure, temperature, density and heat capacity of the liquid and ρ_∞ its density far away from the plate. k is the permeability of the porous medium. λ_e is the effective thermal conduction of water saturated porous medium as measured in the laboratory. μ and β are dynamic viscosity and coefficient of thermal expansion of the liquid in the porous medium respectively. D_f is the diffusion coefficient of the diffusing species in the liquid.

The boundary conditions for our problem are

$$v(x,o) = o,\ T(x,o) = T_w;\ \hat{c}(x,o) = c_s,\ \text{for } x>o \tag{7.3.8}$$

$$u(x,\infty) = v(x,\infty) = 0;\ T(x,\ ) = T_\infty;\ \hat{c}(x,\infty) = 0,\ \text{for } x>o \tag{7.3.9}$$

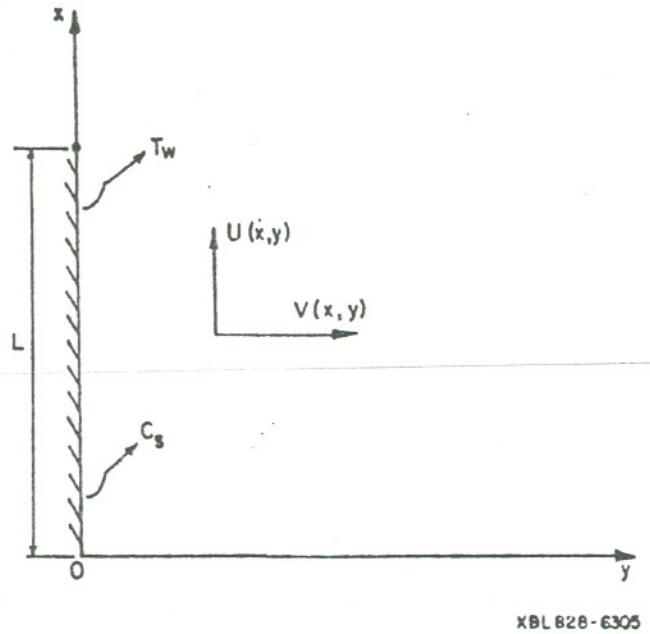

Fig. 7.3.1. Co-ordinate system used in the free convection model.

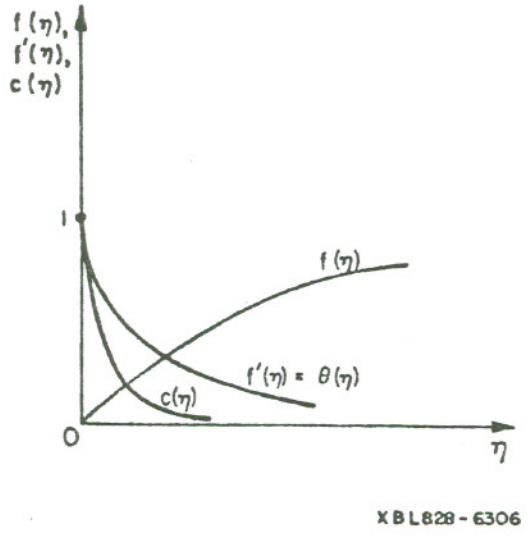

Fig. 7.3.2. Qualitative shape of f(η), f'(η) and c(η) for large Lewis number.

There will be a "slip" condition for the u component of the velocity at the plate surface which is as yet unknown. Furthermore, the temperature difference (T_w-T_∞) which depends among other parameters on the heat release from the cylinder is also determined subsequently.

Eq. (7.3.1) can be satisfied in the usual way by introducing the stream function $\psi(x,y)$ with

$$u(x,y) = \frac{\partial\psi}{\partial y} \; ; \; v(x,y) = - \frac{\partial\psi}{\partial x} \tag{7.3.10}$$

If one differentiates (7.3.2) with respect to y, (7.3.3) with respect to x and then algebraically adds the resulting equations, one obtains with help of (7.3.6) and (7.3.10),

$$(\frac{k}{\mu} \rho_\infty \beta g) \frac{\partial T}{\partial y} = \nabla^2\psi \tag{7.3.11}$$

On the other hand (7.3.4) and (7.3.5), expressed with (7.3.10), give

$$\frac{\partial\psi}{\partial y} \frac{\partial T}{\partial x} - \frac{\partial\psi}{\partial x} \frac{\partial T}{\partial y} = \alpha_e \nabla^2 T \tag{7.3.12}$$

$$\frac{\partial\psi}{\partial y} \frac{\partial\hat{c}}{\partial x} - \frac{\partial\psi}{\partial x} \frac{\partial\hat{c}}{\partial y} = \varepsilon D_f \nabla^2 \hat{c} \tag{7.3.13}$$

One has thus these three governing equations for the determination of the unknown functions ψ,T and $\hat{c}$. For the purpose of establishing the main physical features of the solution, it is convenient to utilize the boundary layer simplifications. These imply that the transport of mass, energy and concentration in the major flow direction (i.e., u) is small compared to that normal to the plate. With

$$\frac{\partial^2\psi}{\partial x^2} << \frac{\partial^2\psi}{\partial y^2} \; , \; \frac{\partial^2 T}{\partial x^2} << \frac{\partial^2 T}{\partial y^2} \; , \; \frac{\partial^2\hat{c}}{\partial x^2} << \frac{\partial^2\hat{c}}{\partial y^2} \tag{7.3.14}$$

Equations 7.3.11-13 result in,

$$\left(\rho_\infty \frac{k}{\mu} \beta g\right) \frac{\partial T}{\partial y} = \frac{\partial^2 \psi}{\partial y^2} \tag{7.3.15}$$

$$\frac{\partial \psi}{\partial y} \frac{\partial T}{\partial x} - \frac{\partial \psi}{\partial x} \frac{\partial T}{\partial y} = \alpha_e \frac{\partial^2 T}{\partial y^2} \tag{7.3.16}$$

$$\frac{\partial \psi}{\partial y} \frac{\partial \hat{c}}{\partial x} - \frac{\partial \psi}{\partial x} \frac{\partial \hat{c}}{\partial y} = \varepsilon D_f \frac{\partial^2 \hat{c}}{\partial y^2} \tag{7.3.17}$$

These equations are subject to the boundary conditions, (see (7.3.8), (7.3.9) and (7.3.10))

$$\frac{\partial \psi(x,o)}{\partial x} = 0, \; T(x,o) = T_w \; ; \; \hat{c}(x,o) = c_s \tag{7.3.18}$$

$$\frac{\partial \psi(x,\infty)}{\partial x} = \frac{\partial \psi(x,\infty)}{\partial y} = 0 \; , \; T(x,\infty) = T_\infty \; ; \; \hat{c}(x,\infty) = 0 \tag{7.3.19}$$

valid for $x>o$.

Equations (7.3.15) and 7.3.16), which are coupled equations for T and ψ, are solved first. One determines thereby the temperature induced stream function $\psi(x,y)$ which describes the free convection flow pattern. With knowledge of ψ, one can then solve for the concentration $\hat{c}(x,y)$ separately. For this reason we concentrate first on the solution of (7.3.15) and (7.3.16). These partial differential equations are reduced to ordinary differential equation by the introduction of the similarity variables

$$\eta = Ra^{1/2} \left(y/\sqrt{xL}\right) \tag{7.3.20}$$

$$\psi = \alpha_e \, (Ra)^{1/2} \left(\frac{x}{L}\right)^{1/2} f(\eta) \tag{7.3.21}$$

$$\theta(\eta) = \frac{T-T_\infty}{T_w-T_\infty} \tag{7.3.22}$$

$$c(\eta) = \frac{\hat{c}}{c_s} \tag{7.3.23}$$

where

$$Ra = \frac{\rho_\infty g}{\alpha_e} \left(\frac{k}{\mu}\right) \beta \, (T_w-T_\infty)L \tag{7.3.24}$$

Here L is the length of the plate and Ra the Rayleigh number of the liquid saturated porous medium. With these variables the governing equations reduce to

$$f'' \, (\eta) - \theta' \, (\eta) = 0 \tag{7.3.25}$$

$$\theta'' \, (\eta) + \frac{1}{2} f \, (\eta) \, \theta' \, (\eta) = 0 \tag{7.3.26}$$

$$\Lambda^{-1} c'' \, (\eta) + \frac{1}{2} f \, (\eta) \, c' \, (\eta) = 0 \tag{7.3.27}$$

where

$$\Lambda = \frac{\alpha_e}{\varepsilon D_f} = Le \tag{7.3.28}$$

is the Lewis number. The boundary conditions transform to

$$f(o) = 0 \; ; \; \theta(o) = 1 \; ; \; c(o) = 1 \tag{7.3.29}$$

$$f'(\infty) = 0 \; ; \; \theta(\infty) = 0 \; ; \; c(\infty) = 0 \tag{7.3.30}$$

as can be seen by introducing the new variables into (7.3.18) and (7.3.19).

A final integral of eq. (7.3.25), which satisfies the boundary conditions (7.3.30) for f' and θ at $\eta = \infty$, is given by

$$f' \, (\eta) = \theta(\eta) \tag{7.3.31}$$

Since the x component of the free convection velocity is determined by

$$u = \frac{\partial \psi}{\partial y} = \left(\frac{\alpha_e}{L} Ra\right) f'(\eta) \qquad (7.3.32)$$

one observes that the normalized vertical velocity $\frac{u(\eta)}{\left(\frac{\alpha_e}{L} Ra\right)}$ and the temperature distribution $\theta(\eta)$ are, according to (7.3.31), of the same form. Thus, the determination of the function $f(\eta)$ is of central importance. To obtain an equation for $f(\eta)$, eliminate θ between equations (7.3.25), (7.3.26) and (7.3.31), with the result that

$$\frac{d^3 f}{d\eta^3} + \frac{1}{2} f \frac{d^2 f}{d\eta^2} = 0 \qquad (7.3.33)$$

Exactly the same differential equation arises in the problem of the boundary layer flow of a viscous fluid over a flat plate, the famous Blasius problem (B2). But in contrast to the boundary conditions $f(o) = f'(o) = 0$, $f'(\infty) = 1$ in that problem, the conditions for the present case read

$$f(o) = 0 \; ; \; f'(o) = 1 \; ; \; f'(\infty) = 0 \qquad (7.3.34)$$

The qualitative shape of the solution $f(\eta)$ of (7.3.33), (7.3.34) and that of its derivative $f'(\eta)$ are shown in Fig. (7.3.2). As already stated, the free convection induced vertical velocity component and the temperature distribution normal to the plate are both characterized by the shape of the $f'(\eta)$ function.

Next we determine the mass transfer from the vertical surface. For this one requires the normal derivative $\left.\frac{\partial \hat{c}}{\partial y}\right|_{y=0}$ which in turn involves $\left.\frac{\partial c}{\partial \eta}\right|_{\eta=0}$. But η contains Ra and in this Rayleigh number there occurs the as yet unknown temperature difference $(T_w - T_\infty)$. $(T_w - T_\infty)$ is determined by the heat flux through the canister surface and the convective and conductive heat

transport into the porous medium. So one must first find (T_w-T_∞). The local heat transfer from the surface of the plate is defined by

$$q'' = - \lambda_e \left.\frac{\partial T}{\partial y}\right|_{y=0}$$

which with (7.3.20) and (7.3.22) yields

$$q'' = - \lambda_e (T_w-T_\infty)^{3/2} \left(\frac{k}{\mu}\frac{\rho_\infty \beta g}{\alpha_e}\right)^{1/2} x^{-1/2} \theta'(o) \qquad (7.3.35)$$

where λ_e is the effective thermal conductive of the saturated porous medium. The total rate of heat transfer from a plate of length and width W is then

$$Q = W \int_o^L q''(x)\, dx$$

$$= - W \lambda_e (T_w-T_\infty)^{3/2} \left(\frac{k}{\mu}\frac{\rho_\infty \beta g}{\alpha_e}\right)^{1/2} 2L^{1/2} \theta'(o) \qquad (7.3.36)$$

Fig. (7.3.3) shows the variation of spent fuel heat generation with time. We now define the magnitude of the average heat flux from the entire plate as

$$\bar{q}'' \equiv \frac{|Q|}{WL}$$

$$= \lambda_e (T_w-T_\infty)^{3/2} \left(4\frac{k}{\mu}\frac{\rho_\infty \beta g}{L\alpha_e}\right)^{1/2} |\theta'(o)| \qquad (7.3.37)$$

Hence the desired temperature difference between plate surface and the porous media is given by

$$(T_w-T_\infty) = \left\{\frac{(\bar{q}'')^2}{4\lambda_e^2 \frac{k}{\mu}\frac{\rho_\infty \beta g}{L\alpha_e}\left[\theta'(o)\right]^2}\right\}^{1/3} \qquad (7.3.38)$$

(T_w-T_∞) is seen to be a function of the average heat flux issuing from the fuel canister and the properties of the porous medium. The assumption

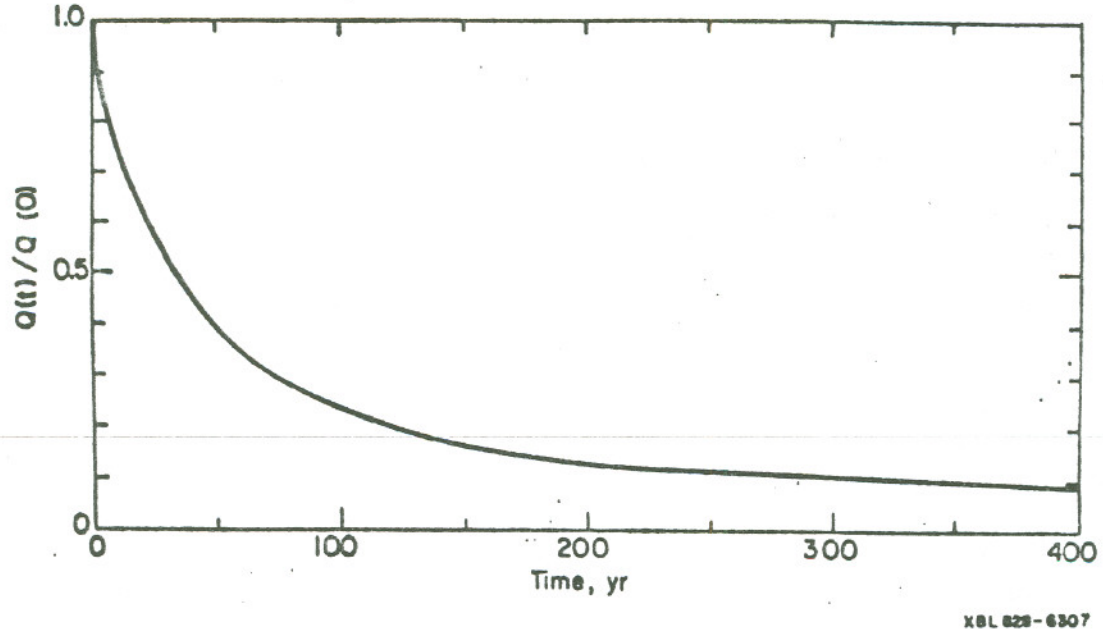

Fig. 7.3.3. Variation of normalized decay heat generation of a spent fuel with time Q (0) is the initial decay heat generation and is equal to 0.55 Kw.

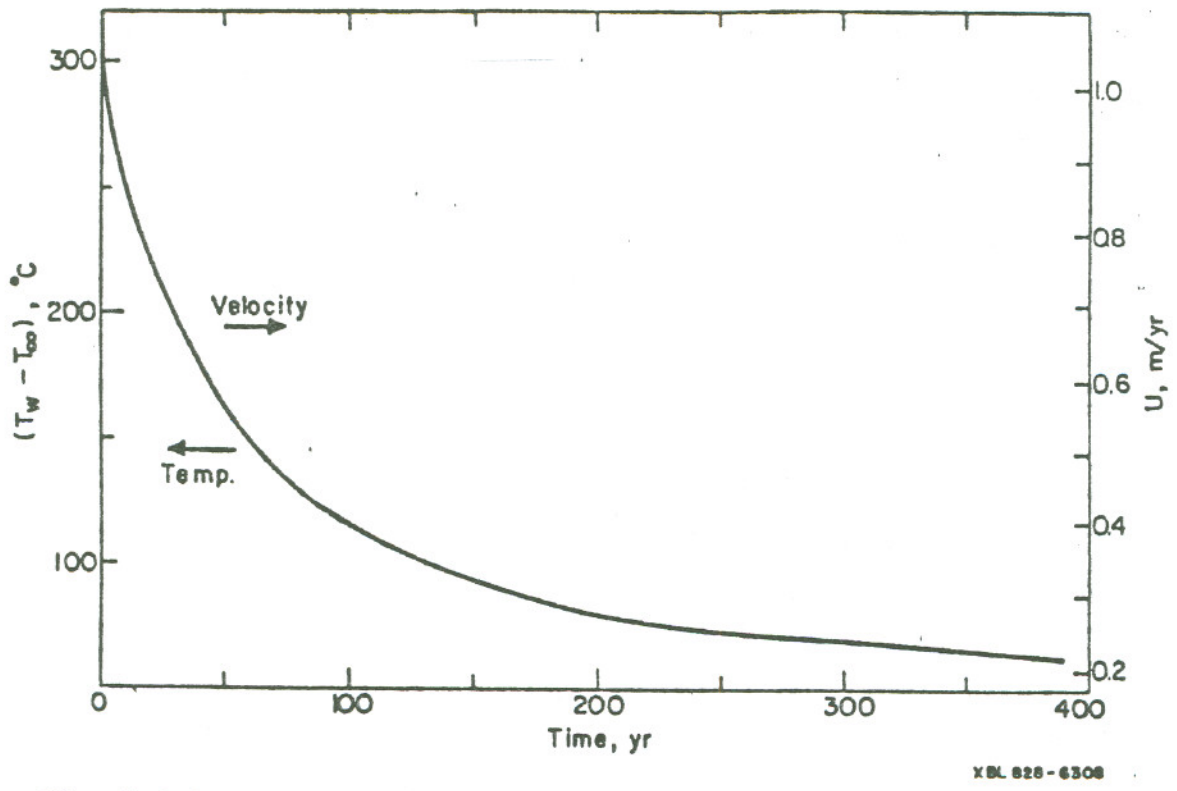

Fig. 7.3.4. Variation of temperature difference $(T_w - T_\infty)$ and free convection velocity with time for a spent fuel canister.

is made that the average heat flux varies so slowly with time so that (7.3.38) can be applied to a quasi-steady state. Fig. (7.3.4) shows a typical trend for this temperature difference as a function of time for a given $\bar{q}''(t)$ descriptive of a spent fuel. The temperature difference drops to 100°C in about 130 years. The calculation is based on the following parameters values

$\lambda = 2.894$ w/m °K (1) $\qquad \beta = 2.07 \times 10^{-4}$ 1/°K

$k = 2.96 \times 10^{-14}$ m^2 (1) $\qquad L = 4.7$ m (2)

$\mu = 5.5 \times 10^{-4}$ kg/m sec $\qquad r = 1.78 \times 10^{-1}$ m (2)

$\rho_\infty = 10^3$ kg/m^3 $\qquad Q(o) = 5.5 \times 10^2$ w (2)

$c_p = 4.184 \times 10^3$ J/kg °K $\qquad \theta'(o) = \frac{-1}{\pi}$

Before proceeding with the mass transfer analysis we estimate next the magnitude of the vertical slip velocity component u for the above data. From (7.3.32) and (7.3.34) the free convection velocity component along the plate surface is given by

$$u = \left(\frac{\alpha_e Ra}{L}\right)$$

$$= \rho_\infty \beta g \, (T_w - T_\infty) \, \frac{k}{\mu} \qquad (7.3.39)$$

For a temperature difference of 100°C one computes u = 0.34 m/yr. This is competitive with commonly assumed groundwater flows of 0.1 to 1 m/yr which are used in the far-field calculations. Fig. (7.3.4) gives the magnitude of the free convection velocity as a function of time.

The local mass transfer rate from the plate is now computed from the solution of (7.3.27) subject to the boundary conditions (7.3.29) and

(7.3.30) for $c(\eta)$. The desired solution is

$$c(\eta) = 1 - \frac{\int_0^{\eta} \exp\left(-\frac{\Lambda}{2}\int_0^{\eta'} f(s)ds\right) d\eta'}{\int_0^{\infty} \exp\left(-\frac{\Lambda}{2}\int_0^{\eta'} f(s)ds\right) d\eta'} \tag{7.3.40}$$

so that the surface mass flux is

$$\vec{j} = -D_f\varepsilon \left.\frac{\partial \hat{c}(y)}{\partial y}\right|_{y=0} = -D_f c_s \varepsilon \left.\frac{\partial \eta}{\partial y}\frac{dc(\eta)}{d\eta}\right|_{\eta=0} \tag{7.3.41}$$

where ε is the porosity of the medium.

In view of (7.3.20) and (7.3.40).

$$\vec{j} = D_f \varepsilon c_s \left(\frac{Ra}{xL}\right)^{1/2} \frac{1}{\int_0^{\infty} \exp\left(-\frac{\Lambda}{2}\int_0^{\eta'} f(s)ds\right) d\eta'} \tag{7.3.42}$$

The definite integral

$$I(\Lambda) = \int_0^{\infty} \exp\left(-\frac{\Lambda}{2}\int_0^{\eta'} f(s)ds\right) d\eta' \tag{7.3.43}$$

involves the function $f(\eta)$, i.e., the solution of (7.3.33) and the Lewis number parameter (7.3.28).

$$\Lambda = \frac{\alpha_e}{\varepsilon D_f} \tag{7.3.44}$$

We shall discuss the complete evaluation of $I(\Lambda)$ for arbitrary Λ values at a later time, but develop now the asymptotic form of this integral for large values of Λ which may arise due to small values of the diffusion coefficient in porous media. In this case the concentration boundary layer is very thin compared with the thermal layer, as sketched in

Fig. (7.3.2). One can then approximate $f(\eta)$ by the first term of its power series expansion, i.e.,

$$f(\eta) = \eta + O(\eta^2) \tag{7.3.45}$$

If one neglects terms of $O(\eta^2)$,

$$I(\Lambda) \simeq \int_0^\infty e^{-\frac{\Lambda}{4}\eta^2} \, d\eta \ ,$$

$$= \sqrt{\frac{\pi}{\Lambda}} \ , \text{ for } \Lambda \text{ large} \tag{7.3.46}$$

Thus (7.3.42) yields,

$$\vec{j} = D_f \varepsilon c_s \left(\frac{Ra}{xL} \frac{\Lambda}{\pi} \right)^{1/2} \ , \text{ for } \Lambda \text{ large} \tag{7.3.47}$$

If one expresses Ra by (7.3.24) one has in terms of the physical parameters

$$\vec{j} = D_f \varepsilon c_s \left(\frac{1}{\pi} \frac{k}{\mu} \frac{\rho_\infty g}{\varepsilon D_f} \beta (T_w - T_\infty) \frac{1}{x} \right)^{1/2} = \frac{D_f \varepsilon c_s}{\ell} \tag{7.3.48}$$

where the length ℓ is given by

$$\ell = \left(\frac{1}{\pi} \frac{k}{\mu} \frac{\rho_\infty g}{\varepsilon D_f} \beta (T_w - T_\infty) \frac{1}{x} \right)^{1/2} \tag{7.3.49}$$

The average rate of mass transfer per unit length of plate for a plate of length L is readily computed from equation (7.3.48).

References

1. M. J. Lippmann, et al, "Modeling Subsidence Due to Geothermal Fluid Production", ASCE Fall Convention and Exhibit, San Francisco, Calif., Oct. 1977.

2. G. E. Raines, et al, "Development of Reference Conditions for Geologic Repositories for Nuclear Waste in the USA", Material Research Society, Nov. 1980.

7.4 A Model for Leach and Diffusion Rates From Glass Bodies

Paul L. Chambré

Experimental evidence indicates that when a typical silica base glass is brought into contact with water two physical processes occur in the dissolution of the glass. One of these is an alkali ion transfer, such as for example, Na^+, across the glass-water interface which gives rise to a gel-like SiO_2 transition layer. The second process appears to be the corrosion of this layer resulting in the dissolution of the glass matrix. A number of theories have been proposed, differing in various detailed mechanistic ways, which attempt to explain qualitatively or quantitatively various aspects of experimental observations on glass dissolution. In the following, we develop a model which is based on only the two, generally accepted, experimental pieces of evidence. These are

i) The movement of the glass interface with a (regression) velocity v, which is initiated by

ii) The diffusion of an alkali ion across the glass-water interface.

Three simplifying assumptions will be made. The interface velocity is assumed to be constant in time. The support for this assumption is indirect. It will be shown in the following analysis that a constant regression velocity leads to the often observed experimental result (M4) that the fractional release of a particular nuclide f(t) follows the empirical formula

$$f(t) = c_1\sqrt{t} + c_2 t \qquad (7.4.1)$$

where c_1 and c_2 are constants. On the other hand there exists also some experimental evidence yielding a different time dependence for f(t)(M3). This has been interpreted by investigators to be due to a corrosion layer which is developing on the glass surface, gradually increasing the resistance

of mass transfer from the interface. In the analysis, the case of accretion, is also included and the f(t) function deduced. The remaining assumptions concern the nature of the diffusion mechanism of the alkali ion. We shall assume a constant diffusion coefficient for the ion in the bulk glass and the gel-like surface transition layer despite the fact that the diffusion coefficient is considerably larger in this layer (H2). Furthermore, we shall ignore the effect of the negative surface potential on the ion transfer. Such a potential is generated when glass is immersed in water. The effects of the latter two assumptions require future study.

The Analysis

The analysis applies to a body of planar, cylindrical and spherical shape. We take as the governing equation

$$\frac{\partial \bar{c}}{\partial t} = D \left\{ \frac{\partial^2 \bar{c}}{\partial r^2} + \frac{m}{r} \frac{\partial \bar{c}}{\partial r} \right\} - \lambda \bar{c} \qquad (7.4.2)$$

Here $\bar{c}(r,t)$ is the concentration of the nuclide, D the diffusion coefficient and λ the radioactive decay constant if the nuclide is radioactive. m describes the geometric character of the diffusion field. For the case of the sphere m = 2, for the cylinder (of infinite length) m = 1 and for the slab m = 0. r is the position variable within the region of interest, t the time and R(t) the position of the movable boundary which will be prescribed below. The initial nuclide concentration is given as c(r) so that

$$\bar{c}(r,0) = c(r), \quad 0 < r < R(0) \equiv a. \qquad (7.4.3)$$

At the surface of the solid

$$\bar{c} \left\{ R(t), t \right\} = 0, \quad t > 0 \qquad (7.4.4)$$

but if the surface concentration is instead $\bar{c}_s \neq 0$, it is always possible

to reduce this to the condition given by eq.(7.4.4) by taking the reference datum for the concentration at $\bar{c}_s$, provided $\lambda = 0$. In addition to the above conditions, one prescribes in case of the sphere and the cylinder that $\bar{c}\ (0,t)$ is bounded and in the case of the slab of thickness 2R(t) that $\partial\bar{c}\ (0,t)/\partial r$ vanishes for all times.

The equation for the moving boundary R(t) is based on the simple hypothesis that

$$R(t) = a - vt, \quad o \leqslant t \leqslant {}^{a}/_{v} \tag{7.4.5}$$

where a is the initial position and v the surface regression velocity. A regressive surface at time $T_L = {}^{a}/_{v}$ the finite sized body has completely dissolved. This limits the time span for the solution. If there is accretion, we take v negative in the expression for R(t) and consider $t \geqslant 0$. The equations(7.4.2) to (7.4.5) completely define the model.

The solution for the different geometric configurations (fig. 7.4.1a) is carried out below. It turns out that the solutions for the sphere, cylinder and slab are very similar. The case of the sphere is treated in detail, then the changes which need to be made in case of the slab are indicated and the final solution is given. These results are exact and are valid for any range of the parameters entering the problem. The cylinder is analyzed by an approximation method which is valid for the large values of the parameter (va/D) usually encountered in practice. By forming the product of the solutions for slabs of different or identical widths one obtains at once the solution to the case of a parallelopiped or cube, respectively. Similarly multiplication of the slab and (infinite) cylinder solutions yields the solution for a cylinder of finite length (fig. 7.4.1b). These results are consequences of some well known theorems and are valid for a time span in which the smallest initial dimension of the body has been reduced to naught by the leaching process.

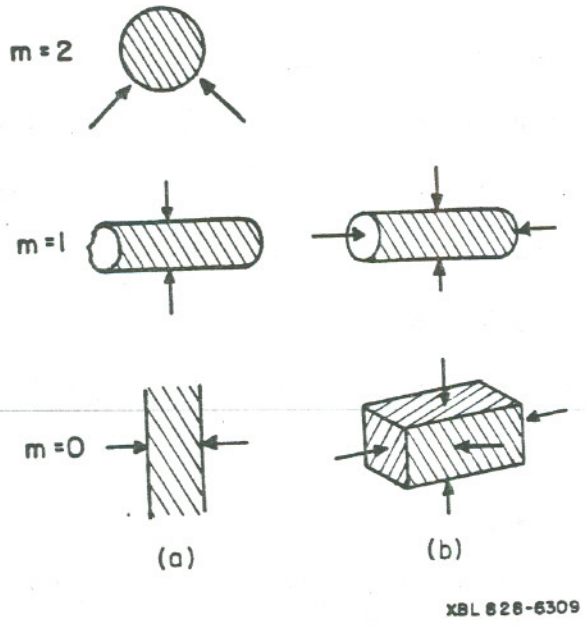

Fig. 7.4.1. Geometries of problems considered (arrows indicate direction of surface regression).

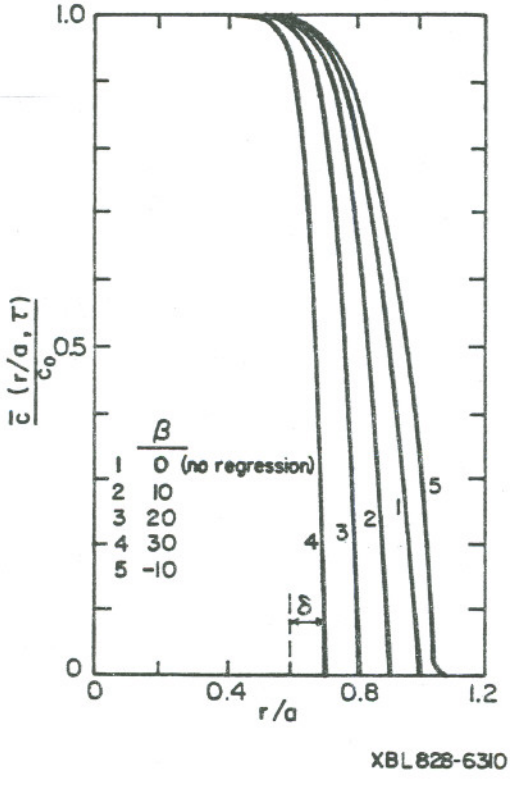

Fig. 7.4.2. Spatial distribution of the concentration inside sphere r = 0.01 for various rates of surface regression (λ=0).

The Sphere

Let

$$c(r,t) = \exp(\lambda t) r\bar{c}_{sp}(r,t) \tag{7.4.6}$$

then eqs. (7.4.2) to (7.4.5) reduce with m = 2 to

$$\frac{\partial c}{\partial t} = D\frac{\partial^2 c}{\partial r^2}, \quad 0 \leq r < a - vt, \quad 0 < t < a/|v| \tag{7.4.7}$$

$$c(r,0) = rc(r) \equiv g(r), \quad 0 \leq r \leq a, \tag{7.4.8}$$

$$c(a - vt,t) = 0 \quad 0 \leq t \leq a/|v| \tag{7.4.9}$$

and on account of the boundedness condition on $\bar{c}$ (0,t),

$$c(0,t) = 0, \quad 0 < t < a/|v| \tag{7.4.10}$$

Now the Kelvin function,

$$\frac{1}{2(\pi Dt)^{1/2}} \exp\left(-\frac{r^2}{4Dt}\right),$$

is a particular solution to eq. (7.4.7). By the super-position principle and the method of images one can construct a more general solution to eq. (7.4.7) which satisfies conditions (7.4.8) and (7.4.10) as a detailed verification shows.

This solution has the form,

$$c(r,t) = \frac{1}{2(\pi Dt)^{1/2}} \left\{ \int_0^a g(s)\, S(r,t;s)\, ds + \int_a^\infty h(s) S(r,t;s) ds \right\}, \tag{7.4.11}$$

$$0 \leq r \leq a - vt, \quad 0 \leq t \leq a/|v|$$

where the source function

$$S(r,t;s) = \exp\left[-\frac{(r-s)^2}{4Dt}\right] - \exp\left[-\frac{(r+s)^2}{4Dt}\right] \quad . \tag{7.4.12}$$

In eq. (7.4.11), g(s) is the initial concentration distribution and h(s) is an as yet unknown source density function which is determined by imposing the last remaining condition on the moving boundary, i.e., eq. (7.4.9),

$$\int_0^a g(s)S(a-vt,t;s)\,ds + \int_a^\infty h(s)S(a-vt,t;s)\,ds = 0. \tag{7.4.13}$$

Now the functions g(s) and h(s) are partly at our disposal. Since g(s) is prescribed only for $0 < s < a$, we analytically continue it in the following manner

$$g(s) = \begin{cases} 0, & |s| > a \\ -g(-s), & |s| < a \ . \end{cases} \tag{7.4.14}$$

Similarly h(s), which must be determined according to the solution (7.4.11) and the condition (7.4.13) in the span $a < s < \infty$, is chosen in the remaining part of the range as

$$h(s) = \begin{cases} h(s), & s > a \\ 0, & |s| < a \\ \text{arbitrary}, & s < -a. \end{cases} \tag{7.4.15}$$

With this choice one can now combine both integrals in eq. (7.4.13) by elementary transformations resulting in integrals with the same integration limits, i.e.,

$$\int_0^\infty \{h(s+a)\exp\left(-\frac{vs}{D}\right) - h(s-a) - g(s-a)\}\exp\left(-\frac{s^2}{4Dt}\right)ds = 0. \tag{7.4.16}$$

The satisfaction of this condition requires that h(s) must obey the ordinary difference equation,

$$h(s+a)\exp(-vs/D) - h(s-a) = g(s-a). \tag{7.4.17}$$

The solution to this equation can be constructed in successive s spans of width 2a, utilizing the properties of the initial distribution g(s) and the continuation properties of h(s) with the result

$$h(s) = g(s-2na)\exp\left[nv(s-na)/D\right]$$

$$(2n-1)a < s < (2n+1)a, \quad n = 1,2,... \tag{7.4.18}$$

Having found the unknown source distribution h(s), c(r,t) given by eq. (7.4.11) can be shown to satisfy all the conditions of the problem. There results, on returning to the original variables, after some minor simplifications

$$\bar{c}_{sp}(r,t) = \frac{\exp(-\lambda t)}{2r(\pi Dt)^{1/2}}\left\{\int_{-a}^{a} sc(s)\exp\left[-\frac{(r-s)^2}{4Dt}\right] ds + \right.$$

$$\left. + \sum_{n=1}^{\infty} \int_{-a}^{a} sc(s)\exp\left[nv(s+na)/D\right] S(r,t;s+2na)\, ds\right\},$$

$$0 \leq r \leq a-vt, \quad 0 \leq t \leq a/|v| \tag{7.4.19}$$

For bounded c(s), the series can be shown to converge for the indicated t range, i.e., for all times for which sphere material remains. It should be noted that, in view of eqs. (7.4.8) and (7.4.14), the initial distribution c(s) must be an even function about s = 0.

A case of practical interest is the one where the initial concentration is uniform throughout the sphere, i.e., $c(r) = c_0$ for $0 \leq r \leq a$. The

integration in eq. (7.4.19) then yields the following explicit result for the concentration in the interior of the sphere,

$$\hat{c}_{sp}(\frac{r}{a},\tau) = \frac{\bar{c}_{sp}(\frac{r}{a},\tau)}{c_o} = \frac{\exp\{(-\lambda a^2/D)\tau\}}{2(r/a)} \quad .$$

$$\cdot\{2(r/a) - (\text{erfc } \varepsilon_1 - \text{erfc } \varepsilon_2) - 2\tau^{1/2} (\text{ierfc } \varepsilon_1 - \text{ierfc } \varepsilon_2) -$$

$$- \sum_{n=1}^{\infty} \Big[(\text{erfc } \theta_{21} + \text{erfc } \theta_{11}) \exp(-n\beta\delta_1) -$$

$$-(\text{erfc } \theta_{22} + \text{erfc } \theta_{12}) \exp(-n\beta\delta_2) + \qquad (7.4.20)$$

$$+ 2\tau^{1/2} (\text{ierfc } \theta_{21} - \text{ierfc } \theta_{11}) \exp(-n\beta\delta_1) -$$

$$- 2\tau^{1/2} (\text{ierfc } \theta_{22} - \text{ierfc } \theta_{12}) \exp(-n\beta\delta_2)\} \ ,$$

where

$$\theta_{ij} \quad \frac{\{2n(1-\beta\tau) + (-1)^i + (-1)^j (r/a)\}}{\left(2\tau^{1/2}\right)}$$

$$\delta_i \equiv n(1-\beta\tau) + (-1)^i (r/a), \qquad (7.4.21)$$

$$\varepsilon_i \equiv \frac{\{1 + (-1)^i (r/a)\}}{\left(2\tau^{1/2}\right)} \quad ,$$

and $\tau \equiv Dt/a^2$; $\beta \equiv va/D$, the interface Peclet number. (7.4.22)

erfc (z) and i^merfc (z) denote, respectively, the complementary error function and the m repeated integral error function which are tabulated in[4].

For $\beta = 0$, this reduces to

$$\frac{\bar{c}_{sp}(\frac{r}{a},\tau)}{c_o} = e^{-\lambda\frac{a^2}{D}\tau}\left\{1 - \frac{a}{r}\sum_{n=o}^{\infty}\left[\text{erfc}\,\frac{(2n+1)-r/a}{2\tau^{1/2}} - \right.\right. \tag{7.4.22a}$$

$$\left.\left. - \text{erfc}\,\frac{(2n+1)+r/a}{2\tau^{1/2}}\right]\right\}$$

The spatial distribution of the nuclide concentration given by eq. (7.4.20) is shown in fig. (7.4.2) for a specific value of the dimensionless time ($\tau = 0.01$) and for different values of the dimensionless regression parameter β. One observes as β increases that the regression of the interface steepens the concentration gradient compared to a stationary interface ($\beta = 0$). Fig. (7.4.2) also shows the effects of accretion. In contrast to the previous case the concentration profile is S-shaped and the surface mass flux shows a marked decrease which indicates a resistance to mass transfer.

A quantity of primary interest to the experimentalist is the fractional release of the radionuclide due to the combined effects of diffusion and interface movement. This may be obtained by integrating the concentration at any time t over the volume of the sphere, dividing the result by the initial amount of diffusant present and subtracting this quotient from unity. Thus for the case of an initially uniform concentration,

$$f(\tau) = 1 - Q(\tau)/Q_o, \tag{7.4.23}$$

$$\text{where } Q(\tau) = \int_0^{(1-\beta\tau)a} 4\pi r^2 \bar{c}_{sp}(r/a,\tau)\, dr,$$

$$Q_o = \frac{4}{3}\pi a^3 c_o\ . \tag{7.4.24}$$

$f(\tau)$ has been evaluated numerically with help of eq. (7.4.20) for $\lambda = 0$.

Fig.(7.4.3) shows the numerical results of the evaluation of eq.(7.4.23) for a number of regression Peclet numbers β and for a limited range of $0 < \tau < 2\times10^{-3}$. One observes that the fractional release is initially a linear function of $\tau^{1/2}$ and then it becomes quadratic in $\tau^{1/2}$. This is exactly the behavior observed in many laboratory leaching experiments as already stated in eq. (7.4.1). More extensive numerical evidence will be given in Section (7.6). To pressage this result, we will show here that eq. (7.4.23) is closely approximated by

$$f(t) = 6\left(\frac{Dt}{\pi a^2}\right)^{1/2} + \frac{3}{2}\left(\frac{vt}{a}\right) \quad 0 \leqslant t \leqslant t^{+} \leqslant 0.4T_L \tag{7.4.25}$$

for both regression (v>o) and accretion (v<o).

The Slab

The system of eqs. (7.4.7) to (7.4.9) describes the diffusion process in a slab of half width (a-vt), with an initial concentration distribution $g(r) = c(r)$, in absence of radioactive decay. If the solid is exposed to regression over both faces, with the center of the slab located at r = 0, the boundary condition is replaced by the symmetry condition

$$\frac{\partial \bar{c}_{sL}(o,t)}{\partial r} = 0, \quad 0 \leqslant t \leqslant a/|v| \tag{7.4.26}$$

In order to satisfy this relation, one chooses as the source function

$$S(r,t;s) = \exp\left[-\frac{(r-s)^2}{4Dt}\right] + \exp\left[-\frac{(r+s)^2}{4Dt}\right], \tag{7.4.27}$$

instead of eq. (7.4.12). The analysis proceeds then along the same lines as

for the sphere. However, the function g(s) must now be defined as follows:

$$g(s) = \begin{cases} 0, & |s| > a \\ \\ g(-s), & |s| < a. \end{cases} \tag{7.4.28}$$

The final result is

$$\bar{c}_{sL}(r,t) = \frac{\exp(-\lambda t)}{2(\pi D t)^{1/2}} \int_{-a}^{a} c(s) \exp\left[-\frac{(r-s)^2}{4Dt}\right] ds$$

$$+ \sum_{n=1}^{\infty} (-1)^n \int_{-a}^{a} c(s) \exp\left[nv(s+na)/D\right] . S(r,t;s + 2na)\, ds\} \tag{7.4.29}$$

$$0 \leqslant |r| \leqslant (a-vt), \quad 0 \leqslant t \leqslant a/|v|$$

For a bounded even function c(s) this result can be shown to converge to the solution of our problem. Again if the initial concentration is uniform throughout the slab one obtains with the shorthand notations introduced in eqs. (7.4.21) and (7.4.22) the following result

$$\hat{c}(\tfrac{r}{a},\tau) = \bar{c}_{sL}(r/a,\tau)/c_o = \tfrac{1}{2} \exp(-\lambda a^2 \tau/D) \{(\operatorname{erf} \varepsilon_2 + \operatorname{erf} \varepsilon_1)$$

$$+ \sum_{n=1}^{\infty} (-1)^n \left[(\operatorname{erf} \theta_{21} - \operatorname{erf} \theta_{12}) \exp(-n\beta\delta_1) + \right. \tag{7.4.30}$$

$$\left. + (\operatorname{erf} \theta_{22} - \operatorname{erf} \theta_{12}) \exp(-n\beta\delta_2)\right] \} .$$

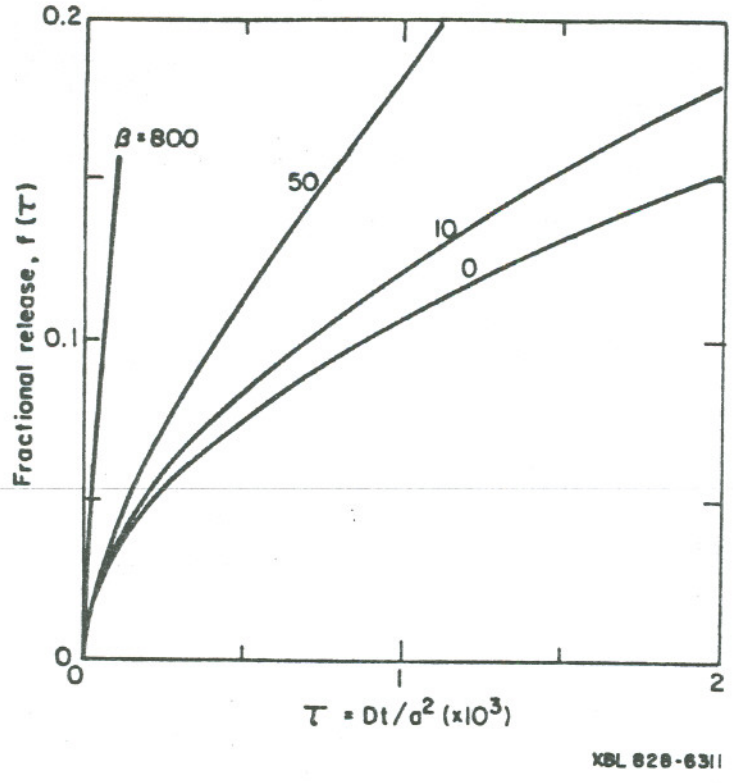

Fig. 7.4.3. Variation of fractional release from sphere (radius = a) with dimensionless time τ for different dimensionless regression speed.

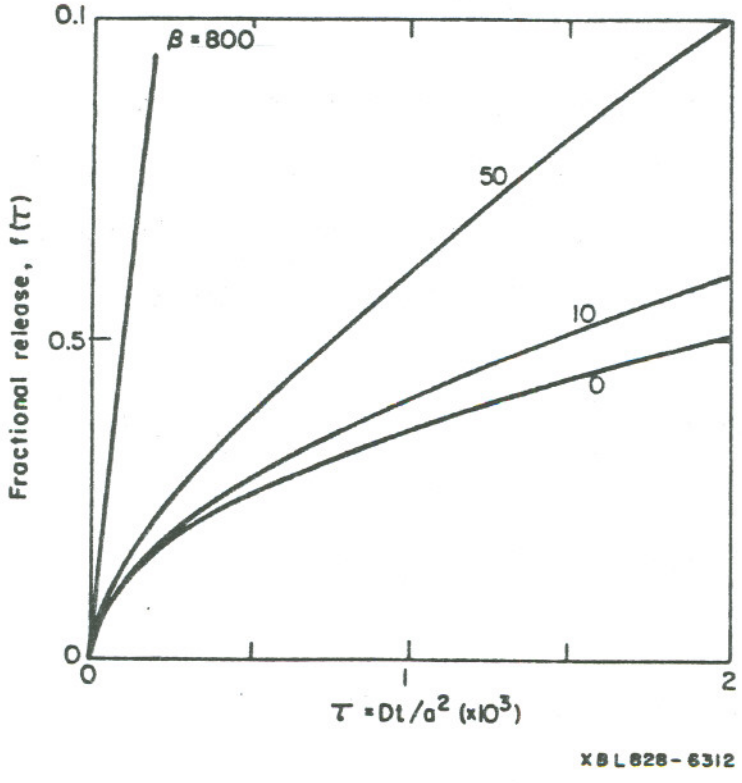

Fig. 7.4.4. Variation of fractional release from slab (initial width 2a) with dimensionless time τ for different dimensionless glass-water interface regression speed β.

For $\beta = 0$, this reduces to

$$\frac{\bar{c}_{sL}\left(\frac{r}{a},\tau\right)}{c_o} = \exp\left(\frac{-\lambda a^2 \tau}{D}\right)\left\{1 - \sum_{n=0}^{\infty} (-1)^n \left[\operatorname{erfc} \frac{(2n+1) - \frac{r}{a}}{2\tau^{1/2}} + \operatorname{erfc} \frac{(2n+1) + \frac{r}{a}}{2\tau^{1/2}}\right]\right\} \tag{7.4.30a}$$

The total fractional release is given by eq.(7.4.23) with

$$Q(\tau) = 2 \int_0^{(1-\beta\tau)a} \bar{c}_{sL}(r/a,\tau)\, dr \tag{7.4.31}$$

$$Q_o = 2ac_o.$$

Performing the integration one obtains

$$f(\tau) = \beta\tau + \tau^{1/2}\left[\operatorname{ierfc}\left(\frac{\beta\tau^{1/2}}{2}\right) - \operatorname{ierfc}\left(\frac{2-\beta\tau}{2\tau^{1/2}}\right)\right] + \sum_{n=1}^{\infty} \frac{(-1)^{n-1}}{2n\beta}\left\{\exp\left[n\beta(n-1)\right].\ (\operatorname{erf}\mu_{11} - \operatorname{erf}\mu_{12}) + \right. \tag{7.4.32}$$

$$\left. + \exp\left[n\beta(n+1)\right].\ (\operatorname{erf}\mu_{22} - \operatorname{erf}\mu_{21}) + \Omega_2(n) - \Omega_1(n)\right\}$$

where

$$\mu_{ij} \equiv \frac{2n + (-1)^i + (-1)^j (1-\beta\tau)}{2\tau^{1/2}}$$

$$\Omega_i(n) \equiv \exp\left\{-n\beta(1-\beta\tau)\left[n+(-1)^i\right]\right\}.\ \sum_{j=1}^{2} (-1)^j \operatorname{erfc}\left[\frac{(1-\beta\tau)\left[2n+(-1)^i\right]+(-1)^j}{2\tau^{1/2}}\right] \tag{7.4.33}$$

For $\beta=0$ this reduces to

$$f(\tau) = 2\tau^{1/2}\left[\frac{1}{\sqrt{\pi}} + 2\sum_{n=1}^{\infty} (-1)^n \operatorname{ierfc} \frac{n}{\tau^{1/2}}\right] \tag{7.4.34}$$

A numerical evaluation for $\lambda = 0$ is shown in Fig. 7.4.4 for some ranges in β and τ.

In section (7.6) we will give numerical evidence that eq. (7.4.32) can be closely approximated by

$$f(t) = 2\left(\frac{Dt}{\pi a^2}\right)^{1/2} + \frac{1}{2}\left(\frac{va}{D}\right)\frac{Dt}{a^2} \qquad (7.4.35)$$

The conclusions for the slab are thus quite comparable to those obtained for a sphere.

The Cylinder

In the case of the cylinder one can proceed in the same manner as above. Instead of the source function eq. (7.4.12) one utilizes the fundamental solution.

$$S(r,t;s) = \{s/(2Dt)\} \exp\left[-(r^2+s^2)/(4Dt)\right] \cdot I_o\{rs/(2Dt)\} \qquad (7.4.36)$$

where $I_o(z)$ is the modified Bessel function of the first kind, zero order. However, this case leads to a rather complicated integral equation for the unknown source density h(s) and for this reason the following approximate solution is recommended.

For large values of the parameter $\beta = va/D$ (about 200 or more) the interface regresses at such a rapid rate compared to temporal changes in the diffusion pattern that the latter is affected primarily in a very thin boundary layer of thickness δ close to the surface as the calculations show, see Fig. 2. Hence, in order to describe the rate of the diffusion of the ion through the interface, it is important to take

account of the steep concentration gradient close to the boundary. For this reason one introduces the transformation

$$c(r,t) = \exp(\lambda t) r^{1/2} \bar{c}_{cy}(r,t) \tag{7.4.37}$$

into eq.(7.4.2), where now m=1. There results

$$\frac{\partial c}{\partial t} = D\left(\frac{\partial^2 c}{\partial r^2} + \frac{c}{4r^2}\right) \tag{7.4.38}$$

Now close to the boundary where the diffusion effects are most prominent the two terms on the right hand side are of entirely different order of magnitudes, $\partial^2 c/\partial r^2 = O(1/\delta^2)$ and $c/4r^2 = O(1/r^2)$. Since δ is very small compared to r, the second term is dropped in favor of the first and there result the eqs. (7.4.6) to (7.4.10) with the initial distribution $g(r) = r^{1/2} c(r)$. Hence the approximate solution to the cylinder problem can be obtained by simply replacing the term $sc(s)$ by $s^{1/2}c(s)$ on the right hand side of eq. (7.4.19). It is worthwhile to point out that if one merely drops the term $(1/r)\partial\bar{c}/\partial r$ in eq. (7.4.1) in favor of $\partial^2\bar{c}/\partial r^2$, one obtains a less accurate approximation to the solution than the one given above.

The exact analysis of the cylinder is planned for the future.

7.5. External Mass Loss Rate and Leach Time for a Glass Cylinder

7.5.1. Introduction

Two mathematical models for the rate of mass transport from a waste cylinder surrounded by groundwater in an infinite porous medium have been developed in sections (7.1) and (7.2). In the first model, the cylinder is approximated by a prolate spheroid and the rate of mass transfer of a species dissolved from the waste solid is assumed to be governed by the rate of molecular diffusion of the dissolved species into stagnant groundwater. This theory is illustrated by analyzing the steady-state mass transfer rate from the cylinder with the dissolved species having a constant concentration on the cylinder surface. The maximum value of this surface concentration is the solubility of the dissolved species in groundwater, and this saturation concentration at the surface is assumed in the illustration.

In the second model, the mass transfer of the dissolved species from the waste surface is due to both molecular diffusion and forced convection by the groundwater moving in D'Arcy's flow in the surrounding porous medium. Again, the theory is applied to the steady-state mass transfer with a constant saturation concentration of the diffusing specie on the cylinder surface. The waste cylinder is idealized as a cylinder of infinite length, and the groundwater is assumed to flow perpendicular to the cylinder axis. This allows one to obtain the rate of mass transfer from a unit length of the cylinder. Numerical calculations are made for a cylinder with the same radius as that of a cylindrical waste form with end effects accounted for.

Calculations are made for the rate of dissolution of silica, in amorphous form, from a borosilicate glass cylinder, and for the rate of

dissolution of low-solubility radioelements in the borosilicate glass, using the two models described above.

In Section 7.5.2, the steady-state mass transfer rate, mass transfer rate per unit length, and average surface mass flux of a species from a prolate spheroid and slender cylinder which is defined as a cylinder with a ratio of height to radius of 10 or greater are given. In Section 7.5.3, the leach times of the prolate spheroid and slender cylinder are derived, subject to the assumptions that the waste form consists of a single species and that the ratio of height to radius of the cylindrical waste-form is constant during the leaching process. In Section 7.5.4, the governing equations for obtaining the dimensions of the prolate spheroid approximating a cylindrical waste form are given. In Section 7.5.5 we present the dimensions of the cylindrical waste-form, calculated dimensions of the equivalent prolate spheroid, diffusivity of a species in a water-saturated porous medium, solubility of amorphous silica in water, and borosilicate glass density. In Section 7.5.6, a comparison between the dissolution rate and the leach time of different waste forms consisting only of amorphous silica are made. These sections deal primarily with the mass transport by molecular diffusion.

In Section 7.5.7, the steady-state mass transfer rate by molecular diffusion and convection are given. The mass transfer rate for a finite cylinder is derived subject to the assumption that the surface mass flux from the ends of the cylinder has the same value as the surface mass flux of the infinitely long cylinder. In Section 7.5.8 the leach time for the cylinder is derived. Section 7.5.9 contains data used for numerical evaluation of mass loss rate and leach time. In Section 7.5.10 a comparison is made between surface mass flux for diffusion and for the diffusion-convection model.

In Section 7.5.11, the diffusion and diffusion-convection models are applied to a silica-base glass cylinder containing low-solubility radio-elements. Section 7.5.12 is the conclusion of the above analyses.

7.5.2. Dissolution Rate Due to Molecular Diffusion

At steady state the mass transfer rate per unit area (surface mass flux) is nonuniform for the prolate spheroid and depends on the position on the surface. The mass flux has a maximum at the poles and a minimum at the equatorial plane (see Fig. 7.1.1 in Section 7.1). The total rate of dissolution $\dot{m}_{ps}$ of a given species of effective surface concentration N_s is obtained by integration of the surface mass flux over the surface area of the prolate spheroid, and is given by (see Section 7.1)

$$\dot{m}_{ps} = \frac{4\pi\varepsilon D_f N_s f}{\log[\coth(\frac{\alpha_s}{2})]} \qquad (7.5.1)$$

where:

$\dot{m}_{ps}$ = the total mass loss rate of the prolate spheroid, g/sec

D_f = molecular diffusivity of diffusing specie in water, cm^2/sec

ε = porosity

$N_s = c_s - c_\infty$ = effective surface concentration, g/cm^3

c_s = solubility limit in groundwater, g/cm^3

c_∞ = concentration in groundwater far from waste surface, g/cm^3

α_s = surface shape factor of the prolate spheroid defined in Section 7.1 by Eq.(7.1.4)

f = focal distance of the prolate spheroid, cm

For a slender cylinder, i.e., $L \geq 10r$, Eq.(7.5.1) simplifies to

$$\dot{m}_{sc} = \frac{2\pi\varepsilon D_f N_s L}{\log(\frac{L}{r})} \qquad (7.5.2)$$

where:

$\dot{m}_{sc}$ = dissolution rate for a slender cylinder, g/sec

L = cylinder length, cm

r = cylinder radius, cm

From Eq.(7.5.1) the dissolution rate per unit length and the average dissolution rate per unit surface area of the prolate spheroid are given by Eqs.(7.5.3) and (7.5.4), respectively

$$\dot{m}^{\ell}_{ps} = \frac{2\pi\varepsilon D_f N_s}{\cosh(\alpha_s)\log[\coth(\frac{\alpha_s}{2})]} \tag{7.5.3}$$

$$\bar{j}_{ps} = \frac{2\varepsilon D_f N_s f}{b(b+ \frac{a}{e} \sin^{-1}e)\log[\coth(\frac{\alpha_s}{2})]} \tag{7.5.4}$$

where:

$\dot{m}^{\ell}_{ps}$ = mass loss rate per unit length of the prolate spheroid, g/cm sec

$\bar{j}_{ps}$ = average surface mass flux of the prolate spheroid, g/cm^2 sec

e = f/a

a = semi-major axis of the prolate spheroid, cm

b = semi-minor axis of the prolate spheroid, cm

7.5.3. Leach Time Derivation

The leach time T is defined as the time interval between the beginning of dissolution and the completion of dissolution of the waste form. Assuming here a waste form consisting of a single species, the time-dependent waste form volume V(t) is given by

$$\frac{d}{dt}(\rho V(t)) = -\dot{m}(t) \tag{7.5.5}$$

where:

ρ = waste form density, g/cm^3

$V(t)$ = waste form volume at time t, cm^3

$\dot{m}(t)$ = mass-loss rate at time t, g/sec given by Eqs.(7.5.1) and (7.5.2).

The initial condition is $V(0) = V_o$, where V_o is the initial volume of the waste form.

Here we assume that at any time t the dissolution rate can be approximated by the steady-state solutions, Eqs.(7.5.1) and (7.5.2), so that Eq.(7.5.5) can be solved for V(t). From definition of the leach time T we have that

$$V(T) = 0 \tag{7.5.6}$$

and leach time is obtained by solving Eq.(7.5.6) for T.

We have for the slender cylinder

$$V_{sc}(t) = \pi r^2(t)\, L(t) \tag{7.5.7}$$

and from (7.5.2)

$$\dot{m}_{sc} = \frac{2\pi\varepsilon\, D_f\, N_s\, L(t)}{\log\left[\frac{L(t)}{r(t)}\right]} \tag{7.5.8}$$

with the initial condition (I.C.) that

$r(0) = r_o$ initial radius, cm

$L(0) = L_o$ initial height, cm

Substituting Eqs.(7.5.7) and (7.5.8) into (7.5.5) yields

$$\frac{d}{dt}\left[\rho\, \pi\, r^2(t)\, L(t)\right] = -\frac{2\pi\varepsilon\, D_f\, N_s\, L(t)}{\log\left[\frac{L(t)}{r(t)}\right]} \tag{7.5.9}$$

with I.C.

$$r(0) = r_o$$

$$L(0) = L_o$$

To solve Eq.(7.5.9), it is necessary to have another relation between L(t) and r(t). We assume that the ratio of height to radius remains constant during the leaching process, i.e.,

$$L(t) = L_o \frac{r(t)}{r_o} \tag{7.5.10}$$

Substituting Eq.(7.5.10) into Eq.(7.5. 9) and solving for r(t) results in

$$r(t) = r_o \left[1 - \frac{4 \varepsilon D_f N_s t}{3 r_o^2 \rho \log(\frac{L_o}{r_o})} \right]^{1/2} \tag{7.5.11}$$

From the definition of leach time we have from (7.5.6-7) that $r(T_{sc}) = 0$, so that

$$T_{sc} = \frac{3 \rho r_o^2 \log \left[\frac{L_o}{r_o} \right]}{4 \varepsilon D_f N_s} \tag{7.5.12}$$

where:

T_{sc} = leach time for the slender cylinder, sec

In deriving the leach time of the prolate spheroid it is assumed that the ratio of the minor axis to the major axis is constant during the leaching process, resulting in the following equation (see Appendix A for details):

$$T_{ps} = \frac{\rho b_o^2 \cosh(\alpha_s) \log \left[\coth(\frac{\alpha_s}{2}) \right]}{2 \varepsilon D_f N_s} \tag{7.5.13}$$

where:

T_{ps} = leach time for the prolate spheroid, sec

b_o = initial semi-minor axis of the prolate spheroid, cm

7.5.4. Approximating a Cylinder by a Prolate Spheroid

We assume that the prolate spheroid has the same volume and surface area as the cylindrical waste form. Thus, equating their volumes,

$$4 \frac{\pi}{3} a\, b^2 = \pi\, r^2\, L \qquad (7.5.14)$$

and equating their surface areas

$$2\, \pi\, b\left(b+\frac{a}{e} \sin^{-1} e\right) = 2\, \pi\, r(r+L) \qquad (7.5.15)$$

Solution of Eqs.(7.5.14) and (7.5.15) for a and b defines the desired prolate spheroid. As is seen from the above equations, a closed-form mathematical solution for a or b cannot be obtained, so a numerical analysis is required.

7.5.5. Parameters of the Problem

The following table shows the physical characteristics of the waste form used in the numerical calculations:

Table 7.5.1. Physical characteristics of waste forms (R1)

Canister dimensions		Commercial high level waste	Defense high level waste
Inner diameter,	cm	30.5	59.1
Length,	cm	2.4×10^2 [a/]	2.4×10^2 [a/]
Surface area,	cm^2	2.446×10^4	5.005×10^4
Volume,	cm^3	1.75×10^6	6.58×10^6
Ratio L/r		15.7	8.1

a/ Assumed that 80% of waste canister is filled with waste glass.

The dimensions of the commercial high level waste form are used in numerical evaluation of the slender cylinder mass loss rate and leach time, listed in Table 7.5.4.

Table 7.5.2 is obtained by approximating the waste forms by a prolate spheroid using Eqs.(7.5.14) and (7.5.15), with the aid of a (computer) program described in Appendix C.

Table 7.5.2. Physical dimensions of prolate spheroid approximating cylindrical waste forms.

Waste Forms	a, cm	b, cm	c, cm	e	α_s
Defense high-level waste	158	31.5	155	0.980	0.202
Commercial high-level waste	145	16.9	144	0.993	0.117

The molecular diffusion coefficient of most nuclides in water-saturated porous media is usually lower than that in the unconfined water. The diffusivity of most species in water is between 1 to 5×10^{-5} cm^2/sec (W2). The molecular diffusion coefficient of silicon dioxide and other species in water is taken to be 1×10^{-5} cm^2/sec.

Table 7.5.3 shows the solubility of two forms of silicon dioxide, i.e., α quartz and amorphous silica, in water at a pressure of 0.1013 MPa, pH of 7.0, and at different temperatures. The solubility of silicon dioxide as a function of pressure and temperature is given (W1) in Appendix B.

Table 7.5.3. Solubility limit of silicon dioxide in water

	Temperature, °C	
	25°C	100°C
Alpha quartz, g/cm^3	4×10^{-6}	5×10^{-5}
Amorphous silica, g/cm^3	1.2×10^{-4}	4.1×10^{-4}

A surface concentration of 1.2×10^{-4} g/cm^3 and a density of 2.8 g/cm^3 are chosen for a pure amorphous silica cylinder. This density corresponds to that of typical borosilicate glass (T1),(M3).

7.5.6. Numerical Results for Dissolution Rate and Leach Time for a Pure Amorphous Silica Cylinder

Table 7.5.4 shows the calculated dissolution rates and leach times, using Eqs.(7.5.1), (7.5.2), (7.5.12), and (7.5.13) with the aid of a computer program (Appendix C). A porosity of 0.01 and the solubility of amorphous silica from Table 7.5.3 were used. The concentration of silicon dioxide in the groundwater far from the waste form is assumed zero.

Table 7.5.4. Mass loss rate and leach time for a pure amorphous silica in stagnant water at 25° C and porosity of 0.01.

	Mass loss rate, g/day	Leach time, yr
Slender cylinder	5.6×10^{-4}	3.54×10^{6}
Commercial high level waste	6.6×10^{-4}	3.03×10^{6}
Defense high level waste	8.8×10^{-4}	8.58×10^{6}

All three waste forms yield similar results. There is reasonable agreement of mass loss rate and leach time between a prolate spheroid approximating the commercial high level waste form and the slender cylinder. Thus, Eqs.(7.5.2) and (7.5.12), derived for the mass loss rate and leach time of the slender cylinder respectively, can be used.

7.5.7. Dissolution Rate Due to Molecular Diffusion and Groundwater Motion

The mass loss rate per unit length of an infinite cylinder with groundwater flow normal to its axis is given by (see Section 7.2)

$$\dot{m}_{\infty}^{\ell} = \frac{8}{\sqrt{\pi}} D_f \varepsilon N_s (Pe)^{1/2} \quad \text{, valid for } Pe \geq 4 \qquad (7.5.16)$$

where:

$\dot{m}_{\infty}^{\ell}$ = mass loss rate per unit length of cylinder, g/cm sec

$Pe = Ur/D_f$, Peclet number

U = groundwater pore velocity, cm/sec

From Eq.(7.5.1), the mass loss rate per unit surface area of the cylinder is obtained

$$\bar{j}_c = \frac{8}{\pi^{3/2}} \varepsilon N_s \left(\frac{U D_f}{r}\right)^{1/2} \quad , Pe \geq 4 \qquad (7.5.17)$$

where:

$\bar{j}_c = \frac{\dot{m}_\infty^\ell}{2\pi r}$ = mass loss per unit surface area of the cylinder, g/cm^2 sec

From this, one obtains the dissolution rate for a cylinder of length L, subject to the assumption that the mass flux from the ends of the cylinder has the same value as the surface mass flux from the cylindrical surface. The result is

$$\dot{m}_c = \frac{8}{\sqrt{\pi}} D_f \varepsilon N_s (r+L) (Pe)^{1/2} \quad , Pe \geq 4 \qquad (7.5.18)$$

where $\dot{m}_c$ = dissolution rate from cylinder, g/sec

7.5.8. Leach Time for a Cylinder, Diffusion and Convection

As a result of dissolution, the radius decreases with time as does the Peclet number. The leach time T is defined as the time interval from the beginning of the steady-state dissolution of an infinitely long cylinder until the cylinder has completely dissolved. For simplicity it is assumed that Eq.(7.5.16) is also valid for Peclet numbers less than four. The following expression for the leach time is obtained (see Appendix A for derivation).

$$T_c = \frac{\pi^{3/2} \rho r_o^2}{6 \varepsilon D_f N_s Pe_o^{1/2}} \quad , Pe_o \equiv \frac{U r_o}{D_f} \qquad (7.5.19)$$

where:

T_c = leach time for the cylinder located in flowing groundwater, sec

r_o = initial radius of the cylinder, cm

7.5.9. Parameters of the Problem

Groundwater pore velocities of 10, 5, and 1 m/yr are assumed. The radius of the cylinder is 15.2 cm, which is the same as that of a commercial high level waste glass cylinder. The cylinder consists of silicon dioxide. The surface concentration of silicon dioxide is 1.2×10^{-4} g/cm^3 and the concentration of silicon dioxide in the groundwater far from the cylinder is assumed to be zero. The diffusivity of SiO_2 in groundwater is taken to be 1×10^{-5} cm^2/sec. The porosity of the medium is 0.01.

7.5.10. Numerical Results for Surface Mass Flux

In Table 7.5.5 are presented the calculated average surface mass fluxes for diffusion and convection in flowing groundwater (Eq. 7.5.17) and for diffusion in stagnant groundwater (Eq. 7.5.4), using the computer program described in Appendix C. A porosity of 0.01 is chosen.

Table 7.5.6 Average surface mass flux of silicon dioxide g/cm^2 day for the diffusion and diffusion-convection models, porosity = 0.01, $N_s = 1.2 \times 10^{-4}$ g/cm^3, $D_f = 1 \times 10^{-5}$ cm^2/sec, r = 15.2 cm, and L = 2.4 m.

	Groundwater pore velocity, m/yr			
	10	5	1	0[a/]
Surface mass flux, g/cm^2 day	3.5×10^{-7}	2.5×10^{-7}	1.1×10^{-7}	2.7×10^{-8}

a/Molecular diffusion model, Eq.(7.5.4)

For the pure amorphous silica cylinder (r = 15.2 cm) emplaced in a medium with porosity of 0.01 and groundwater pore velocity of 10 m/yr, from Eq.(7.5.19), we obtain $T_c = 2.3 \times 10^5$ yr. The proper value may be less, if an accurate solution for Pe< 4 were available. Such an analysis is presently being completed. For example, from Eq.(A.29), we find that after 1.7×10^5 years the cylinder radius has decreased from the initial value of 15.2 cm to 1.2 cm when the Peclet number becomes four.

7.5.11. Solubility Limited Dissolution of Silica and Low-Solubility Radioelements in a Silica-Base Glass Cylinder

In the previous sections two mathematical models of dissolution from a cylinder with only one diffusing component were considered. In this section, a silica-base glass cylinder containing additional low solubility components, such as various radioelements, is considered.

The time-dependent fractional dissolution rate of component j is defined as

$$\dot{f}_j(t) = \dot{m}_j(t) / M_j(t) \qquad (7.5.20)$$

where:

$\dot{f}_j(t)$ = fractional dissolution of component j at time t, 1/sec

$\dot{m}_j(t)$ = dissolution rate of component j at time t given by Eq.(7.5.1) for molecular diffusion and Eq.(7.5.18) for the molecular diffusion-convection models, g/sec

$M_j(t) = V_j(t)\, n_j(t)$ = mass of j at time t in glass, g

$V_j(t)$ = volume of undissolved waste at time t, cm^3

$n_j(t)$ = density of j in undissolved solid waste at time t, g/cm^3

Substituting the $\dot{m}_j(t)$ given by Eqs.(7.5.1) and (7.5.18) into (7.5.20) yields

$$\dot{f}_j(t) = \frac{N_{s,j}}{n_j(t)} \cdot \left\{ \begin{array}{l} \dfrac{3\varepsilon D_f^j e}{b^2 \log\left[\coth\left(\frac{\alpha_s}{2}\right)\right]}, \text{ molecular diffusion} \\ \dfrac{8\varepsilon D_f^j (Pe^j)^{1/2} (1+\frac{r}{L})}{\pi^{3/2} r^2}, \text{ molecular diffusion-convection} \\ \qquad Pe^j \equiv \dfrac{Ur}{D_f^j} \geq 4 \end{array} \right\}$$

$$, \; 0 \leq t \leq T \qquad (7.5.21)$$

where:

$N_{s,j}$ = difference between the concentration of j in the groundwater on the waste surface and concentration of j in groundwater far from waste surface, g/cm^3

D_f^j = diffusion coefficient of specie j in groundwater, cm^2/sec

T = leach time given by Eq.(7.5.13) and Eq.(7.5.19), sec

In the above equation it is assumed that the ratio of the major axis to the minor axis of the prolate spheroid is constant during the leaching process. In Eq.(7.5.21) r and b are functions of time, with functional forms given by Eqs.(A.29) and (A.10), respectively.

To apply Eq.(7.5.21), it is assumed that the rate of bulk dissolution of the solid waste is controlled by dissolution of the silica matrix, i.e., the preferential release of a waste-component by diffusion in solid is neglected. As the silica matrix dissolves, all the components in the silica matrix are released congruently from the solid but are not necessarily dissolved. If the solubility of an individual waste component is so low that its fractional dissolution rate is less than that of the waste matrix, then precipitates of the low-solubility component will form. It is assumed that the precipitates remain on the waste surface and slowly dissolve at a rate given by the rate of mass transfer of the low-solubility species into the surrounding liquid, with the concentration of the low-solubility species in the liquid adjacent to the waste surface given by the solubility of that species in groundwater. The possibility of forming colloids or other non-dissolved suspended particulates within the groundwater is neglected.

These assumptions can be written as

$$\dot{f}_j(t) = \text{Min}\ (\dot{f}_{silica}\ (t),\ \dot{f}_j\ (t)) \quad j = 1,2,..,N \qquad (7.5.22)$$

where:

Min (X,Y) = minimum value of X or Y

For numerical demonstration we consider a borosilicate waste glass with r = 15.2 cm and L = 2.40 m emplaced in a porous medium with a porosity of 0.01 and groundwater pore velocity of 1 m/yr. The concentration of each of the components in the groundwater far from waste cylinder is assumed zero. The molecular diffusion coefficient in groundwater is assumed to be $1x10^{-5}$ cm^2/sec for all the diffusing components. The initial inventories and solubilities of constituents in groundwater and the corresponding calculated fractional release rates are given in Table 7.5.7. Table 7.5.8 shows the calculated fractional release rate of the constituents from the above waste glass in absence of groundwater flow. For this case the prolate spheroid has the same volume and surface area as the waste cylinder.

Table 7.5.8 also shows the experimental results of fractional release rate for some radionuclides(M1). The experimental results are adjusted for the surface area of the waste cylinder on the assumption that the release rate is proportional to surface area exposed. Comparison between these calculated values indicate that in the repository conditions dissolution of the low-solubility radionuclides is controlled by the concentration boundary layer and not by the kinetics inside the glass matrix.

7.5.12. Conclusion

Two solubility-limited dissolution models were developed in Sections 7.1 and 7.2. The models permit one to calculate the steady-state dissolution rate of a diffusing species from a cylinder which is embedded in a water saturated porous medium. In one model the mass loss is due to molecular diffusion only, while in the other it is governed by molecular diffusion and groundwater convection.

The models are applied to an amorphous silica cylinder embedded in a medium with porosity of 0.01. The cylinder radius of 15.2 cm and height of 2.4 m are used, which are dimensions of a commercial high level waste

glass cylinder. For the diffusion model an average surface mass flux of 2.7×10^{-8} g/cm^2 day and leach time of 3×10^6 yr are calculated.

The models are applied to a borosilicate high level waste glass. The fractional release rates of some low-solubility components are calculated. The numerical results indicate that if the solubility of these constituents is low enough, and their initial inventories high enough, they will not initially dissolve congruently with the waste matrix. Comparison of fractional release rates due to diffusion and those due to diffusion-convection indicates that the groundwater pore velocity of 1 m/yr causes a four fold increase in dissolution rate. This indicates a narrow range for dissolution rates obtained by the two models.

Comparison between calculated fractional release rate and experimental values indicates that for low-solubility glass components the dissolution rate may be controlled by concentration boundary layer, porosity of the medium, and groundwater pore velocity and not by kinetics inside the glass matrix or solid-liquid interactions. Therefore, interior cracks of the waste solid, devitrification, and other mechanisms that could increase the rate of solid-liquid interaction would not be expected to affect the solubility-limited dissolution rate, unless they have some affect on the solubilities. If the solubility is sufficiently large, then the kinetics of interaction between the solid waste and water may be dominant.

Table 7.5.7 Calculated fractional release rates for borosilicate glass waste in flowing groundwater.

Waste cylinder: r = 0.152 m, L = 2.40 m, fission-product and actinide oxides from 460 kg of uranium fuel. Groundwater pore velocity of 1 m/yr.

Constituent	Initial species concentration in the waste, g/cm^3	Solubility, g/cm^3	Fractional Dissolution rate, yr^{-1}
SiO_2	1.6 a/	1.2×10^{-4} c/	3.4×10^{-6}
Tc	1.92×10^{-3} b/	3×10^{-9} d/	7×10^{-8}
U	1.22×10^{-2} b/	2×10^{-9} d/	8×10^{-9}
Np	1.92×10^{-3} b/	2.4×10^{-11} d/	5.7×10^{-10}
Pu	1.15×10^{-4} b/	1×10^{-9} d/	4×10^{-7}
Am	3.56×10^{-4} b/	1.8×10^{-12} d/	2.3×10^{-10}

a/ Reference (M2).

b/ Assumed 0.5% U and Pu and all fission products and actinides (B1).

c/ For amorphous SiO_2 (S1).

d/ Reference (K1).

Table 7.5.8 Calculated fractional dissolution rates for borosilicate glass waste in stagnant groundwater.

Waste cylinder: r = 0.152 m, L = 2.40 m, fission-product and actinide oxides from 460 kg of uranium fuel.

Constituent	Initial specie concentration in the waste, g/cm^3	Solubility, g/cm^3	Fractional dissolution rate, yr^{-1}	
			Calculated	Observed [a]
SiO_2	1.6 [b]	1.2×10^{-4} [d]	8.7×10^{-7}	1.6×10^{-3}
Tc	1.92×10^{-3} [c]	3.0×10^{-9} [e]	1.8×10^{-8}	--
U	1.22×10^{-2} [c]	2.0×10^{-9} [e]	1.9×10^{-9}	1.5×10^{-6}
Np	1.92×10^{-3} [c]	2.4×10^{-11} [e]	1.5×10^{-10}	6.6×10^{-4}
Pu	1.15×10^{-4} [c]	1.0×10^{-9} [e]	1.0×10^{-7}	2.6×10^{-5}
Am	3.56×10^{-4} [c]	1.8×10^{-12} [e]	5.8×10^{-11}	2.7×10^{-6}

a/ Reference (M1).

b/ Reference (M2).

c/ Assumed 0.5% U and Pu and all the fission products and actinides (B1).

d/ For amorphous SiO_2.

e/ Reference (K1).

7.5.13 Nomenclature

a	Semi-major axis of the prolate spheroid cm
b	Semi-minor axis of the prolate spheroid cm
b_o	Initial semi-minor axis of the prolate spheroid cm
c_s	Solubility limit in groundwater g/cm^3
c_∞	Concentration in groundwater far away from waste surface g/cm^3
D_f	Molecular diffusivity in water cm^2/sec
D_f^j	Molecular diffusivity of component j in water cm^2/sec
e	Eccentricity of prolate spheroid
f	Focal distance of the prolate spheroid
$f_j(t)$	Fractional dissolution rate of component j at time t sec^{-1}
$\bar{j}_c$	Average surface mass flux of infinitely long cylinder in flowing groundwater g/cm^2sec
$\bar{j}_{ps}$	Average surface mass flux of the prolate spheroid g/cm^2 sec
L	Cylinder height cm
L_o	Initial cylinder height cm
$L(t)$	Cylinder height at time t after dissolution begins cm
$\dot{m}(t)$	Dissolution rate at time t g/sec
$\dot{m}_j(t)$	Dissolution rate of component j at time t g/sec
$\dot{m}_{ps}$	Total dissolution rate of the prolate spheroid g/sec
$\dot{m}_p^L$	Dissolution rate per unit length of the prolate spheroid g/cm sec
$\dot{m}_{sc}$	Dissolution rate for a slender cylinder g/sec
$\dot{m}_c$	Dissolution rate from a cylinder in flowing groundwater
$\dot{m}_c^\ell$	Dissolution rate per unit length of infinitely long cylinder in flowing groundwater g/cm sec
$M_j(t)$	Mass of j at time t in the waste glass g
$n_j(t)$	Density of j in undissolved waste at time t g/cm^3
N_s	Difference between concentration in the liquid adjacent to waste surface and concentration in the groundwater far away from waste surface g/cm^3

$N_{s,j}$ Difference between concentration of component j in liquid adjacent to the waste surface and concentration in the groundwater far away from waste surface g/cm^3

r Cylinder radius cm

$r(t)$ Cylinder radius at time t after dissolution begins cm

r_o Initial cylinder radius cm

T Leach time (sec)

T_{ps} Leach time for prolate spheroid sec

T_{sc} Leach time for slender cylinder sec

T_c Leach time for the infinitely long cylinder in flowing groundwater sec

U Groundwater pore velocity cm/sec

$V_j(t)$ Volume of undissolved waste at time t cm^3

$Pe \equiv \frac{Ur}{D_f}$ Peclet number

$Pe_o \equiv \frac{Ur_o}{D_f}$

$Pe^j \equiv \frac{Ur}{D_f^j}$

Greek letters

ρ = waste form density g/cm^3

ε = porosity

$\alpha_s = \cosh^{-1}(\frac{1}{e})$ Surface shape factor of prolate spheroid Defined by Eq.(7.1.4)

7.6 Calculations of Dissolution of a Glass Matrix by Internal Molecular Diffusion and Surface Regression

P. L. Chambré and S. J. Zavoshy

1. Introduction

In this paper we consider the dissolution of a glass matrix containing sodium oxide. It is experimentally observed that sodium molecular diffusion and ion-exchange at the glass-water interface depletes the glass matrix of sodium ion. Further, the glass matrix is dissolved by water. This matrix dissolution is viewed as regression of dissolved glass-water interface. The fractional release of sodium from the glass has a form of $c_1 t^{1/2}+c_2 t$, where c_1 and c_2 are two constants (H1,M3). A dissolution model that yields a fractional release which is initially parabolic (proportional to $t^{1/2}$), and then becomes linear function of time (proportional to t), is developed in section 7.4.

A mathematical dissolution model is developed based upon these two observed phenomena, i.e., internal molecular diffusion and glass surface regression. It is assumed that the loss of the diffusing ion from the interior of the glass due to molecular diffusion will lessen the integrity of the glass matrix. Furthermore, it is assumed that the glass-water interface has a constant velocity during the dissolution process. The regression speed is positive for the case of a regressive glass-water interface, zero for stationary interface, and negative for the progressive interface. The concentration inside the glass and fractional release of the diffusant from the glass are obtained for a sphere and slab of finite width.

For numerical evaluation a ternary sodium-borosilicate glass is considered. Sodium is the diffusing nuclide. The concentration of sodium

at the glass-water interface is chosen to be zero. The radius and half width of the slab are equal to the radius of a spent fuel canister. A range of regression speeds from -9.7×10^{-13} to 3.9×10^{-11} cm/sec is chosen. The normalized concentration, surface mass flux, and fractional release of sodium are evaluated.

2. Governing equations for the normalized concentration, surface mass flux, and fractional release.

Case 1. Finite slab

The following equation defines the normalized concentration of the diffusing specie in the slab of width 2a

$$c^n_{sL}(x,t) = N^s + N^o \hat{c}_{sL}(x,t) \qquad (7.6.1)$$

where:

$c^n_{sL}(x,t)$ = normalized concentration of diffusing specie in the slab

$\hat{c}_{sL}(x,t)$ = normalized concentration of the stable diffusing specie in the slab with zero concentration on the boundary (see Eq. (7.4.30) in section 7.4 with $\lambda=o$)

$N^s = \frac{c_s}{c_o}$

$N^o = (c_o - c_s) / c_o$

c_s = surface concentration of the diffusing specie, g/cm^3

c_o = initial bulk density of diffusing specie in the glass, g/cm^3

x = position from center of slab, cm

t = time, sec

The fractional release is obtained by the following equation:

$$f_{sL}(t) = 1 - N^s(1-vt/a) - N^o \int_o^{1-\beta\tau} \hat{c}_{sL}(y,t)\, dy \qquad (7.6.2)$$

where:

$f_{sL}(t)$ = fractional release of diffusing specie at time t from the finite slab

$\beta = va/D$

a = initial half width of finite slab, cm

D = molecular diffusion coefficient of diffusing specie in the glass matrix, cm^2/sec

$\tau = Dt/a^2$

v = regression speed, cm/sec

An asymptotic form for $f_{sL}(t)$ is obtained which is

$$f_{sL}(t) = \frac{2}{\sqrt{\pi}} N^o (D/a^2)^{1/2} t^{1/2} + vt/2d \qquad (7.6.3)$$

The surface mass flux is given by

$$j_{sL} = - D (c_o - c_s) \frac{\partial \hat{c}_{sL}}{\partial x}\Big|_{a-vt} + v c_s \qquad (7.6.4)$$

where j_{sL} is the surface mass loss of diffusing specie from the finite slab, g/cm^2 sec.

Case 2. Sphere.

The normalized concentration of the diffusing specie in the sphere is given by

$$c^n_{sp}(r,t) = N^s + N^o \hat{c}_{sp}(r,t) \qquad (7.6.5)$$

where:

$c^n_{sp}(r,t)$ = normalized concentration of the diffusing specie in the sphere

$\hat{c}_{sp}(r,t)$ = normalized concentration of stable diffusing specie in the sphere with zero concentration at the boundary (see Eq. (7.4.20) in section 7.4 with λ=o)

r = radial position from center of sphere, cm

From Eq. (7.6.5) we obtain the surface mass flux, i.e.,

$$j_{sp} = -D\,(c_o - c_s)\,\frac{\partial \hat{c}_{sp}}{\partial r}\Bigg|_{R-vt} + v\,c_s \qquad (7.6.6)$$

where j_{sp} is the surface mass loss of diffusing specie from sphere, g/cm^2 sec

The fractional release is obtained by

$$f_{sp}(t) = 1 - N^s\,(1-vt/R)^3 - 3\,N^o \int_o^{1-\beta\tau} \hat{c}_{sp}(y,t)\,y^2 dy \qquad (7.6.7)$$

where:

$f_{sp}(t)$ = the fractional release of diffusing specie from sphere at time t

$\beta = vR/D$

R = initial radius of sphere, cm

An asymptotic form of $f_{sp}(t)$ for early period of dissolution is

$$f_{sp}(t) = \frac{6N^o}{\sqrt{\pi}}\,(D/R^2)^{1/2} + 3\,(vt/2R)\,(1+N^s) \qquad (7.6.8)$$

and as the total dissolution time is approached the following asymptotic relation is obtained

$$f_{sp}(t) = 1 - (1 - vt/R)^3 \qquad (7.6.9)$$

This is due to time dependency of surface area of the sphere.

3. Parameters of the problem

The values of a and R were chosen to be 17.8 cm, equal to the radius of a spent fuel canister. The glass density is taken to be 2.8 g/cm^3. Table 7.6.1 gives the value of molecular diffusion coefficient of sodium in a ternary sodium-borosilicate glass at 100° and 200°C. Table 7.6.1 was obtained by applying the following equation (F1)

$$D(T) = D_o \mathrm{Exp}(-Q/RT) \qquad (7.6.10)$$

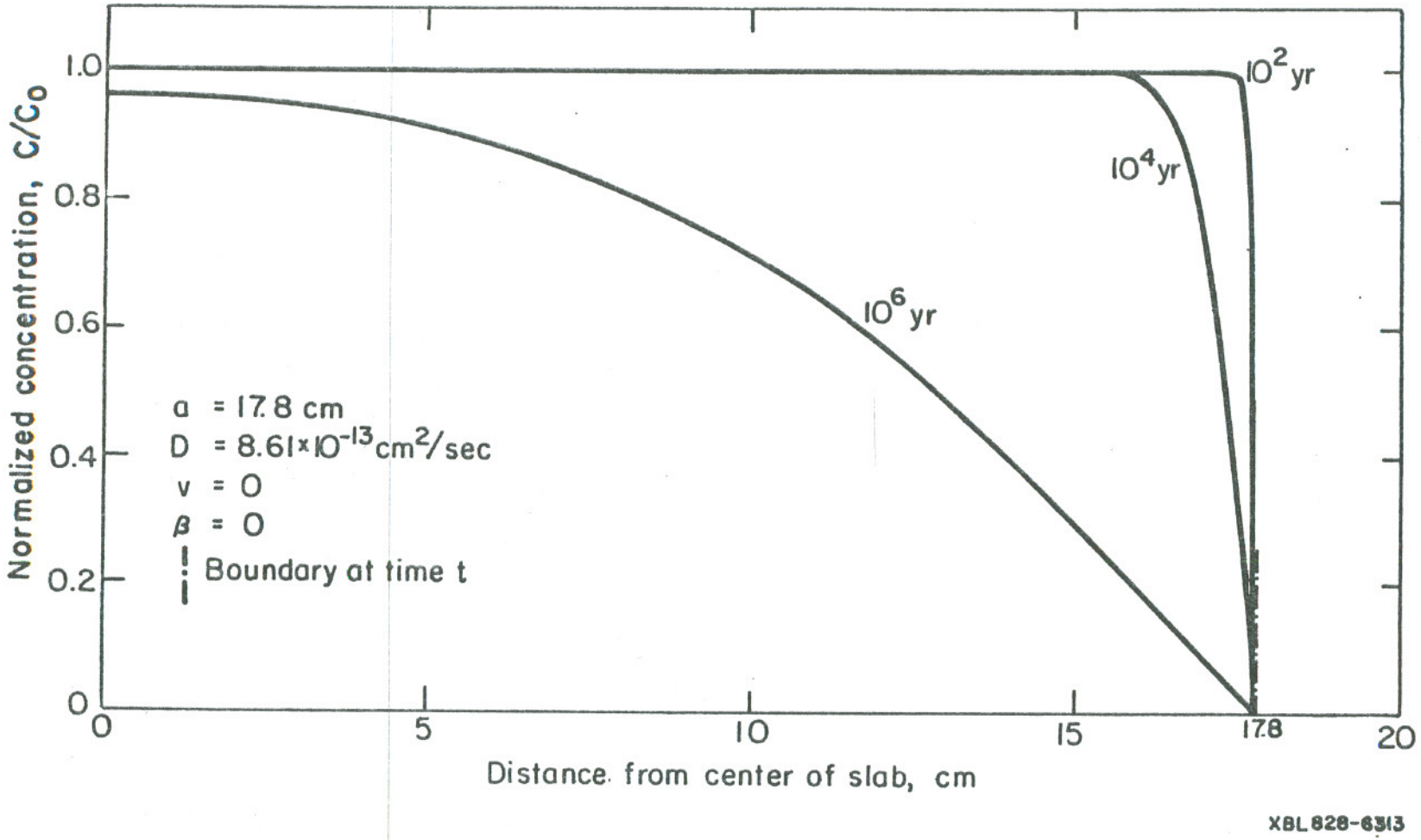

Fig. 7.6.1. Variation of Na normalized concentration in the slab (initial width 2a) with position at different times after glass dissolution begins.

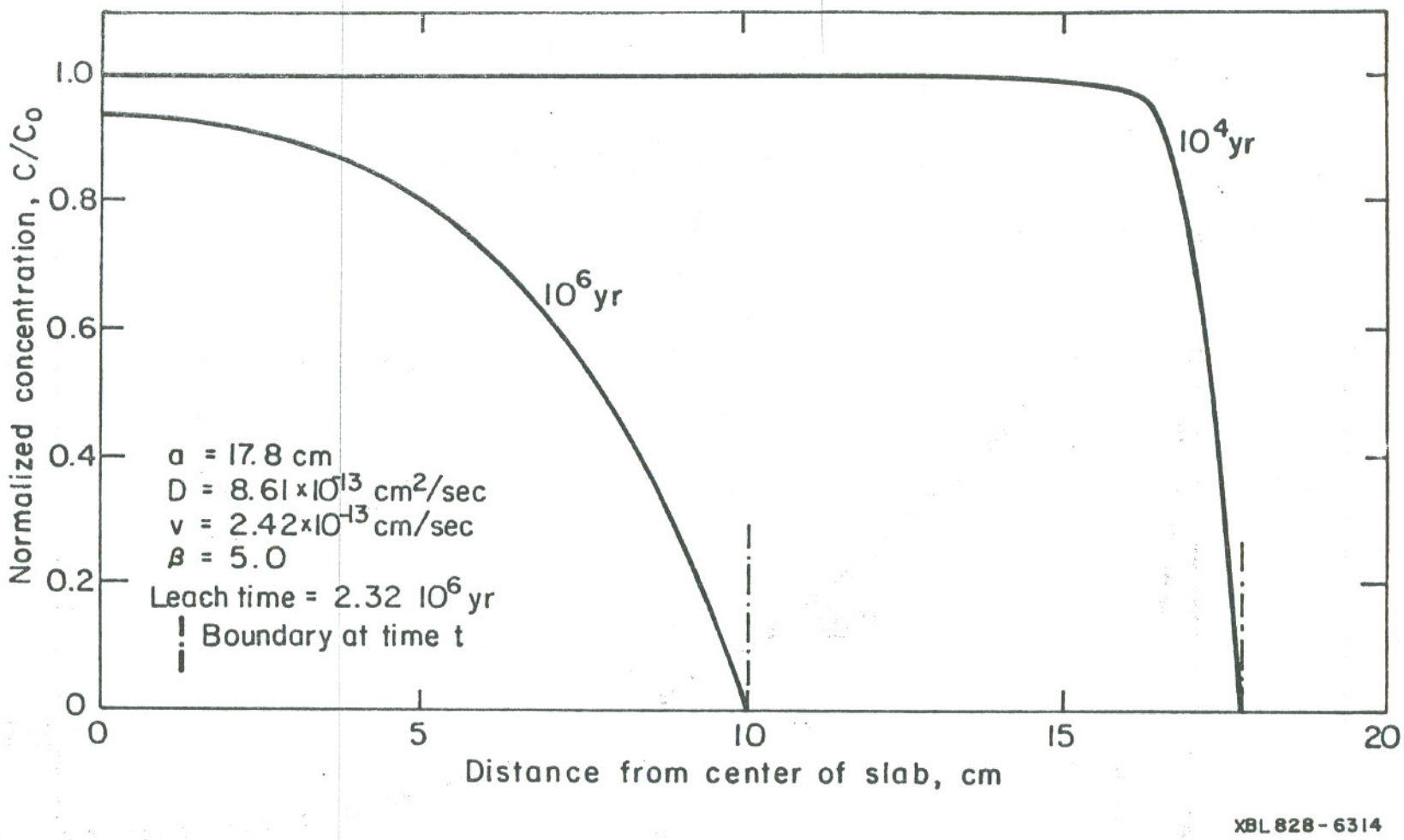

Fig. 7.6.2. Variation of Na normalized concentration in the slab (initial width 2a) with position at different times after glass dissolution begins.

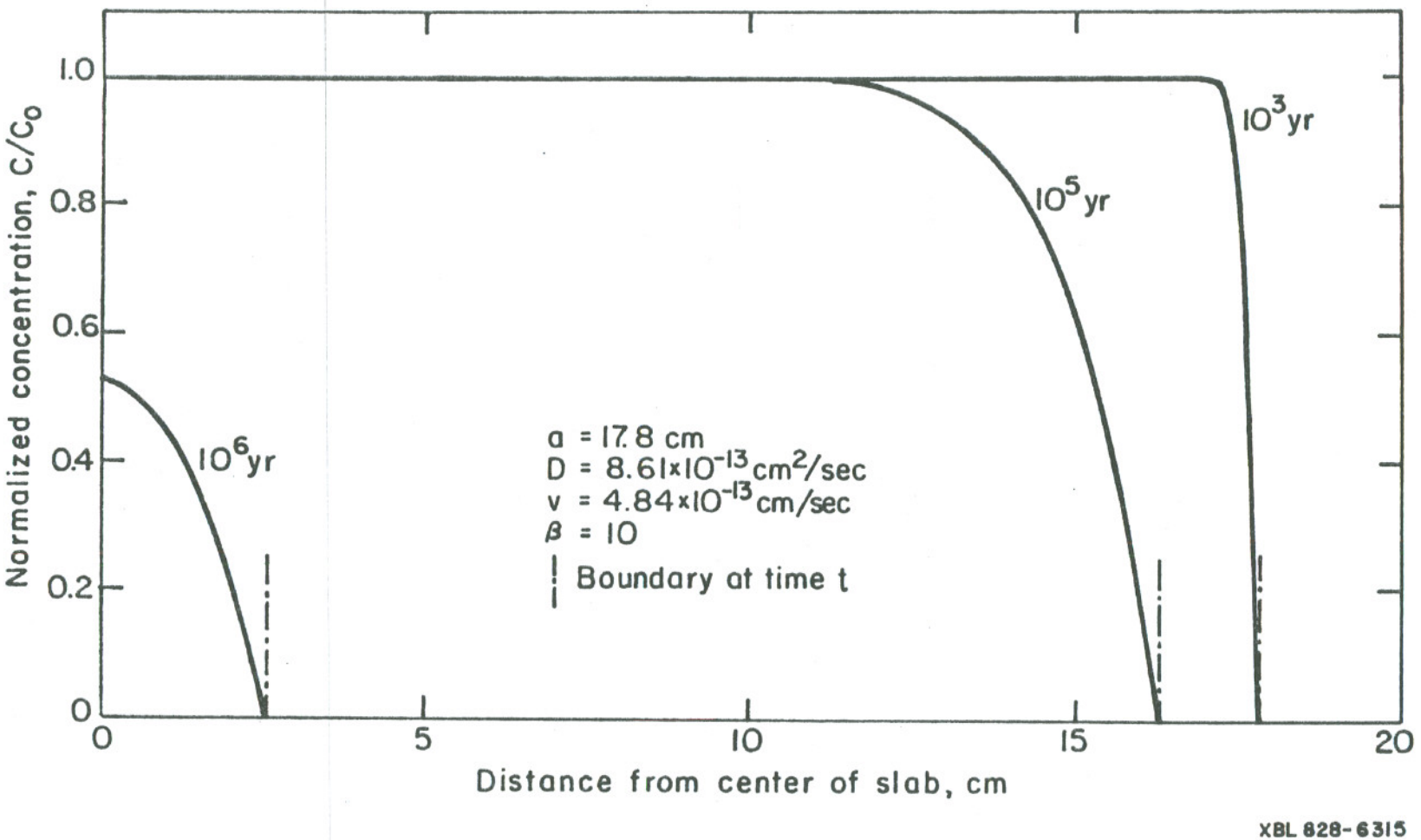

Fig. 7.6.3. Variation of Na normalized concentration in the slab (initial width 2a) with position at different times after glass dissolution begins.

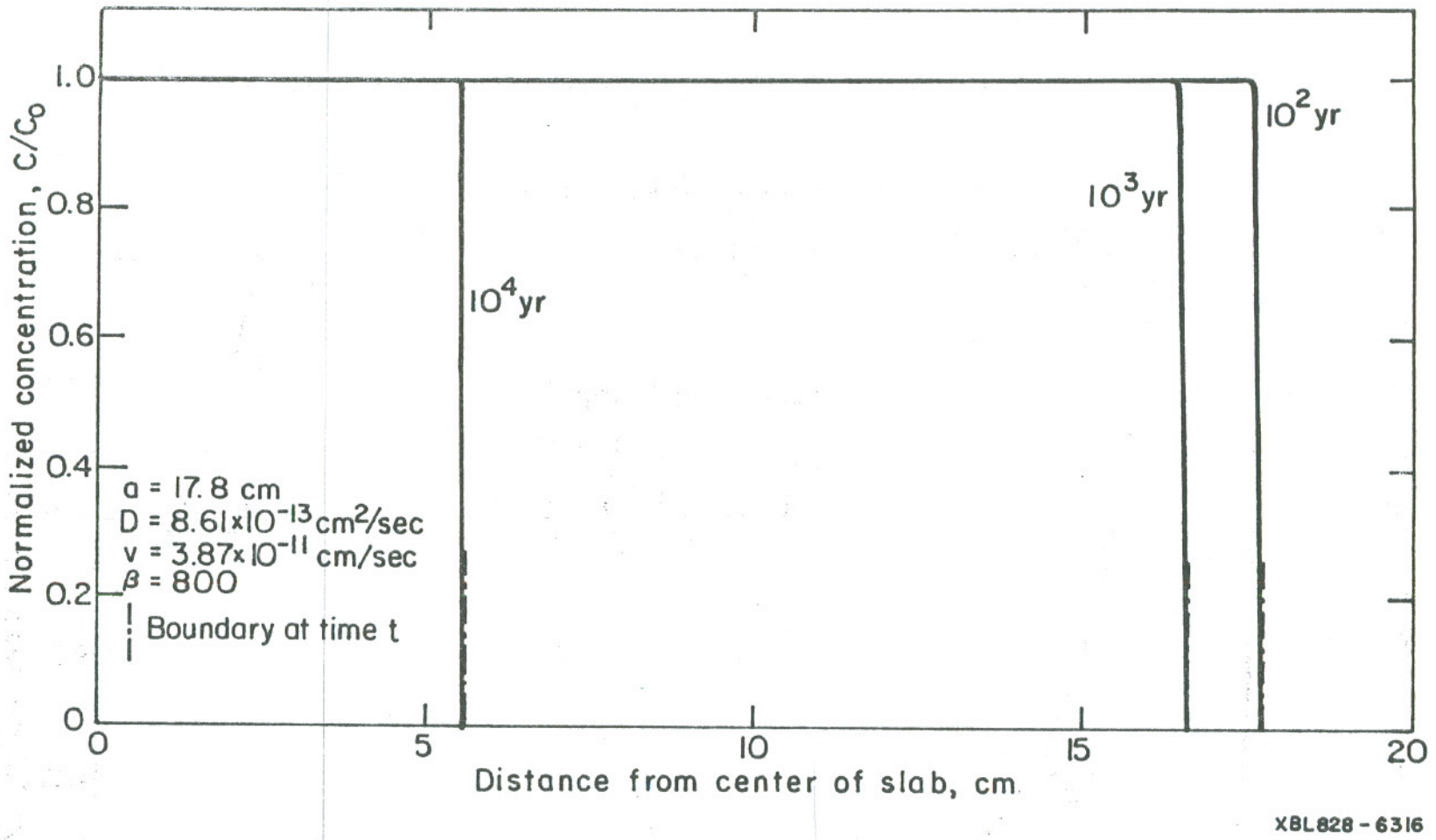

Fig. 7.6.4. Variation of Na normalized concentration in the slab (initial width 2a) with position at different times after glass dissolution begins.

where:

$D(T)$ = sodium diffusion coefficient at temperature T, cm^2/sec

D_o = frequency factor, cm^2/s

Q = activation energy, Kcal/mole

R = gas constant = 1.99×10^{-3} Kcal/mole °K

T = temperature in degrees Kelvin, °K

Table 7.6.1. Na self-diffusion in ternary Na_2O-B_2O_3-SiO_2 glasses (F1)

Na_2O/B_2O_3 mole%	$D_o(cm^2/s)$ a/	Q(Kcal/mole) a/	$D_{100}(cm^2/s)$ b/	$D_{200}(cm^2/s)$ c/
31.3/6.25	5.01×10^{-6}	11.5	9.36×10^{-13}	2.84×10^{-11}
30.9/9.10	6.31×10^{-6}	11.7	9.00×10^{-13}	2.52×10^{-11}
28.6/14.3	3.98×10^{-5}	13.1	8.61×10^{-13}	3.59×10^{-11}
32.3/3.22	5.01×10^{-4}	13.4	7.24×10^{-12}	3.29×10^{-10}
31.7/4.76	1.21×10^{-4}	13.0	3.00×10^{-12}	1.22×10^{-10}

a/ For temperature range of 100° to 250°C.

b/ At 100°C.

c/ At 200°C.

For numerical evaluation a ternary sodium-borosilicate glass at 100°C with the composition 28.6 Na_2O/14.3 B_2O_3 mole % was considered. From Table 7.6.1 we obtain $D=D_{100} = 8.61 \times 10^{-13}$ cm^2/s. The surface concentration is taken to be zero.

Values of β = -20, -10, -5, 0, 5, 10, 50, and 800 were chosen. Value of β = 800 corresponds to $v = 3.3 \times 10^{-6}$ cm/day.

4. Numerical results and discussion

The numerical results are obtained with the aid of four computer

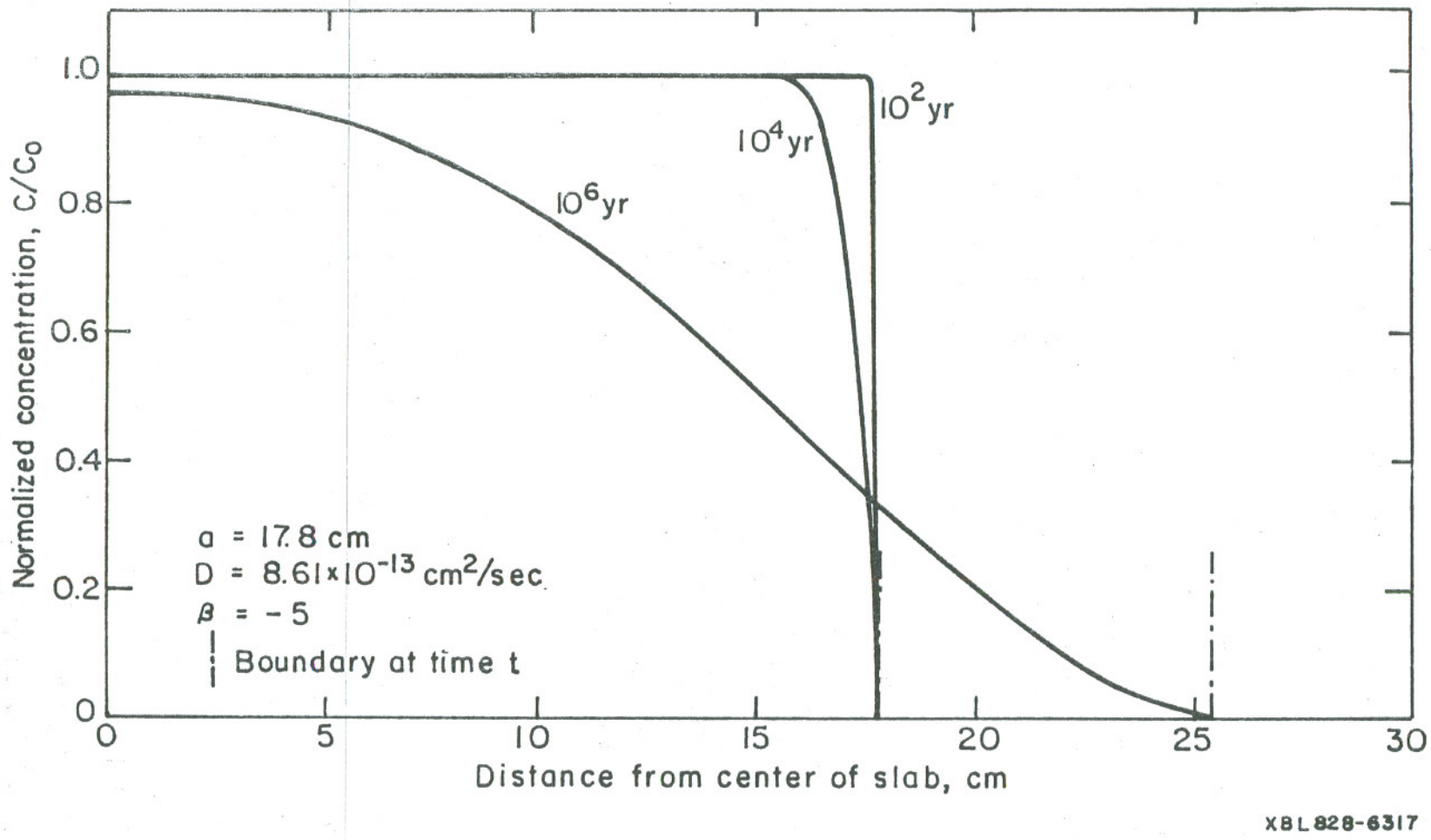

Fig. 7.6.5. Variation of Na normalized concentration in the slab (initial width 2a) with position at different times after glass dissolution begins.

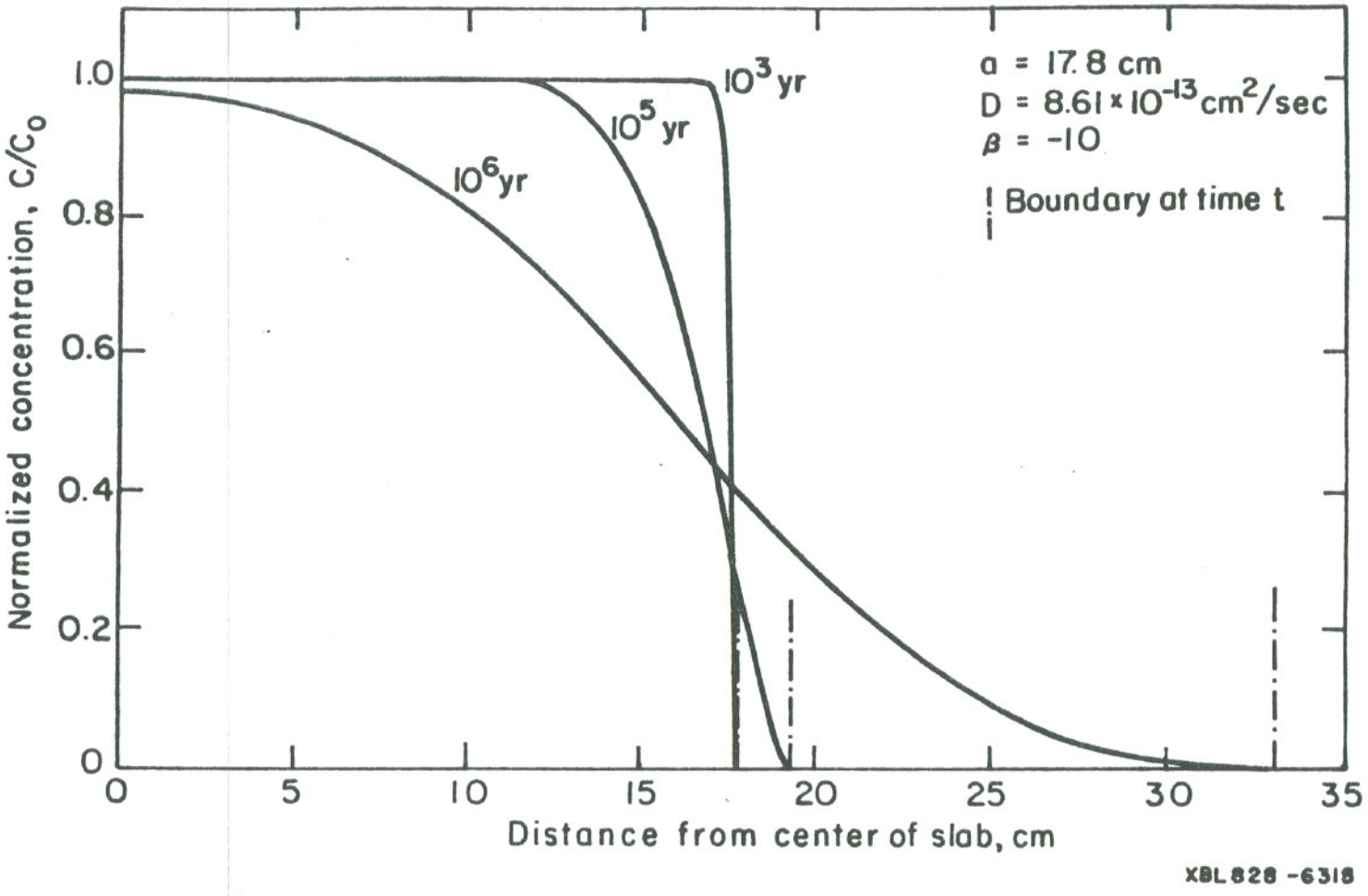

Fig. 7.6.6. Variation of Na normalized concentration in the slab (initial width 2a) with position at different times after glass dissolution begins.

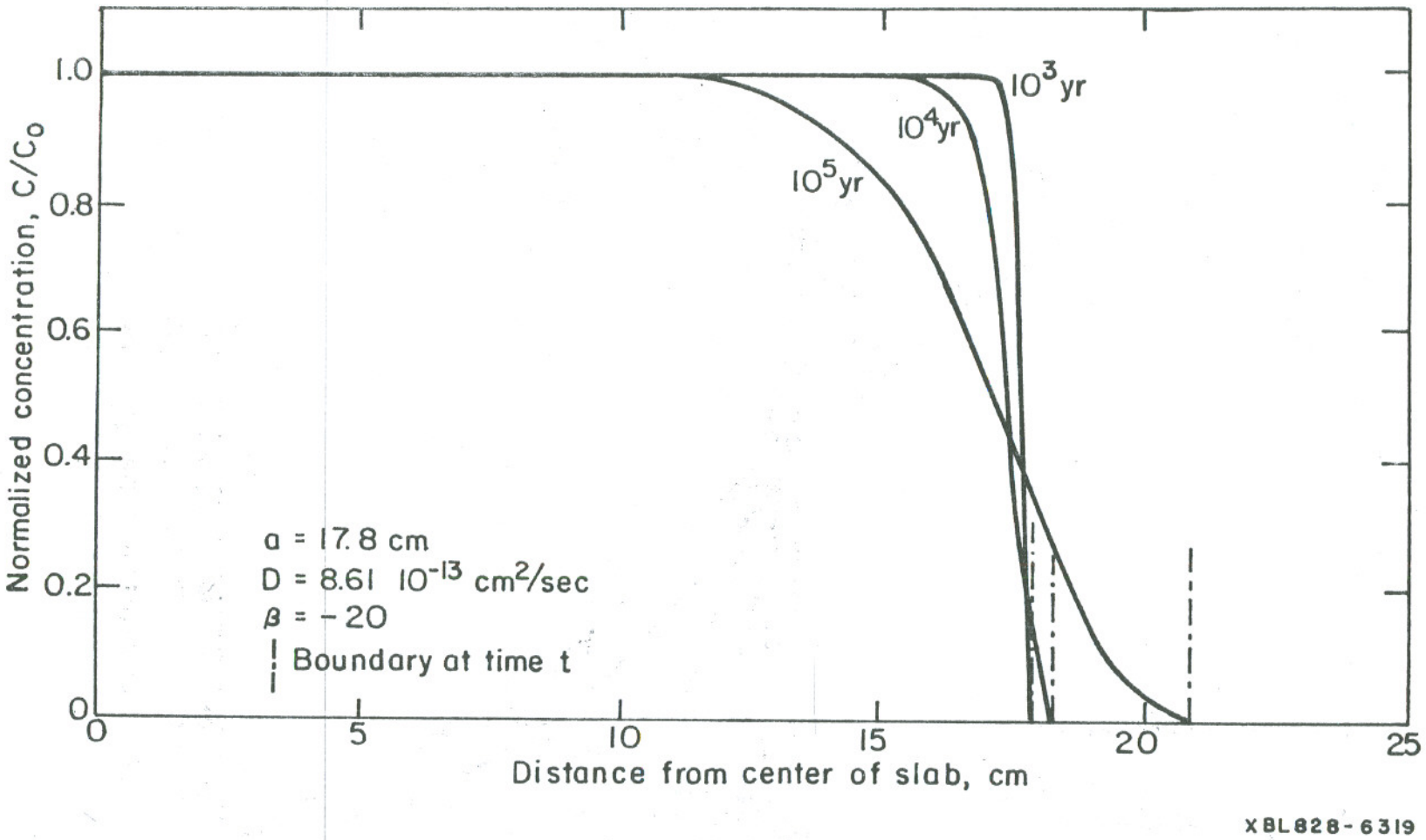

Fig. 7.6.7. Variation of Na normalized concentration in the slab (initial width 2a) with position at different times after glass dissolution begins.

programs (see Appendix A for the program details). The cut off time for calculations is the leach time T_L. This is defined as

$$T_L = | L/v | \quad , v \neq 0 \qquad (7.6.11)$$

where:

T_L = leach time, sec

L = initial characteristic length of the problem, cm

(half width of the finite slab or sphere radius).

The value of T_L corresponds to total dissolution of the glass matrix if $v > 0$, and doubling of L if $v < 0$. The surface mass flux was obtained by numerical differentiation of Eqs. (7.6.4) and (7.6.6).

Figs. 7.6.1 - 7.6.7 show the normalized concentration vs. half width of the finite slab, for β = 0, 5, 10, 800, -5, -10, and -20 respectively. For $v > 0$, increase in v, (β) will result in steepening of the concentration profile at the glass-water interface. This effect can be best seen in Fig.7.6.4, where β = 800. Also, the absolute value of the concentration gradient at the interface is increased as v increases. For negative values of v, the normalized concentration profile becomes S-shaped, see Fig. 7.6.5.

Fig.7.6.8 shows the variation of the normalized surface mass flux of the finite slab with time ($\tau = Dt/a$) for different values of β, (v). At the early period of glass dissolution the normalized surface mass flux is proportional to $t^{-1/2}$ and is independent of the regression velocity. This indicates the diffusion-controlled mass loss. For β = 800, after approximately 100 years, a constant surface mass flux of 2.4×10^{-6} g sodium/cm^2 day is obtained.

Fig.7.6.9 shows the variation of the fractional release with time for

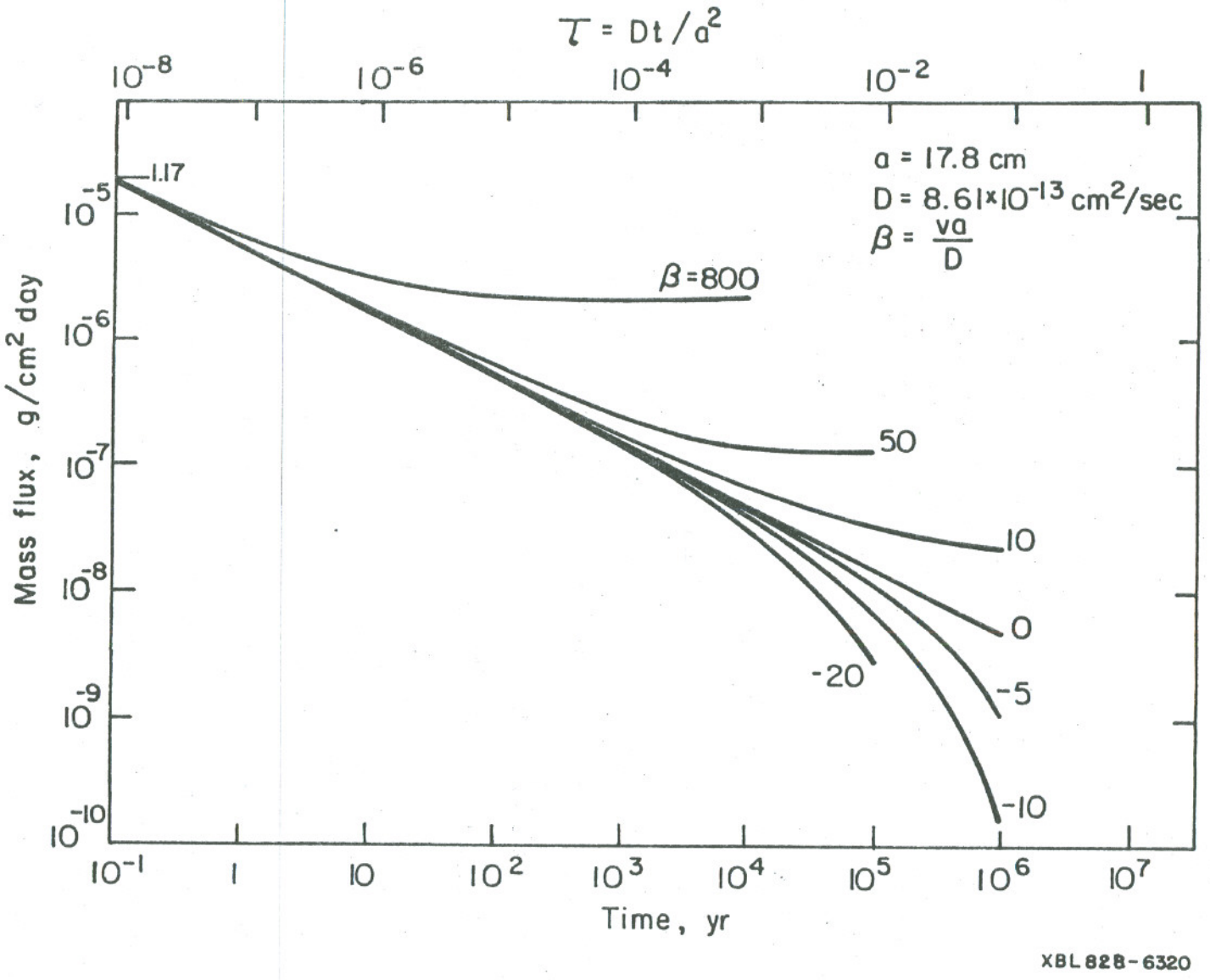

Fig. 7.6.8. Variation of Na surface mass flux from slab (initial width 2a) with time for different β (glass-water interface regression speed).

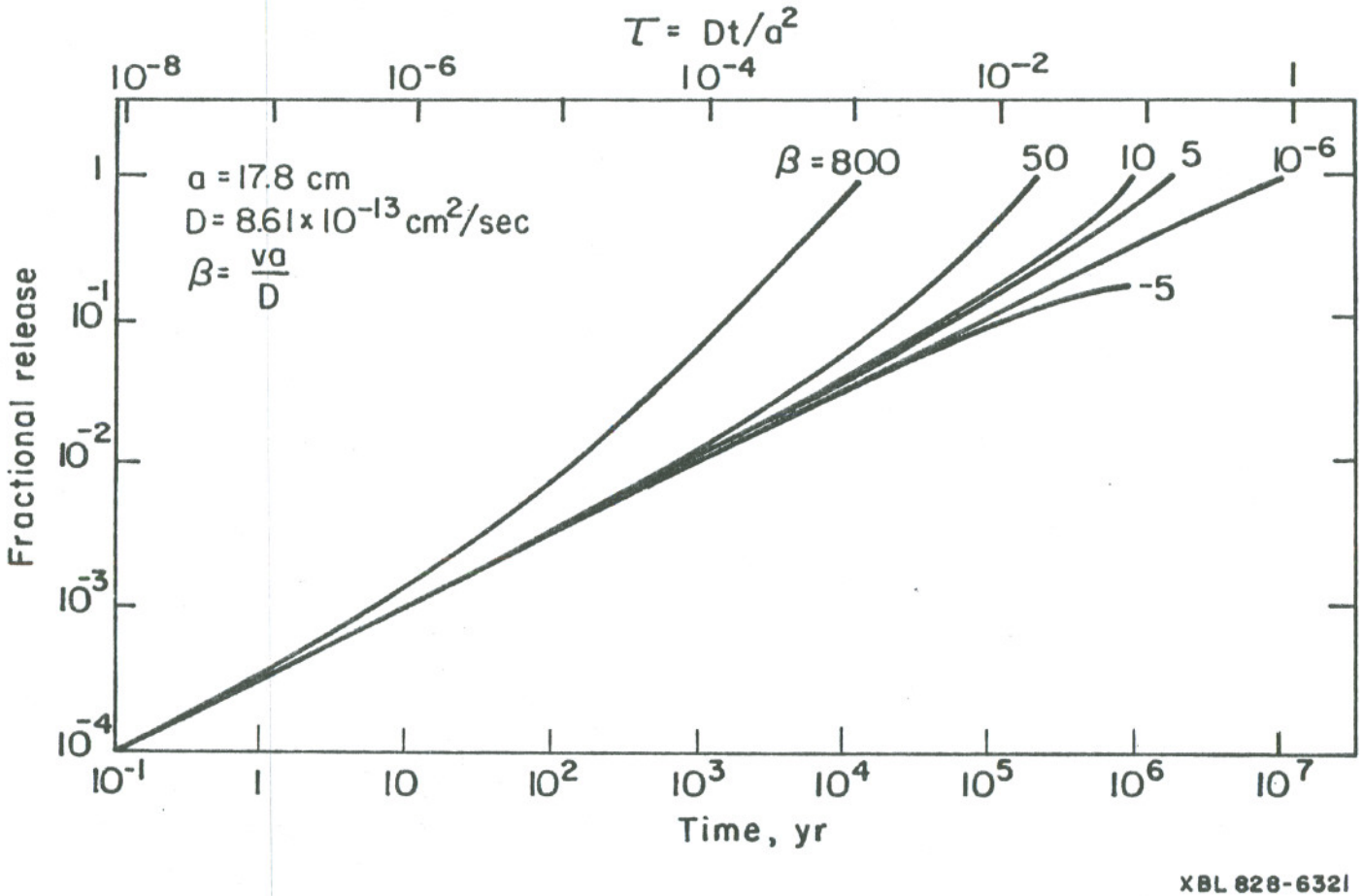

Fig. 7.6.9. Variation of Na fractional release from slab (initial width 2a) with time (τ) for different glass water interface regression speed (β).

different values of v. Fractional release has a behavior of the form $c_1 t^{1/2} + c_2 t$, where c_1 and c_2 are two constants, see Eq. (7.6.6) for values of c_1 and c_2.

Figs. 7.6.10 - 7.6.13 apply to the sphere and show the normalized concentration vs. radius of sphere for β = 0, 10, -5, and -10 respectively. Comparison with Figs. 7.6.1, 3, 5 and 6 indicates that sodium depletion is faster for the sphere than for the slab. The plot obtained for β = 800 is identical to Fig. 7.6.7, thus it is not reproduced..

Fig. 7.6.14 shows the variation of the normalized surface mass flux of the sphere with time (τ) for different values of β, (v). As leach time is approached there is a drop in surface mass flux due to depletion of sodium inside the sphere.

Fractional release for the sphere case is obtained by way of numerical integration of the normalized concentration. Fig. 7.6.15 shows the variation of fractional release with time (τ) for different values of β, (v).

5. Conclusion

A glass dissolution model based upon two observed phenomena, i.e., internal molecular diffusion and glass surface regression, is developed. An asymptotic equation is obtained for fractional dissolution of diffusant from the glass. The asymptotic equation has a form of $c_1 t^{1/2} + c_2 t$ where c_1 and c_2 are a function of molecular diffusion coefficient and regression speed. The experimental results of fractional dissolution of component 'i' is of the form $C_1 t^{1/2} + C_2 t$, where C_1 and C_2 are two constants which depend on the diffusing component. Values of C_1 and C_2 are obtained from glass dissolution experiment. By fitting Eq. (7.6.3) or (7.6.8) to the

experimentally observed f(t) we can obtain the internal molecular diffusion coefficient of component 'i' and the glass-water regression speed. This is presently under study.

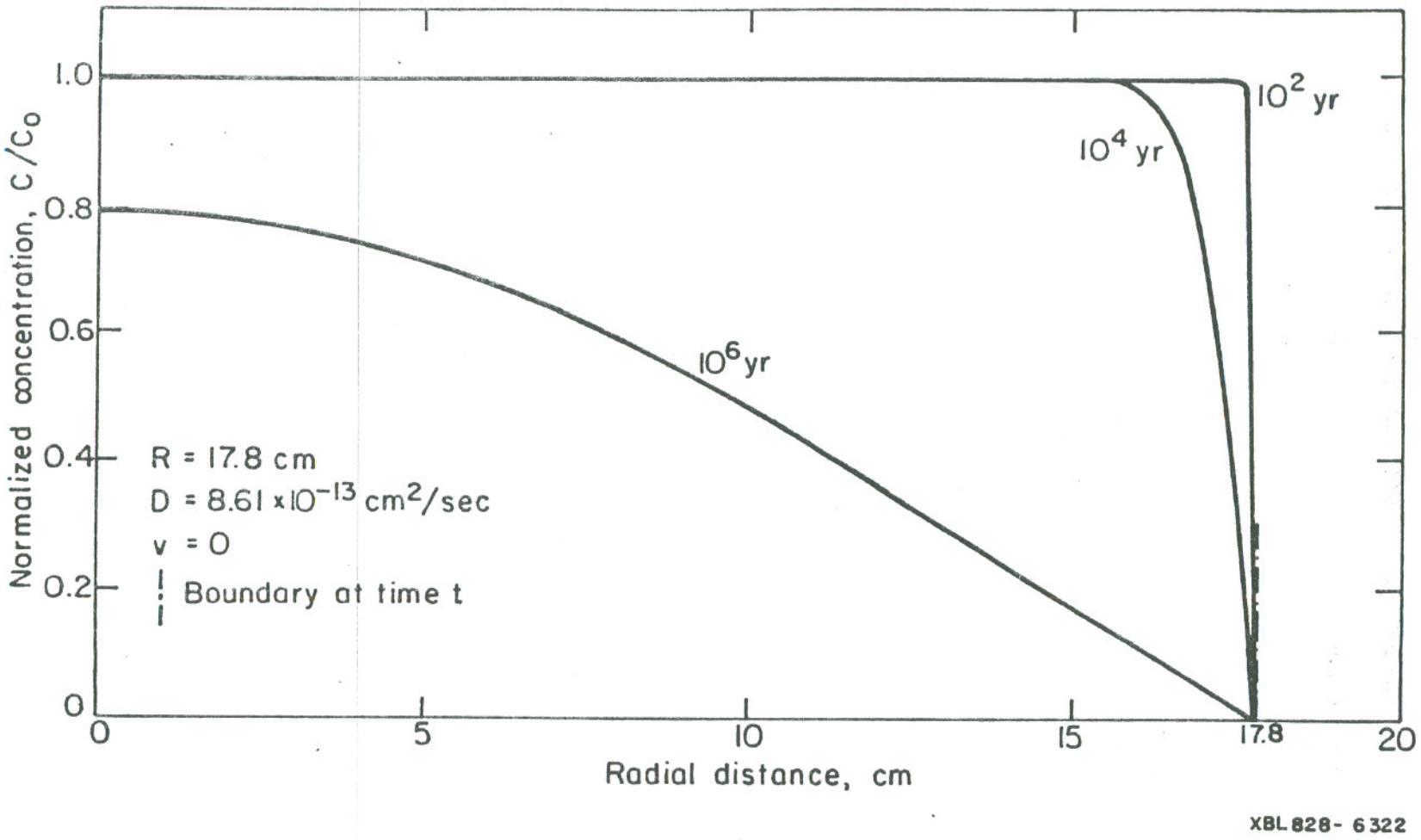

Fig. 7.6.10. Variation of Na normalized concentration in the sphere with radial position at different times after glass dissolution begins.

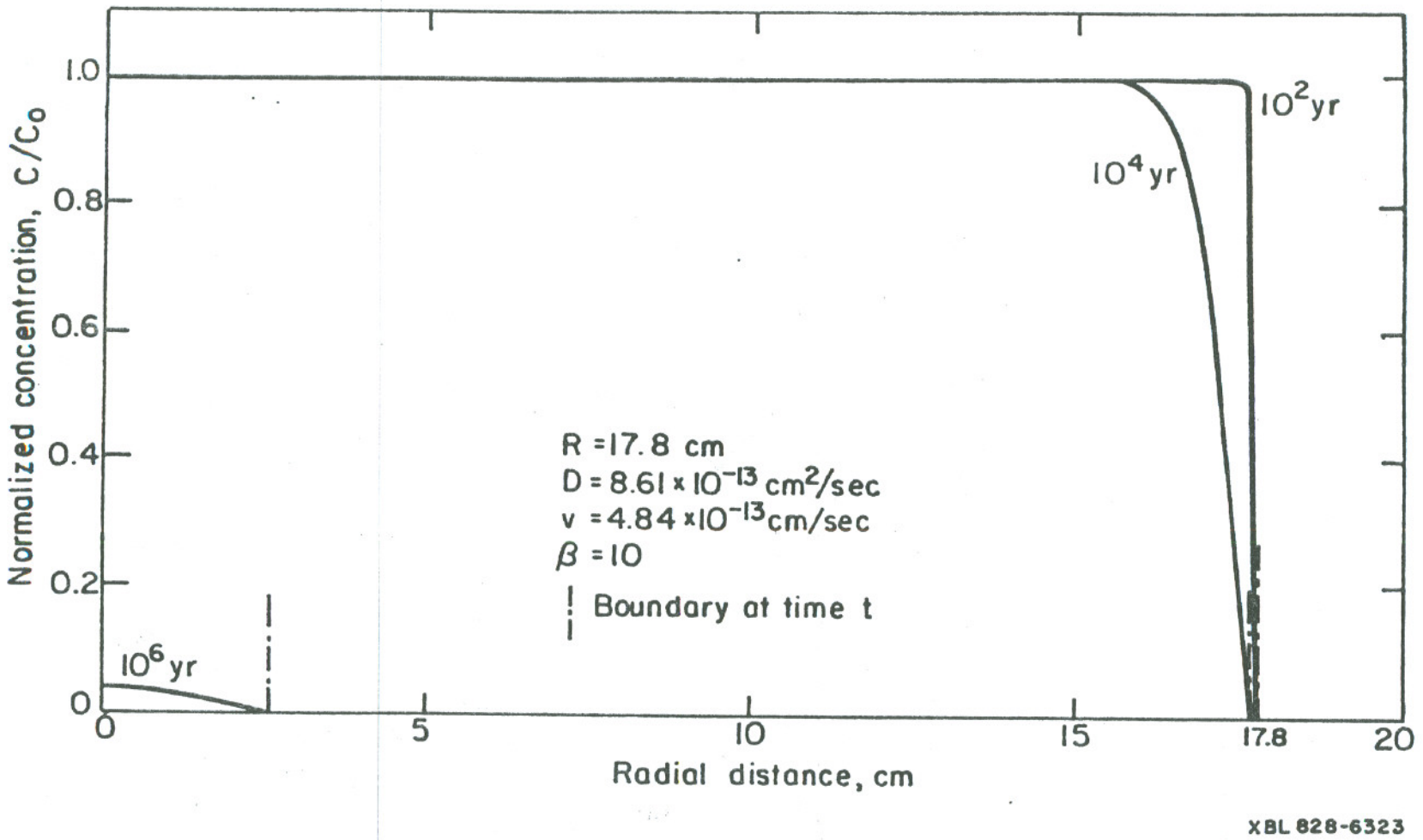

Fig. 7.6.11. Variation of Na normalized concentration in the sphere with radial position at different times after glass dissolution begins.

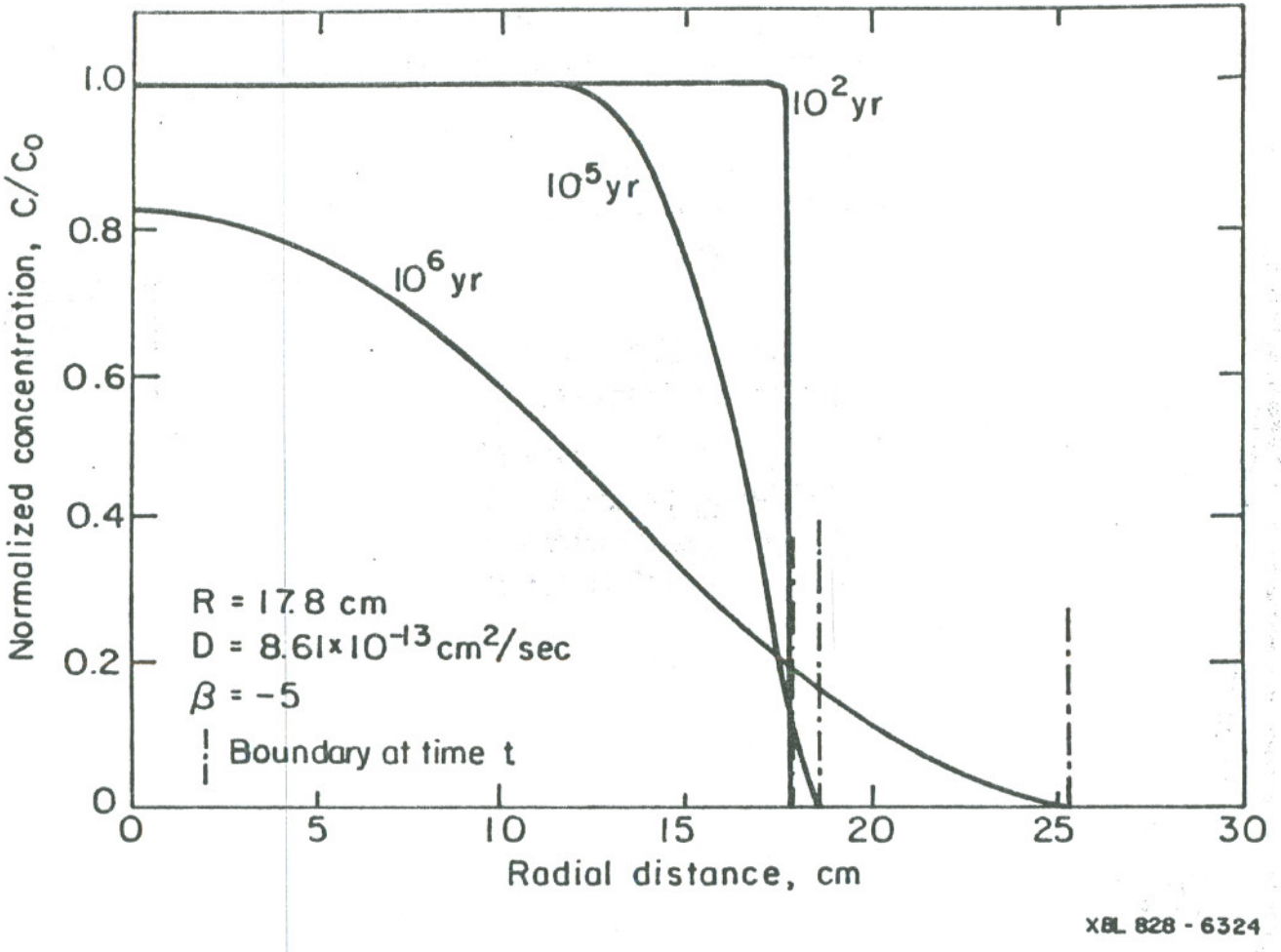

Fig. 7.6.12. Variation of Na normalized concentration in the sphere with radial position at different times after glass dissolution begins.

7.7 Literature References

B1. M. Benedict, T. H. Pigford, H. Levi, "Nuclear Chemical Engineering", 2nd Ed., Chapter 8, pp 369, McGraw-Hill Book Co., 1981.

B2. Blasius, 1908, Z. Math. Phys. 561.

F1. G. H. Frischat, Ionic Diffusion in Oxide Glasses, Trans. Tech. Publications, Ohio, U.S.A., 1975.

H1. Heimerl, et al, 'Research on Glasses for Fission Product Fixation', Hahn-Meitner Institut, HMI-B109, Sept. 1971.

H2. L. Holland, "The Properties of Glass Surfaces", John Wiley and Sons, Inc., New York, 1964.

K1. Krauskopf, K. K., Private communication, March 1, 1982.

K2. F. Kreith, "Principles of Heat Transfer", 2nd Ed., pp 404, International Textbook Co., 1966.

L1. W. Lobrich, VDI-Forsch.-Heft No. 322, 1929.

M1. McVay, G. L., Bradley, D. J., and Kricher, J. F., "Elemental Release from Glass and Spent Fuel", in press in, "Advances in the Science and Technology of Management of High-Level Nuclear Waste", 1982.

M2. G. L. McVay, Private communication, 1982.

M3. Mendel, et al, 'A State-of-the-Art Review of Materials Properties of Nuclear Waste Forms', PNL-3802, April 1981.

M4. W. F. Merrit, "High-Level Waste Glass: Field Leach Test", Nuclear Technology, Vol. 32, 88, Jan. 1977.

R1. G. E. Raines, L. D. Rickertsen, H. C. Caliborne, J. L. McElroy, and R. W. Lynch, 'Development of Reference Condition for Geological Repositories for Nuclear Waste in the U.S.A.', Proc. Mtg. Material Research Societies, Boston, 1980.

S1. Seidell, A., 'Solubilities Inorganic and Metal-Organic Compound' 4th Ed., Vol. 2, pp 1452, American Chemical Soc., Washington, DC, 1965.

T1. Tymochowicz, S., 'A Collection of Results and Methods on the Leachability of Solidified High Level Radioactive Waste', Hahn-Meitner Institut, HMI-B241, April 1977.

W1. Walther, J. V. and Helgson, H. C., 'Calculation of the Thermodynamic Properties of Aqueous Silica and Solubility of Quartz and Its Polymorphs at High Pressures and Temperatures', American J. of Science, V277 (1977).

W2. Weast, R. C., Astle, M. J., Handbook of Chemistry and Physics, 61st Ed., pp F-62, CRC Press, 1980-1981.

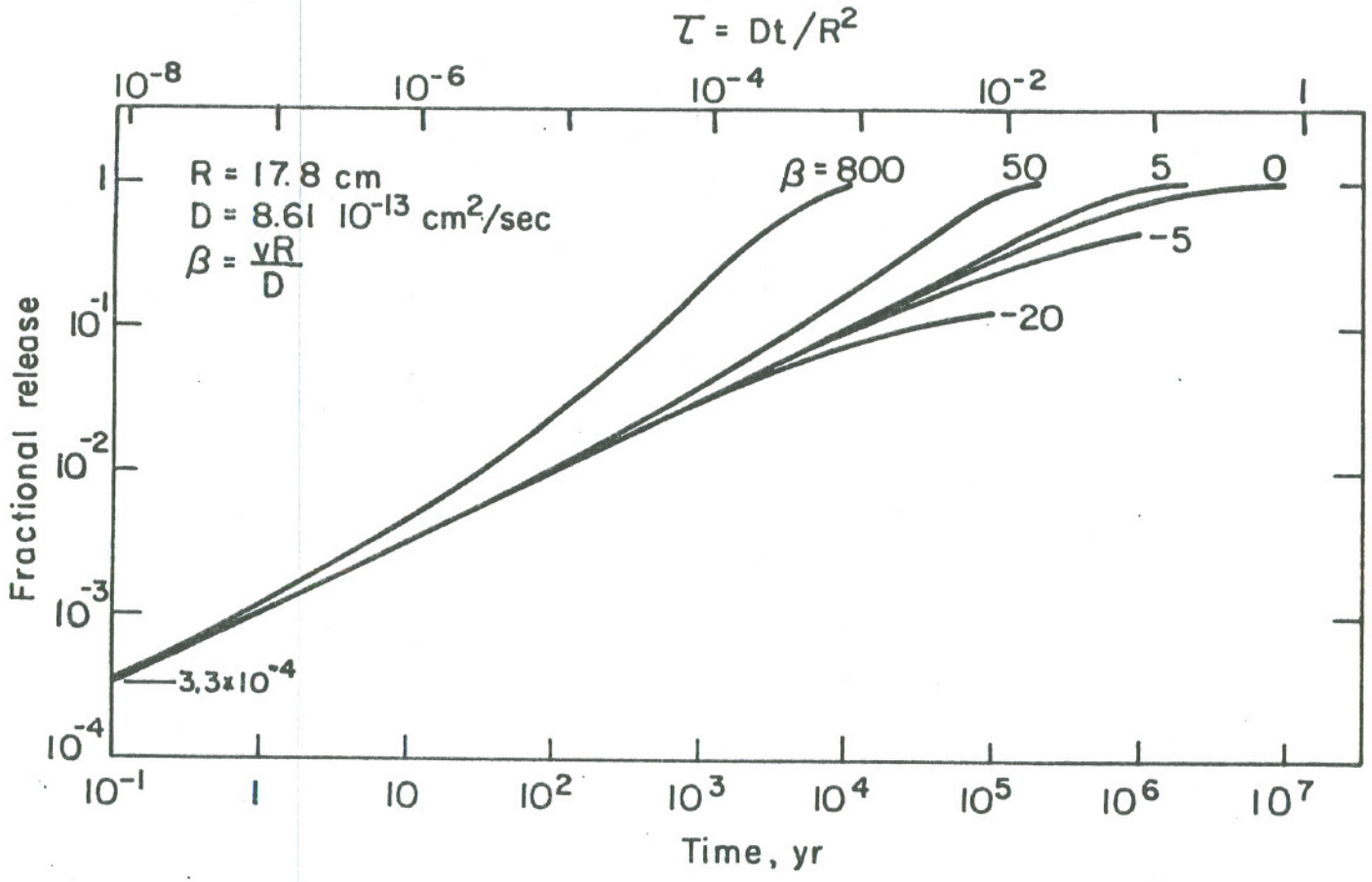

Fig. 7.6.15. Fractional release of Na from sphere against time (τ) for different values of β.

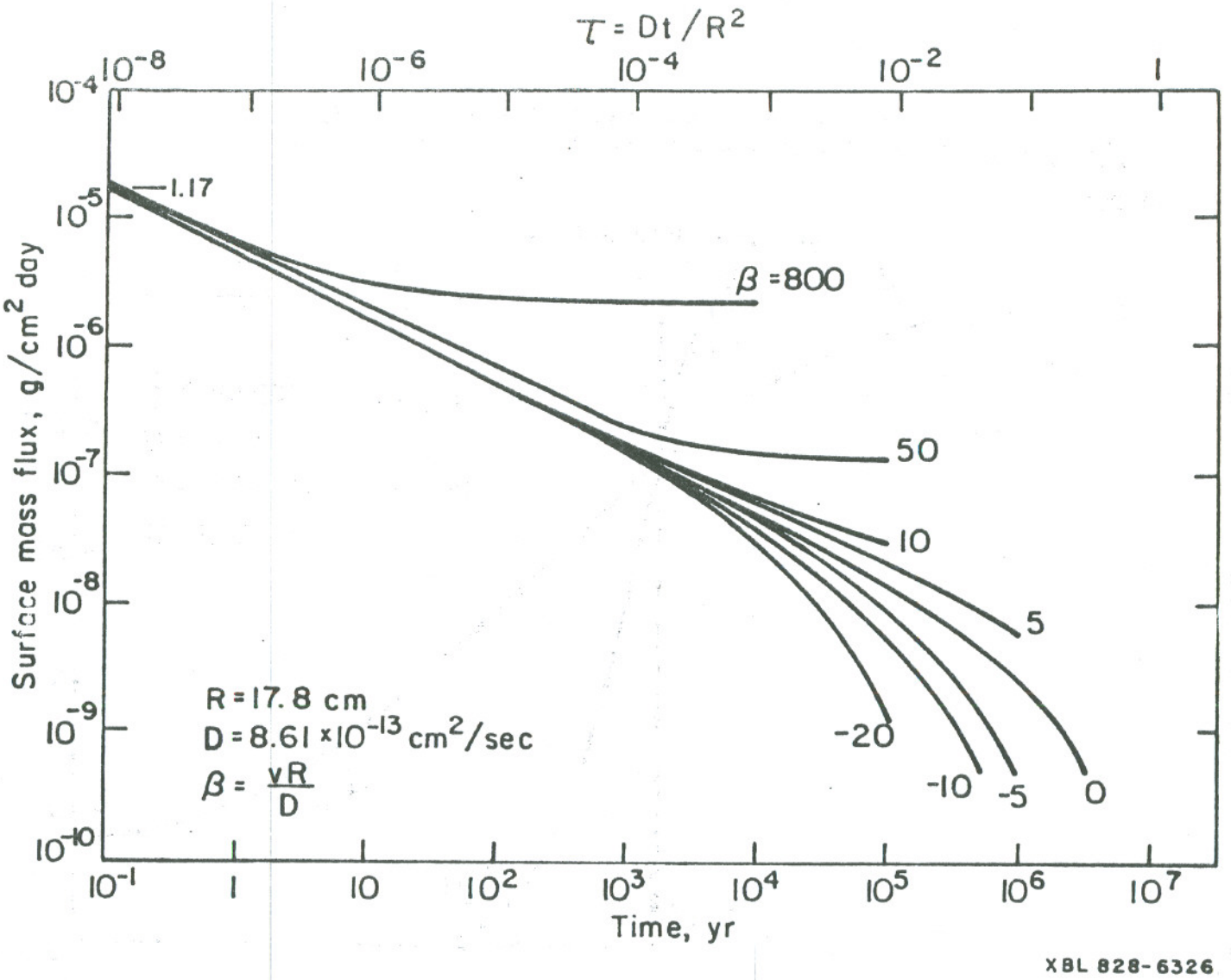

Fig. 7.6.14. Variation of surface mass flux of Na from sphere with time (τ) for different values of β.

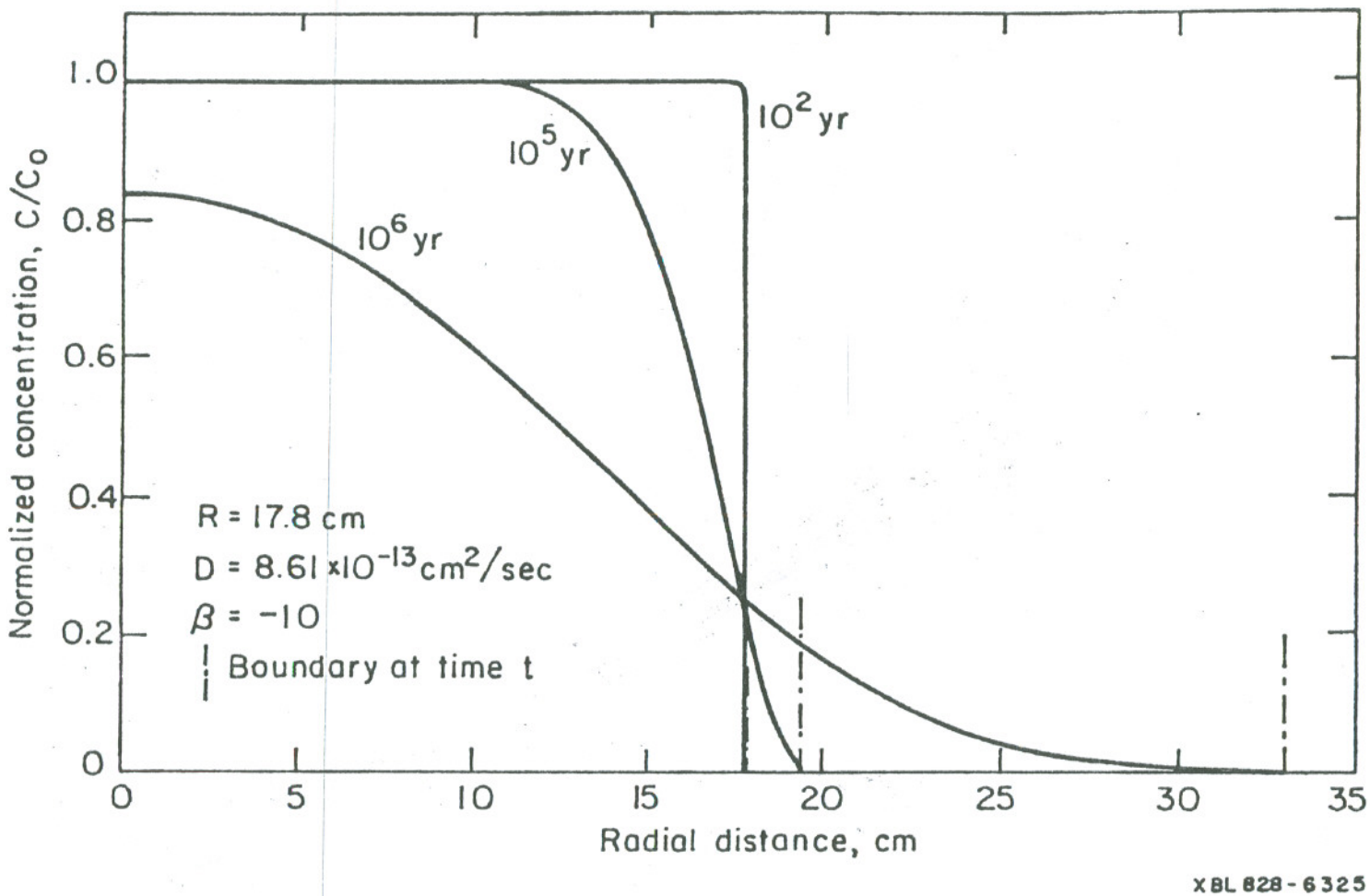

Fig. 7.6.13. Normalized Na concentration in the sphere as a function of radial position at different times after glass dissolution begins.

Appendix A

Derivation of the leach time for sphere, prolate ellipsoid, slender cylinder, and infinite cylinder.

Conservation of mass is the governing equation which for a quasi-steady state is

$$\frac{\partial}{\partial t}(\rho V(t)) = -\dot{m}(t) \tag{A1}$$

where:

ρ = density (g/cm^3)

$V(t)$ = volume at time t (cm^3)

$\dot{m}(t)$ = mass loss rate at time t (g/sec)

With the proper initial condition ($V(0) = V_o$, initial volume), Eq. (A1) can be solved. The following geometries are considered and analyzed.

1. The sphere radius is r, the concentration on the surface is constant and denoted by N_s, the concentration in the liquid tends to zero as r tends to infinity. For the sphere we have

$$V = \frac{4}{3}\pi r^3 \tag{A2}$$

$$\dot{m} = 4\pi r D_e N_s \ , \ D_e \equiv \varepsilon D_f \tag{A3}$$

Initial condition $r(0) = b_o'$ (initial radius)

Substituting Eqs. (A2) and (A3) into Eq. (A1) and after some algebraic manipulation yields

$$\rho r\, dr = -D_e N_s\, dt \tag{A4}$$

Initial condition $r(0) = b_o'$

Integrating with respect to time from t = 0 to t yields

$$(b_o')^2 - r^2(t) = 2 D_e N_s t/\rho \tag{A5}$$

For total dissolution of the sphere we require that $r(T_{sphere}) = 0$, hence

$$T_{sphere} = \frac{\rho (b_o')^2}{2 D_e N_s} \tag{A6}$$

where:

T_{sphere} = leach time for sphere (sec)

2. The concentration on the surface of the prolate ellipsoid is constant (N_s), and the concentration far away from the ellipsoid tends to zero. For the prolate ellipsoid case we have

$$V = \frac{4}{3} \pi ab^2 = \frac{4}{3} \pi f^3 \sinh^2 \alpha \cosh \alpha \tag{A7}$$

$$\dot{m} = \frac{4 \pi D_e N_s f}{\log \left[\coth \left(\frac{\alpha_s}{2}\right)\right]} \tag{A8}$$

Initial condition $\alpha (0) = \alpha_s$ initial surface shape factor

$f (0) = f_o$ initial focal distance

Substituting Eqs. (A7) and (A8) into Eq. (A1) yields

$$\frac{\partial}{\partial t} (f^3 \sinh^2 \alpha \cosh \alpha) = - \frac{3 D_e N_s f}{\rho \log \left[\coth \left(\frac{\alpha}{2}\right)\right]} \tag{A9}$$

Initial condition $f (0) = f_o$

$\alpha (0) = \alpha_s$

Eq. (A9) cannot be solved since there are two unknowns and one equation. It is necessary to have another relation between f and α. To overcome this difficulty we assume that either f, α, or some function of f and α is constant during leaching. Hence, we analyze the following two cases.

Case 1. α is constant and is equal to α_s.

The above assumption can also be stated as: the ratio of major axis to minor axis is constant throughout the leaching. Thus, Eq. (A9) is simplified to

$$f \frac{df}{dt} = - D_e N_s \left[\rho \sinh^2 (\alpha_s) \cosh (\alpha_s) \log(\coth (\frac{\alpha_s}{2})\right]^{-1} \qquad (A10)$$

Initial condition $f(0) = f_o$

By integrating Eq. (A10) from t = 0 to t, we obtain

$$f_o^2 - f^2(t) = 2D_eN_s \left[\rho \sinh^2(\alpha_s)\cosh(\alpha_s)\log(\coth(\frac{\alpha_s}{2}))\right]^{-1} t \qquad (A11)$$

For total dissolution of the prolate ellipsoid we require that $f(T_p) = 0$ and obtain

$$T_p = \frac{\rho b_o^2}{2D_eN_s} \cosh (\alpha_s) \log(\coth(\frac{\alpha_s}{2})) \qquad (A12)$$

where:

T_p = leach time of prolate ellipsoid (sec)

b_o = initial semi-minor axis (cm)

Case 2. The minor axis is constant.

From the above assumption implies that after sufficient time the prolate ellipsoid has shrunk to a sphere with radius equal to the semi-minor axis. The volume and mass loss rate are rewritten as

$$V = \frac{4}{3} \pi ab^2 = \frac{4}{3} \pi b_o^3 \coth \alpha \qquad (A13)$$

$$\dot{m} = 4 \pi D_e N_s b_o \left[\sinh \alpha \log(\coth(\frac{\alpha}{2}))\right]^{-1} \qquad (A14)$$

Initial condition $\alpha(0) = \alpha_s$

Substituting Eqs. (A13) and (A14) into Eq. (A1) yields

$$\rho\, b_o^2 \sinh\alpha \log(\coth(\tfrac{\alpha}{2}))\, \frac{d}{dt}(\coth\alpha) = -\,3D_e\, N_s \qquad \text{(A15)}$$

Initial condition $\alpha(0) = \alpha_s$

After some simplifications, we obtain

$$\frac{3\, D_e\, N_s}{\rho\, b_o^2}\, dt = \frac{\log\left[\coth(\frac{\alpha}{2})\right]}{\sinh\alpha}\, d\alpha \qquad \text{(A16)}$$

Initial condition $\alpha(0) = \alpha_s$

Integrating the above equation between t = 0 to t yields

$$\frac{6\, D_e\, N_s\, t}{\rho\, b_o^2} = \left[\log(\coth(\tfrac{\alpha_s}{2}))\right] - \left[\log(\coth(\tfrac{\alpha}{2}))\right]^2 \qquad \text{(A17)}$$

From Eq. (A17), we obtain T_p^s, the time that will take the prolate ellipsoid to reduce to a sphere with radius b_o, i.e., $\alpha \to \infty$

$$T_p^s = \frac{\rho\, b_o^2}{6\, D_e\, N_s}\left[\log(\coth(\tfrac{\alpha_s}{2}))\right]^2 \qquad \text{(A18)}$$

The leach time for total dissolution of the prolate ellipsoid is viewed as the sum of two time intervals. The first time interval corresponds to reduction of the prolate ellipsoid to a sphere. The second time interval is the leach time of the sphere. Thus, from equation (A18) and (A6) we have

$$T_p = T_p^s + T_{sphere} \qquad \text{(A19)}$$

or

$$T_p = \frac{\rho\, b_o^2}{2\, D_e\, N_s}\left(1+\left[\log\left(\coth\left(\frac{\alpha_s}{2}\right)\right)\right]^2/3\right) \qquad \text{(A20)}$$

Comparison of Eqs. (A12) and (A20) shows that the leach two different cases differ only by a multiplier. From table of the hyperbolic functions, we have

$\alpha_s/2$	$1+\left[\log\left(\coth\left(\frac{\alpha_s}{2}\right)\right)\right]^2/3$	$\cosh(\alpha_s)\log\left(\coth\left(\frac{\alpha_s}{2}\right)\right)$
0.05	4	3.01
0.07	3.36	2.68
0.13	2.40	2.11

Therefore, both cases yield similar results. This does not prove nor disprove the validity of the assumptions used in their derivations. The first case (α constant) is chosen as the criterion for establishing leach time.

3. Slender cylinder ($L \geqslant 10r$)

For the slinder cylinder, we have

$$V = \pi\, r^2 L \qquad \text{(A21)}$$

$$\dot{m} = 2\,\pi\, D_e\, N_s\, L/\log(L/r) \qquad \text{(A22)}$$

Initial condition $r(0) = r_d$ initial radius

$L(0) = L_o$ initial height

We assume that the ratio of height to radius is constant during leaching. This is written as

$$r = r_o\, q(t) \qquad \text{(A23)}$$

$$L = L_o\, q(t) \qquad \text{(A24)}$$

Initial condition $q(0) = 1$

Substituting Eqs. (A21), (A22), (A23), and (A24) into Eq. (A1) and after some transformations, we obtain

$$q(t)\,\frac{dq}{dt} = -\frac{2\,D_e\,N_s}{3\,\rho\,r_o^{\,2}\,\log(L_o/r_o)} \tag{A25}$$

Initial condition $q(0) = 1$

Integrating with respect to time from $t = 0$ to t yields

$$q(t) = \left(1 - \frac{4\,D_e\,N_s\,t}{3\,r_o^{\,2}\,\rho\,\log(\frac{L_o}{r_o})}\right)^{1/2} \tag{A26}$$

From definition of the leach time we require that $q(T_{sc}) = 0$, and obtain

$$T_{sc} = \frac{3\,r_o^{\,2}\,\rho\,\log(\frac{L_o}{r_o})}{4\,D_e\,N_s} \tag{A27}$$

4. Infinitely long cylinder

The mass balance in a unit length results in

$$\frac{d}{dt}\,(\pi\,r^2\rho) = -\frac{8}{\sqrt{\pi}}\;D_e\,N_s\,(Pe)^{1/2},\quad Pe \geq 4 \tag{A28}$$

Initial condition $r(0) = r_o$

Integrating with respect to time from $t = 0$ to t for $r(t)$ yields

$$r^{3/2}(t) - r_o^{\,3/2} = -\frac{6}{\pi^{3/2}}\;N_s\,D_e\,t\,(U/D_f)^{1/2}/\rho \tag{A29}$$

From definition of the leach time $r(T_\infty) = 0$, we obtain

$$T_\infty = \frac{\pi^{3/2}\,\rho r_o^{\,2}}{6D_e\,N_s\,P_e^{\,1/2}},\quad Pe \equiv \frac{Ur_o}{D_f} \tag{A30}$$

Appendix B: The solubility limit of silica in water as a function of temperature and pressure (Ref. W1).

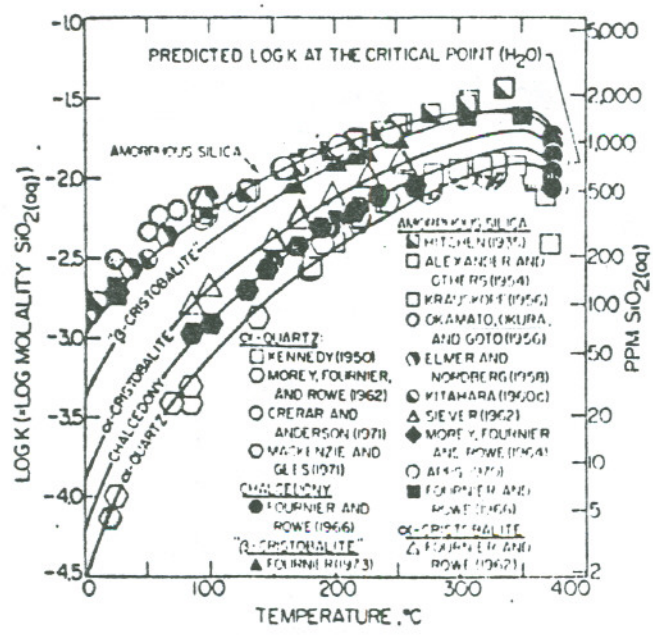

Fig. B.1 Solubility of silica variation with temperature. Pressure corresponds to the liquid-vapor equilibrium curve for H_2O. The symbols correspond to experimental values.

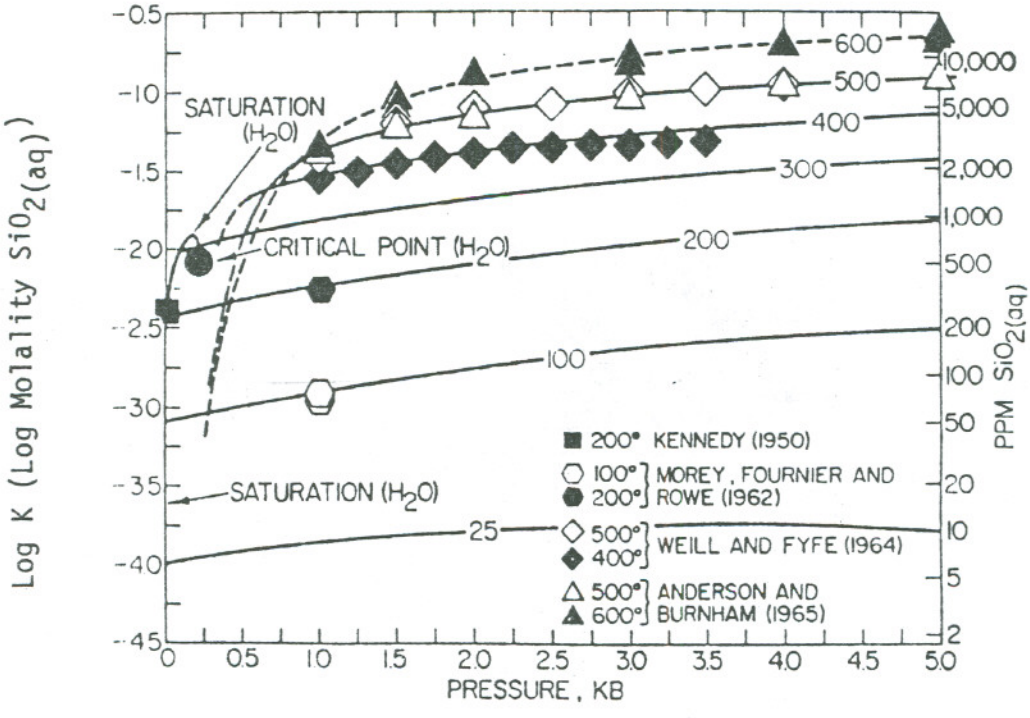

Fig. B.2 Solubility of α quartz variation with pressure at different temperatures in degrees C. The symbols correspond to experimental results.

Reference

W1. Walther, J. V. and Helgson, H. C., 'Calculation of the Thermodynamic Properties of Aqueous Silica and Solubility of Quartz and Its Polymorphs at High Pressures and Temperatures', American J. of Science, V277 (1977).

Appendix C The Computer Programs

UCB NE 70, 71, 72, 73, 74

The following computer programs are written in Fortran IV and have been executed on CDC-7600.

UCBNE-70 Calculates the surface mass flux and leach time due to diffusion and diffusion-convection for a given glass cylinder.

Description of Data Cards:

1st Card: Free Format

Icont	0, stop the program execution; otherwise continue.
Ipara	0, same parameters as previous run; otherwise read new input parameters.
Ivel	0, same groundwater pore velocity as previous run; otherwise read the new value.
Igeo	0, same geometry as previous run; otherwise read the new values.

2nd Card: Free Format. Consists of 4 pieces of information.

1st	surface concentration g/cm^3
2nd	porosity
3rd	diffusivity in groundwater cm^2/sec
4th	glass density

3rd Card: Free Format

1st	groundwater pore velocity m/yr

4th Card: Free Format

1	glass cylinder radius cm
2	glass cylinder height cm

UCBNE-71 Calculates the normalized concentration of a species in a slab with regressive surface.

UCBNE-72 Calculates the fractional release of a species from a slab with regressive surface.

UCBNE-73 Calculates the normalized concentration and surface mass flux of species from sphere with regressive surface.

UCBNE-74 Calculates the fractional release of a diffusing species from a sphere with regressive surface.

```
C                    * UCBNE-70 *
C             AUTHOR    SHAW J. ZAVOSHY
C             DATE    OCT. 1981
C
C       THIS PROGRAM CALCULATES THE SURFACE MASS FLUX FROM A GLASS CYLINDER.
C       THE INPUT PARAMETERS ARE
C       CSE SURFACE CONCENTRATION (G/CM3)
C       EPSE POROSITY
C       DWE DIFFUSIVITY IN WATER (CM2/SEC)
C       RO E DENSITY    (G/CM3)
C       UE GROUNDWATER VELOCITY (M/YR)
C       RE GLASS CYLINDER RADIUS (CM)
C       HTE GLASS CYLINDER HEIGHT (CM)
C     ***************************************************************
```

```
      PROGRAM NONNY  (INPUT,OUTPUT,TAPE5=INPUT,TAPE6=OUTPUT)
      DIMENSION Y(10),X(10),F(10),E(10)
1000  CONTINUE
      READ(5,*)ICONT,IPARA,IVEL,IGEO
      IF(ICONT .EQ. 0) GO TO 6000
      IF(IPARA .EQ. 0) GO TO 700
      READ(5,*)CS,EPS,DW,RO
700   IF(IVEL .EQ. 0) GO TO 800
      READ(5,*)U
800   IF(IGEO .EQ. 0) GO TO 900
      READ(5,*) R,HT
900    CONTINUE
      NNN=0
      V1=3.*R*R*HT/4.
      DE=DW*EPS
      DH=1.E-4
      S1=R*(R+HT)
      X(1)=HT/2.
      Y(1)=SQRT(V1/X(1))
1     Y(1)=Y(1)-DH
      DO 13 I=1,3
      X(I)=V1/Y(I)/Y(I)
      E(I)=SQRT(X(I)*X(I) - Y(I)*Y(I))/X(I)
      F(I)=S1- Y(I)*(Y(I) + X(I)*ASIN(E(I))/E(I))
13    Y(I+1)=Y(I)+DH
      NNN=NNN+1
      FP=(F(3)-F(1))/2./DH
      ACC=F(2)/FP
      ACD=F(2)
      IF(ABS(ACD).LE.0.001) GO TO 101
      Y(1)=Y(2)-ACC
       IF(NNN.GE.50) GO TO 500
      GO TO 1
101    CONTINUE
      A=X(2)
      B=Y(2)
      IF(B.GE.A) GO TO 500
      C=SQRT(A*A-B*B)
      ECC=C/A
```

```
      SHAPE=ALOG((A+B)/C)
      PI=ACOS(-1.)
      S=2.*PI*B*(B+(A*ASIN(ECC)/ECC))
       CTS=-ALOG(TANH(SHAPE/2.))
      AREA=2.*PI*R*(R+HT)/10000.
      VOLUM=PI*R*R*HT/1000000.
      WRITE(6,2)
2      FORMAT(1H1,*--------DIMENSIONS OF GLASS CYLINDER---------*)
      WRITE(6,5)R,HT/100.,AREA,VOLUM
5      FORMAT(//,*      RADIUS (CM)=*,F10.2   ,6X,*HEIGHT (M)=*, F10.2 ,6X
     1,*SURFACE AREA (M2)=*, F10.2 ,6X,*VOLUME (M3)=*,F10.2)
      WRITE(6,15)DW,EPS,DE
15     FORMAT(/,*DIFFUSIVITY IN WATER (CM2/SEC)=*,1PE15.7,6X,*POROSITY=*,
     11PE15.7,6X,*EFFECTIVE DIFFUSIVITY (CM2/SEC)=*,1PE15.7)
      WRITE(6,6)CS
1      FORMAT(//,6X,*  CS (G/CM3) =*,1PE15.7)
      WRITE(6,7)
7      FORMAT(/,*----DIMENSION OF APPROX. PROLATE ELLIPSOID-----*)
      WRITE(6,10)A/100.,B,C/100.
10     FORMAT(//,*  A (M)=*,1PE15.7,6X,*B (CM)=*,1PE15.7,6X,*C (M)=*,1PE1
     15.7)
      WRITE(6,12)ECC,SHAPE,S/10000.
12     FORMAT(*  E@C/A =*,F12.6,6X,*SURFACE SHAPE FACTOR=*,F12.6,6X,*S (M
     12)=*,1PE15.7)
      DY=86400.
      ZTOTAL=(4.*PI*DE*CS*C)/CTS
      ZTOTAL=DY*ZTOTAL
      ZLENGT=ZTOTAL/2./A
      ZSURF=ZTOTAL/S
       PELT=(RO*B*B*COSH(SHAPE)*CTS)/(2.*DE*CS)
      PELT=PELT/DY/365.25
      WRITE(6,30)ZTOTAL,PELT
30      FORMAT(//,*  P.E. MASS LOSS RATE (GR/D)=*,1PE15.7,9X,*P.E.LEACH T
     1IME (YR)=*,1PE15.7)
      WRITE(6,32) ZLENGT,ZSURF
32     FORMAT(*  P.E. MASS LOSS PER UNIT LENGTH (GR/DAY)=*,1PE15.7,6X,
```

```
     1*SURFACE MASS FLUX (GR/CM2 DAY)=*,1PE15.7)
      ZSCYL=(2.*PI*DE*CS*HT)/(ALOG(HT/R))
      ZSCYL=ZSCYL*DY
      SCLT=(3.*R*R*RO*ALOG(HT/R))/(4.*DE*CS)
      SCLT=SCLT/DY/365.25
       WRITE(6,35)HT/R,ZSCYL,SCLT
35     FORMAT(//,*  S.CYL.RATO=*,F10.2,7X,*S.CYL. MASS LOSS RATE (GR/D)=
     1*,F14.7,7X,*S.CYL. LEACH TIME (YR)=*,1PE10.2)
      WRITE(6,75)
75     FORMAT(//,*-------INFINITE CYLINDER-------*)
500    CONTINUE
      V=(U*100.)/365.25/86400.
      PE=V*R/DW
      IF(PE.LT.4.) GO TO 5000
      WRITE(6,40) V*DY*3.6525,PE,DW
40     FORMAT(///,*  U (M/YR)=*,1PE10.3,6X,* PECLET NO.=*,1PE10.3,6X,*DW
     1(CM2/SEC)=*,1PE10.3)
      ZUL=4.5135*DE*CS*SORT(PE)
      ZUL=ZUL*DY
      ZUS=ZUL/(2.*PI*R)
      RI=4.*DW/V
      ZLT=0.9281*RO*(R*SORT(R)-RI*SORT(RI))/(CS*DE*SORT(V/DW))
      ZLT=ZLT/DY/365.25
      WRITE(6,50)R,RI,ZUL
50     FORMAT(//,* INITIAL RADIUS (CM)=*,1PE10.3,6X,*FINAL RADIUS (CM)=*
     1,1PE10.3,6X,*MASS LOSS PER UNIT LENGTH (GR/CM DAY)=*,1PE15.7)
      WRITE(6,55) ZUS,ZLT
55     FORMAT(*  SURFACE MASS FLUX (GR/CM2 DAY)=*,1PE15.7,6X,*LEACH TIME
     1(YR)=*,1PE15.7)
5000   CONTINUE
      GO TO 1000
1000   CONTINUE
      STOP
      END
```

```
C       ***********  UCENE-71   ***************
C                   AUTHOR : SHAW J. ZAVOSHY
C                   DATE  JUL. 1981
C       THIS PROGRAM CALCULATES THE NORMALIZED CONCENTRATION AND SURFACE
C       MASS FLUX OF A DIFFUSING SPECIES FROM A SLAB WITH INITIAL HALF
C       WIDTH OF 2A. THE INPUT PARAMETERS ARE
C       AE  INITIAL HALF WIDTH (CM)
C       DE  DIFFUSION COEFFICIENT (CM2/SEC)
C      BETHA=V*A/D=DIMENSIONLESS GLASS-WATER REGRESSION SPEED
C       ***************************************************************
C
      PROGRAM NOME   (INPUT,OUTPUT,TAPE5=INPUT,TAPE6=OUTPUT)
        DIMENSION X(22),C(20)
       DIMENSION DD(10),BETHV(10)
      H=1.E-6
      RO=.672
      ROS=0.
      CEFF=RO-ROS
         A=17.8
      DD(1)=8.61*(10.**(-13))
      DD(2)=3.59*(10.**(-11))

       BETHV(1)=0.
       BETHV(2)=5.
       BETHV(3)=10.
       BETHV(4)=50.
       BETHV(5)=800.
       BETHV(6)=1600.
       BETHV(7)=-5.
      BETHV(8)=-10.
      BETHV(9)=-20.
      NBI=9
      NDI=2
       DO 6000 ND=1,NDI
      D=DD(ND)
      DO 5000 NB=1,NBI
      BETH=BETHV(NB)

      T=.1
       T=T*86400.*365.25
      RO1=(RO-ROS)*D*8640.
       V=BETH*D/A
      WRITE(6,2)A,V,D,BETH
2     FORMAT(1H1,*HALF WIDTH(CM)=*,F12.6,6X,*V(CM/SEC)=*,1PE15.7,6X,
     1*D (CMXCM/SEC)=*,1PE15.7,6X,*BETHA=(VXA/D)=*,1PE15.7)
      WRITE(6,13)RO
13    FORMAT(/,* DENSITY (GR/CM3)=*,1PE15.7)

      IF(V.EQ.0.) GO TO 7
```

```
      TLY=A/V/86400./365.25
      WRITE(6,3)TLY
3     FORMAT(/,*LEACH TIME(YR)=*,1PE15.7)
7     CONTINUE
C
C       BEGINNING OF TIME DO LOOP . MULTIPLIER=10
C
      DO 100 K=0,25
      IF(V.EQ.0.) GO TO 15
      IF(T.GE.ABS(A/V)) GO TO 500
15      TA=DT/A/A

        SQ=2.*SQRT(TA)
        PX=1.-BETH*TA
       DX=PX/10.

      WRITE(6,10)PX*A,DX*A,T/86400./365.25
10    FORMAT(//,*W(T)(CM)=*,F10.4,6X,*DX(CM)=*,F10.5,6X,*TIME(YR )=*,1PE
     114.6)
C
C     BEGINNING OF NODAL LOOP.
C
      DO 50 I=1,23
      IF(I.GE.11) GO TO 150
         X(I)=(I-1)*DX
       GO TO 200
150    X(I)=X(I-1)+.1*DX
       IF(I.GE.21) GO TO 101
       GO TO 200

101     M=I-20
       X(I)=PX-M*H/A
200     C(1)=(ERF((1.+X(I))/SQ)+ERF((1.-X(I))/SQ))/2.
         Z=1.-X(I)
         Y=1.+X(I)
C      BEGINNING OF SUMMATION OF INFINITE SERIES. MAX. OF 40 TERMS.
      DO 20 N=1,40

        AR=N*PX
       S1=EXP(-N*BETH*(AR-X(I)))*(ERF((2.*AR+Z)/SQ)-ERF((2.*AR-Y)/SQ))
         S1=S1/2.
      S2=EXP(-N*BETH*(AR+X(I)))*(ERF((2.*AR+Y)/SQ)-ERF((2.*AR-Z)/SQ))/2.
           S=(S1+S2)*((-1)**N)

       C(N+1)=C(N)+S
       IF(C(N+1).EQ.0.) GO TO 35

      EPS=S/C(N+1)
      IF(ABS(EPS).LE.ABS(C(N+1))/1000.) GO TO 35
20      CONTINUE
```

```
35      IF(I.GE.21) GO TO 77
        C(N+1)=(ROS+CEFF*ABS(C(N+1)))/RO
        C(1)=C(1)*CEFF/RO
          WRITE(6,36)X(I)*A,ABS(C(N+1)),N,C(N+1)-C(1)
36      FORMAT(/,*POSITION (CM)=*,F10.4,12X,*CONCENTRATION=*,F10.4,6X,
     1*N=*,I2,6X,*SUM(N)=*,F12.6)
        GO TO 50

77      DERIV=-C(N+1)/H/M
        WRITE(6,45)M*H,DERIV,-RO1*DERIV,N
45      FORMAT(/,*H(CM)=*,1PE15.7,6X,*DERIVATIVE=*,1PE15.7,6X,*MASS FLUX
     1(GR/CM2 DAY)=*,1PE15.7,6X,I2)
        TOTJ=-RO1*DERIV +V*ROS*86400.
        WRITE(6,55) TOTJ
55      FORMAT(//,*  TOTAL MASS LOSS RATE (G/CM2 DAY)=*,1PE15.7)
50      CONTINUE
100       T=T*10.
500     CONTINUE
5000    CONTINUE
6000    CONTINUE
        STOP
        END
```

```
C                    *** UCBNE-72   ***
C                  AUTHOR  SHAW J. ZAVOSHY
C                  DATE  AUG. 1981
C     THIS PROGRAM CALCULATES THE FRACTIONAL RELEASE OF A DIFFUSING
C     RADIO-NUCLIDE FROM A SLAB WITH INITIAL WIDTH OF 2A. THE INPUT
C     PARAMETERS ARE
C     A= INITIAL HALF WIDTH (CM)
C     DC= DECAY CONSTANT (1/YR)
C     D= DIFFUSION COEFFICIENT (CM2/SEC)
C     B= V*A/D @ THE DIMENSIONLESS GLASS -WATER REGRESSION SPEED
C     ****************************************************************
C     THE FRACTIONAL RELEASE IS CALCULATED BY DIRECT EVALUATION
C     OF THE EQUATION FOR B .LE. 90, AND ASYMPTOTIC AND UPPER AND LOWER BOUND
C     OF THE EQUATION FOR B .LE. 90, AND ASYMPTOTIC AND UPPER
C     BOUND LOWER BOUND ARE USED FOR B .GT. 90.
C    ******************************************************************
C
      DIMENSION SU(50),SL(50)
      DIMENSION S(50),AR(5),AE(5),ASFC(5)
      DIMENSION DD(10),BV(10)
      RO=.672
      ROS=0.
      CEFF=RO-ROS
      DC=0.
      DCYY=DC*86400.*365.25
      A=17.8
      DD(1)=8.61*(10.**(-13))
      DD(2)=3.59*(10.**(-11))
      BV(1)=.000001
      BV(2)=5.
      BV(3)=10.
      BV(4)=50.
      BV(5)=800.
      BV(6)=1600.
      BV(7)=-5.
```

```
      TIN=.001
      NDI=2
      NBI=7
      DO 6000 ND=1,NDI
      D=DD(ND)
      DO 5000 NB=1,NBI
      B=BV(NB)
      V=D*B/A
      WRITE(6,2)A,V,D,B
2     FORMAT(1H1,*HALF WIDTH(CM)=*,F12.6,6X,*V(CM/SEC)=*,1PE15.7,6X,
     1*D (CMXCM/SEC)=*,1PE15.7,6X,*BETHA=*,1PE15.7)

      WRITE(6,13) RO
13    FORMAT(//,* DENSITY (G/CM3) =*,1PE15.7)
      IF(DC.EQ.0.) GO TO 17
      WRITE(6,8)DCYY,.693/DCYY
8     FORMAT(/,2X,*DECAY CONSTANT(1/YR) =*,1PE15.7,6X,*HALF LIFE(YR)=*,
     11PE10.4)
17    CONTINUE
      IF(V.EQ.0.) GO TO 7
      TLY=A/V/86400./365.25
      WRITE(6,3)TLY
3     FORMAT(/,*LEACH TIME(YR)=*,1PE15.7)
7     T=TIN
      T=T*86400.*365.25
      IF(B.GE.90.) GO TO 234

      WRITE(6,789)
789   FORMAT(////,*---------- DIRECT CALCULATION ------------*)
C
C     BEGINNING OF TIME DO LOOP.MULTIPLIER IS 10.
C
      DO 30 K=0,20
      IF(V.EQ.0.) GO TO 21
      IF(ABS(T).GE.ABS(A/V)) GO TO 5000
21    TA=D*T/A/A
```

```
      TETH=1.-TA*B
      C=2.*SQRT(TA)
      F1=(1.+TETH)/C
      F2=(1.-TETH)/C

      TI=(1.+TETH)*ERF(F1)-(1.-TETH)*ERF(F2)
      S(1)=TI+C*(EXP(-F1*F1)-EXP(-F2*F2))/1.772454
      O=1.-S(1)/2.
      S(1)=O
C
C     BEGINNING OF INFINITE SUM DO LOOP. MAX. OF 40 TERMS.
C
      DO 10 N=1,40
      IF(N.EO.40) GO TO 30
      E1=EXP(-N*B*TETH*(N-1))
      E2=EXP(-N*B*TETH*(N+1))
      E=2.*N-1.
      F=2.*N+1.
      A1=E*TETH
      A2=F*TETH

      P1=E1*(ERF((A1+1.)/C)-ERF((A1-1.)/C))
      P2=E2*(ERF((A2-1.)/C)-ERF((A2+1.)/C))
      P3=EXP(N*B*(N-1))*(ERF((E-TETH)/C)-ERF((E+TETH)/C))
      P4=EXP(N*B*(N+1))*(ERF((F+TETH)/C)-ERF((F-TETH)/C))
      PS=((-1.)**(N+1))*(P1+P2+P3+P4)/(2.*N*B)
      S(N+1)=PS+S(N)
      IF(S(N+1).EO.0.) GO TO 100
      EPS=(S(N+1)-S(N))/S(N+1)
      IF(ABS(EPS).LE.ABS(S(N+1))/1000.) GO TO 100
10    CONTINUE

100   S(N+1)=1.+(S(N+1)-1.)*CEFF/RO -ROS*(1.-V*T/A)/RO
      WRITE(6,105)T/86400./365.25,S(N+1),S(N+1)*EXP(-DC*T),N
105   FORMAT(/,* TIME(YR)=*,1PE10.4,6X,*FRACTINAL RELEASE=*,1PE15.7,6X
     1,*FRAC. REL. WITH DECAY=*,1PE15.7,4X,*N=*,I2)
```

```
   30  T=T*10.
       GO TO 5000
  234  CONTINUE
       WRITE(6,456)
  456  FORMAT(////,*---------- ASYMPTOTIC METHOD USED ----------*)
C
C      BEGINNING OF TIME DO LOOP.MULTIPLIER IS 10.
C
       DO 31 K=0,20
       IF(V.EQ.0.) GO TO 22
       IF(ABS(T).GE.ABS(A/V)) GO TO 235
   22  TA=D*T/A/A
       TETH=1.-TA*B
       C=2.*SQRT(TA)
       F1=(1.+TETH)/C
       F2=(1.-TETH)/C
       TI=(1.+TETH)*ERF(F1)-(1.-TETH)*ERF(F2)
       S(1)=TI+C*(EXP(-F1*F1)-EXP(-F2*F2))/1.772454
       O=1.-S(1)/2.
       S(1)=O
C
C      BEGINNING OF INFINITE SUM DO LOOP. MAX. OF 40 TERMS.
C
       DO 11 N=1,40
       IF(N.EQ.40) GO TO 31
       E1=EXP(-N*B*TETH*(N-1))
       E2=EXP(-N*B*TETH*(N+1))
       E=2.*N-1.
       F=2.*N+1.
       A1=E*TETH
       A2=F*TETH
       AR(1)=(E+TETH)/C
       AR(2)=(E-TETH)/C
       AR(3)=(F-TETH)/C
       AR(4)=(F+TETH)/C
       AE(1)=N*B*(N-1)-AR(1)*AR(1)
```

```
      AE(2)=N*B*(N-1)-AR(2)*AR(2)
      AE(3)=N*B*(N+1)-AR(3)*AR(3)
      AE(4)=N*B*(N+1)-AR(4)*AR(4)

      DO 400 J=1,4
      ASYM=1.
      DO 300 NN=1,4
      AFT=2.*J+1.
      AFB=J+1.
      FT=GAMFN(AFT,IERR)
      FB=GAMFN(AFB,IERR)
      SS=FT/(FB*((4.*AR(J)*AR(J))**NN))
300   ASYM=ASYM+(-1)**NN*SS
400   ASFC(J)=EXP(AE(J))*ASYM/AR(J)/SQRT(3.1415)
      P1=E1*(ERF((A1+1.)/C)-ERF((A1-1.)/C))
      P2=E2*(ERF((A2-1.)/C)-ERF((A2+1.)/C))
      IF(N.GE.2) GO TO 250
      P3=ERF(AR(2))-ERF(AR(1))
      P4=ASFC(3)-ASFC(4)
      GO TO 75
250   P3=ASFC(1)-ASFC(2)
      P4=ASFC(3)-ASFC(4)
75    PS=((-1.)**(N+1))*(P1+P2+P3+P4)/(2.*N*B)
      S(N+1)=PS+S(N)
      IF(S(N+1).EQ.0.) GO TO 101
      EPS=(S(N+1)-S(N))/S(N+1)
      IF(ABS(EPS).LE.ABS(S(N+1))/1000.) GO TO 101
11    CONTINUE
101   S(N+1)=1.+(S(N+1)-1.)*CEFF/RO -ROS*(1.-V*T/A)/RO
      WRITE(6,106)T/86400./365.25,S(N+1),S(N+1)*EXP(-DC*T),N
106   FORMAT(/,* TIME(YR)=*,1PE10.4,6X,*FRACTINAL RELEASE=*,1PE15.7,6X
     1,*FRAC. REL. WITH DECAY=*,1PE15.7,4X,*N=*,I2)
31    T=T*10.
235   CONTINUE
C
      WRITE(6,576)
```

```
576   FORMAT(/,*  BOUND METHOD IS USED. U.B.@ UPPER BOUND FRACTIONAL REL
     1EASE. DELTA@U.B. - L.B. *)
      T=TIN*86400.*365.25
      DO 32 K=0,20
      IF(V.EQ.0.) GO TO 23
      IF(ABS(T).GE.ABS(A/V)) GO TO 5000
23    TA=D*T/A/A
      TETH=1.-TA*B
      C=2.*SORT(TA)
      F1=(1.+TETH)/C
      F2=(1.-TETH)/C
      TI=(1.+TETH)*ERF(F1)-(1.-TETH)*ERF(F2)
      S(1)=TI+C*(EXP(-F1*F1)-EXP(-F2*F2))/1.772454
      O=1.-S(1)/2.
      SL(1)=O
      SU(1)=O
C
C     BEGINNING OF INFINITE SUM DO LOOP. MAX. OF 40 TERMS.
C
      DO 12 N=1,40
      E1=EXP(-N*B*TETH*(N-1))
      IF(N.EQ.40) GO TO 32
      E2=EXP(-N*B*TETH*(N+1))
      E=2.*N-1.
      F=2.*N+1.
      A1=E*TETH
      A2=F*TETH
      AR(1)=(E+TETH)/C
      AR(2)=(E-TETH)/C
      AR(3)=(F-TETH)/C
      AR(4)=(F+TETH)/C
      AE(1)=N*B*(N-1)-AR(1)*AR(1)
      AE(2)=N*B*(N-1)-AR(2)*AR(2)
      AE(3)=N*B*(N+1)-AR(3)*AR(3)
      AE(4)=N*B*(N+1)-AR(4)*AR(4)
      CL31=AR(1)+SORT(AR(1)*AR(1)+2.)
```

```
      CL32=AR(2)+SQRT(AR(2)*AR(2)+1.2732)
      CU31=AR(1)+SQRT(AR(1)*AR(1)+1.2732)
      CU32=AR(2)+SQRT(AR(2)*AR(2)+2.)
      CL41=AR(3)+SQRT(AR(3)*AR(3)+2.)
      CL42=AR(4)+SQRT(AR(4)*AR(4)+1.2732)
      CU41=AR(3)+SQRT(AR(3)*AR(3)+1.2732)
      CU42=AR(4)+SQRT(AR(4)*AR(4)+2.)
      BLP3=SQRT(1.2732)*(EXP(AE(1))/CL31-EXP(AE(2))/CL32)
      BUP3=SQRT(1.2732)*(EXP(AE(1))/CU31-EXP(AE(2))/CU32)
      BLP4=SQRT(1.2732)*(EXP(AE(3))/CL41-EXP(AE(4))/CL42)
      BUP4=SQRT(1.2732)*(EXP(AE(3))/CU41-EXP(AE(4))/CU42)
      P1=E1*(ERF((A1+1.)/C)-ERF((A1-1.)/C))
      P2=E2*(ERF((A2-1.)/C)-ERF((A2+1.)/C))
      IF(N.GE.2) GO TO 50
      BLP3=ERF(AR(2)) -ERF(AR(1))
      BUP3=BLP3
50    PSU=(-1)**(N+1)*(P1+P2+BUP3+BUP4)
      PSL=(-1)**(N+1)*(P1+P2+BLP3+BLP4)
      PSL=PSL/(2.*N*B)
      PSU=PSU/(2.*N*B)
      SU(N+1)=SU(N)+PSU
      SL(N+1)=SL(N)+PSL
      EPSU=(SU(N+1)-SU(N))/SU(N+1)
      EPSL=(SL(N+1)-SL(N))/SL(N+1)
      IF(ABS(EPSU).LE.SU(N+1)/1000.) GO TO 410
      GO TO 12
410   IF(ABS(EPSL).LE.SL(N+1)/1000.) GO TO 550
12    CONTINUE
550   SU(N+1)=1.+(SU(N+1)-1.)*CEFF/RO -ROS*(1.-V*T/A)/RO
      SL(N+1)=1.+(SL(N+1)-1.)*CEFF/RO -ROS*(1.-V*T/A)/RO
      WRITE(6,107)T/86400./365.25,SU(N+1),ABS(SU(N+1)-SL(N+1)),SU(N+1)*
     1EXP(-DC*T),N
107   FORMAT(/,* TIME(YR)=*,1PE10.4,4X,*U.B.=*,1PE15.7,6X,*DELTA=*,1PE1
     15.7,6X,*U.B. WITH DECAY=*,1PE15.7,4X,*N=*,I2)
32    T=T*10.
5000  CONTINUE
```

```
1000  CONTINUE
      STOP
      END
```

```
C
C     THIS PROGRAMM CALCULATES CONCENTRATIN AND MASS FLUX.
C      CASE SPHERE.
C
C                                  UCBNE-73
C                              Author  Shaw J. Zavoshy
C                                 Date  August 1981
C
      DIMENSION C(50),X(30),ERC(10),ERFC(10),XX(10)
      DIMENSION FRAC(30),QAV(30),SDIR(5)
      DIMENSION TIME(30)
      DIMENSION DD(10),BETHV(10)
      A=17.8
      RO=.672
      ROS=0.
      COEF=RO-ROS
      DD(1)=8.61*(10.**(-13))
      DD(2)=3.59*(10.**(-11))
      NDI=1
      NBI=9
      BETHV(1)=0.
      BETHV(2)=5.
      BETHV(3)=10.
      BETHV(4)=50.
      BETHV(5)=800.
      BETHV(6)=1600.
      BETHV(7)=-5.
      BETHV(8)=-10.
      BETHV(9)=-20.
      H=.00001
      DO 6000 ND=1,NDI
      D=DD(ND)
      DO 5000 NB=1,NBI
      BETH=BETHV(NB)
      POI=(RO-ROS)*D*86400.
      V=BETH*D/A
      T=.1
      T=T*86400.*365.25
      WRITE(6,2)A,V,D,BETH
2     FORMAT(1H1,*  RADIUS  (CM)=*,F12.6,5X,*V(CM/SEC)=*,1PE15.7,6X,
     1*D  (CMXCM/SEC)=*,1PE15.7,6X,*BETHA=(VXA/D)=*,1PE15.7)
      WRITE(6,13)RO
13    FORMAT(/,* DENSITY (GR/CM3)=*,1PE15.7)
      IF(V.EQ.0.) GO TO 7

      TLY=A/V/86400./365.25
      TTRANS=D/V/V
      WRITE(6,3)TLY,TTRANS/86400./365.25
3     FORMAT(/,*LEACH TIME(YR)=(A/V)=*,1PE15.7,5X,*TRANSITION TIME(YR)=
     1(D/V2)= *,1PE15.7)
7     CONTINUE
C
C       BEGINNING OF TIME DO LOOP . MULTIPLIER=10
C
      IJK=25
      DO 100 K=0,IJK
      SDIR(1)=0.
      IF(V.EQ.0.) GO TO 17
      IF(T.GE.ABS(A/V)) GO TO 500

      GO TO 301
```

```
17      IJK=9
301     CONTINUE
         TA=D*T/A/A

         SQ=2.*SQRT(TA)
         PX=1.-BETH*TA
        IF(PX.LE. .001/A ) GO TO 500
        DX=PX/10.

       WRITE(6,10)T/86400./365.25,PX*A,DX*A
10     FORMAT(//,*-------- TIME(YR)=*,1PE13.2,6X,* R(I) (CM)=*,F12.4,6X,
      1* DR(CM)=*,F12.5)
C
C      BEGINNING OF NODAL POINTS.
       DO 50 I=1,23
       IF(I.GE.11) GO TO 150
          X(I)=(I-1)*DX
        X(1)=.001/A

          GO TO 200
150     X(I)=X(I-1)+.1*DX
        IF(I.GE.21) GO TO 101
        GO TO 200

101      M=I-20
        X(I)=PX-M*H/A
200        Z=1.-X(I)

           Y=1.+X(I)
        SI=2.*X(I)
        XX(1)=Z/SQ
        XX(2)=Y/SQ

        DO 40 II=1,2
        ERC(II)=ERFC(XX(II))
40      ERIFC(II)=.56419*EXP(-XX(II)*XX(II)) -XX(II)*ERC(II)
       C(1)=1.-(ERC(1)-ERC(2) +SQ*(ERIFC(1)-ERIFC(2)))/SI
C
C       BEGINNING OF SUMMATION OF INFINITE SERIES. MAX. OF 40 TERMS.
C
       DO 20 N=1,40
       IF(N.GE. 40) GO TO 100
         AR=N*PX
        ARE1=N*BETH*(N*PX-X(I))
        ARE2=N*BETH*(N*PX+X(I))

        E1=EXP(-ARE1)
        E2=EXP(-ARE2)
        XX(1)=(2.*AR+Z)/SQ
        XX(2)=(2.*AR-Y)/SQ
        XX(3)=(2.*AR+Y)/SQ
        XX(4)=(2.*AR-Z)/SQ

        DO 88 II=1,4
        ERC(II)=ERFC(XX(II))
88      ERIFC(II)=.56419*EXP(-XX(II)*XX(II)) -XX(II)*ERC(II)

       SUM1=-E1*(ERC(1)+ERC(2))/SI
       SUM2= E2*(ERC(3)+ERC(4))/SI
        SUM3=-SQ*E1*(ERIFC(1)-ERIFC(2))/SI
        SUM4= SQ*E2*(ERIFC(3)-ERIFC(4))/SI
```

```
      S=SUM1+SUM2+SUM3+SUM4
      C(N+1)=C(N)+S
      IF(C(N+1).EQ.0.) GO TO 35

      EPS=S/C(N+1)
      IF(ABS(EPS).LE.ABS(C(N+1))/1.E4 ) GO TO 35
20    CONTINUE
35    IF(I.GE.21) GO TO 77
      C(N+1)=(ROS+COEFF*ABS(C(N+1)))/RO
      C(1)=C(1)*COEFF/RO
      WRITE(6,36)X(I)*A,ABS(C(N+1)),N,C(N+1)-C(1)
36    FORMAT(/,*POSITION (CM)=*,F10.4,12(,*CONCENTRATION=*,F10.4,6X,
     1*N=*,I2,6X,*SUM(N)=*,F12.6)

      GO TO 50
77    DERIV=-C(N+1)/H/M

      WRITE(6,45)M*H,DERIV,-RO1*DERIV,N
45    FORMAT(/,*H(CM)=*,1PE15.7,6X,*DERIVATIVE=*,1PE15.7,6X,*MASS FLUX
     1(GR/CM2 DAY)=*,1PE15.7,6X,I2)
      TOTJ=-RO1*DERIV +V*ROS*86400.
      WRITE(6,55) TOTJ
55    FORMAT(//,*  TOTAL MASS LOSS RATE (G/CM2 DAY)=*,1PE15.7)
      SDIR(M+1)=SDIR(M)+DERIV
50      CONTINUE

        I=3
      DIRAV=SDIR(I+1)/3.
      FLUXAV=-RO1*DIRAV
      FLUXT=12.56637*FLUXAV*A*A*PX*PX

      WRITE(6,300)DIRAV,FLUXAV,FLUXT
300   FORMAT(/,*AVERAGE DIR.=*,1PE15.7,6(,*AVERAGE FLUX(GR/CM2 DAY)=*,
     11PE15.7,6X,*MASS LOSS(GR/DAY)=*,1PE15.7)
C
100   T=T*10.
500     CONTINUE
5000    CONTINUE
6000    CONTINUE
        STOP
        END
```

```
C
C       ********** UCBNE-74  **************
C                  AUTHOR  SHAW J. ZAVOSHY
C                  DATE  SEP. 1981
C       THIS PROGRAM CALCULATES THE FRACTICNAL RELEASE OF A DIFFUSING
C       SPECIES FROM SPHERE. THE INPUT PARAMETERS ARE
C      A= RADIUS CM
C       RO= DENSITY OF DIFFUSANT G/CM3
C       ROS= CONCENTRATION ON THE SURFACE G/CM3
C       DE DIFFUSION COEFFICIENT (CM2/SEC)
C      BETHA=V*A/D = DIMENSIONLESS REGRESION SPEED
C       ***************************************************************
       DIMENSION X(999),C(999),YP(999),YPP(999),YZ(999),W(999,3),ANS(5)
       DIMENSION ERC(10),XX(10),ERIFC(10)
        DIMENSION DD(10),BETHV(10)
        A=17.8
       RO=.672
       ROS=0.
       CEFF=RO-ROS
       DD(1)=8.61*(10.**(-13))
       DD(2)=3.59*(10.**(-11))
        NDI=1
       NBI=9
        BETHV(1)=0.
        BETHV(2)=5.
        BETHV(3)=10.
        BETHV(4)=50.
        BETHV(5)=800.
        BETHV(6)=1600.
        BETHV(7)=-5.
       BETHV(8)=-10.
       BETHV(9)=-20.
       H=.00001
        DO 6000 ND=1,NDI
       D=DD(ND)
       DO 5000 NB=1,NBI
       BETH=BETHV(NB)
        V=BETH*D/A
        T=.1
        T=T*86400.*365.25
       WRITE(6,2)A,V,D,BETH
2      FORMAT(1H1,*  RADIUS  (CM)=*,F12.6,6X,*V(CM/SEC)=*,1PE15.7,6X,
      1*D (CMXCM/SEC)=*,1PE15.7,6X,*BETHA=(VXA/D)=*,1PE15.7)
       WRITE(6,13)RO
13     FORMAT(/,* DENSITY (GR/CM3)=*,1PE15.7)
       IF(V.EQ.0.) GO TO 7

        TLY=A/V/86400./365.25
       TTRANS=D/V/V
       WRITE(6,3)TLY,TTRANS/86400./365.25
3      FORMAT(/,*LEACH TIME(YR)=(A/V)=*,1PE15.7,6X,*TRANSITION TIME(YR)=
      1(D/V2)= *,1PE15.7)
7      CONTINUE
C
C        BEGINNING OF TIME DO LOOP . MULTIPLIER=10
C
       IJK=25
        DO 100 K=0,IJK
       IF(V.EQ.0.) GO TO 17
       IF(T.GE.ABS(A/V)) GO TO 500
```

```
      GO TO 301
17     IJK=9
301    CONTINUE
        TA=D*T/A/A

        SQ=2.*SQRT(TA)
        PX=1.-BETH*TA
       IF(PX.LE. .001/A ) GO TO 500
      DX=PX/100.

      WRITE(6,10)T/86400./365.25,PX*A,DX*A
10    FORMAT(//,*-------- TIME(YR)=*,1PE10.2,6X,* R(T) (CM)=*,F12.4,6X,
     1* DR(CM)=*,F12.5)
C
C      BEGINNING OF NODAL LOOP.
      NNN=992
       DO 50  I=1,NNN
      IF(I .GE. NNN) GO TO 101
      IF(I.GE.92) GO TO 150
         X(I)=(I-1)*DX
       X(1)=.001/A

         GO TO 200
150    X(I)=X(91)+PX*(I-91)/9000.
      GO TO 200

101     X(I)=PX-H/A
200      Z=1.-X(I)

         Y=1.+X(I)
       SI=2.*X(I)
       XX(1)=Z/SQ
       XX(2)=Y/SQ

       DO 40 II=1,2
       ERC(II)=ERFC(XX(II))
40     ERIFC(II)=.56419*EXP(-XX(II)*XX(II)) -XX(II)*ERC(II)
      C(1)=1.-(ERC(1)-ERC(2) +SQ*(ERIFC(1)-ERIFC(2)))/SI
C
C      BEGINNING OF SUMMATION OF INFINITE SERIES. MAX. OF 40 TERMS.
C
      DO 20 N=1,40
      IF(N.GE. 40) GO TO 100
        AR=N*PX
       ARE1=N*BETH*(N*PX-X(I))
       ARE2=N*BETH*(N*PX+X(I))

       E1=EXP(-ARE1)
       E2=EXP(-ARE2)
       XX(1)=(2.*AR+Z)/SQ
       XX(2)=(2.*AR-Y)/SQ
       XX(3)=(2.*AR+Y)/SQ
       XX(4)=(2.*AR-Z)/SQ

       DO 88 II=1,4
       ERC(II)=ERFC(XX(II))
88     ERIFC(II)=.56419*EXP(-XX(II)*XX(II)) -XX(II)*ERC(II)

      SUM1=-E1*(ERC(1)+ERC(2))/SI
      SUM2= E2*(ERC(3)+ERC(4))/SI
       SUM3=-SQ*E1*(ERIFC(1)-ERIFC(2))/SI
       SUM4= SQ*E2*(ERIFC(3)-ERIFC(4))/SI
```

```
      S=SUM1+SUM2+SUM3+SUM4
     C(N+1)=C(N)+S
      IF(C(N+1).EQ.0.) GO TO 35

     EPS=S/C(N+1)
     IF(ABS(EPS).LE.ABS(C(N+1))/1.E4 ) GO TO 35
20    CONTINUE
35   YZ(I)=3.*X(I)*X(I)*ABS(C(N+1))

50     CONTINUE
     YPN=-YZ(NNN)/H
      YPN=YPN*PX*PX
     A1= -.5
     AN=-.5

      NNN=NNN-1
     N=NNN
     YP1=0.

     B1=3.*((YZ(2)-YZ(1))/(X(2)-X(1))-YP1)/(X(2)-X(1))
     BN=-3.*((YZ(N)-YZ(N-1))/(X(N)-X(N-1))-YPN)/(X(N)-X(N-1))
     CALL SPLIFT(X,YZ,YP,YPP,NNN,W,IERR,0,A1,B1,AN,BN)
     NUP=1

     XLO=X(1)
     XUP=X(NNN)
     CALL SPLIQ(X,YZ,YP,YPP,NNN,XLO,XUP,NUP,ANS,IERR2)

      FRAC=1.-ROS*(1.-V*T/A)**3./RO -CEFF*ABS(ANS(1))/RO
     WRITE(6,300)IERR,IERR2,FRAC
300   FORMAT(//,*  IE=*,I2,6X,*IE2=*,I2,6X,* FRAC.=*,1PE15.7)
100   T=T*10.
500    CONTINUE
5000   CONTINUE
6000   CONTINUE
       STOP
      END
```